General Disclaimer

One or more of the Following Statements may affect this Document

- This document has been reproduced from the best copy furnished by the organizational source. It is being released in the interest of making available as much information as possible.

- This document may contain data, which exceeds the sheet parameters. It was furnished in this condition by the organizational source and is the best copy available.

- This document may contain tone-on-tone or color graphs, charts and/or pictures, which have been reproduced in black and white.

- This document is paginated as submitted by the original source.

- Portions of this document are not fully legible due to the historical nature of some of the material. However, it is the best reproduction available from the original submission.

NASA CR-54571
SEPTEMBER 1968
Allison EDR 5863

Single-Stage Experimental Evaluation of Boundary Layer Bleed Techniques for High Lift Stator Blades

III — Data and Performance of Unslotted 0.75 Hub Diffusion Factor Stator

Prepared for

NATIONAL AERONAUTICS AND SPACE ADMINISTRATION

Contract NAS3-7900

Allison Division • General Motors

Indianapolis, Indiana

Requests for copies of this report should be referred to

National Aeronautics and Space Administration
Scientific and Technical Information Facility
P. O. Box 33
College Park, Maryland 20740

NASA CR 54571
SEPTEMBER 1968
Allis n EDR 5863

Single-Stage Experimental Evaluation of Boundary Layer Bleed Techniques for High Lift Stator Blades

III — Data and Performance of Unslotted 0.75 Hub Diffusion Factor Stator

by

G. Seren and R. H. Carmody

Prepared for

NATIONAL AERONAUTICS AND SPACE ADMINISTRATION

Contract NAS3-7900

Technical Management
NASA-Lewis Research Center
Cleveland, Ohio

Lewis Project Manager: William L. Beede
Lewis Reseach Advisor: L. Joseph Herrig

Allison Division • General Motors

Indianapolis, Indiana

ABSTRACT

The test described in this report is part of an overall program to establish experimentally the extent to which it is feasible to increase compressor stator loading and stall-free flow margin by employing suction surface boundary layer bleed techniques. The unslotted stator vanes in this test are used with the objective of providing a basis of comparison for the blade suction surface boundary layer control using blowing and bleed techniques. During this test, the only attempt to control the flow in the boundary layer was done by means of varying hub and case wall bleeds. A secondary objective of this test was to obtain blade element data for design use.

In this test, overall and blade element performance of a row of 0.75 diffusion factor unslotted stator vanes was measured with varying wall bleed rates for boundary layer control. In addition, the vane static pressure distribution was obtained at three radial locations and for three different wall bleed rates at design speed. Overall and blade element performance was also obtained for the rotor and compared to data previously obtained for this rotor without stator vanes. Preliminary discussion of test results and correlations of data are presented.

TABLE OF CONTENTS

LIST OF ILLUSTRATIONS

LIST OF TABLES

SINGLE-STAGE EXPERIMENTAL EVALUATION OF BOUNDARY LAYER BLEED TECHNIQUES FOR HIGH LIFT STATOR BLADES

III. DATA AND PERFORMANCE OF UNSLOTTED 0.75 HUB DIFFUSION FACTOR STATOR

By

G. Seren and R. H. Carmody
Allison Division, GM

SUMMARY

To establish the feasibility of increasing compressor stator loading and stall-free flow margin by the use of boundary layer blowing and bleed techniques and to determine the extent to which such concepts may be employed, a series of investigations were made of a single-stage compressor provided with single- and double-slotted blowing stator rows and single- and triple-slotted bleed stator rows. These stators were designed with NACA 65-series airfoils and with hub diffusion factors of 0.65 and 0.75. The results of tests performed with 0.65 hub diffusion factor single-slotted blowing and bleed stators and the single- and double-slotted 0.75 hub diffusion factor blowing stators were discussed in previous reports. This report presents the results of an investigation with an unslotted stator which was carried out to provide data which could be used for evaluating the performance improvements of the blowing and bleed stators. This stator was also designed with NACA 65-series airfoils and had a hub diffusion factor of 0.75 as did the single- and double-slotted blowing stators (References 1 and 2). To ensure an attached stator end wall boundary layer and to minimize secondary flows, annulus wall bleeding was employed, starting from a point upstream of the stator leading edge and extending to a point downstream of the stator trailing edge. During these tests the rates of wall annulus bleed were varied to evaluate the effects of compressor wall boundary layer control on performance and stator blade element data. For this purpose, an optimized bleed rate and two reduced bleed rates were used. The flow into this stator row during the test was generated by the same state-of-the-art flow generation rotor as used for the tests reported in References 1 and 2.

Overall performance of the rotor and inlet guide vanes was evaluated separately for this stage test. Compared with rotor design values of 1.37 pressure ratio, 88.2 lb/sec inlet flow, and 88.8% overall adiabatic efficiency, at the design pressure ratio the corrected inlet flow was 95.0 lb/sec and the adiabatic efficiency was 93%. The overall rotor performance remained essentially unchanged while the wall bleed rates were varied. In general, this performance agreed well with the flow generation rotor performance without

stators reported in Reference 1. The stage exceeded its design requirements on both pressure ratio and efficiency at design flow. Overall performance for the complete stage with optimum wall bleed was found to have a pressure ratio of 1.315 and adiabatic efficiency of 84.0% at the 95.0 lb/sec airflow corresponding to the flow generation rotor design pressure ratio. The overall performance obtained for the mean and minimum wall bleed rates was 1.325 pressure ratio and 83.5% adiabatic efficiency and 1.333 pressure ratio and 83.0% adiabatic efficiency, respectively. Stage design values are 1.35 pressure ratio and 84.9% adiabatic efficiency at 88.2 lb/sec flow rate.

Blade element performance was obtained for the rotor blade and stator vane row. Experimental values are presented in terms of diffusion factor, deviation angle, and loss coefficient as a function of incidence for various annulus heights, with rotative speed as a parameter. Minimum loss values are determined and compared with the NACA loss parameter versus diffusion factor correlation curves. Radial variations of experimental rotor and stator blade element parameters near their design inlet flow conditions are also compared with the design values for all three of the annulus wall bleed rates employed.

Surface pressure distributions and wake surveys were obtained for the stator. A hysteresis test with acquisition of rotating stall characteristics was also obtained at 60% corrected speed for the complete stage. Hysteresis effects for the stage were observed while recovering from stall. Onset of stall was found to be abrupt at all speeds with stall cells first appearing in the hub region.

The 0.75 hub diffusion factor stator performance met or exceeded the design flow turning values at the end walls. The total pressure losses were higher than design at these loadings. Blade element performance loss correlations for these stators with suction at the end wall generally were below an extension of the existing NACA correlations at the mean and hub regions, but fell above these NACA correlations in the tip region.

Suction surface static pressure distributions along the mean line indicated a boundary layer separation at 55 to 65% chord at incidence angles greater than design. The hub and tip static pressure distributions appeared to be extremely erratic, indicating a possible separation at about 40 to 50% chord throughout the entire range of tests. There was, however, some indication of reattachment and the observed losses were much lower than would be expected under conditions of severe flow separation.

INTRODUCTION

Advanced airbreathing propulsion systems require lightweight compact compressors capable of high levels of performance. These compressors should have a broad range of operation and a large stall margin. High reliability and relative insensitivity to inlet flow distortion are generally required for all compressors. In meeting the more demanding compressor design requirements, compromises must be made that are strongly dependent on the particular application. New applications are steadily increasing the range of requirements which the compressor must meet.

Compressor technology has been advanced continuously by extending, among other parameters, the usable rotational speeds; increasing stage loadings or diffusion factors; and reducing stage length through the use of high blade aspect ratios. Whereas further advancements can be made through optimizations and improved combinations of these parameters, severe aerodynamic limitations such as increasing losses and decreased stall margin are being encountered. Significant advancements in compressor technology require the application of advanced concepts in terms of improved blading for high flow Mach numbers and application of high lift devices to extend the stall-free flow range for compressor rotors and stators. Advanced concepts in these areas may result in sizable reductions in the number of compressor stages and in improved performance.

Airfoils designed to provide high lift experience steep blade surface pressure gradients which become steeper as angle of incidence is increased. As a result, the suction surface boundary layer separates and high total pressure losses and a decrease in stall-free flow margin result. To some extent, however, separation of the suction surface boundary layer can be delayed by energizing it with high energy air. In view of these considerations, an experimental single-stage compressor rig was designed and constructed to test high loaded stators using internal blowing and boundary layer suction concepts to reduce losses and improve stall-free flow margin.

The objectives of this program are to establish experimentally the feasibility of increasing blade loading and stall-free flow margin by stator boundary layer bleed and blowing and to determine the extent to which these may be employed. A secondary objective is to obtain blade element data for design use. The stator designs were to be representative of those for middle and latter stages of highly loaded axial-flow compressors. Stator inlet flow was to be generated by a state-of-the-art flow generation rotor. This report presents the test results for the unslotted 0.75 hub diffusion factor stator. Test results of single- and double-slotted 0.75 hub diffusion factor blowing stators are presented in References 1 and 2, respectively. The performances of these stators are compared with the performance of the unslotted stators in this report. Reference 1 also includes a presentation of the flow generation

rotor performance without stators. The performance characteristics of the 0.65 hub diffusion factor blowing and bleed stators are presented, respectively, in References 3 and 4. The design characteristics of the stators that are employed in the series of tests for the evaluation of boundary layer bleed techniques are presented in Reference 5.

SYMBOLS

A_a	Annulus area, ft^2
c	Airfoil chord, in.
D_f	Diffusion factor
g	Gravitational constant, 32.2 ft-lb_m/lb_f-sec^2
H	Hysteresis loop data point
i	Incidence angle based on mean camber line, degrees
M	Mach number
n	Number of blades per row
N	Rotational speed, rpm
P_t	Total pressure, psia
p	Static pressure, psia
q	Dynamic pressure, psia
R	Radius, in.
$\mathcal{R}$	Gas constant, 53.35 lb_f-ft/lb_m-°R
R_c	Pressure ratio
S	Airfoil surface pressure coefficient, Equation (A13)
T_t	Total temperature, °R
t	Static temperature, °R
t/c	Thickness-to-chord ratio

V	Air velocity, ft/sec
W_a	Compressor airflow, lb_m/sec
W_{BL}	Annulus wall bleed flow, lb_m/sec
x	Distance from blade leading edge, in.

Greek

β	Air angle measured from axial direction, degrees
γ	Ratio of specific heats
γ°	Blade chord angle, degrees
δ	Ratio of total pressure to standard sea level pressure of 14.7 psia
δ°	Deviation angle, degrees
Δ	Incremental value
η	Efficiency
θ	Ratio of total temperature to standard sea level temperature of 518.6°R
κ	Blade metal angle measured from axial direction, degrees
ρ	Density, lb_m/ft^3
σ	Blade row solidity
ϕ	Camber angle, degrees
ω	Angular velocity of rotor, radians/sec
$\bar{\omega}$	Total pressure loss coefficient
$\frac{\bar{\omega}\cos\beta}{2\sigma}$	Loss parameter

Subscripts

0	Guide vane inlet
1	Rotor inlet

2	Stator inlet or rotor exit
3	Stator exit
θ	Tangential direction
ad	Adiabatic
m	Mean or 50% streamline
ma	Mass averaged
z	Axial direction

Superscripts

'	Relative value, rotor property

APPARATUS AND PROCEDURES

TEST FACILITY

A general arrangement of the test facility is shown in Figure 1. Air enters the test compressor after passing through the test facility filter house, an inlet duct, plenum, and bellmouth and is exhausted to the atmosphere through a diffuser. Provisions exist for maintaining compressor inlet pressures above or below atmospheric if necessary.

Two power units can be used simultaneously to drive the test compressor. One is a T56 power turbine with combustors which burn fuel mixed with high pressure air from test facility compressors; the other is a complete T56 power section. The two units are coupled by a primary gearbox whose output shaft drives a secondary gearbox which in turn drives the test compressor. Test compressor speed is controlled by throttling the turbine air supply with a hydraulically-operated valve and by independent fuel controls for each unit.

COMPRESSOR TEST RIG

The mechanical arrangement of the test compressor is shown in Figure 2. It consists of a cylindrical inlet section, the test compressor section, and an exhaust diffuser. The single-stage rotor is supported on two bearings whose housings are linked by a vertically-split compressor case. The compressor case houses the inlet guide vanes, the rotor tip abradable coating, the stator vanes, and the case and hub bleed manifolds. The abradable coating on the

compressor cases over the rotor blade tip permits low running clearances between the blade tips and the case. The rotor is designed with an interference fit such that the rotor blade tip will run into the abradable coating at design speed. Radial growth due to centrifugal force and temperature expansion is considered. Nominal design clearances for this rotor are -0.0025 in. at 100% speed and -0.0045 in. at 110% speed. Nominal static clearance is 0.0075 in. The design of the rig allows the rapid exchange of inlet guide vanes, if ncessary, without dismantling the remainder of the compressor, and the exchange of stator vanes without disassembly of the entire test rig.

Airflow rate and pressure ratio are varied by throttle plates located in the exhaust diffuser. The throttles are linked by a ring and operated by a common actuator.

Provision is made in the rig for bleeding the wall boundary layers at stator tip and hub. This is accomplished by fabricating the stator flow passage walls from perforated sheet metal. Manifolds behind the perforated metal surfaces are connected by multiple tubes to separate vacuum headers for tip and hub wall bleeds.

BLADING

The design of the stator vanes, rotor blades, and design inlet guide vanes is described in detail in Reference 5. Selected types of airfoil sections are: (1) 63-006-series for the inlet guide vanes, (2) double circular arc for the rotor blades, and (3) 65-series thickness distribution with circular arc meanline for the stator vanes. For convenience, however, the principal geometric details of these components are repeated in Table I.

INSTRUMENTATION

Instrumentation was provided to obtain blade element performance for the rotor and stator row and to measure overall performance. The locations of instrumentation planes are shown in Figure 3; Figure 4 shows schematically the circumferential location of the instruments installed at each plane. The radial element locations at each plane were selected along streamlines passing through the 10, 30, 50, 70, and 90% annulus height stations from the tip at the stator inlet measurement plane. The streamline locations are shown schematically in Figure 5. Dimensioned sketches of the probes used are shown in Figure 6. Instrumentation was distributed so as to minimize area blockages and prevent immersion in upstream instrument wakes. Except at the inlet guide vane exit station, duplicate instrumentation was distributed so as to average out any inlet guide vane effects.

Compressor Inlet Conditions

Weight flow was measured with an ASME thin plate orifice located in each branch of the triple inlet header. Six total pressure probes and two 6-element temperature rakes were located in the cylindrical section approximately three feet upstream of the test compressor inlet for measurement of inlet total pressure and temperature. See Figure 4a. Inlet static pressure was measured at the same axial station by two static taps in the inlet wall.

Rotor Inlet—Station 1

Four approximately equally spaced static pressure taps were located on both the inner and outer walls as shown in Figure 4b. An 8-degree wedge static pressure traverse probe was also installed to measure the radial static pressure distribution. Three radial traverse combination total pressure and yaw angle probes were used to measure the distribution of these parameters across the annulus. Total temperature was obtained from plenum thermocouples.

Stator Inlet or Rotor Exit—Station 2

Four approximately equally spaced static pressure taps were located on both the inner and outer walls, and the radial distribution of static pressure was measured by two 8-degree wedge static pressure traverse probes as shown in Figure 4c. Three radial traverse combination probes were installed at this station to measure the radial distribution of total pressure, total temperature, and flow angle.

Stator Exit—Station 3

Four approximately equally spaced static pressure taps were located on both inner and outer walls and two 8-degree wedge static pressure traverse probes were installed for measurement of the radial static pressure distribution as shown in Figure 4d. One traverse combination total pressure, total temperature, and yaw probe was installed primarily to measure flow angle. A 16-element total pressure circumferential rake, shown in Figure 6d, was installed at this station to measure discharge total pressure and stator vane wake. This rake spanned 1.08 vane spaces at the 10% streamline and 1.43 vane spaces at the 90% streamline. Total temperature was measured by four 5-element radial rakes. Inner and outer wall boundary layers were surveyed by fixed 5-element total pressure probes. All taps, probes, and radial rakes were located on extensions of mid-channel streamlines.

Special Instrumentation

In addition to the instrumentation enumerated for blade element and overall performance, the following special instrumentation was installed.

At the rotor exit, two fixed and one traverse hot wire anemometers were installed to signal the onset of compressor stall and to provide rotating stall data. Shaft whip was monitored by means of a whip pickup mounted in the plane of the rotor blades, and strain gages were mounted on eight rotor blades to monitor blade stresses.

The 10, 50, and 90% streamline sections of the unslotted stator vanes were each provided with 12 suction surface and 7 pressure surface static pressure taps as indicated in Figure 7. The 19 static pressure taps for each streamline section were distributed among 4 vanes.

DETERMINATION OF ANNULUS WALL BLEED FLOW FOR STATOR VANE TESTS

With the compressor operating at design speed and stage pressure ratio, the circumferential total pressure rake at the stator exit was set at the streamline station 10% from the tip. Hub and tip wall bleeds were set at a nominal flow of less than 1% of compressor flow. The stator wake pattern at this bleed flow was noted, and the tip wall bleed was then increased until no further improvement in wake pattern was visually observed on a manometer bank. This bleed flow rate was defined as the "optimum" bleed rate. One limiting consideration set as a reasonable upper value, however, was to extract no more than 2.5% of compressor inlet flow per wall at design conditions.

The circumferential rake was then set at the streamline station 90% from the tip. The tip wall bleed flow rate was reset at its original low value, and the procedure described was repeated for the hub bleed.

After hub and outer wall bleed flows had been optimized, the circumferential rake was moved to the mean position. Hub and outer wall bleeds were varied simultaneously in increments from the original nominal flow rate to optimum flow. The effects on the stator wake at mean depth were studied to check that optimum hub and tip wall bleeds coincided with an optimum wake at mid-span. The valve settings for the optimum bleed flow rate were left unchanged for all subsequent speed and flow conditions, except in the case where the wall bleed was varied to compare the effect of various bleed rates on overall and blade element performance. The hub and tip bleed rates were then set at the minimum wall bleed flow as limited by a condition of no back pressure on the perforated wall material and overall performance and blade element data were obtained for design speed. A similar investigation of overall performance and blade element data was also made with a mean bleed flow which was approximately half-way between the optimum and minimum bleed flow rates.

HYSTERESIS TEST

The following method was employed to determine the characteristics of this stage at entry into and when recovering from stall. With corrected speed set at 60%, the throttle was closed until stall cells were indicated by the three hot-wire anemometers (two of which were at the 10% and one at the 90% station from the tip) thus signalling the onset of stall. The first hysteresis point data recording was made prior to the onset of stall. At this near stalled condition, a partial data recording, which consisted of data required for airflow and pressure ratio calculation, was obtained.

The throttle was then closed further in steps, following the onset of stall, and partial data recordings were made at intermediate points before stage pressure ratio levelled off at a lower pressure ratio and a fourth partial data recording was obtained. The throttle was then gradually opened in steps and three other partial recordings, two at intermediate points and one very close to the stall point, were made before indications of stall, as signalled by the hot-wire anemometers, just disappeared. At this point an eighth short data cycle was recorded.

Rotor blade stresses were monitored continuously during the hysteresis test to ensure that excessive vibratory stresses were not encountered.

OVERALL AND BLADE ELEMENT PERFORMANCE DATA

Overall and blade element performance data were obtained at a sufficient number of points per speed line to define rotor or stage performance between maximum flow and stall. The stage stall point is defined as the onset of a steady stall cell indication on the hot-wire anemometers. Performance at design speed was obtained for the minimum and mean wall bleed rates as well as the optimum wall bleed rate. The near-stall test points were taken as close to the rotating stall condition as could be set without actually being in rotating stall. This type of near-stall setting permitted a full data point recording. At each full data point, fixed and traverse pressure and temperature data were recorded at five radial locations corresponding to streamlines passing through the 10, 30, 50, 70, and 90% span stations at the stator inlet measurement plane.

DATA REDUCTION

Overall performance and blade element data reduction is accomplished in one program. A second program is used to calculate pressure coefficients for the stator vanes.

In the first program, raw data from the test stand is read in and printed. The program converts wedge probe static pressure transducer readings to inches of mercury absolute and applies a Mach number correction. All yaw units are converted to degrees. Data recording system corrections, wire

calibrations, and Mach number corrections are applied to all temperatures. Pressures recorded on the data recording system are corrected to standard inlet total pressure. The corrected data is then printed.

Circumferential arithmetic averages of total pressures, static pressures, total temperatures, and yaw angles are calculated and printed. Individual data readings were compared with the averages to validate the data. Any individual reading which differs from its respective average by more than the prescribed deviation (0.5 in. Hg for pressures, 3° for yaw angles, 1.5, 2, and 3°R, respectively, for reference, inlet, and all other temperatures), is not used in the final calculations. Mass-averaged values required for performance calculations are determined using the averaged and validated data.

The program provides a choice of two radial distributions of static pressure: (1) the distributions measured by the wedge probes and (2) a linear distribution across the flow annulus calculated from the arithmetically-averaged hub and case wall static pressure taps. Overall and blade element performances are calculated and printed using the two static pressure distributions mentioned. If a continuity check at any data measurement station is not satisfied within 5%, a simple radial equilibrium solution is provided to give an indication of the problem.

Overall performance values are calculated for the inlet guide vane and rotor and for the complete stage. The following operations were performed to determine these values.

At the inlet plenum station, two total temperatures are arithmetically averaged at each radial station. Mass flow is integrated radially, assuming that averaged wall static pressure exits over the entire cross section. Total pressures and temperatures are then mass averaged. Behind the rotor, wall static pressures are arithmetically averaged circumferentially and all total pressures and total temperatures are arithmetically averaged circumferentially at each radial station. Mass flow is radially integrated and total pressures and temperatures are radially mass averaged.

At the stator exit, four total temperatures are arithmetically averaged circumferentially at each radial station. Incremental mass flow is computed using an arithmetic average of the circumferential rake total pressure readings spanning a stator vane passage at each radial station. A radial integration is made for weight flow. For performance calculations, the total pressures at each radial station are mass averaged circumferentially and the total pressures and temperatures are mass averaged radially. The overall pressure ratio and efficiencies are obtained using the radially mass averaged values of total pressure and temperature.

The calculation of performance variables, as programmed in the data reduction programs, is delineated in the Appendix.

PRESENTATION OF RESULTS

Experimental results obtained in the test program are summarized herein in detail for the unslotted 0.75 hub diffusion factor stator vane with flow generation rotor with the design inlet guide vane set. The reduced data presented were based on a linear static pressure distribution across the annulus at each axial survey station rather than on the static wedge survey values. Comparison of results using both linear and wedge static data (Reference 1) showed that, when the wedge data were considered reliable, differences in reduced data were small; there was a tendency, however, for the wedge static data to be erratic for some test points. Use of the linear static data gives a consistent basis for comparison over the test range and with the data from other tests.

OVERALL PERFORMANCE OF FLOW GENERATION ROTOR AND STAGE

Overall pressure ratio and adiabatic efficiency are each plotted versus corrected inlet flow with corrected speed as a parameter. These are presented in Figures 8 and 9 for the flow generation rotor during this stage test, and Figures 10 and 11 for the stage.

To indicate whether the rotor or the unslotted stator caused the stage to choke or stall, rotor incidence range is summarized in Table II for the flow generation rotor test of Reference 1 and the flow generation rotor of the unslotted 0.75 D_f stator stage test.

Stage rotating stall characteristics at the stall points and hysteresis points are summarized in Table III.

BLADE ELEMENT PERFORMANCE

Rotor blade and stator vane blade element characteristics were computed on the five streamline positions previously defined. The blade element characteristics chosen to present the detailed performance of each blade row are as follows.

Blade element parameter
Incidence angle, i or i'
Total pressure loss coefficient, $\bar{\omega}$ or $\bar{\omega}'$
Diffusion factor, D_f
Deviation angle, $\delta°$
Inlet flow angle, β or β'
Flow turning, $\Delta\beta$ or $\Delta\beta'$
Inlet axial velocity, V_z
Inlet Mach number, M or M'

Rotor blade element data are plotted as a function of incidence with corrected speed as a parameter for each of the streamline stations. The blade element data obtained during the stage test are shown in Figure 12 for the points run at optimum wall bleed and Figure 13 for the points run at design speed with optimum, mean, and minimum wall bleed. For comparison and to aid the analysis of the rotor blade performance, blade element data for the rotor blade, with optimum, mean, and minimum wall bleed, are plotted versus percent annulus height in Figures 14 through 16 for the flow providing the best approximation of the design incidence angle at design speed. Design values are also plotted for comparison. Mass flux distribution out of the rotor corresponding to the design flow rate is plotted and compared with the design flow distribution in Figure 17. Rotor blade element performance is evaluated, in Figure 18, by comparing the loss parameter versus diffusion factor at the 10, 50, and 90% streamline stations from the tip with the NACA correlation curve in Reference 6.

Stator vane blade element data are also plotted as a function of incidence angle with corrected speed as a parameter for each streamline station. The blade element data for the unslotted stator run at optimum wall bleed are plotted in Figure 19. The stator blade element data for the design speed with optimum, mean, and minimum wall bleeds are presented in Figure 20. The annulus wall bleed rates plotted against stage pressure ratio are presented in Figure 21. Blade element data of the unslotted stator vane, for conditions nearest to the design incidence angle, with optimum, mean, and minimum wall bleed, are plotted against the percent annulus height in Figures 22 through 24, respectively, to aid stator vane performance analysis and comparison of the effect of varying the annulus wall bleed rates. Stator vane blade element performance is also evaluated in Figure 25 where the loss parameter versus diffusion factor for 10, 50, and 90% streamline stations from tip is compared with the NACA correlation curve in Reference 6.

The pressure distributions along the 10, 50, and 90% streamlines from the tip of the unslotted stator suction and pressure surfaces are presented in Figures 26 through 32.

Selected stator wakes are plotted in Figure 33 to show the variation of stator wakes with Mach number at fixed incidence angle, and also to show the effect of incidence angle at a fixed Mach number, at optimum wall bleed. The selected stator wakes, plotted in Figure 34, at mean wall bleed, and in Figure 35, at minimum wall bleed are used to show the effects of wall bleed in addition to the Mach number and incidence angle variations. The variation of the stator wake during wall bleed optimization, at the design pressure ratio, is presented in Figure 36.

To enable compressor designers to evaluate and apply the results of this test, detailed summaries of vector diagrams, blade element characteristics, and losses at each streamline station are provided in Table IV.

DISCUSSION OF RESULTS

The method of presentation using the overall and blade element parameter for evaluating the performance has been described in detail. Since the figures and tables are self-explanatory, only general observations are made.

OVERALL PERFORMANCE

Flow Generation Rotor

The design point pressure ratio and efficiency are 1.37 and 88.8%, respectively, at a design flow rate of 88.2 lb/sec with the design inlet guide vanes. Flow generation rotor pressure ratio and adiabatic efficiency measured during the test with the stator are given in Figures 8 and 9. At the design equivalent rotor speed, maximum efficiency was 96.8% with corresponding pressure ratio of 1.44 and flow rate of 90.5 lb/sec. At the design pressure ratio of 1.37 the flow rate was 7.7% higher than design, at 95.0 lb/sec with an adiabatic efficiency of 93%.

The pressure ratio results are in good agreement with the rotor test results without stator vanes (Figure 10 of Reference 1). When the maximum value of the rotor adiabatic efficiencies are examined at a 100% corrected speed, however, a value of 96.8% is obtained from the results of the stage test, Figure 9, as opposed to 92.5% from the flow generation rotor test without stator vanes (Figure 11 of Reference 1) both at the same measured airflow rate. This apparent discrepancy is the result of a reduction in the average total temperature across the stator due to bleeding the inner and outer walls of the stator passage and the method used to compute the efficiency (See Equation (A2) in the Appendix). The mass averaged total temperature at the stator exit is, in general, lower with wall bleed than without. This reflects in a higher rotor efficiency. Figure 9 then indicates the trend in efficiency due to bleed rather than absolute level. The rotor pressure ratio observed with the reduced wall bleeds was similar to that observed with optimum wall bleed.

A prime concern during the design phase of the flow generation rotor, discussed in Reference 1, was that sufficient flow range would be available to avoid excessive limitations on the stator operating range by the rotor. In this report, Table II gives a summary of rotor incidence angles near stall and maximum flow, at hub, mean, and tip streamlines. The stall incidence angles correspond to the minimum flow rate due to either rotor or stator stall. The choke incidence angles correspond to the maximum flow rate due either to rotor choke, stator choke, or facility pressure loss limitations. Rotor incidence angle differences at stall observed between the stator test and the flow generation rotor test of Reference 1 are small, and the stage stall may be primarily due to rotor stall. The comparison of incidence angles at maximum flow indicates that the stator limited the maximum flow at 60 and 80% corrected speed. At 100% corrected speed, the approximately equal rotor incidence angles for both

tests indicate that the rotor or stator is choking at nearly the same flow or the facility pressure loss was controlling. The flow at the hub may, however, be limited by the stator hub choking prior to the mean and tip regions. It is believed that the facility exit duct pressure loss is controlling at these relatively low pressure ratios with high flow rate conditions.

Complete Stage

The overall stage pressure ratio and adiabatic efficiency are shown in Figures 10 and 11, respectively. During these tests only the design inlet guide vanes were employed.

Stage design values for the pressure ratio and adiabatic efficiency are 1.35 and 85.5%, respectively, at a design flow rate of 88.2 lb/sec. At the design equivalent rotor speed, a maximum stage adiabatic efficiency of 87.9% was obtained with a pressure ratio of 1.392 and a flow rate of 90.5 lb/sec. At the flow generation rotor condition of 95.0 lb/sec corrected flow rate the stage pressure ratio was 1.315 and adiabatic efficiency was 84.0%. At this corrected flow rate the values obtained for the pressure ratio and efficiency of the stators with mean and minimum wall bleed rates were 1.325 and 83.5%, and 1.333 and 83%, respectively. For simplicity, the calculated stage adiabatic efficiency, presented herein, is not penalized by the case and hub wall bleed flows. Inasmuch as the rotor loading is not compatible with the stator loading, the stage efficiency is of secondary interest.

The stator is designed to remove all of the tangential whirl imparted by the rotor and the inlet guide vane. This tangential whirl if produced by the rotor alone would give the equivalent of a 1.66:1 pressure ratio level at the stator inlet. Maintaining the same average pressure recovery in the stator of 0.986, a 1.5- to 2.0-point increase in overall stage efficiency would be realized.

Annulus Wall Bleed for Stator Test

Annulus wall bleed over the stator row at tip and hub surface was defined at 100% corrected speed and rotor pressure ratio of 1.37 by visually monitoring the circumferential rake and boundary layer total pressure rakes at tip and hub. Except at very low wall bleed flows of about 0.5%, where stator wakes were still relatively large, the boundary layer total pressure rakes indicated an attached boundary layer. That is, total pressures increased away from the wall. Once the wall boundary layer attached, additional wall bleed essentially affected only the end regions. Optimum wall bleed was selected as the condition where increased bleed did not result in improvement of the stator wake. The bleed valves were held fixed at this setting for all testing defined as optimum bleed flow rate. The wall bleed rate was later varied, at design speed, to determine the influence of the wall bleed on the overall performance and blade element data. The wall bleed flow was first adjusted to its minimum allowable value then to a rate corresponding to approximately half the flow between optimum and minimum values.

The tip and hub wall bleed rates experienced throughout this test with the fixed bleed line valve settings are summarized in Figure 21. The minimum and mean wall bleed rates at design speed are also indicated in Figure 21.

Hysteresis and Rotating Stall Results—Complete Stage

This test was made to determine whether the stall of this stage was gradual or abrupt, and whether the stall would disappear and the stage recover smoothly. The onset of rotating stall at each corrected speed was indicated by the hot wire anemometer located at the 90% streamline. Rotor stall first appeared at the hub and was abrupt at all speeds. The stall zone then progressed to the tip of the rotor with only a slight increase in back pressure.

At 60% corrected speed, an eight-point hysteresis loop test was conducted. The pressure ratio-flow rate points are shown in Figure 10. A hysteresis effect, in terms of pressure ratio and flow rate, was observed from measurements defining the path from point H_1 to H_8.

The maximum transient blade stresses encountered during the hysteresis test were 16,700 psi. There were indications, from the frequent recurrence of stress peaks, that these maximum transient stresses prevailed for a significant period during the hysteresis test. These blade stresses were considered to be at a potentially damaging level. Their magnitudes were appreciably higher than the prescribed stress limit which was 11,250 psi.

Rotative speed, frequency, and number of stall zones are summarized in Table III. Following the onset of stall, a stall zone was recorded in the hub and in the tip regions. The rotative speeds of the cells in both span regions ranged from 27 to 47% rotor speed in the direction of rotation. Multiple stall cells at the tip and hub were recorded during rotating stall tests at design speed. In deep stall, rotative speed was approximately 44% rotor speed in the direction of rotation and the frequency was 110 cps. High rotor blade transient stresses prevented radial traversing of the hot wire probe. It appears, however, that the stall zone extended across the blade span.

BLADE ELEMENT PERFORMANCE

As reported in Reference 1, an extensive study of the inlet guide vanes was made both at design and off-design conditions. Investigation into the possible persistence of the inlet guide vane wakes through the rotor, at the design flow rate condition, indicated the attenuation of these wakes before entering the stator rows. In view of these results, repeated study of inlet guide vane flow for each test was found unnecessary.

Rotor

Figure 12 is a summary of diffusion factor, deviation angle, and loss coefficient data throughout the rotor operating range for the complete stage test at optimum wall bleed. Data at design speed and at all three wall bleed rates are compared in Figure 13. In general, the measured loss coefficients are found to be lower than the design values in the vicinity of the 0° design incidence angle at the 10, 30, 50 and 70% streamline stations and about equal to design values at the 90% streamline station for all the speeds tested using the optimized wall bleed. There were no significant changes in rotor losses as the wall bleed rates were reduced.

Primary rotor blade element performance for the double circular arc blade during the stator test is shown in Figures 14, 15, and 16 for the optimum, mean, and minimum wall bleeds, respectively. Rotor blade measured data for both the flow generation rotor and the complete stage tests operating near the design incidence angle at corrected speed are compared with the design values. The selection of measured data was based on the best agreement with the design incidence angle values since the rotor exceeded its design airflow rate at design pressure ratio. In general, the values obtained for the deviation angles were lower than design and those of the diffusion factor were higher than design.

Values of deviation angle and diffusion factor, differing significantly from the design values, were also evidenced in Reference 1. The lower than design deviation angles result in an effective overcambering of the rotor blades, producing an excessive amount of work on the flow. The combination of higher work input and lower axial exit velocity results in the higher than design values of the diffusion factors.

The radial distribution of mass flux at the rotor outlet for the flow generation rotor and the complete stage test is compared with design values in Figure 17. A flow shift to the tip is indicated, experimentally, with respect to the design distribution. This can be attributed to the low deviation angles in the tip region of the rotor. An additional mass flow shift was observed between the measured test values of the flow generation rotor test, Reference 1, and the 0.75 hub diffusion factor stator test.

Rotor loss parameter data at the 10, 50, and 90% streamlines are shown in Figure 18. When they could be defined, minimum loss coefficient values are indicated in Figure 18 as filled symbols. The minimum values are selected at the data point nearest to the minimum value of the curve drawn through data points in Figure 12. Minimum loss data for the tip region or 10% streamline are found to lie on the lower band of the data scatter (Reference 6). The minimum loss data for the mid-span and hub region are found to agree well with the NACA correlation curves in the test diffusion factor range.

Stator

Figure 19 presents diffusion factor, deviation angle, and loss coefficient over the entire test operating range for the 10, 30, 50, 70, and 90% streamline stations. The measured values of deviation angle are appreciably lower than design values. The tip losses are appreciably higher than the design values. A study of Figure 19 also indicates that the choke or minimum incidence angle limit may not be clearly defined except at the 90% streamline. Further study also shows, however, that the loss coefficient versus incidence angle curve is quite flat over a wide range except at the 70 and 90% streamline height. The lowest hub losses were obtained with the optimum wall bleed rates as shown in Figure 20. The losses at the tip were quite scattered and no firm conclusion could be drawn with respect to the effect of wall bleed rate on tip losses.

The radial variations of blade element data for the stator, at a point where the values of the incidence angle provided the best approximation to design incidence, is compared with the design values in Figures 22 through 24 for the optimum, mean, and minimum wall bleeds, respectively. Inlet axial velocity and incidence angle plots indicate a mass flow shift to the tip with respect to the design value. Other significant results, shown in Figures 22 through 24, are that flow turning was greater than expected or deviation angles much less than designed for over the entire span of the blade and particularly so at the tip. The apparent turning and deviation angles, particularly at the hub and tip, differ greatly from design values, and this margin of difference increases with decreasing wall bleed flow rates. The effect of the varying wall bleed is displayed more prominently at the hub and becomes even more significant as stall incidence is approached. The deviation angles obtained with optimum and mean wall bleed at the hub and tip are considerable less than the design values. The margin between measured and design values increased with decreasing wall bleed flow. This deviation angle result agrees with the measured deviation angles for the single- and double-slotted 0.75 diffusion factor stator of References 1 and 2. Measured losses, in general, were found to be greater than the design values.

Minimum loss coefficient points obtained from Figures 19 and 20 are compared with an extension of the NACA loss parameter versus diffusion factor correlation curves (Reference 6) in Figure 25 for the 10, 50, and 90% streamlines from the tip. The minimum loss coefficient points for the stator for the 10% streamline are generally greater than the values on an extension of the NACA correlation. The data for the 50% streamline agree favorably with the extension of NACA correlation curves with minimum values generally less than the values of the curve.

Typical stator wake distributions are shown in Figures 33 through 35. Selected cases nearest to -3° incidence which show the increasing wake pressure depressions as inlet Mach number increases are given in Figures

33a through 33c, 33e and 33i for optimum wall bleed. The effects of incidence angle at inlet Mach number near 0.7 are illustrated in Figures 33d through 33h for optimum wall bleed, Figures 34a through 34d for mean wall bleed, and Figures 35a through 35d for minimum wall bleed. The wake surveys at high positive incidence angles, in Figures 33h and 33j, with optimum wall bleed flow show low total pressure peaks at the hub, indicated by the rake elements 6 and 7. The wakes presented in Figures 34d, for the mean wall bleed, and Figure 35d, for the minimum wall bleed, show a similar behavior at the hub region.

Wake survey data was recorded during the wall bleed optimization runs at the design stage pressure ratio of 1.35 and 100% corrected speed. The effect of reduced stator losses with increasing wall bleed rate is shown in Figure 36. It is evident in Figure 34 and from the wake surveys at design speed that increased wall bleed reduced the end wall region flow disturbance and stator losses, particularly at the hub. Higher wall bleed rates above the 30.2 and 30 in. H_2O orifice pressure differential at tip and hub, respectively, had little effect on increasing wake total pressure at these depth locations. A comparison of the tip and hub wakes during optimization also indicates that the hub total pressure losses are reduced more effectively by the wall bleeds while the improvements at the tip are less marked. This indicates that a system where the hub and tip wall bleeds are controlled independently may be desirable to further improve stator wakes by means of wall bleeds.

Stator Static Pressure Distributions

Suction surface static pressure distributions along the meanline for the stator indicate the presence of boundary layer separation at 55 to 65% chord for incidence angles greater than the design incidence angle at all the wall bleeds, as shown in Figures 26 through 32. The determination of the apparent boundary layer separation is based on the study of the static pressure distribution along the 50% streamline. The reason for this choice is the difficulty experienced in analyzing the 10 and 90% streamlines for separation. These streamlines are greatly influenced by the secondary flow and end wall effects to varying degrees, depending on the bleed rates applied at the annulus walls. The pressure distributions along 10 and 90% streamlines indicate possible existence of separation further upstream along the suction surface.

The apparent separation point was observed to move upstream as the incidence angle was increased. In cases of high stator incidence angle, some of the static pressure distributions indicate almost totally detached flow at the hub. These cases also indicate separation at the tip occurring further upstream than it appears where the incidence angles are smaller.

The 10% and 90% streamline pressure distributions obtained for high incidence angles at a 110% design speed, in Figures 32e and 32f, indicate separation occurring almost at the leading edge for the hub and tip while it is retarded to about 50% chord along the 50% streamline. Some of the operating conditions indicate the existence of reattachment of the boundary layer. These observed changes in the static pressure distribution may be attributed to the existence of wall bleeds. The similarity in the pressure distributions obtained with varying wall bleed rates made it difficult to determine the direct effects the bleed technique had on the surface pressure distributions.

CONCLUDING REMARKS

Discussion of the experimental results has been based on the work completed to date. Analysis of the data indicates the following points.

1. The overall performance of the flow generation rotor agreed favorably with the results of the rotor without stator vanes in Reference 1. The stage exceeded its design requirements on both pressure ratio and efficiency. The rotor overall performance was not affected by the variations in the wall bleeds. The stage overall performance showed little change in pressure ratio but a drop in efficiency with decreasing wall bleed flow was noted.

2. A hysteresis effect was observed in terms of pressure ratio and mass flow rate at 60% design speed. Stall point tests indicated abrupt stall at all speeds. During the hysteresis tests at 60% speed and the stall point tests above 60% speed, rotor blade stresses frequently exceeded the prescribed stress limit which was 11,250 psi. The maximum stress values, during the hysteresis tests, were 16,700 psi.

3. The wall bleed technique provided a means of controlling the boundary layer flow and reducing losses. Losses were reduced, more effectively at the hub than at the tip, by increasing wall bleed flow rates.

4. The blade surface static pressure distributions along the meanline gave evidence of possible flow separation at 55 to 65% chord, for angles greater than the design incidence angle. The apparent separation point was detected further upstream at the 10 and 90% annulus height locations. Flow turning and pressure loss levels did not indicate severe flow separation on the vane suction surface. Also, there was some indication of flow reattachment.

5. The 0.75 hub diffusion factor stator performance met or exceeded the design flow turning values at the end walls. The total pressure losses were higher than design at these loadings. Blade element performance loss correlations for these stators with suction at the end wall generally were below an extension of the existing NACA correlations at the mean and hub regions, but fell above these NACA correlations in the tip region.

REFERENCES

1. Miller, M. L. and Beck, T. E. Single-Stage Experimental Evaluation of Boundary Layer Blowing Techniques for High Lift Stator Blades, II—Data and Performance of Flow Generation Rotor and Single-Slotted 0.75 Hub Diffusion Factor Stator. NASA CR-54565, Allison Division, GM, EDR 5691, February 1968.

2. Carmody, R. H. and Seren, G. Single-Stage Experimental Evaluation of Boundary Layer Blowing Techniques for High Lift Stator Blades, IV—Data and Performance of Double-Slotted 0.75 Hub Diffusion Factor Stator. NASA CR-54567, Allison Division, GM, EDR 5861, August 1968.

3. Miller, M. L. and Seren, G. Single-Stage Experimental Evaluation of Boundary Layer Blowing Techniques for High Lift Stator Blades, III—Data and Performance of Flow Generation Rotor and Single-Slotted 0.65 Hub Diffusion Factor Stator. NASA CR-54566, Allison Division, GM, EDR 5759, June 1968.

4. Seren, G. and Carmody, R. H. Single-Stage Experimental Evaluation of Boundary Layer Bleed Techniques for High Lift Stator Blades, II—Data and Performance of Single-Slotted 0.65 Hub Diffusion Factor Stator. NASA CR-54570, Allison Division, GM, EDR 5862, August 1968.

5. Chapman, D. C. and Miller, M. L. Single-Stage Experimental Evaluation of Boundary Layer Bleed Techniques for High Lift Stator Blades, I—Compressor Design. NASA CR-54569, Allison Division, GM, EDR 5636, February 1968.

6. Aerodynamic Design of Axial Flow Compressors. NACA SP-36, 1965.

APPENDIX

PERFORMANCE EQUATIONS

The following overall and blade element performance parameters were calculated for the analysis of test data and the evaluation of the unslotted stator performance.

WEIGHT FLOW

Overall performance is presented as a function of corrected weight flow, defined as

$$\frac{W_a\sqrt{\theta}}{\delta} \tag{A1}$$

ADIABATIC EFFICIENCY

Adiabatic efficiency for the inlet guide vane and rotor combination is

$$\eta_{ad_2} = \frac{\left(\frac{P_{t_{2,ma}}}{P_{t_0}}\right)^{(\gamma-1)/\gamma} - 1}{\frac{T_{t_{3,ma}}}{T_{t_0}} - 1} \tag{A2}$$

and for the guide vane, rotor, and stator is

$$\eta_{ad_3} = \frac{\left(\frac{P_{t_{3,ma}}}{P_{t_0}}\right)^{(\gamma-1)/\gamma} - 1}{\frac{T_{t_{3,ma}}}{T_{t_0}} - 1} \tag{A3}$$

DIFFUSION FACTOR

For the rotor, diffusion factor is defined as

$$D_{f_2} = 1 - \frac{V_2'}{V_1'} + \frac{V_{\theta_2} - V_{\theta_1}}{2\sigma V_1'} \tag{A4}$$

and for the stator as

$$D_{f_3} = 1 - \frac{V_3}{V_2} + \frac{V_{\theta_2} - V_{\theta_3}}{2\sigma V_2} \tag{A5}$$

These quantities are calculated using the appropriate velocity triangle values previously computed by the program.

DEVIATION ANGLE

Rotor blade deviation is defined as

$$\delta^{\circ}_2 = \beta'_2 - \kappa'_2 \tag{A6}$$

and stator deviation as

$$\delta^{\circ}_3 = \beta_3 - \kappa_3 \tag{A7}$$

where κ'_2 is the rotor blade exit metal angle based on the mean camber line for a double-circular arc airfoil and κ_3 is the stator vane exit metal angle based on the circular arc camber line for the 65-series airfoil.

INCIDENCE ANGLE

Rotor blade incidence is defined as

$$i'_1 = \beta'_1 - \kappa'_1 \tag{A8}$$

and stator incidence as

$$i_2 = \beta_2 - \kappa_2 \tag{A9}$$

where κ'_1 is the rotor blade inlet metal angle based on the mean camber line for a double-circular arc airfoil and κ_2 is the stator vane inlet metal angle based on the circular arc camber line.

TOTAL PRESSURE LOSS COEFFICIENT

Total pressure loss coefficient for the rotor is defined as

$$\bar{\omega}' = \frac{\left[1 + \frac{\gamma-1}{2}\frac{(\omega R_2)^2}{\gamma g \mathcal{R} T'_{t_1}}\left(1 - \frac{R_1^2}{R_2^2}\right)\right]^{\gamma/(\gamma-1)}\left[1 - \frac{P_{t_2}/P_{t_1}}{(T_{t_2}/T_{t_1})^{\gamma/(\gamma-1)}}\right]}{1 - \left[1 + \frac{\gamma-1}{2}(M'_1)^2\right]^{-\gamma/(\gamma-1)}} \tag{A10}$$

and for the inlet guide vanes as

$$\bar{\omega} = \frac{1 - \frac{P_{t_1}}{P_{t_0}}}{1 - \left[1 + \frac{\gamma - 1}{2}(M_0)^2\right]^{-\gamma/(\gamma-1)}} \tag{A11}$$

and stator as

$$\bar{\omega} = \frac{1 - \frac{P_{t_3}}{P_{t_2}}}{1 - \left[1 + \frac{\gamma - 1}{2}(M_2)^2\right]^{-\gamma/(\gamma-1)}} \tag{A12}$$

PRESSURE COEFFICIENT

Pressure coefficient (S) is defined by

$$S = \frac{P_{t_2} - p}{q_2} \tag{A13}$$

where:

P_{t_2} = total pressure at stator inlet

p = static pressure at a given point on the vane surface

$q_2 = \frac{\gamma p_2 M_2^2}{2}$ = dynamic pressure at stator inlet

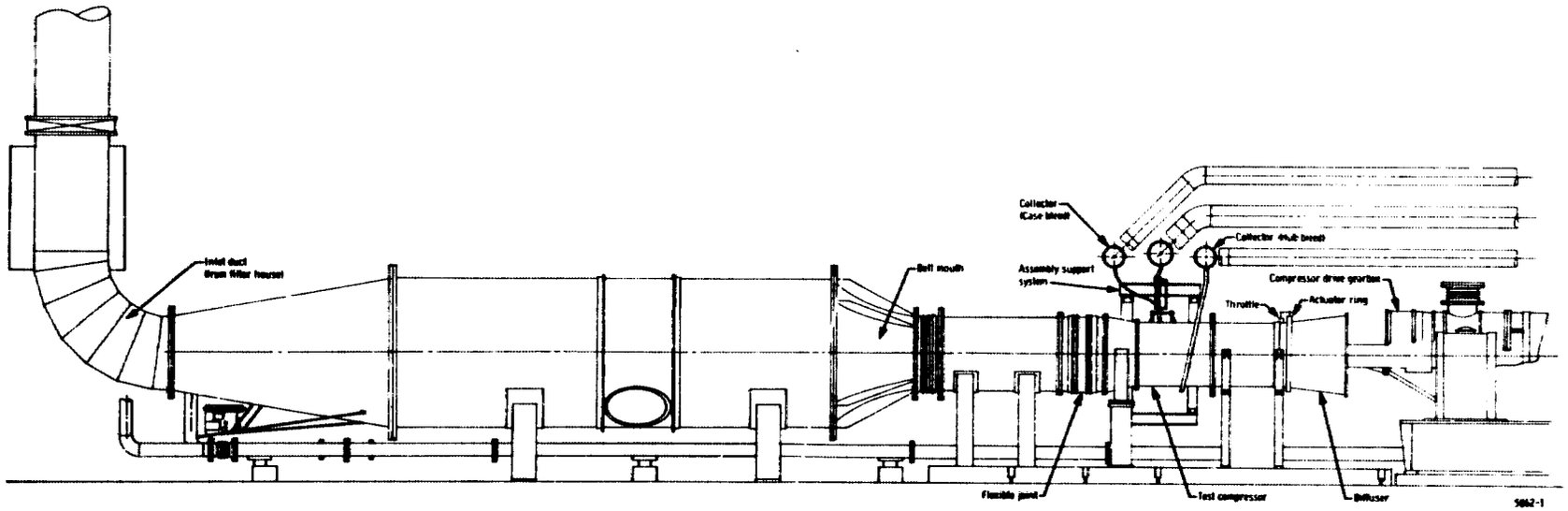

Figure 1. Compressor test facility.

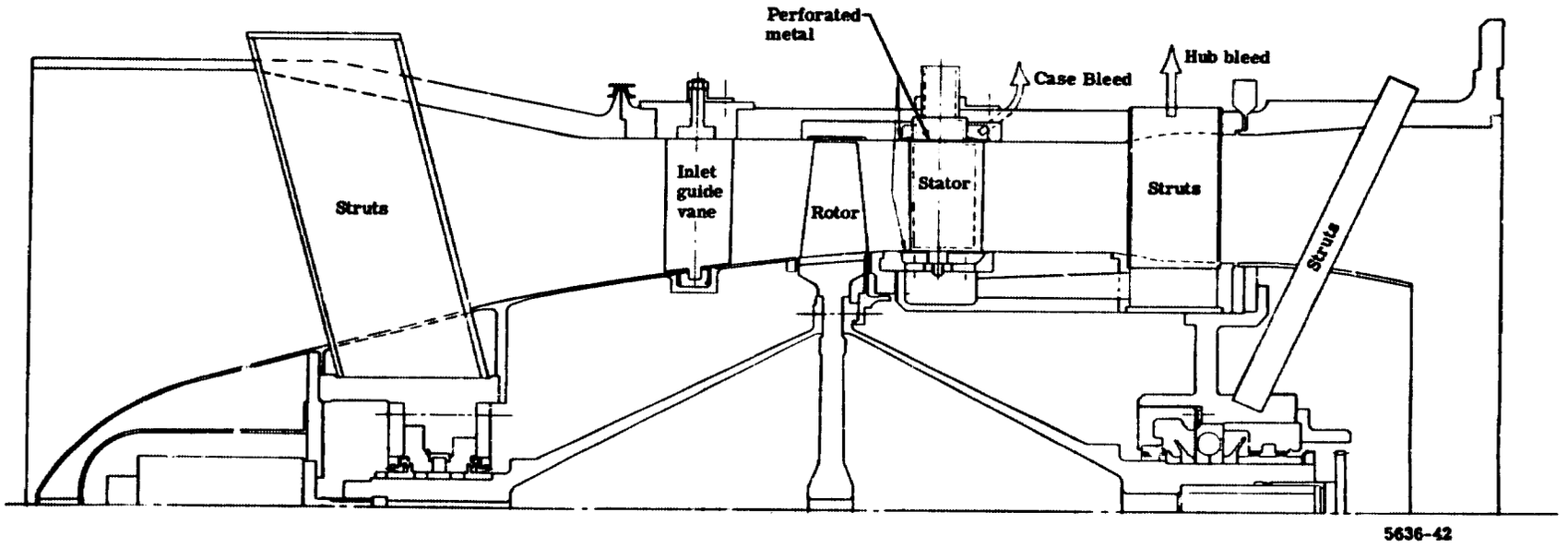

Figure 2. Layout of compressor test rig.

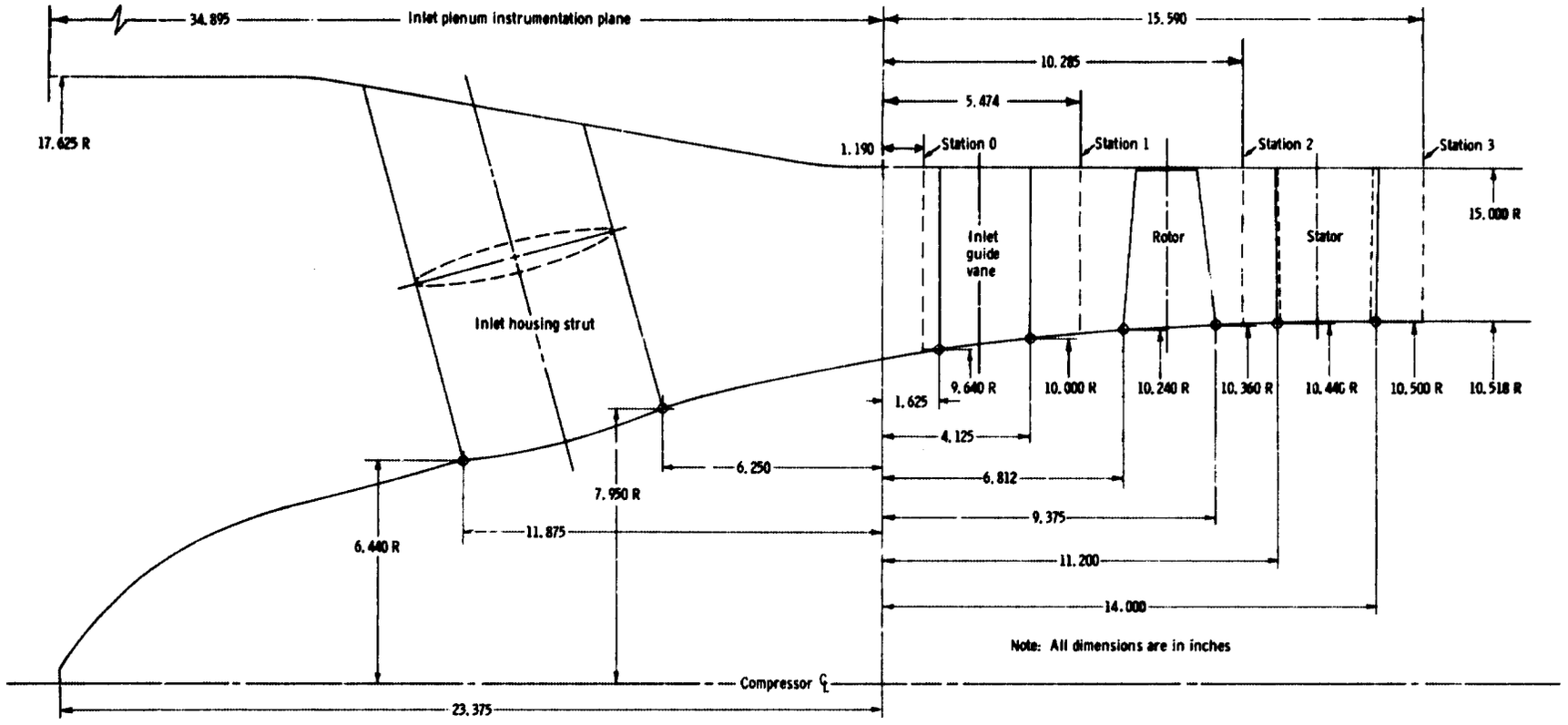

Figure 3. Test rig flow path.

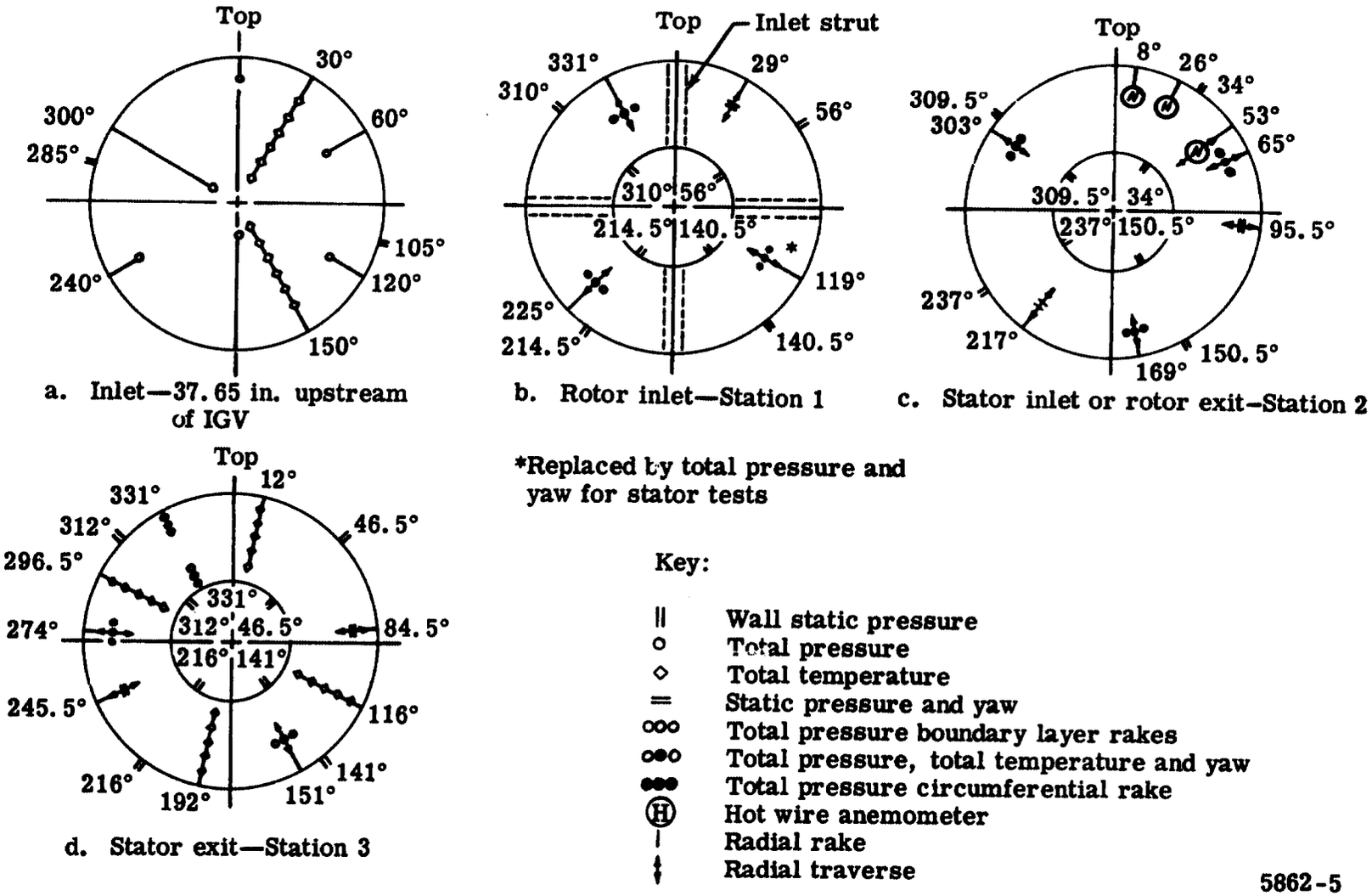

Figure 4. Circumferential location of instrumentation viewed downstream.

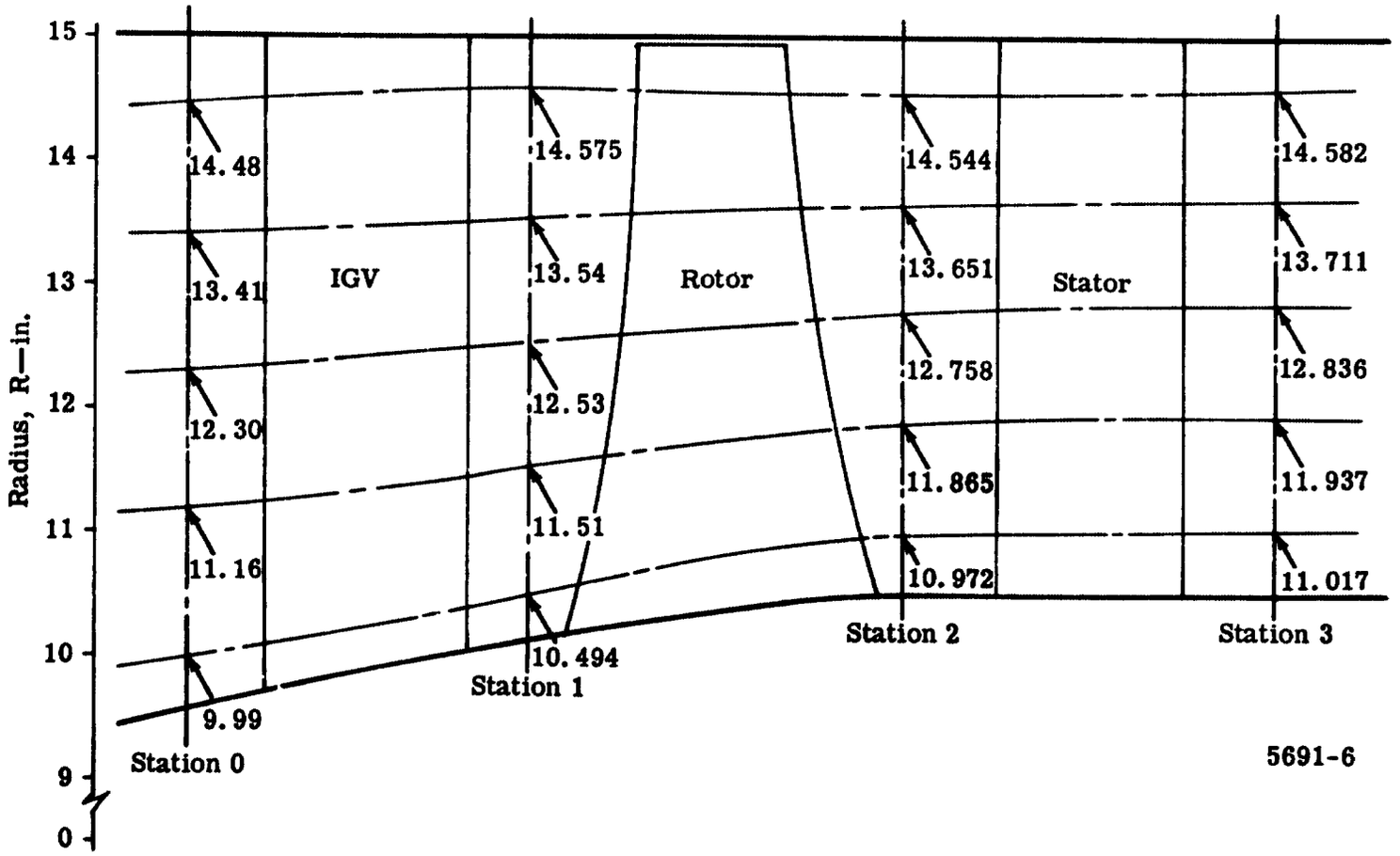

Figure 5. Radial location of streamlines for instrumentation positions.

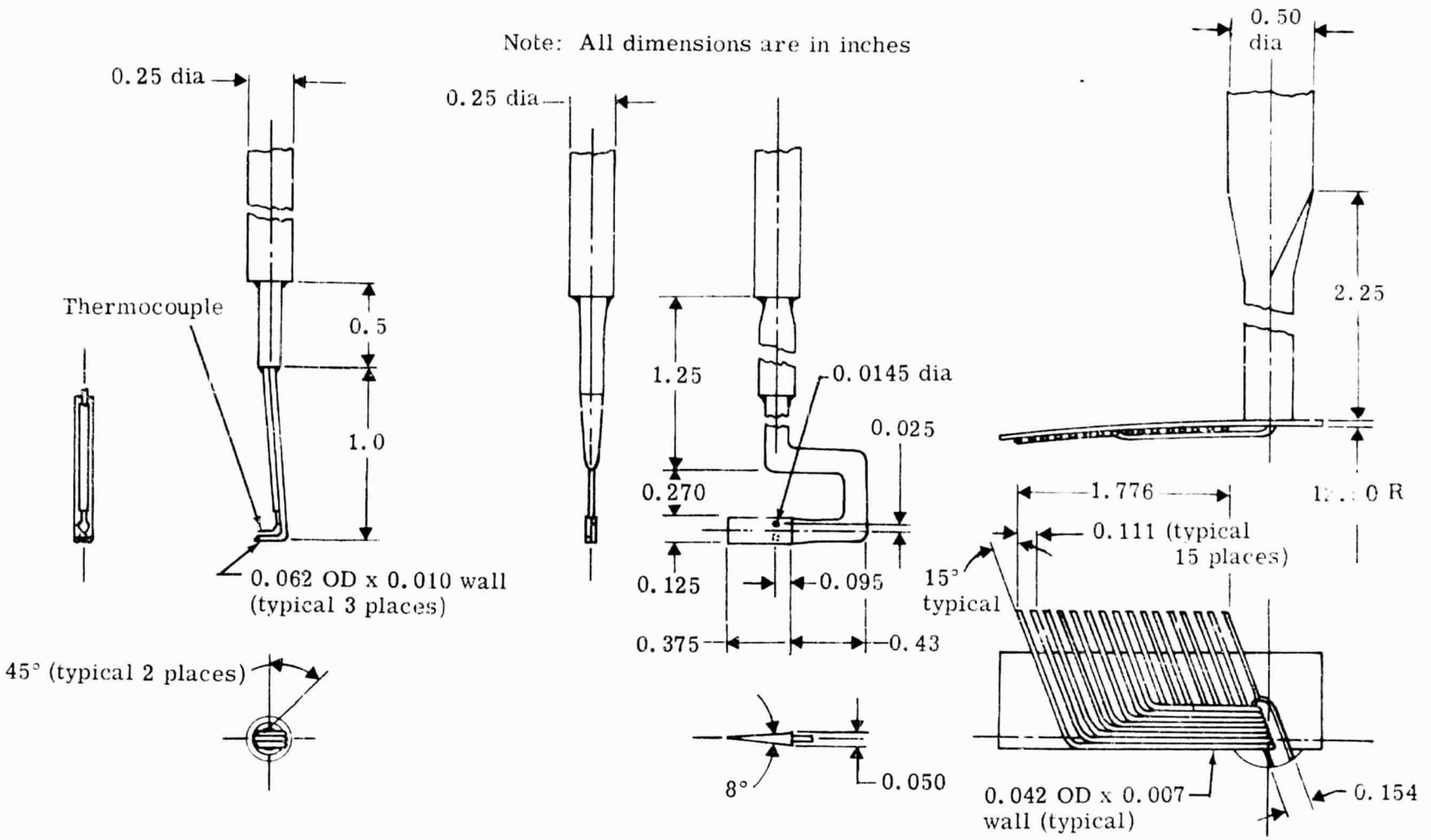

a. Total pressure, total temperature, and yaw probe

b. Static pressure and yaw probe

c. IGV circumferential rake

Figure 6. Schematics of survey instrumentation.

Note: All dimensions are in inches

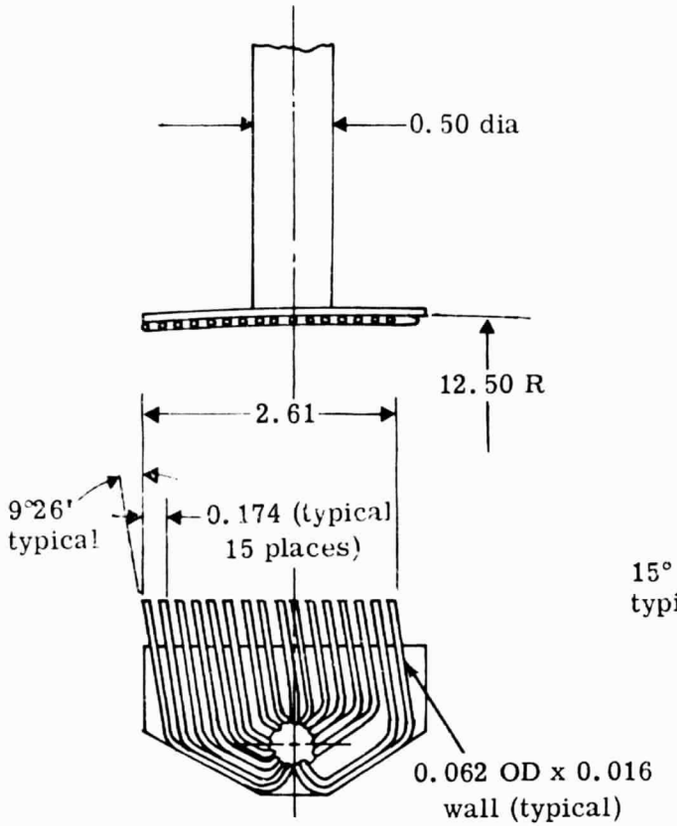

d. Stator circumferential rake

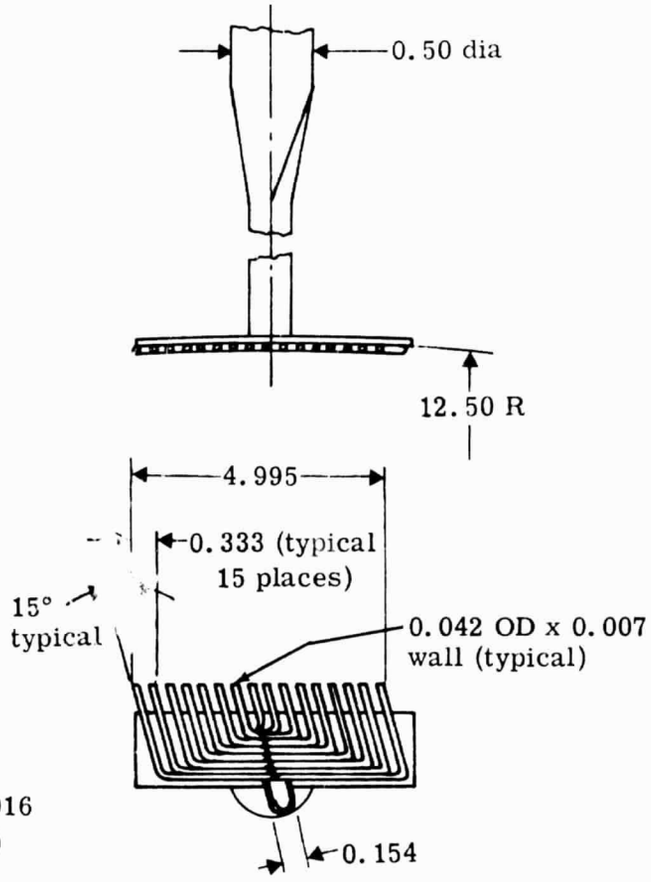

e. IGV wake persistence circumferential rake

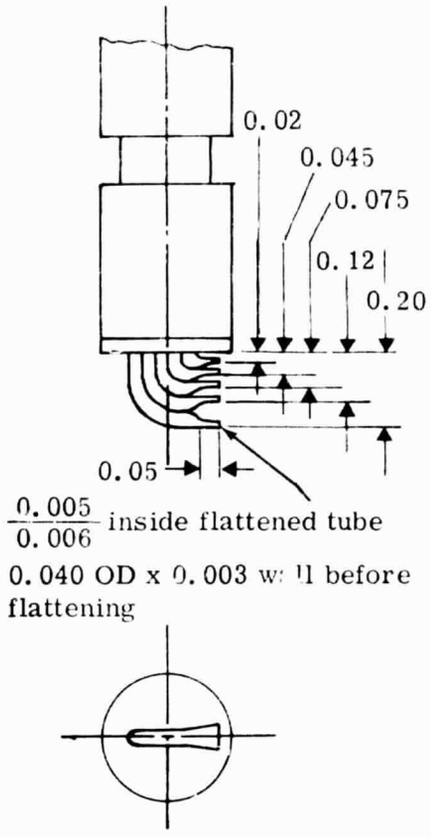

f. Boundary layer probe for tip and hub

5691-8

Figure 6. Schematics of survey instrumentation.

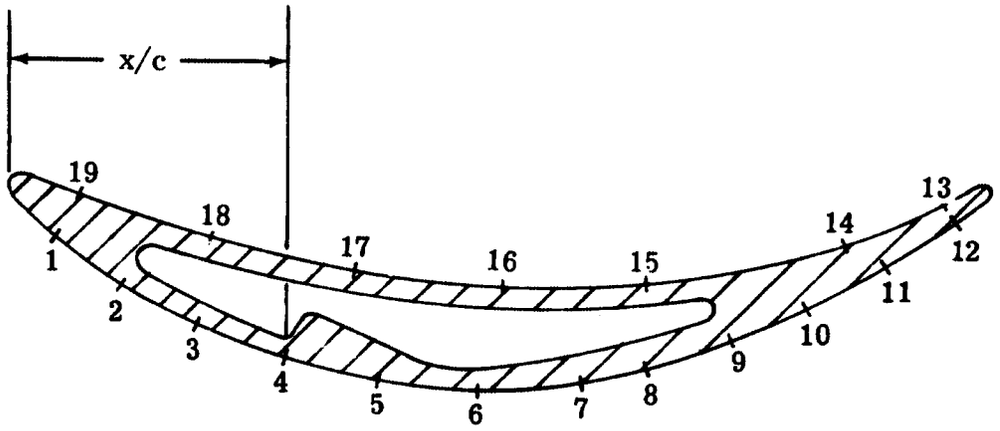

Tap	1	2	3	4	5	6	7	8	9	10	11	12
x/c—%	4.98	11.62	19.59	28.22	38.18	48.14	58.43	65.07	73.37	81.34	88.98	96.61
Vane No.	1	2	3	4	1	2	3	4	1	2	3	4

Tap	13	14	15	16	17	18	19
x/c—%	94.29	84.66	65.41	50.46	35.52	20.92	6.64
Vane No.	1	2	3	4	1	2	3

5863-8

Figure 7. Unslotted stator vane static pressure tap locations at 10, 50, and 90% streamlines.

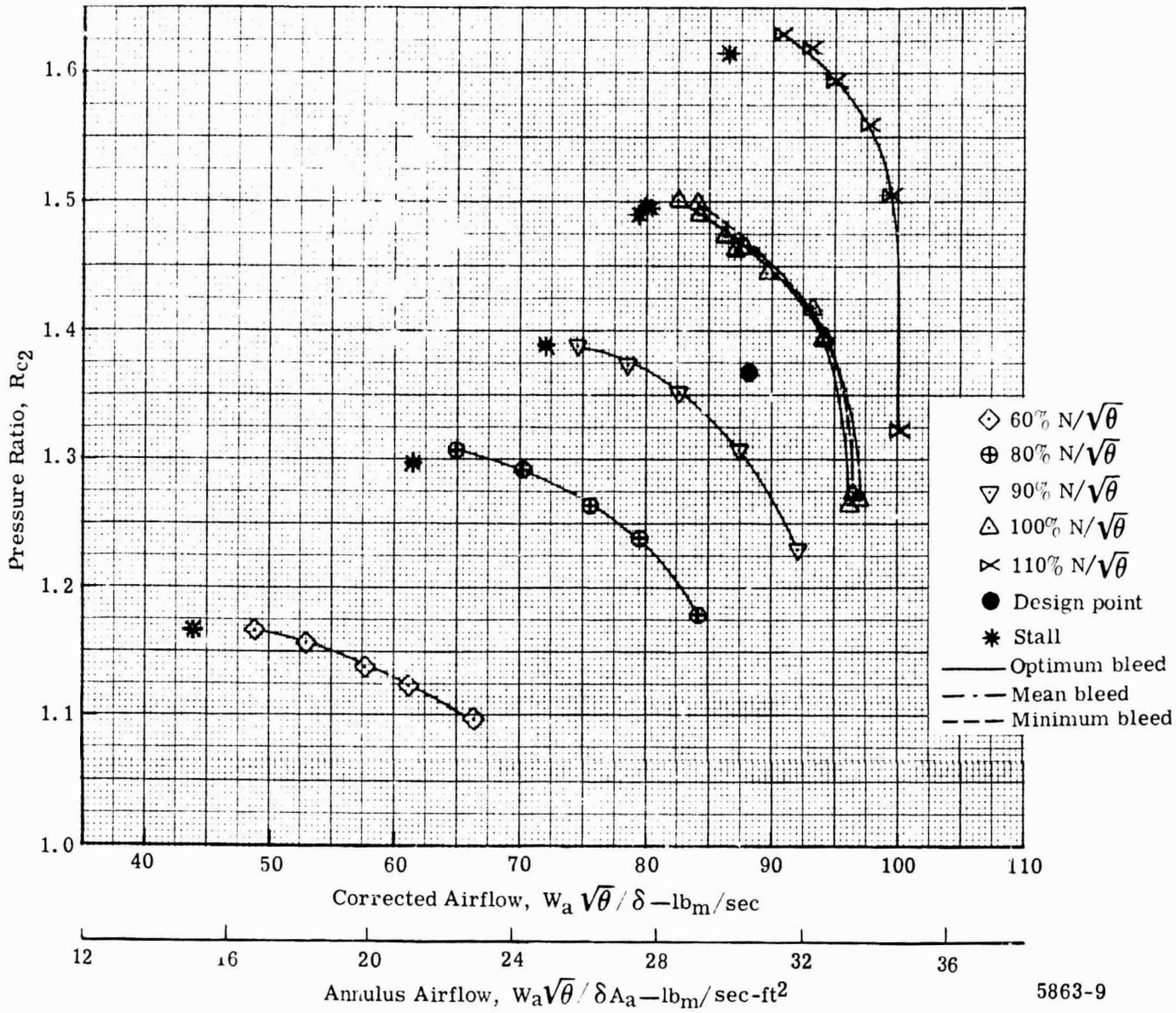

Figure 8. Flow generation rotor overall performance in stage test—pressure ratio.

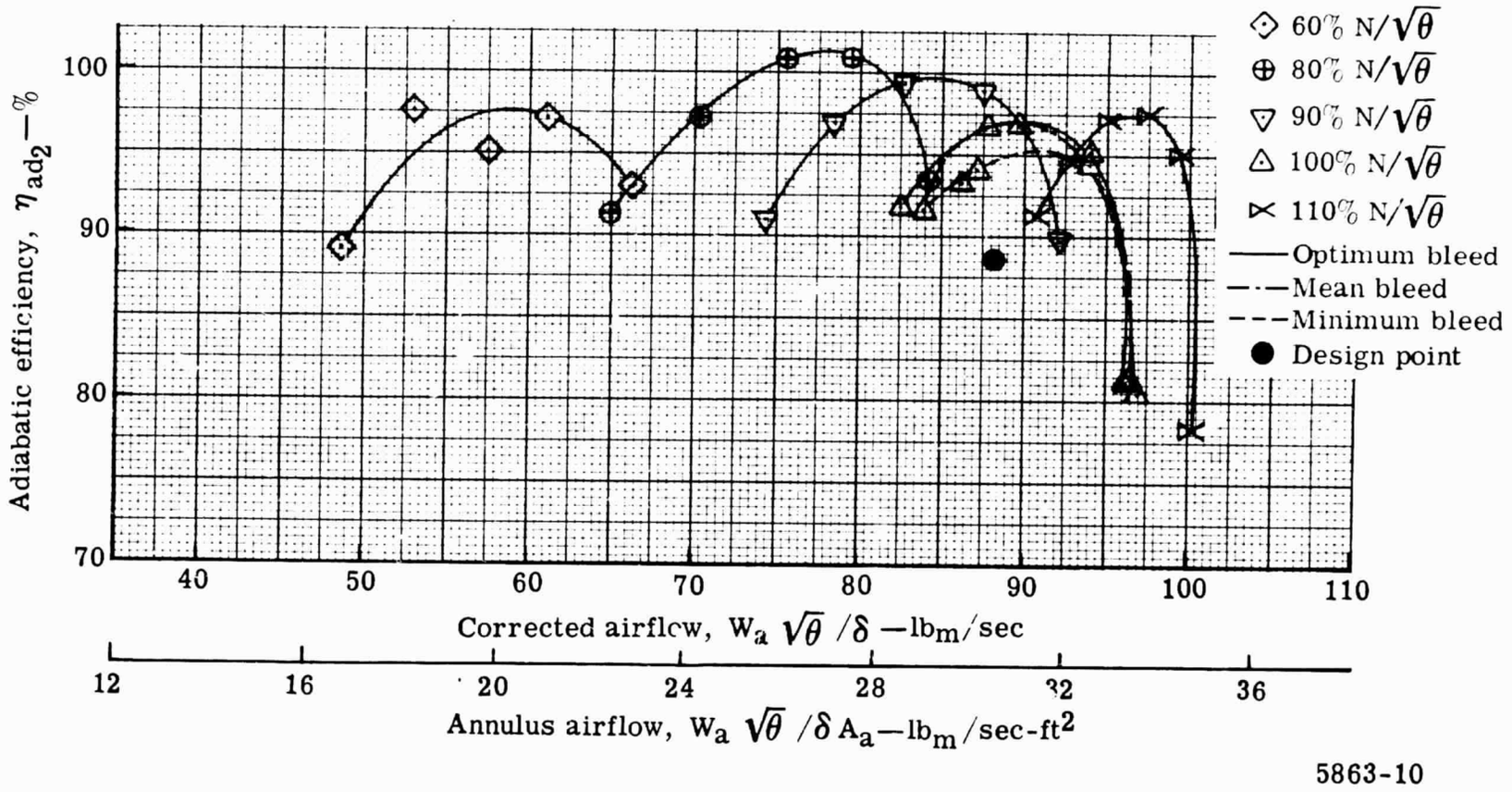

Figure 9. Flow generation rotor overall performance in stage test—adiabatic efficiency.

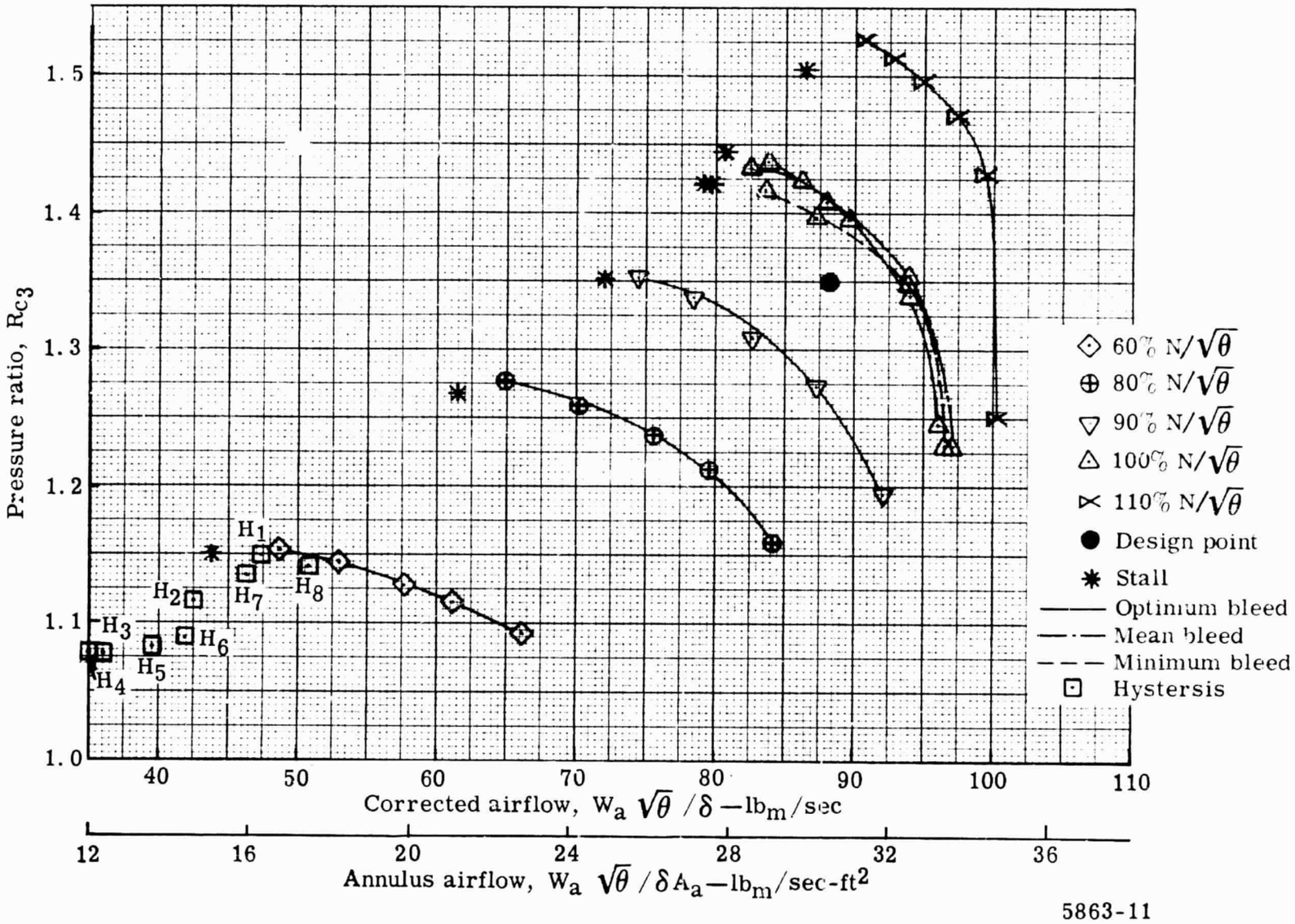

Figure 10. Stage overall performance—pressure ratio.

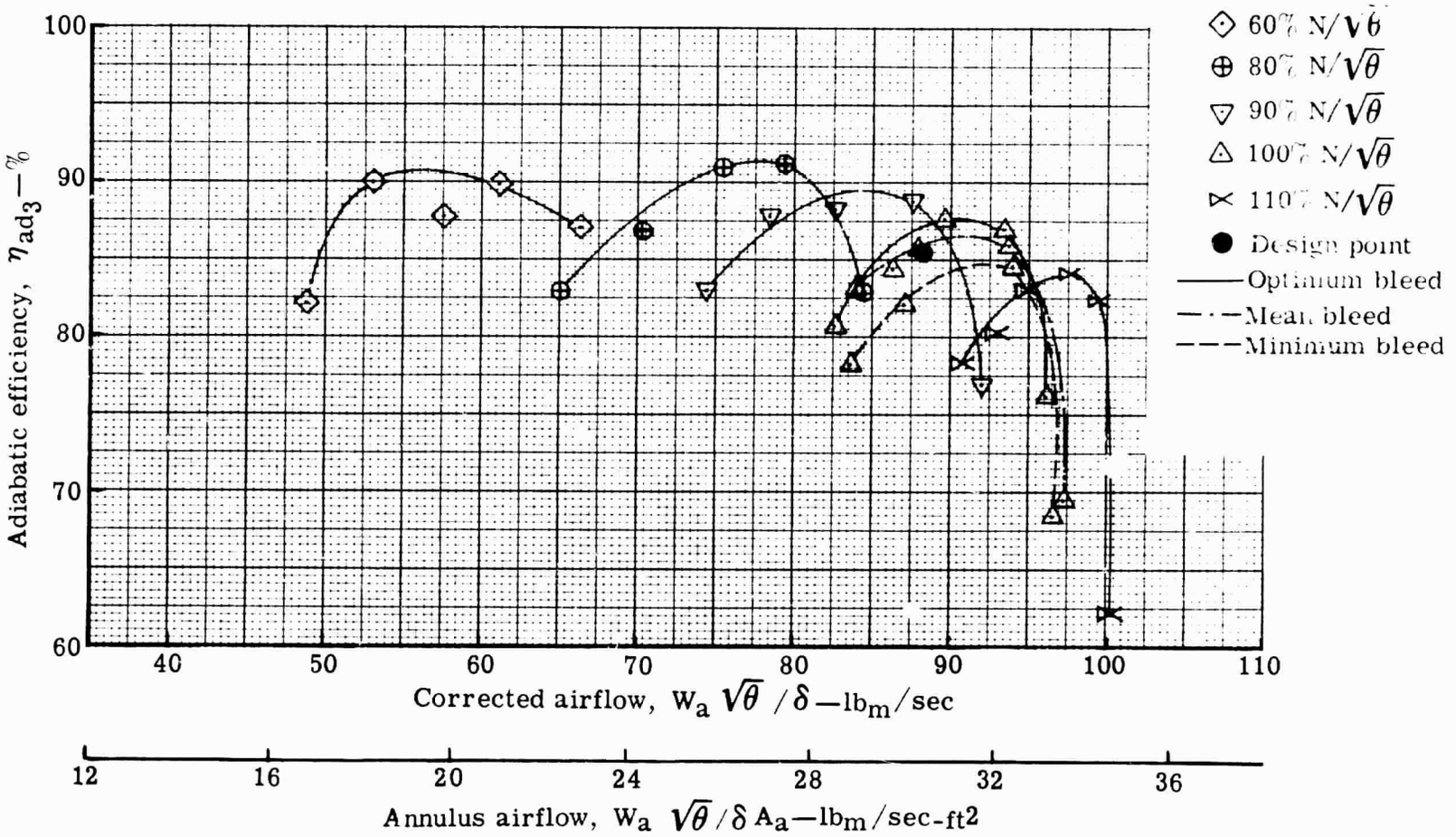

Figure 11. Stage overall performance—adiabatic efficiency.

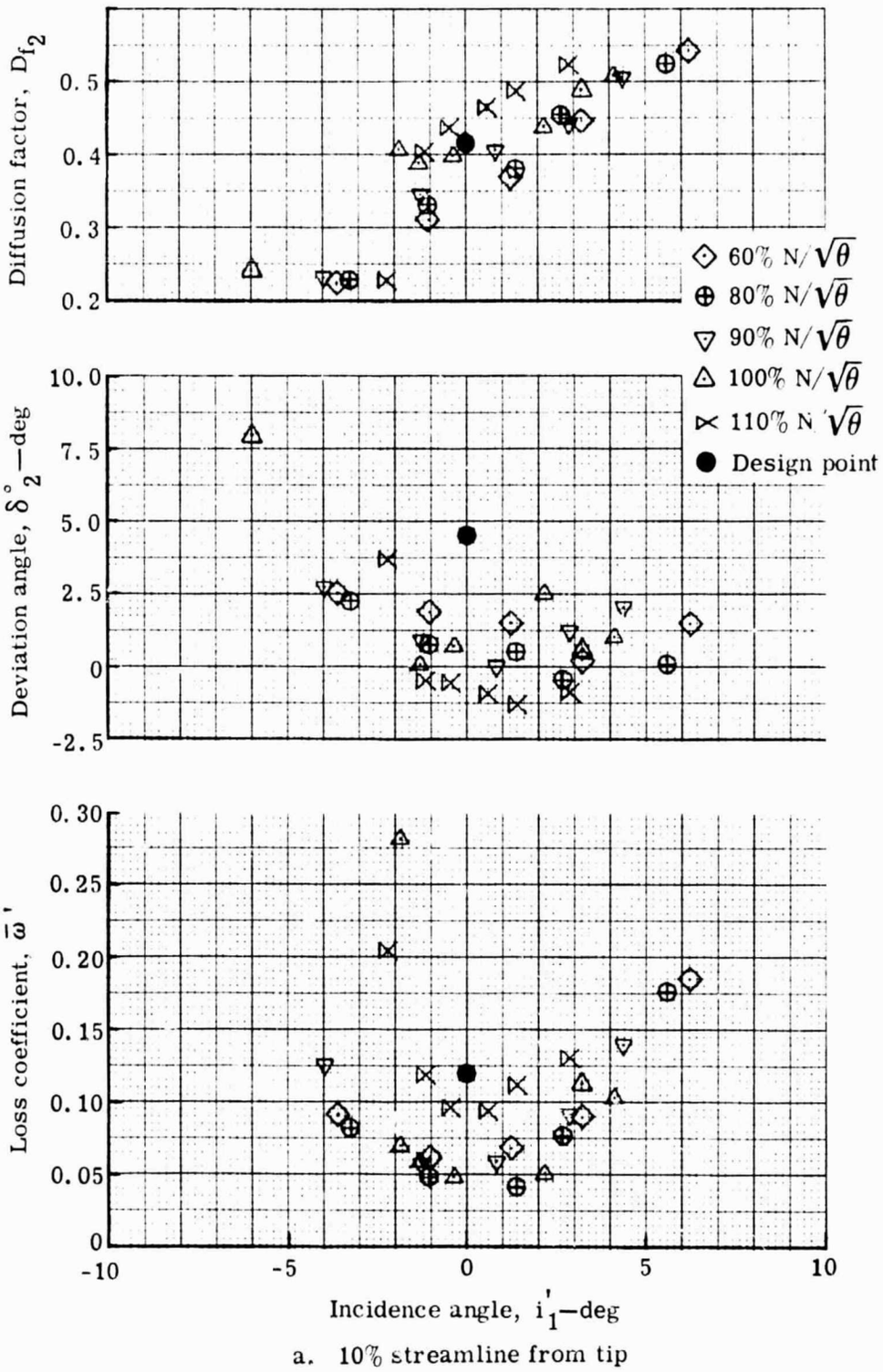

a. 10% streamline from tip

5863-13

Figure 12. Rotor blade element performance at optimum wall bleed—stage test.

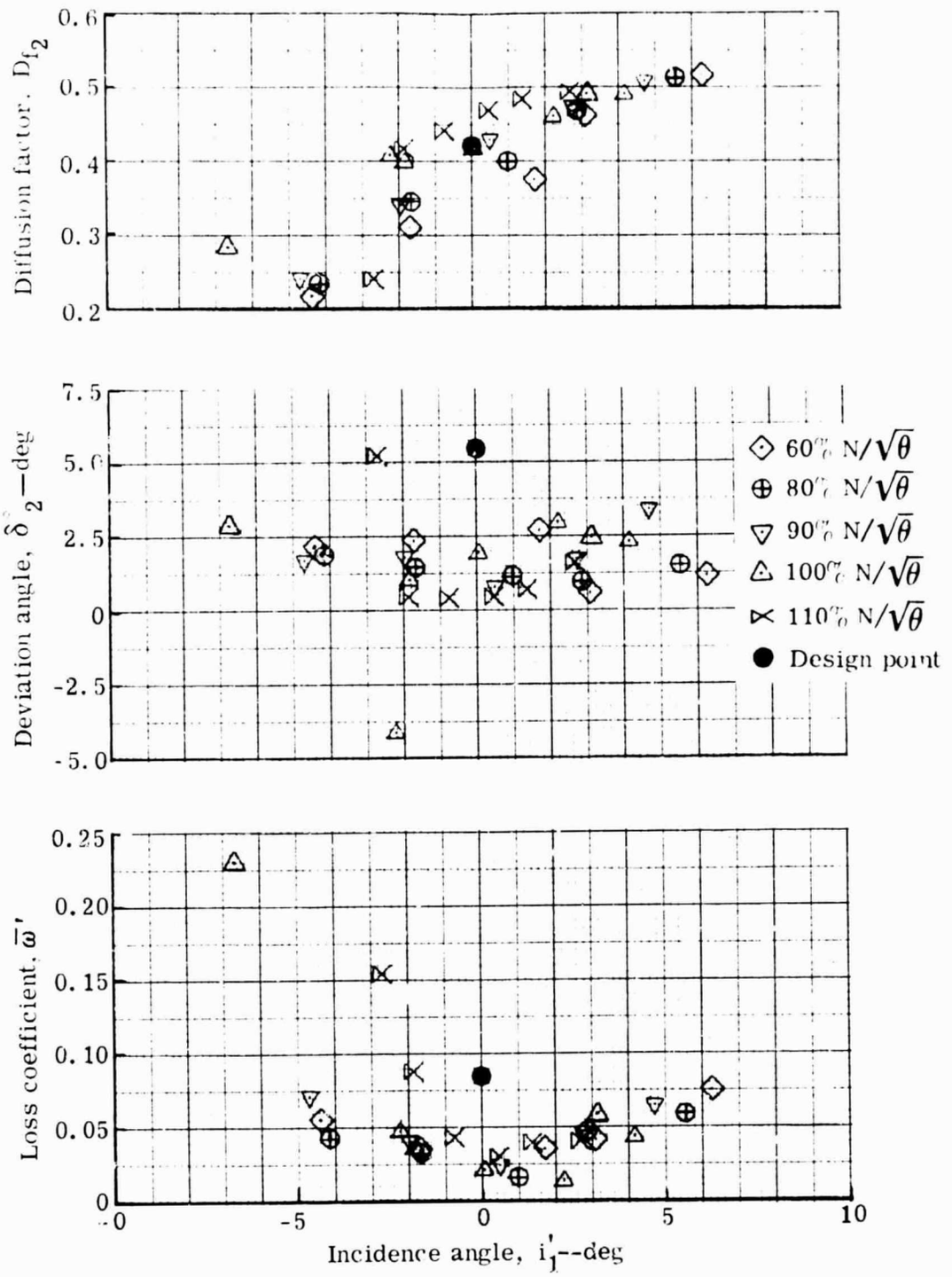

b. 30% streamline from tip

5863-14

Figure 12. Rotor blade element performance at optimum wall bleed—stage test.

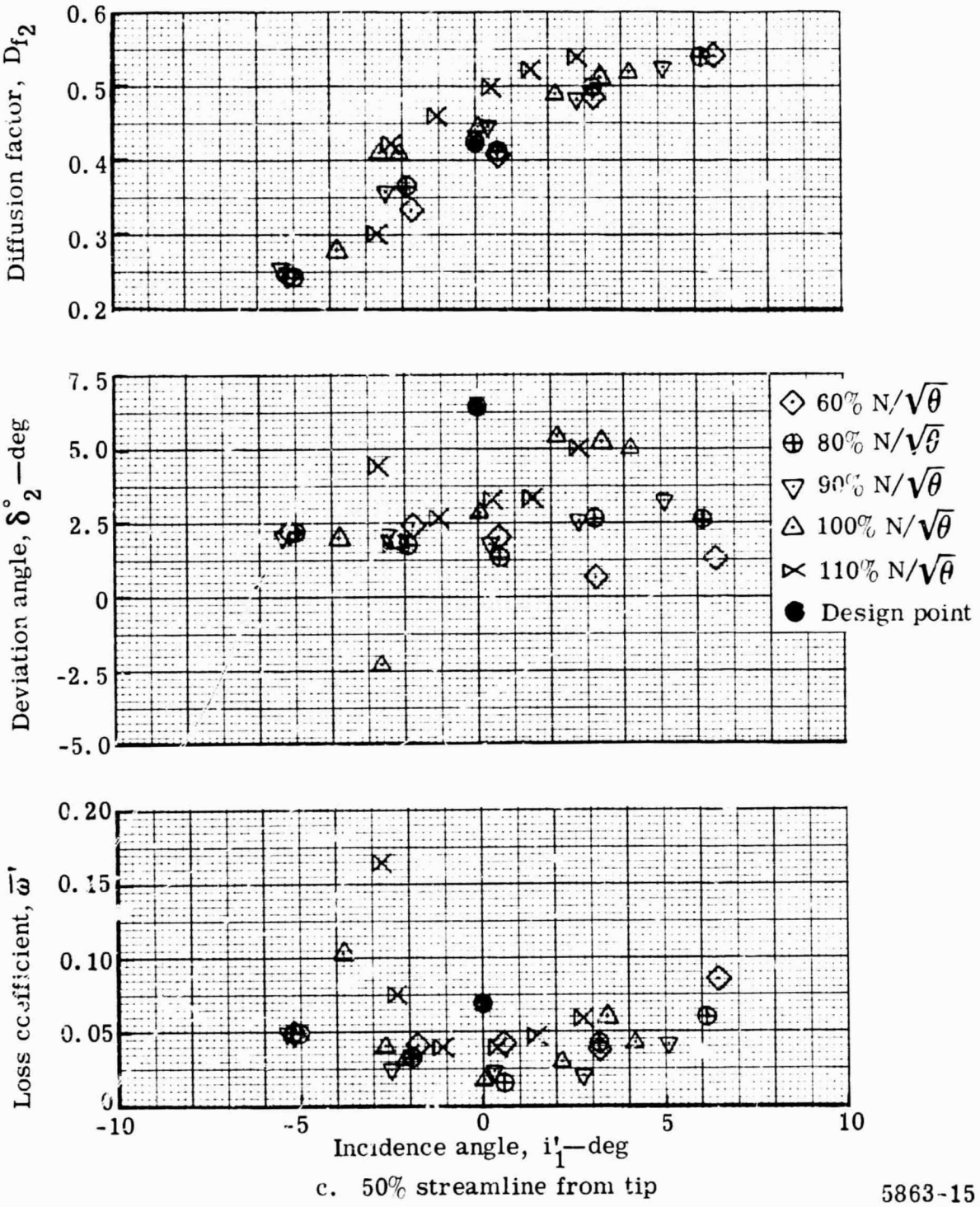

Figure 12. Rotor blade element performance at optimum wall bleed—stage test.

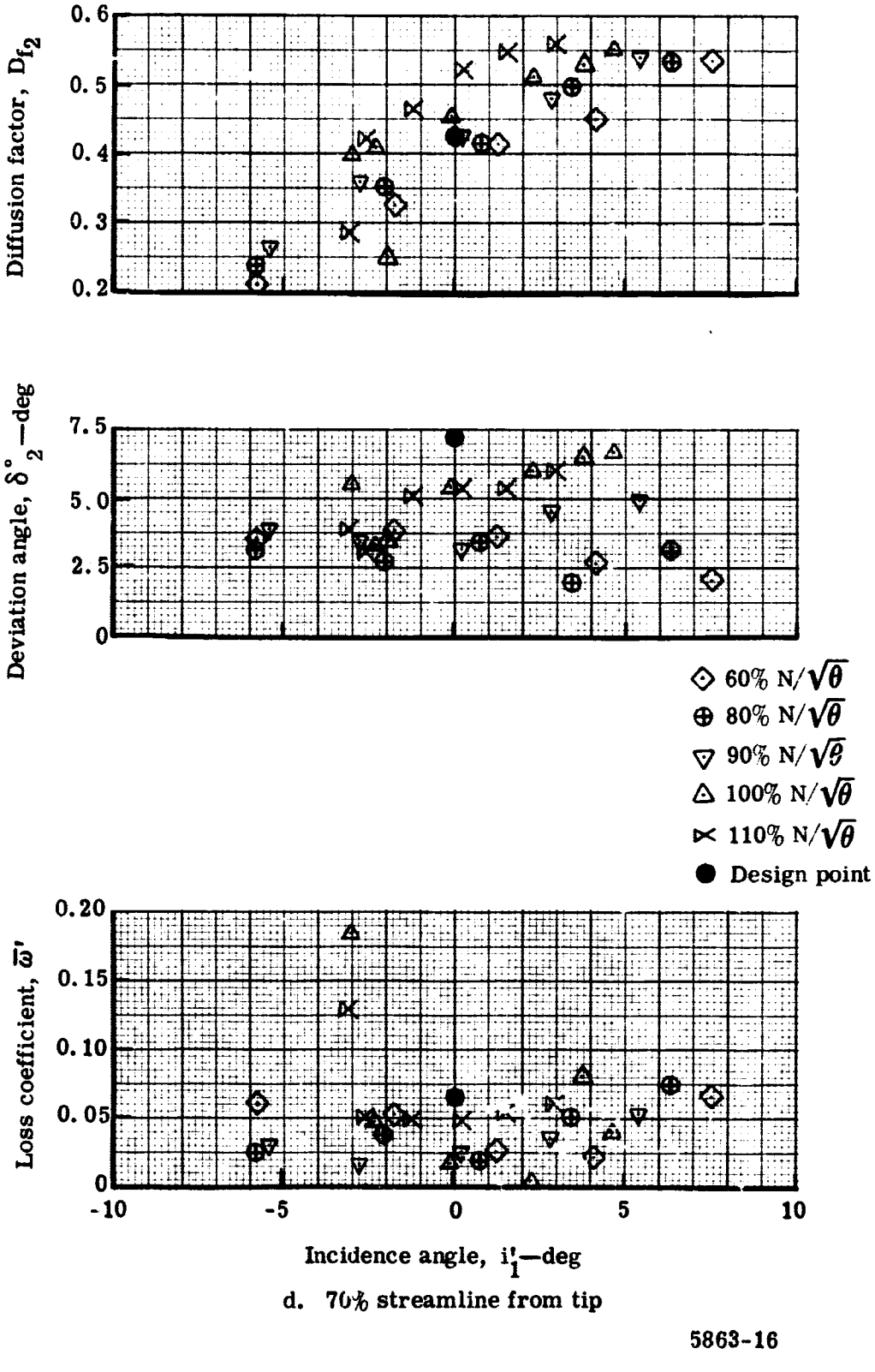

Figure 12. Rotor blade element performance at optimum wall bleed—stage test.

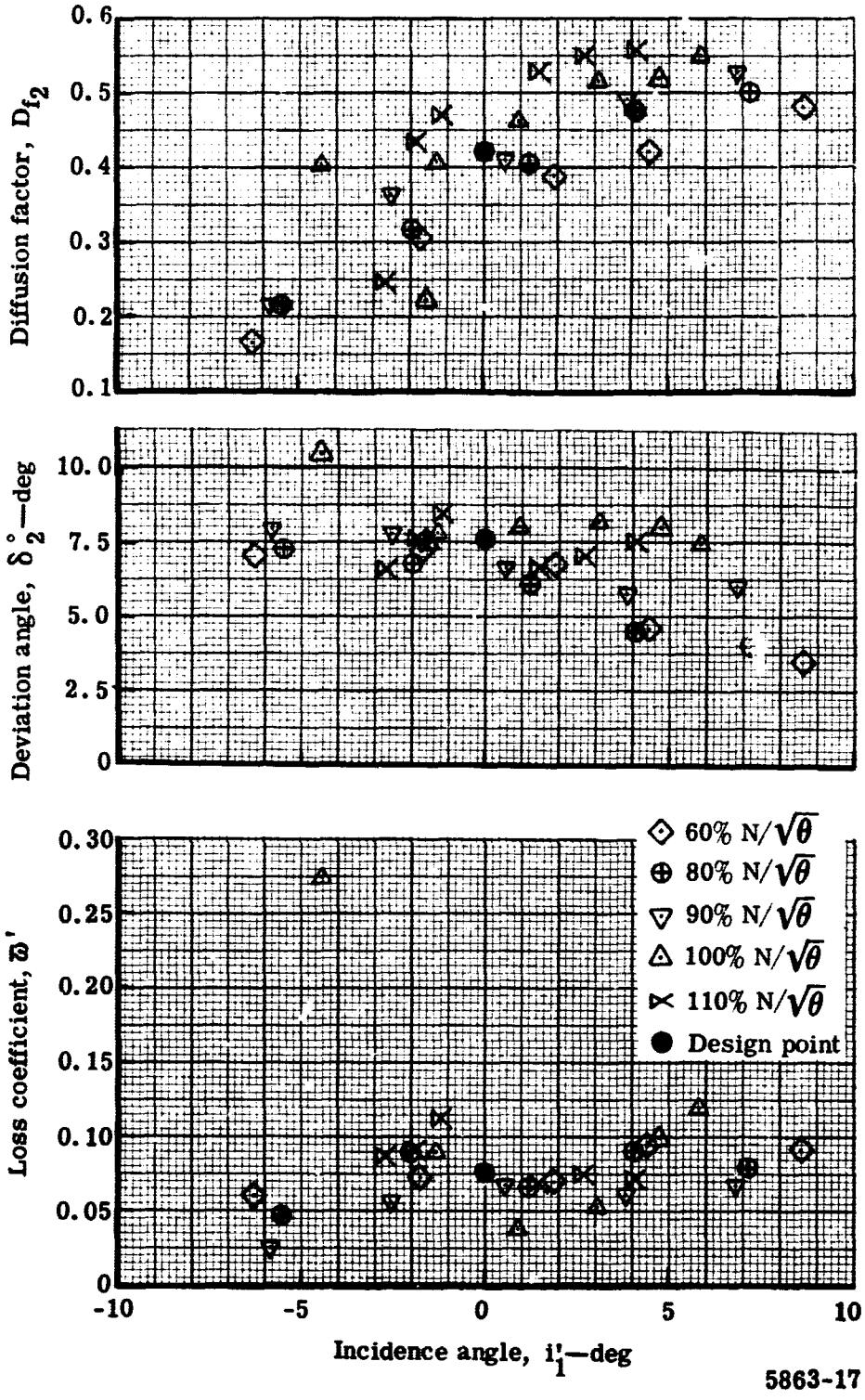

e. 90% streamline from tip

Figure 12. Rotor blade element performance at optimum wall bleed—stage test.

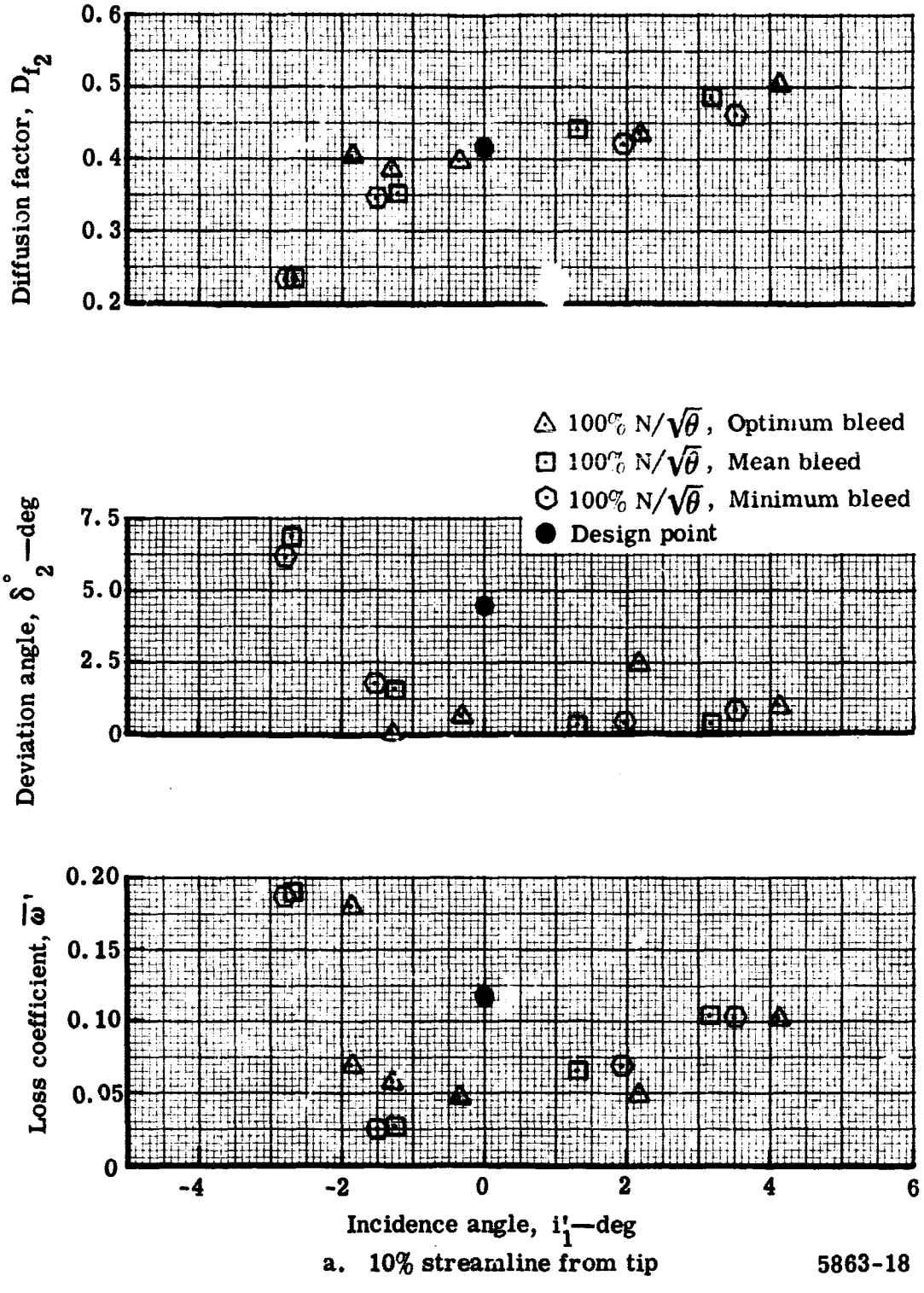

Figure 13. Rotor blade element performance for 100% design speed with varying wall bleed rates—stage test.

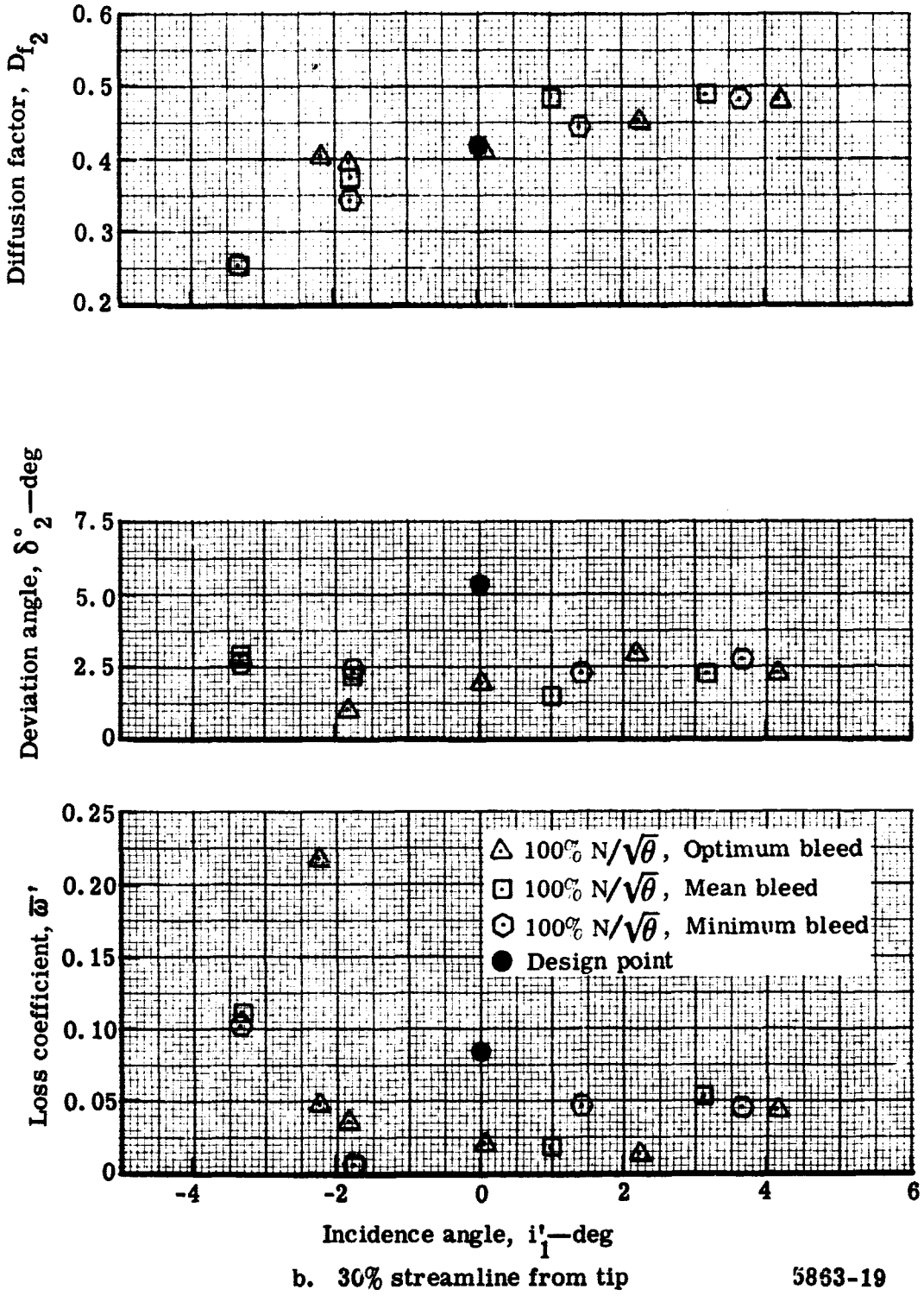

b. 30% streamline from tip

Figure 13. Rotor blade element performance for 100% design speed with varying wall bleed rates—stage test.

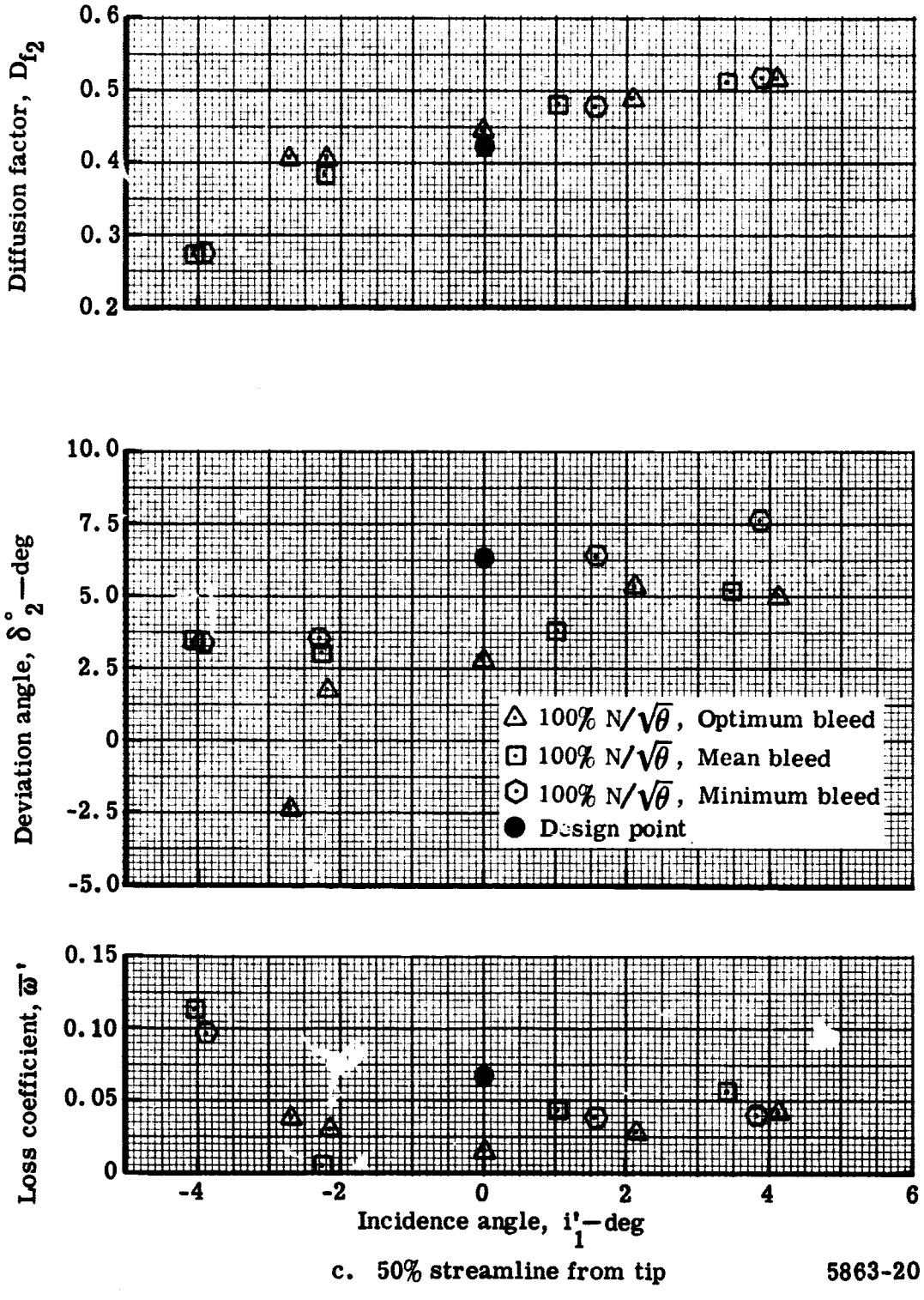

Figure 13. Rotor blade element performance for 100% design speed with varying wall bleed rates—stage test.

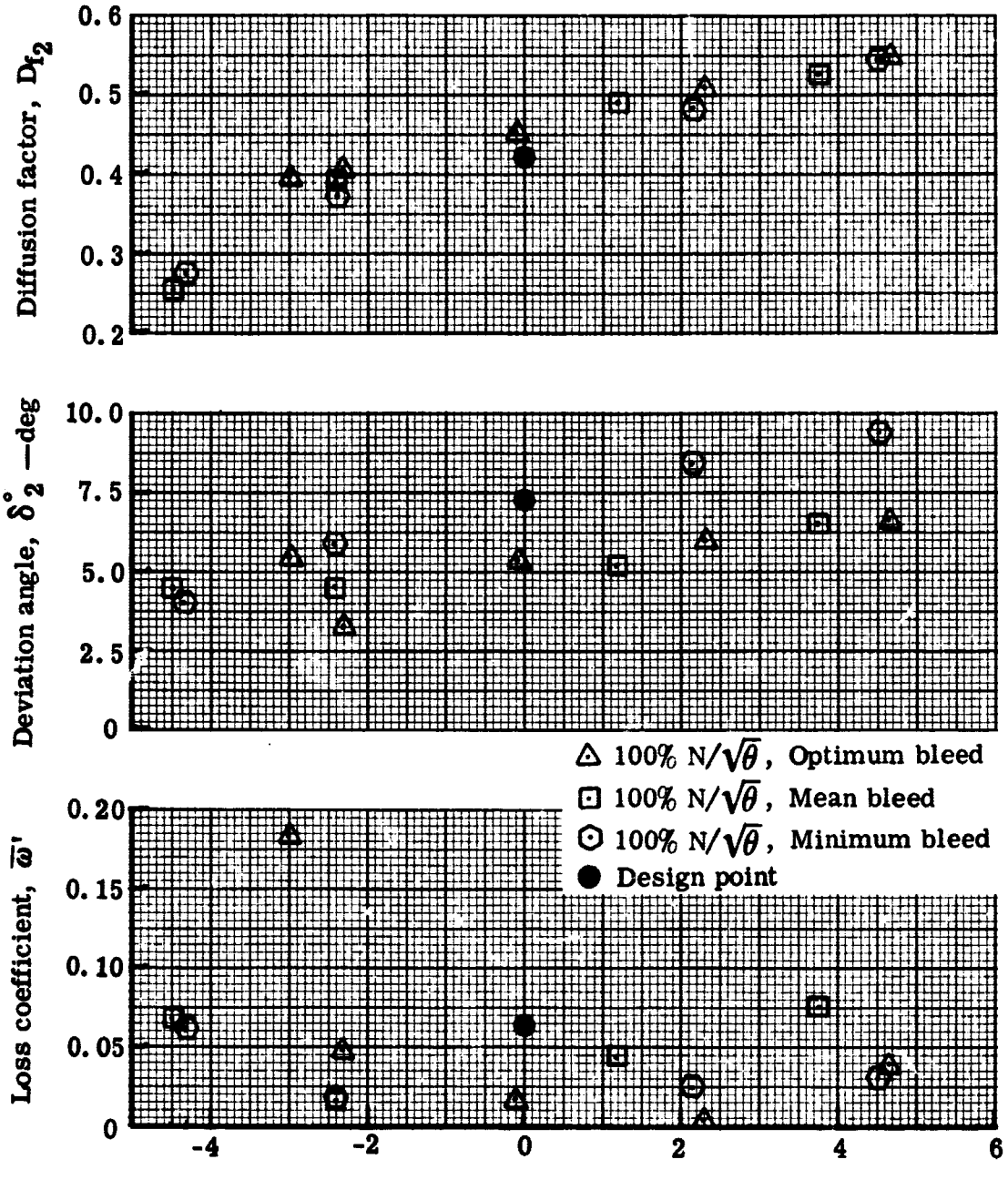

d. 70% streamline from tip

Figure 13. Rotor blade element performance for 100% design speed with varying wall bleed rates—stage test.

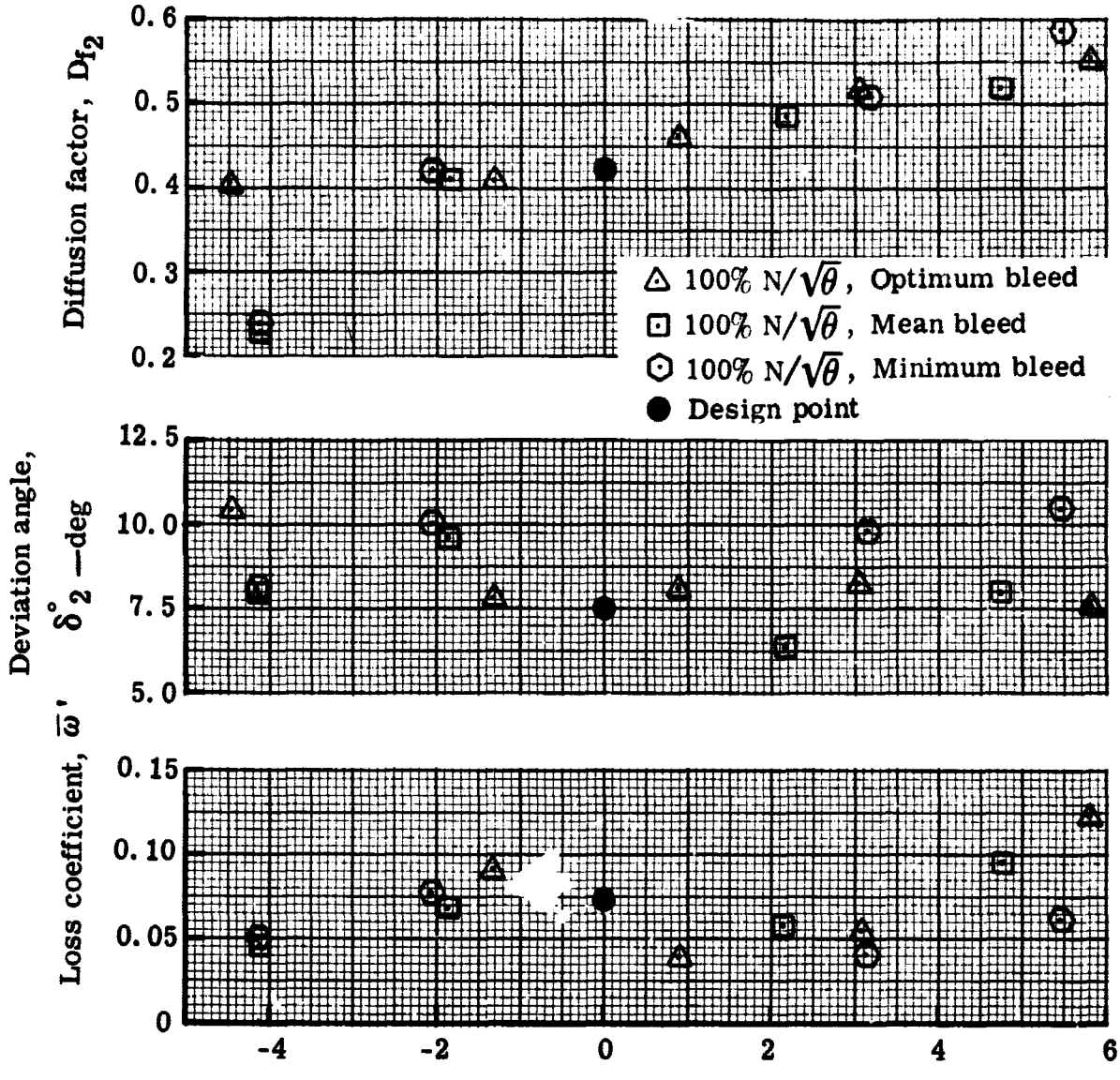

e. 90% streamline from tip

Figure 13. Rotor blade element performance for 100% design speed with varying wall bleed rates—stage test.

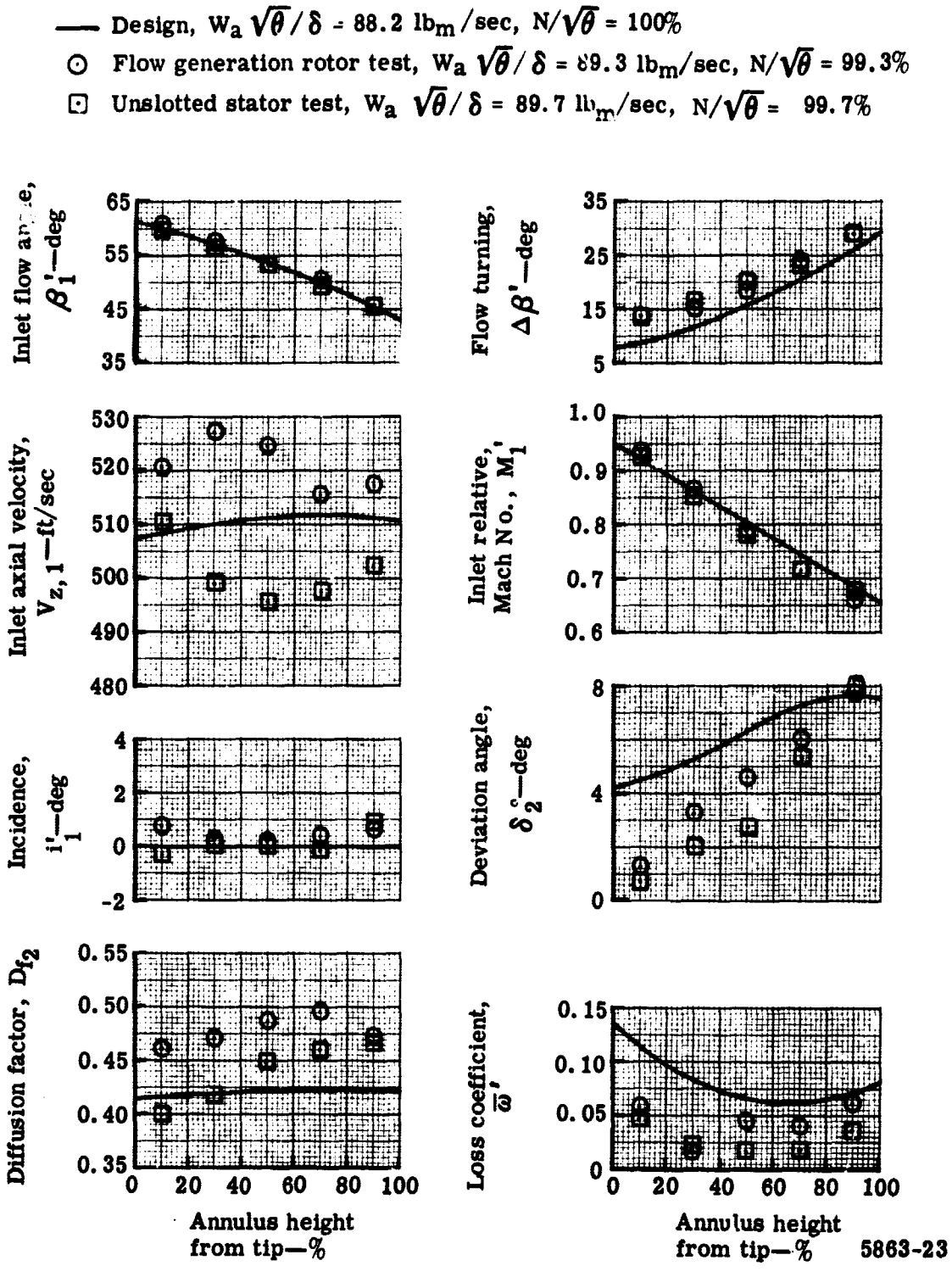

Figure 14. Radial variation of rotor blade element performance with optimum wall bleed.

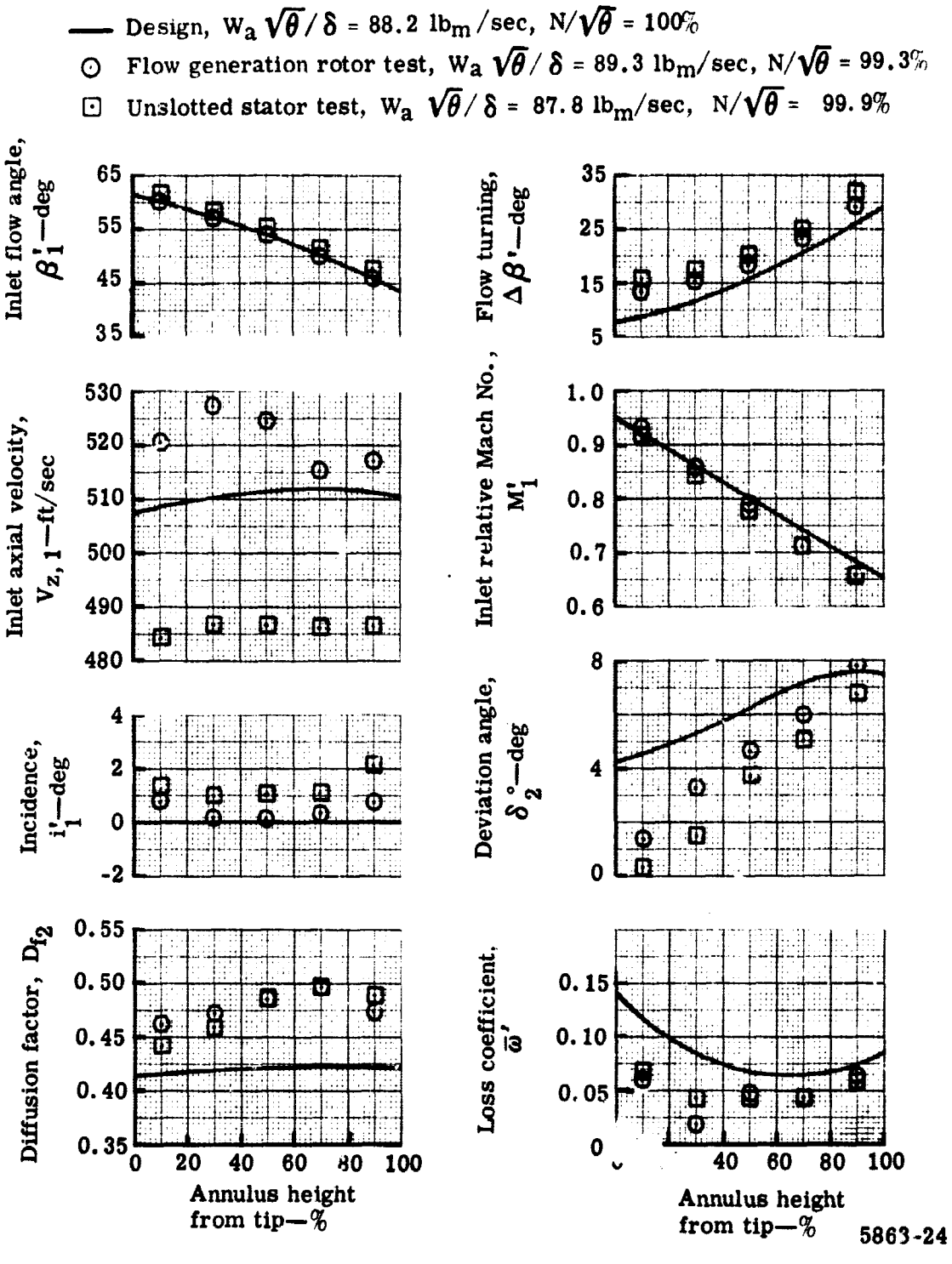

Figure 15. Radial variation of rotor blade element performance with mean wall bleed.

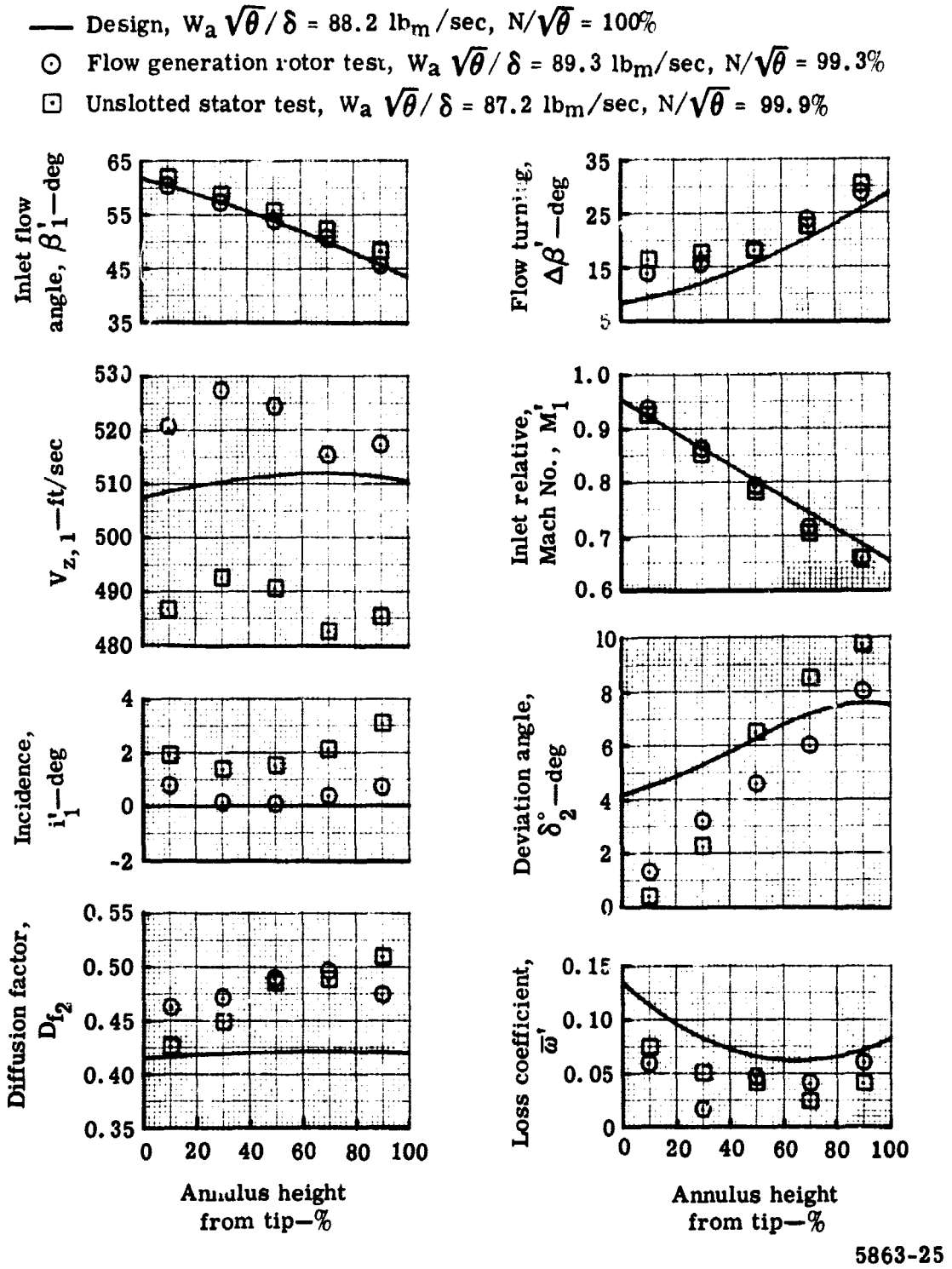

Figure 16. Radial variation of rotor blade element performance with minimum wall bleed.

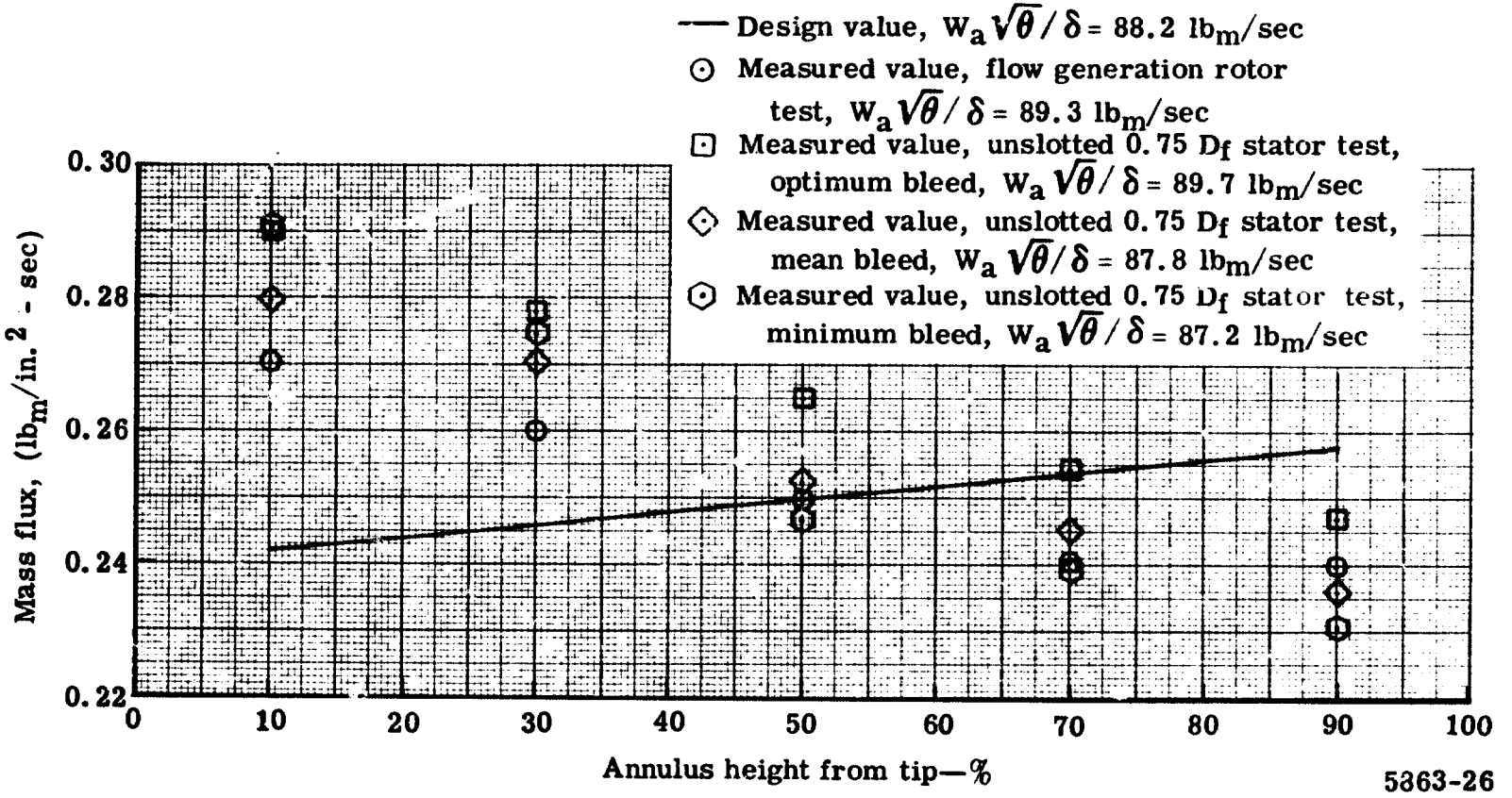

Figure 17. Rotor out radial mass flux distribution at design speed with varying wall bleed rates.

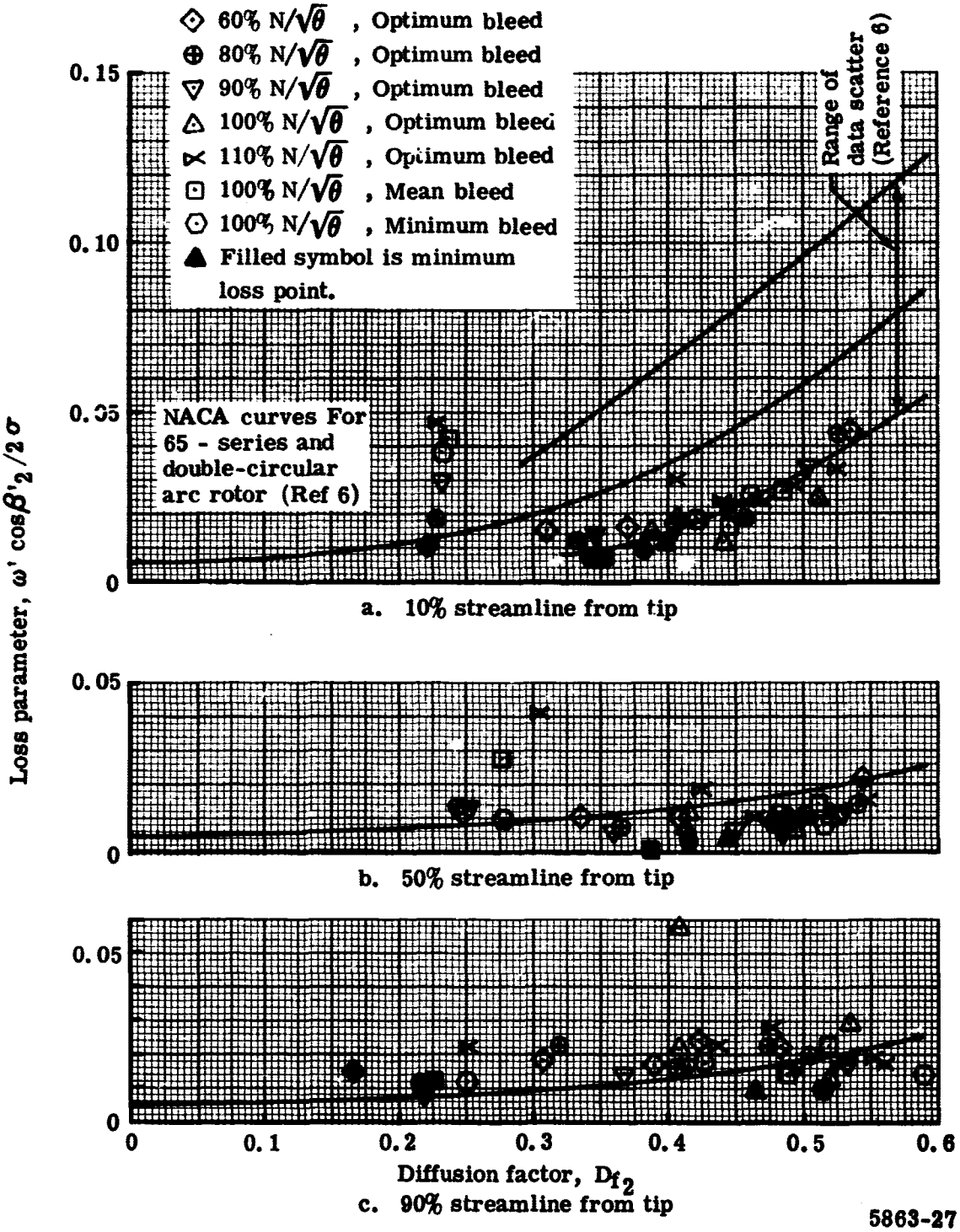

Figure 18. Rotor loss parameter versus diffusion factor.

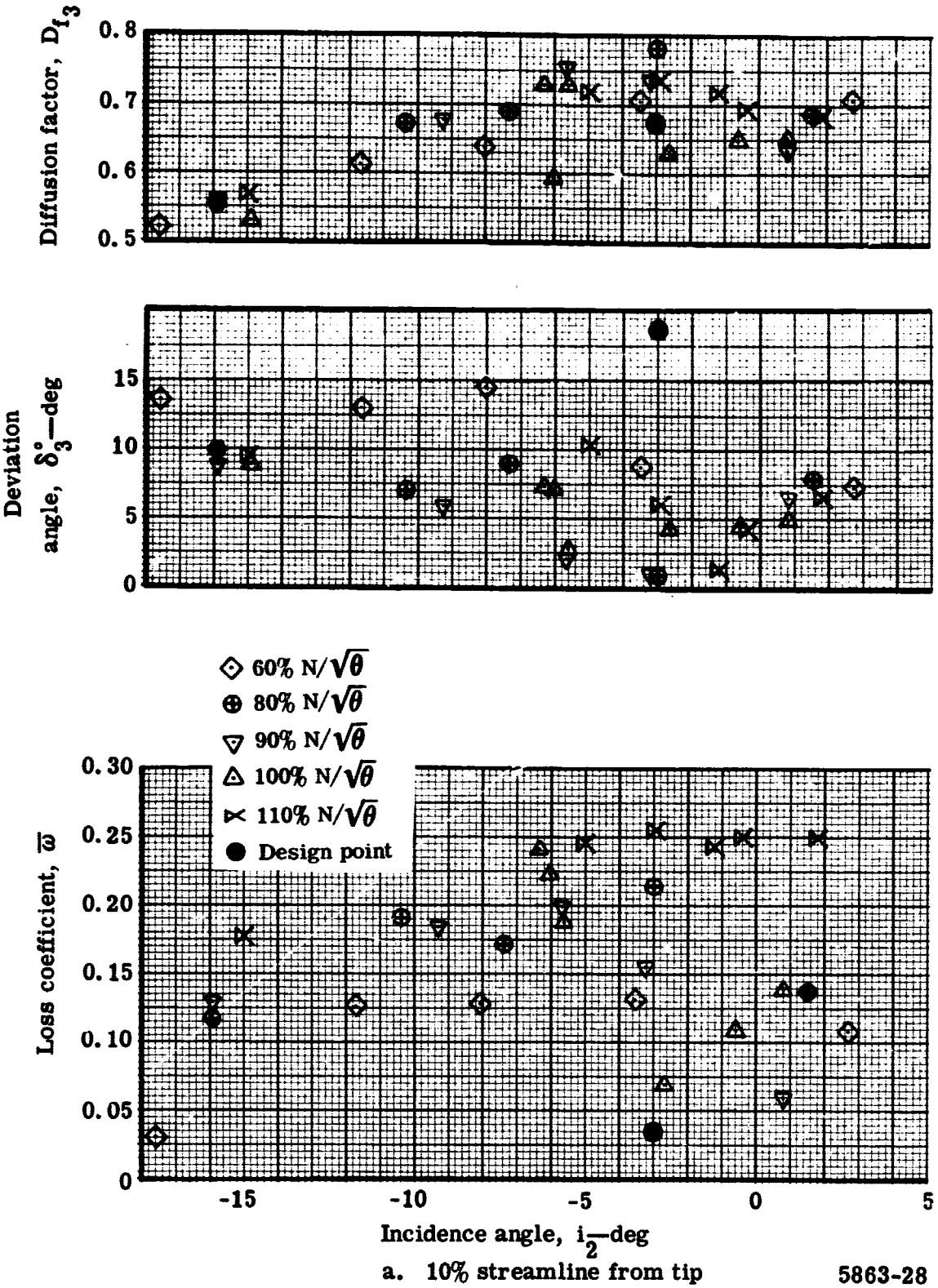

Figure 19. Stator blade element performance with optimum wall bleed.

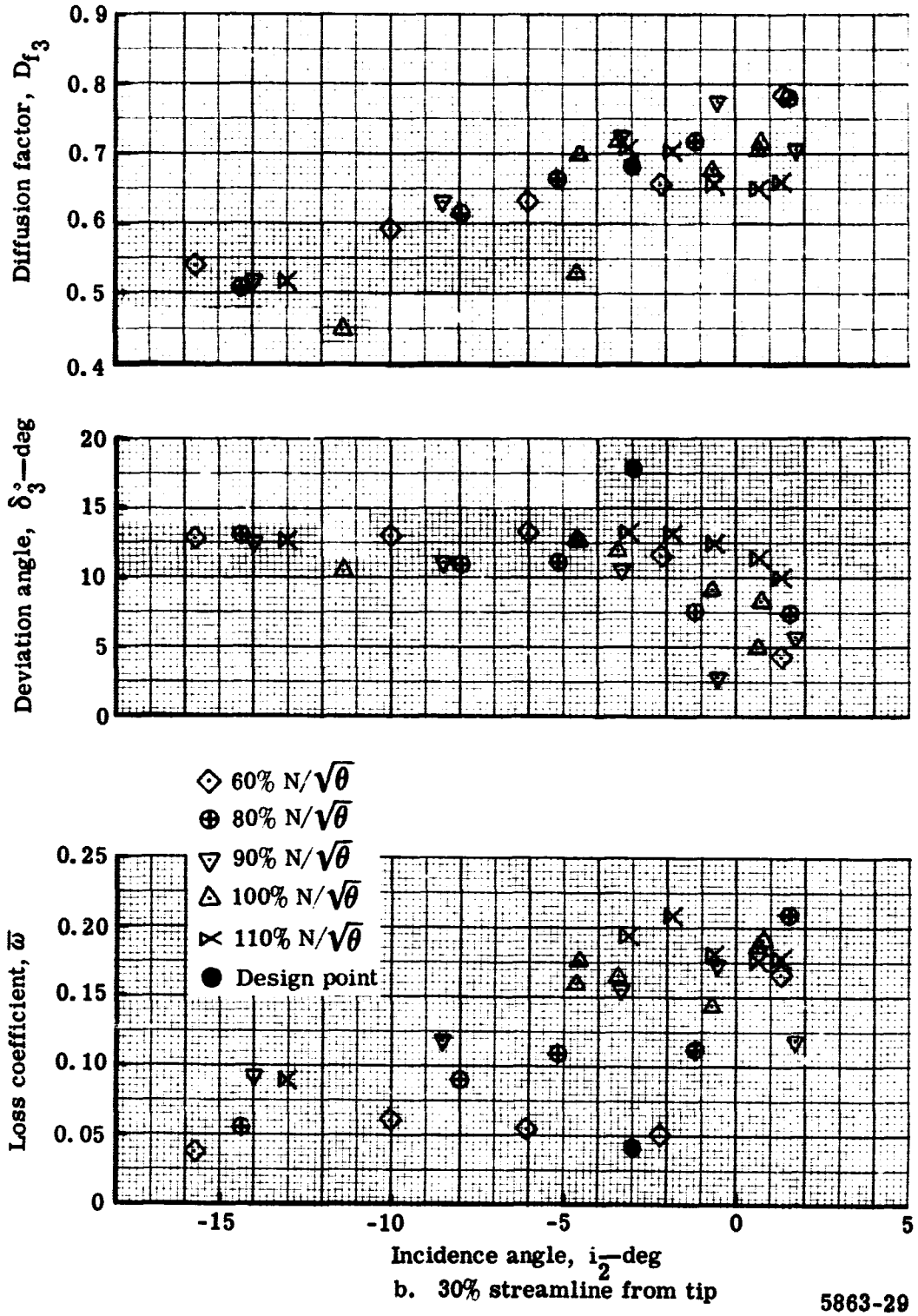

Figure 19. Stator blade element performance with optimum wall bleed.

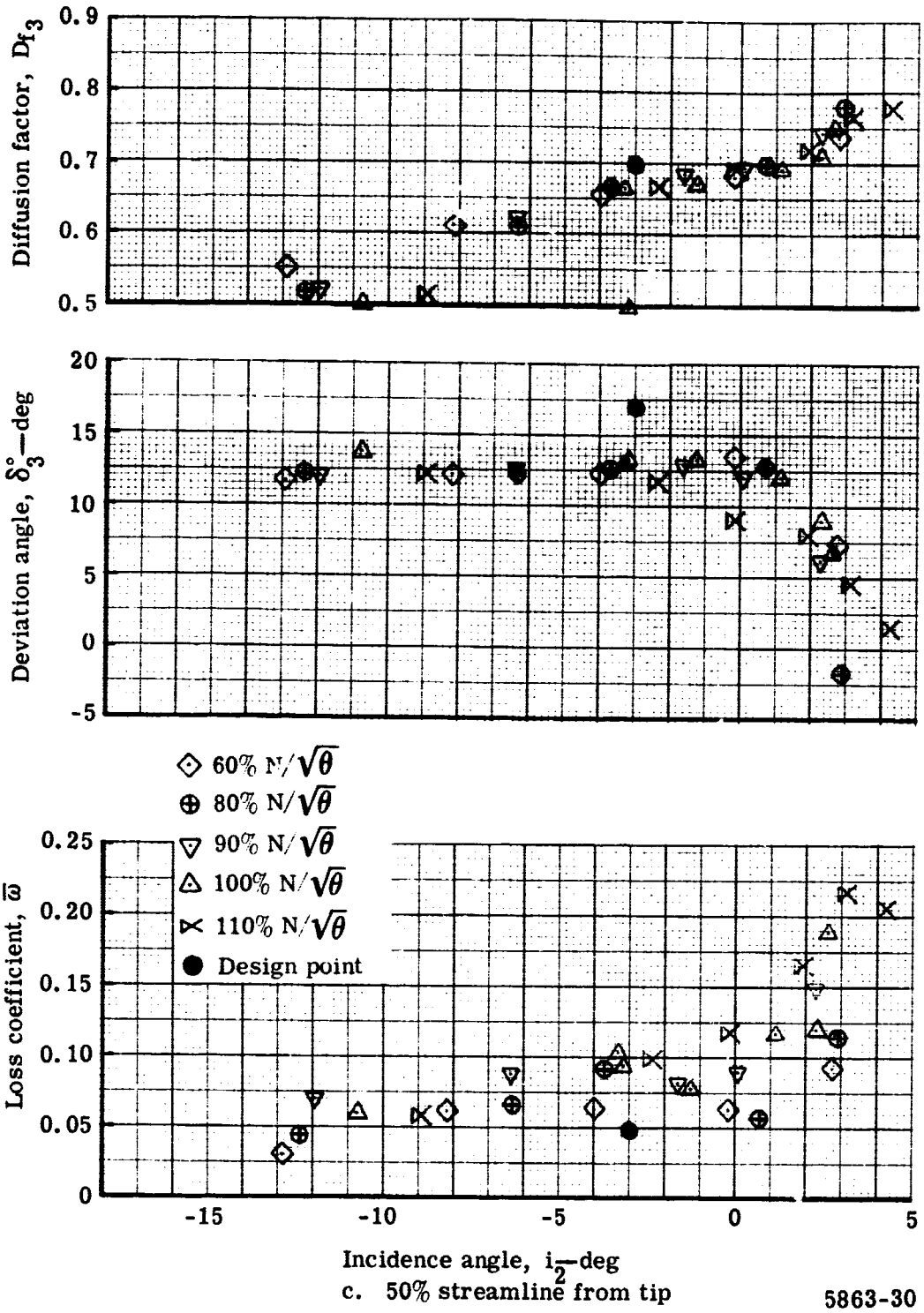

Figure 19. Stator blade element performance with optimum wall bleed.

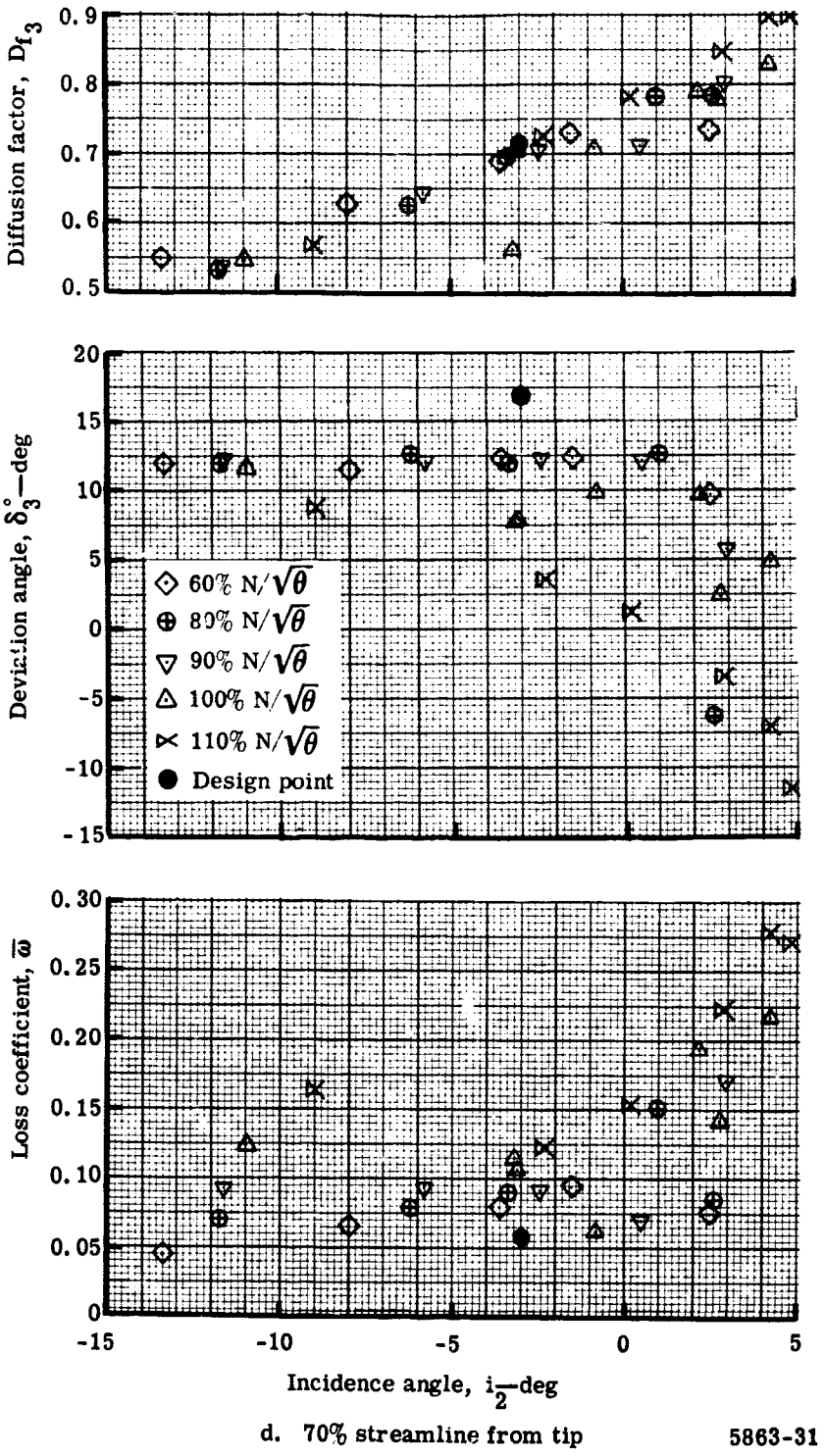

Figure 19. Stator blade element performance with optimum wall bleed.

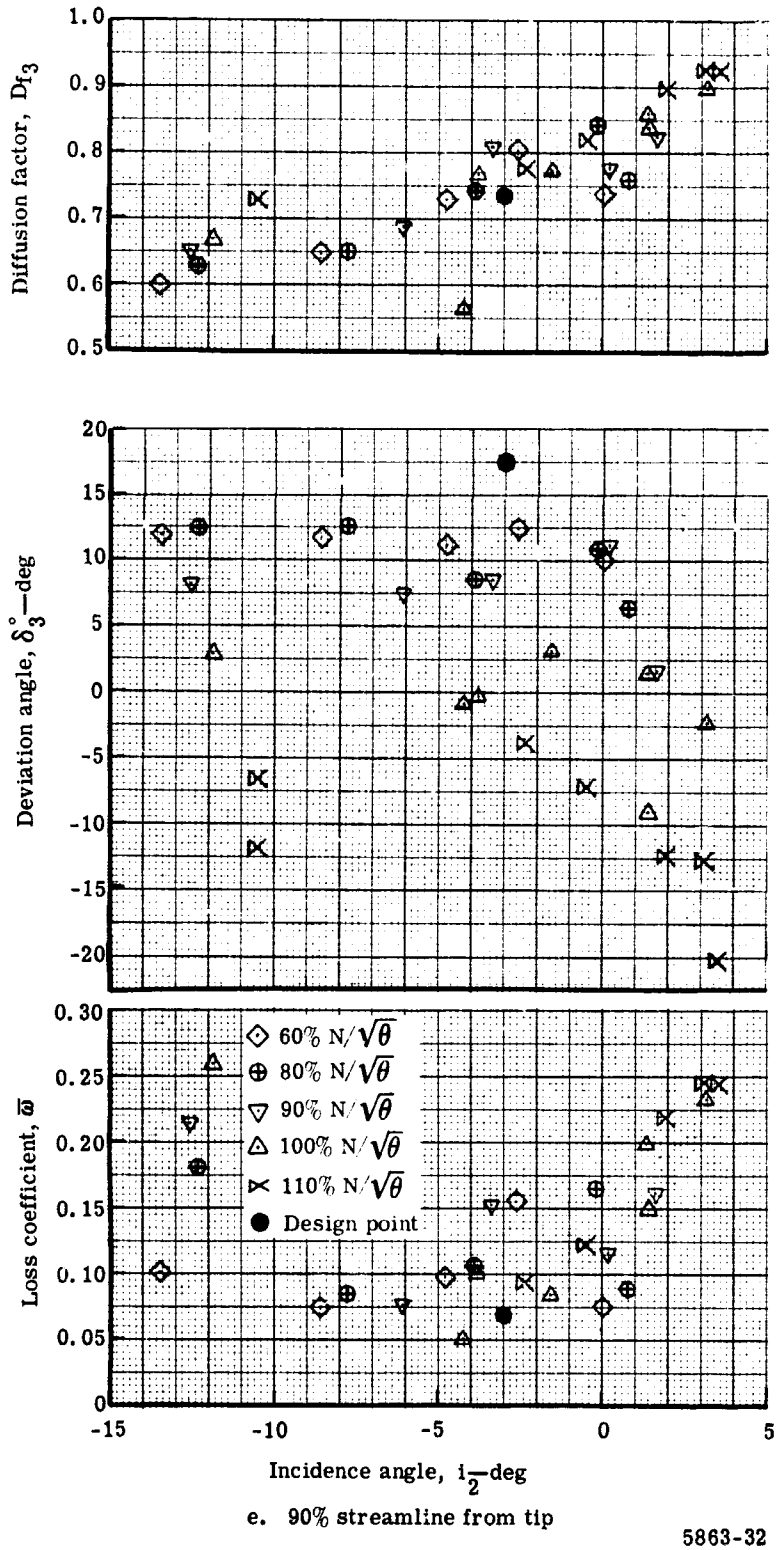

e. 90% streamline from tip

5863-32

Figure 19. Stator blade element performance with optimum wall bleed.

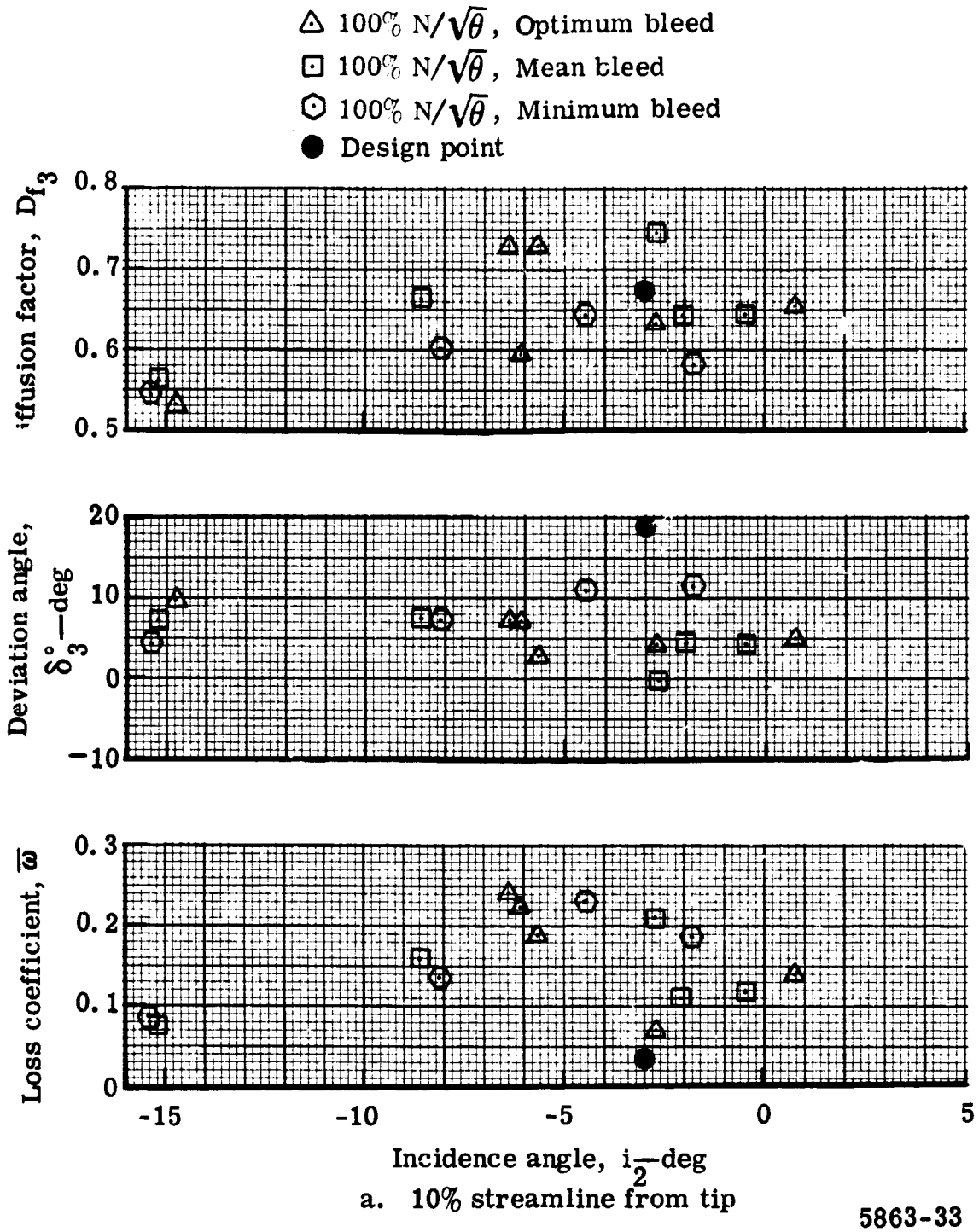

Figure 20. Stator blade element performance for 100% design speed with varying wall bleed rates.

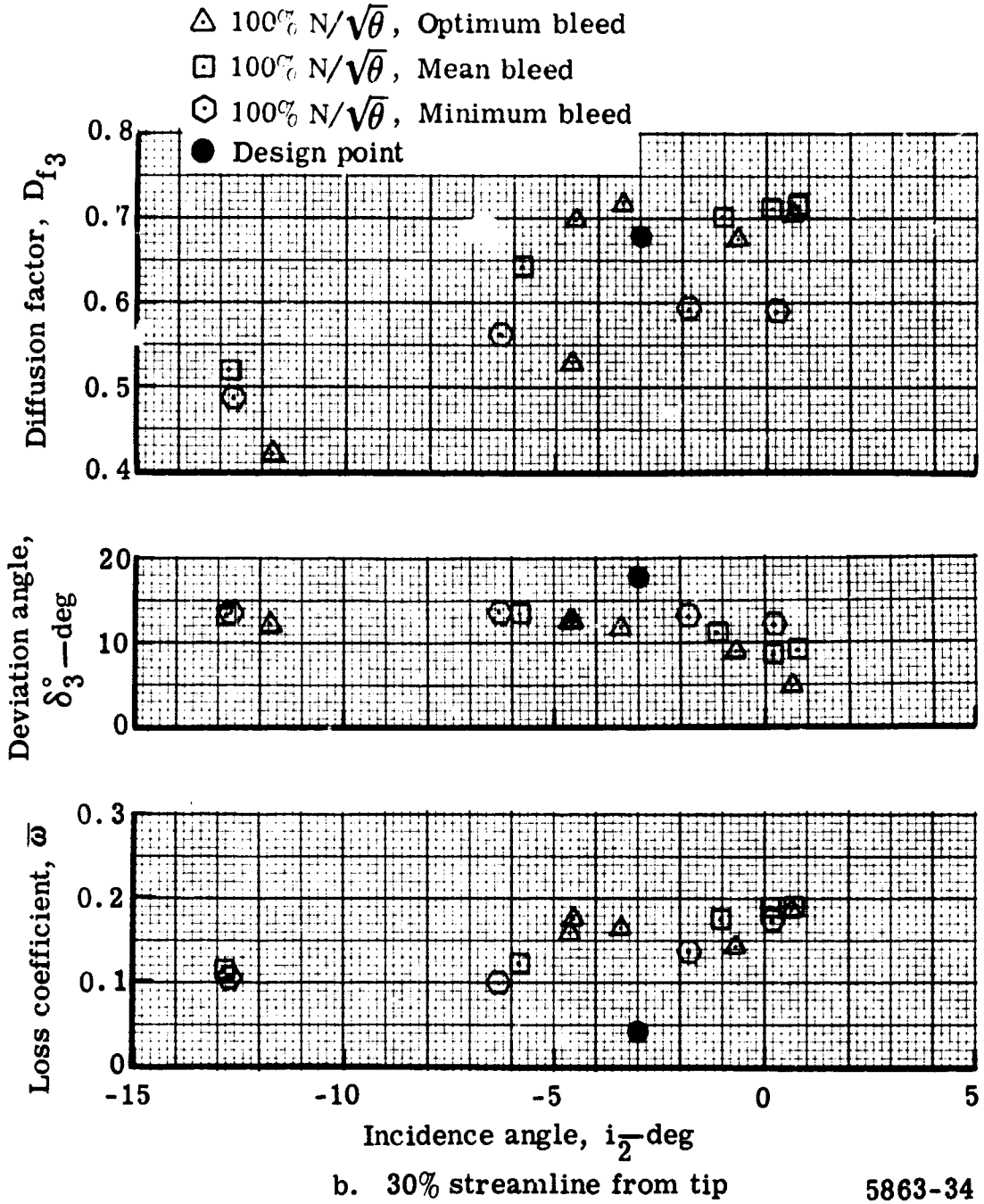

Figure 20. Stator blade element performance for 100% design speed with varying wall bleed rates.

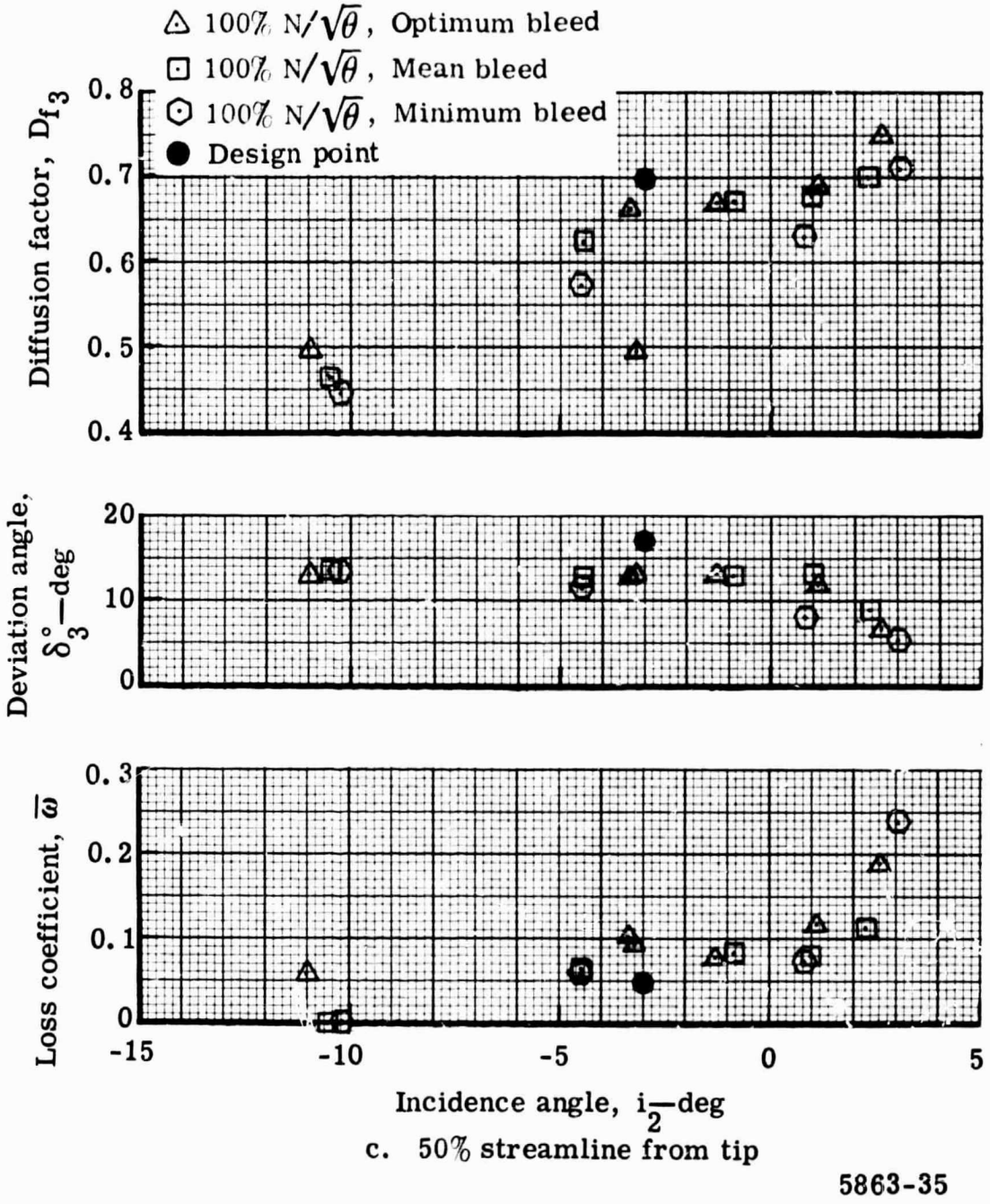

Figure 20. Stator blade element performance for 100% design speed with varying wall bleed rates.

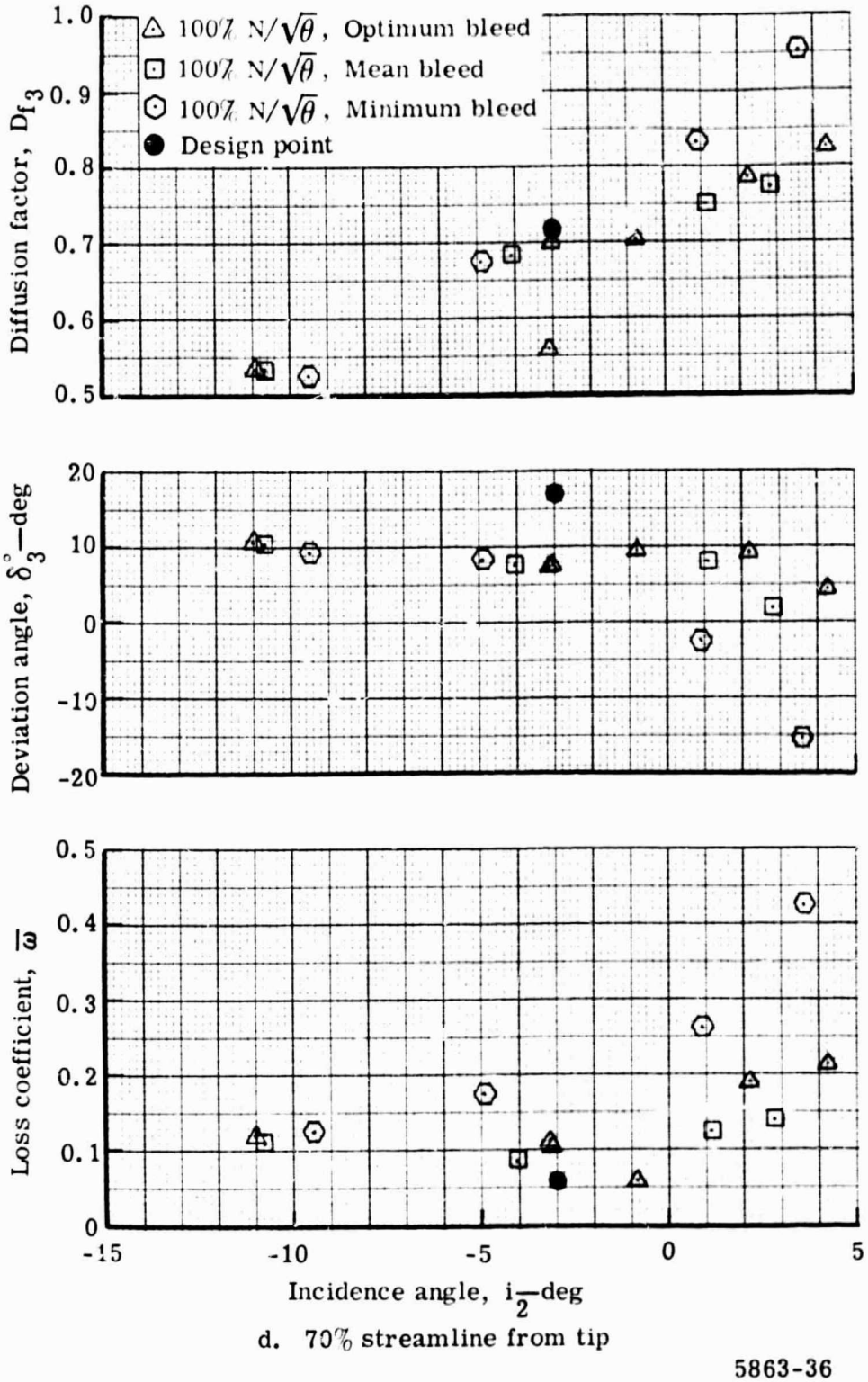

d. 70% streamline from tip

5863-36

Figure 20. Stator blade element performance for 100% design speed with varying wall bleed rates.

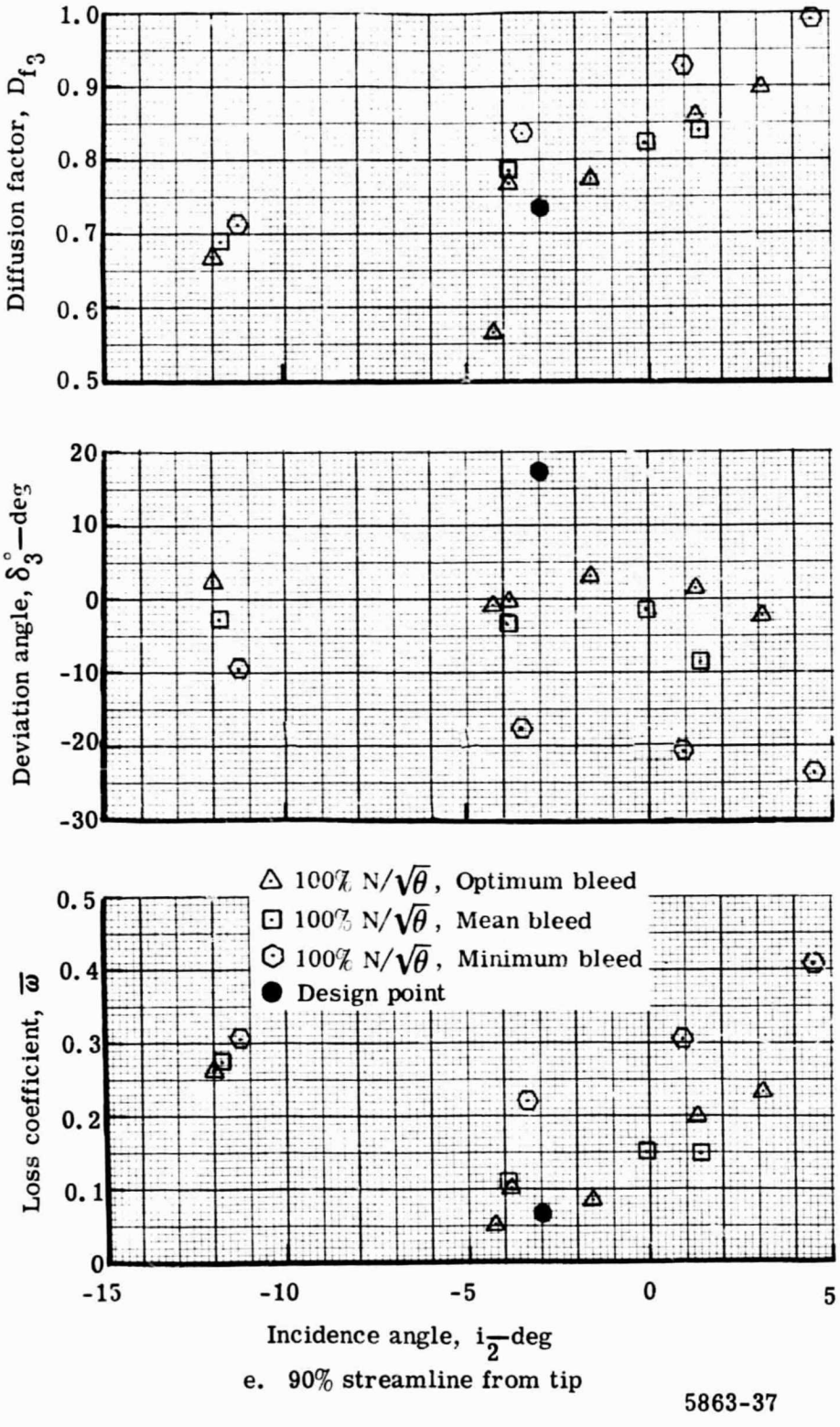

Figure 20. Stator blade element performance for 100% design speed with varying wall bleed rates.

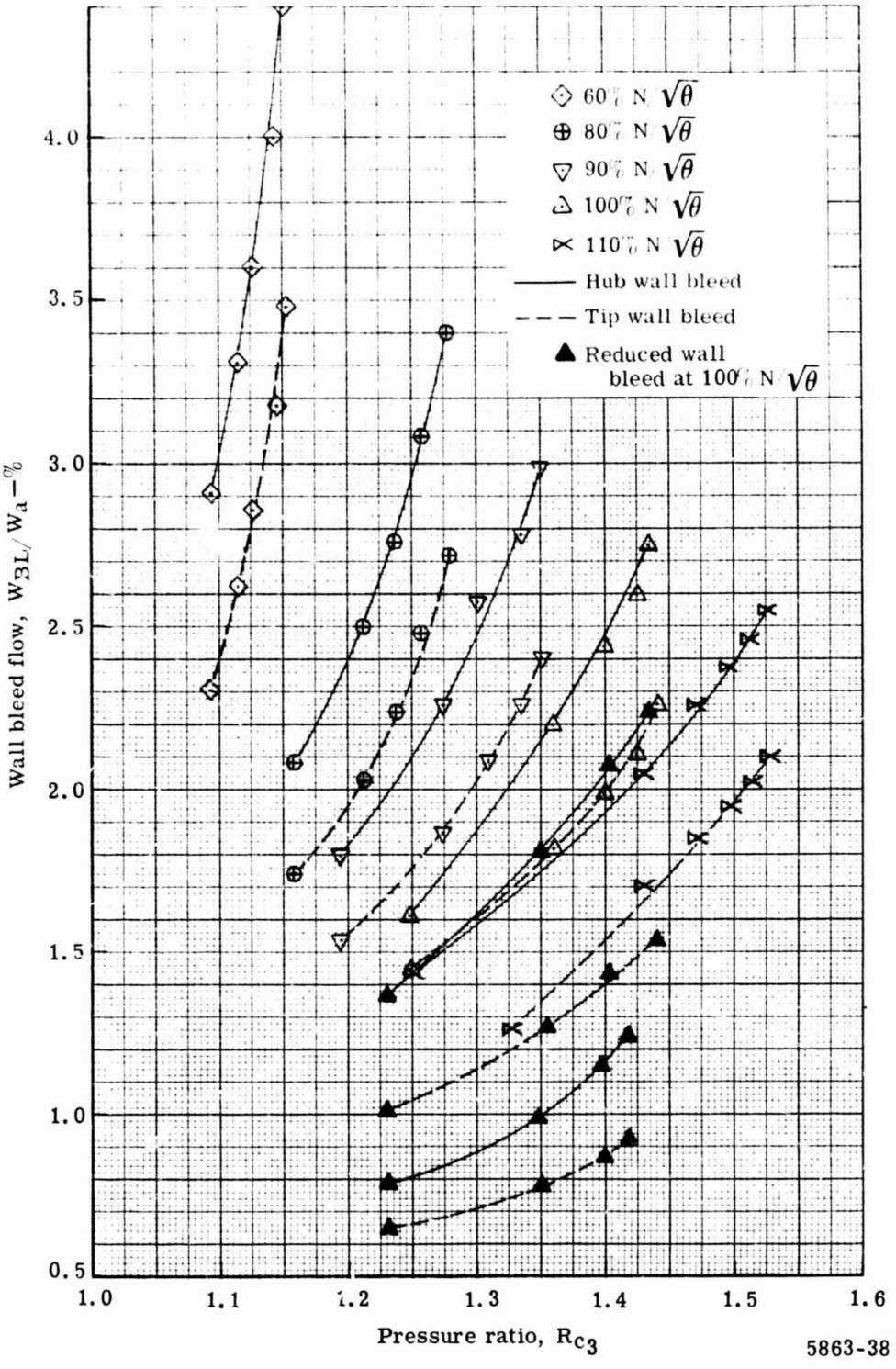

Figure 21. Variation of wall bleed flows with stage pressure ratio.

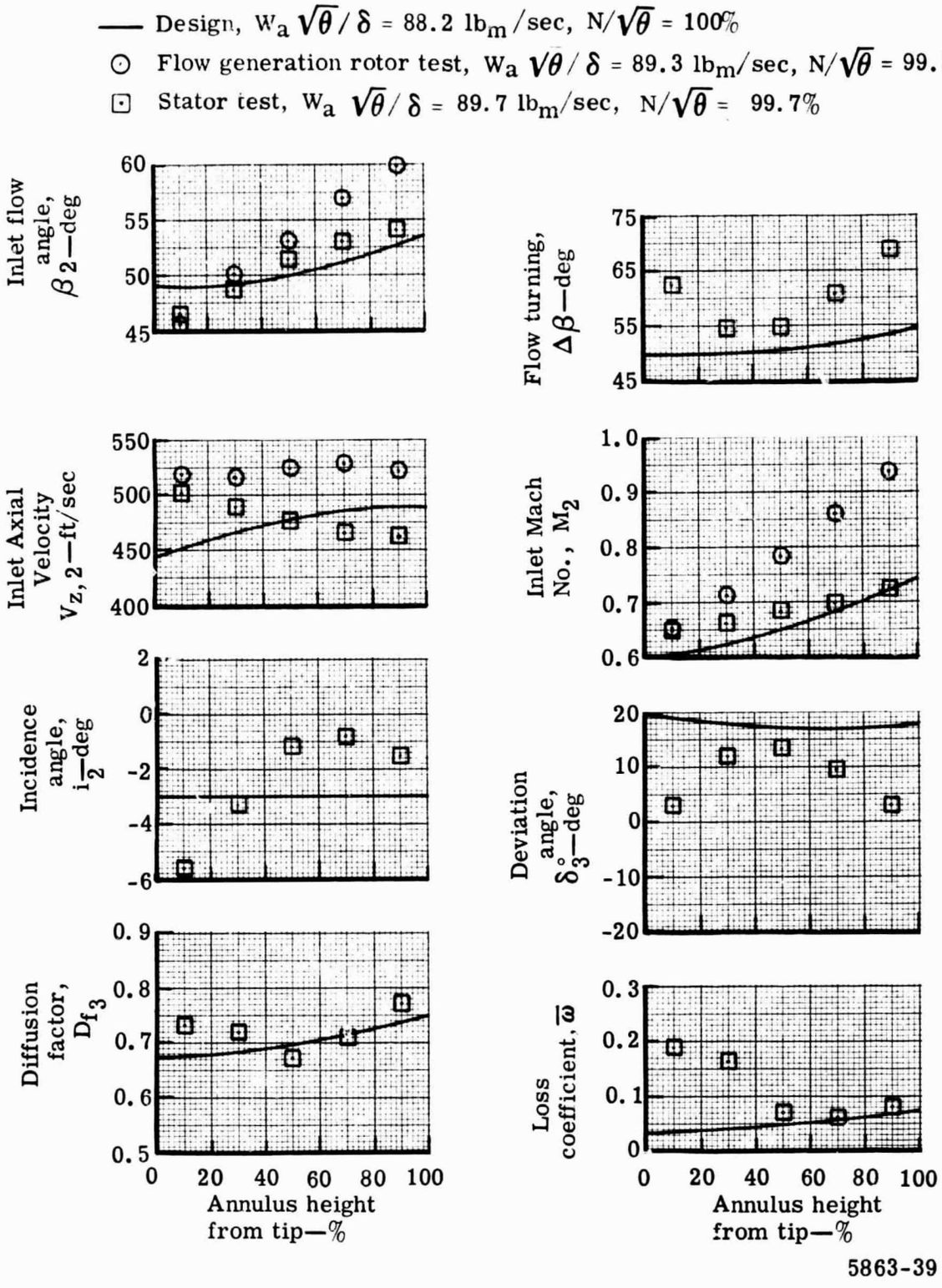

Figure 22. Radial variation of 0.75 D_f stator blade element performance with optimum wall bleed.

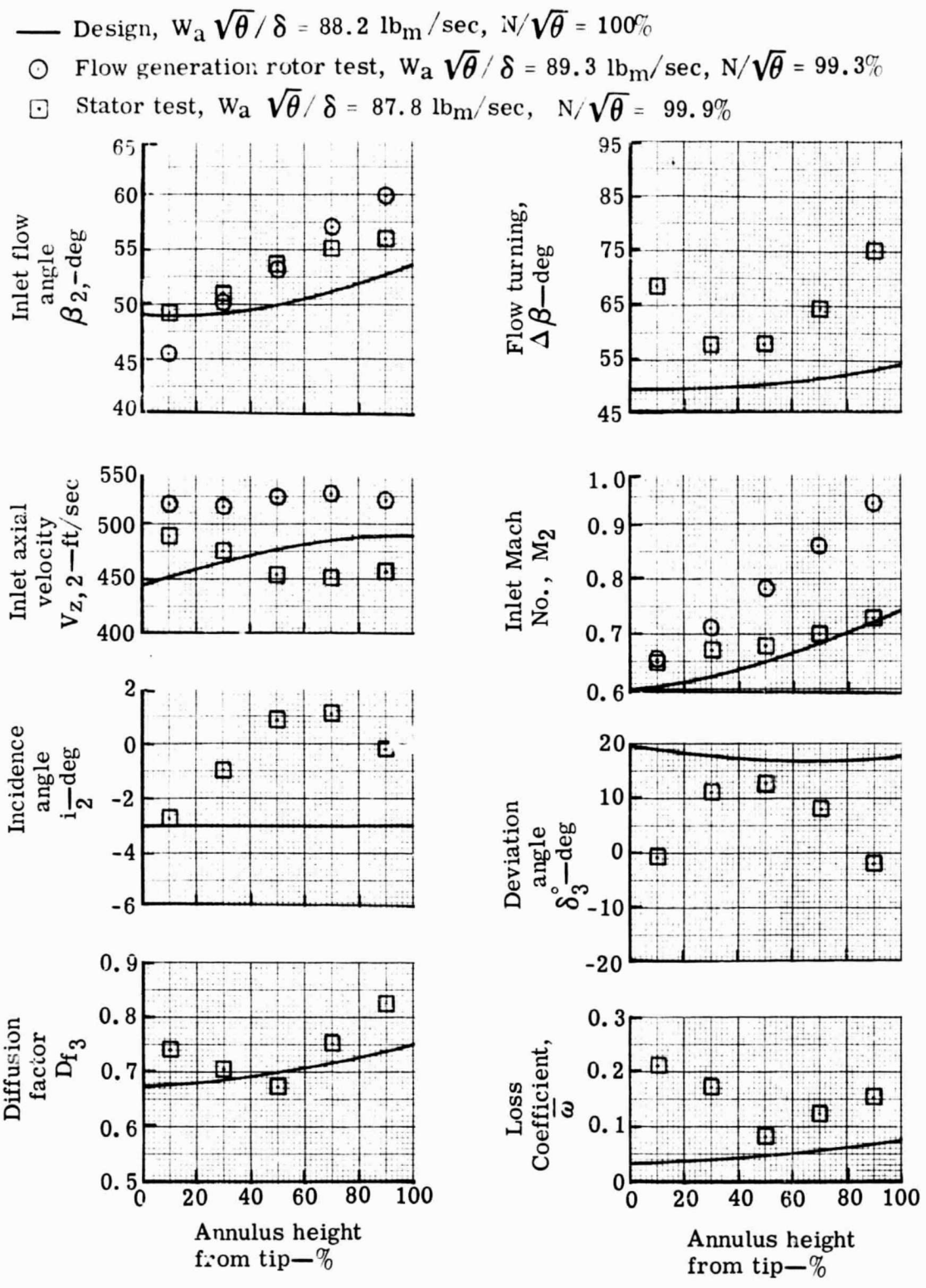

Figure 23. Radial variation of 0.75 D_f stator blade element performance with mean wall bleed.

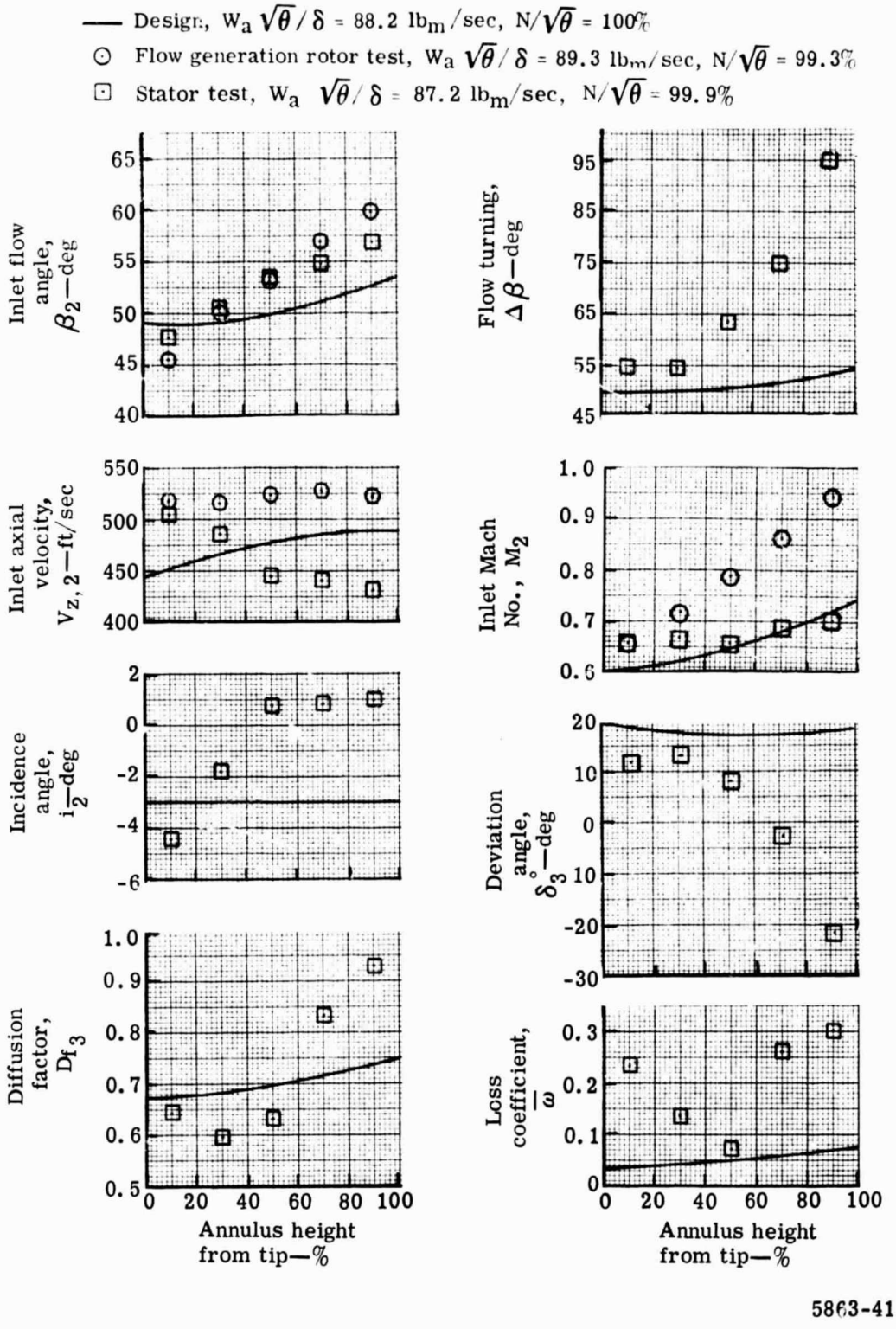

Figure 24. Radial variation of 0.75 D_f stator blade element performance with minimum wall bleed.

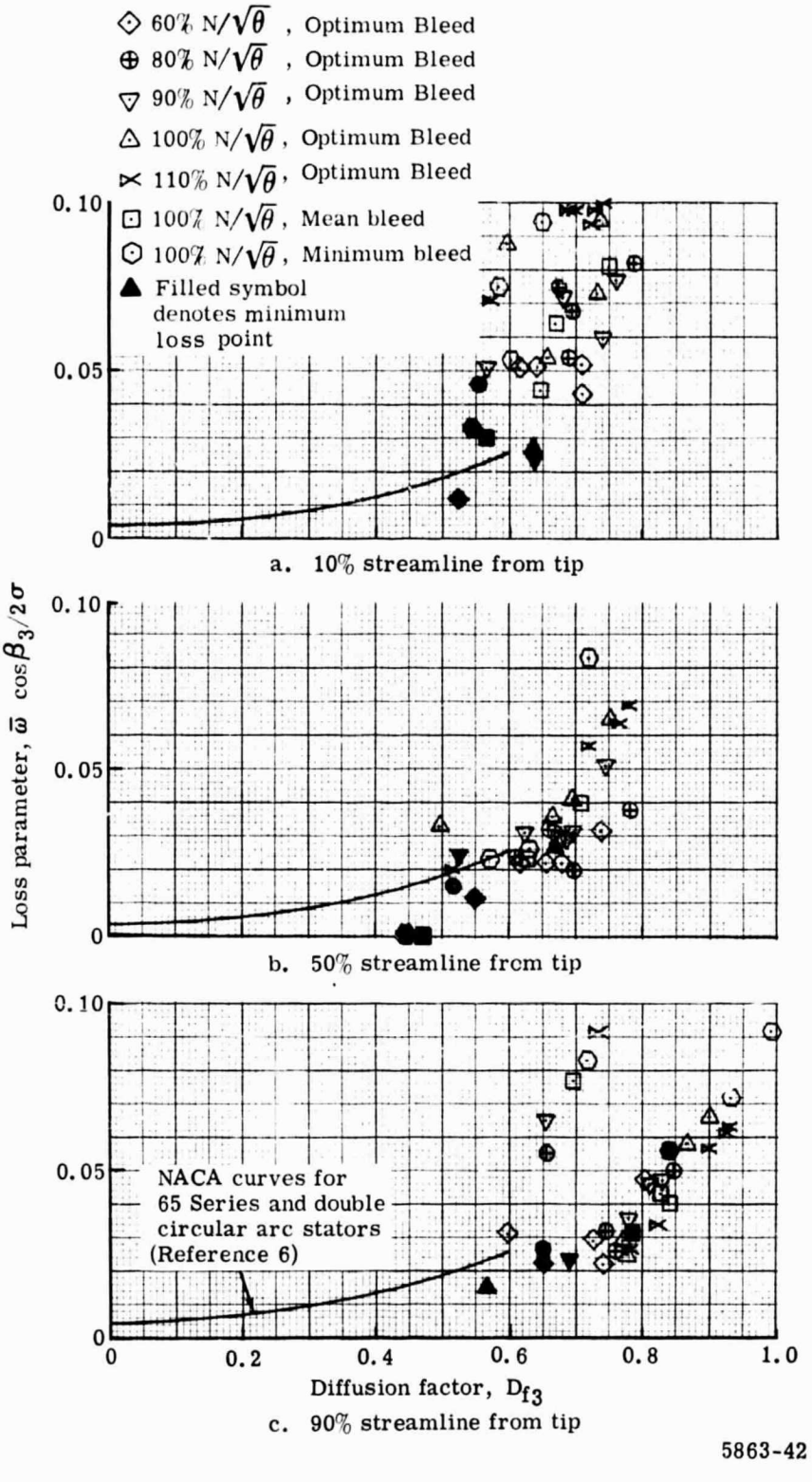

Figure 25. Stator loss parameter versus diffusion factor.

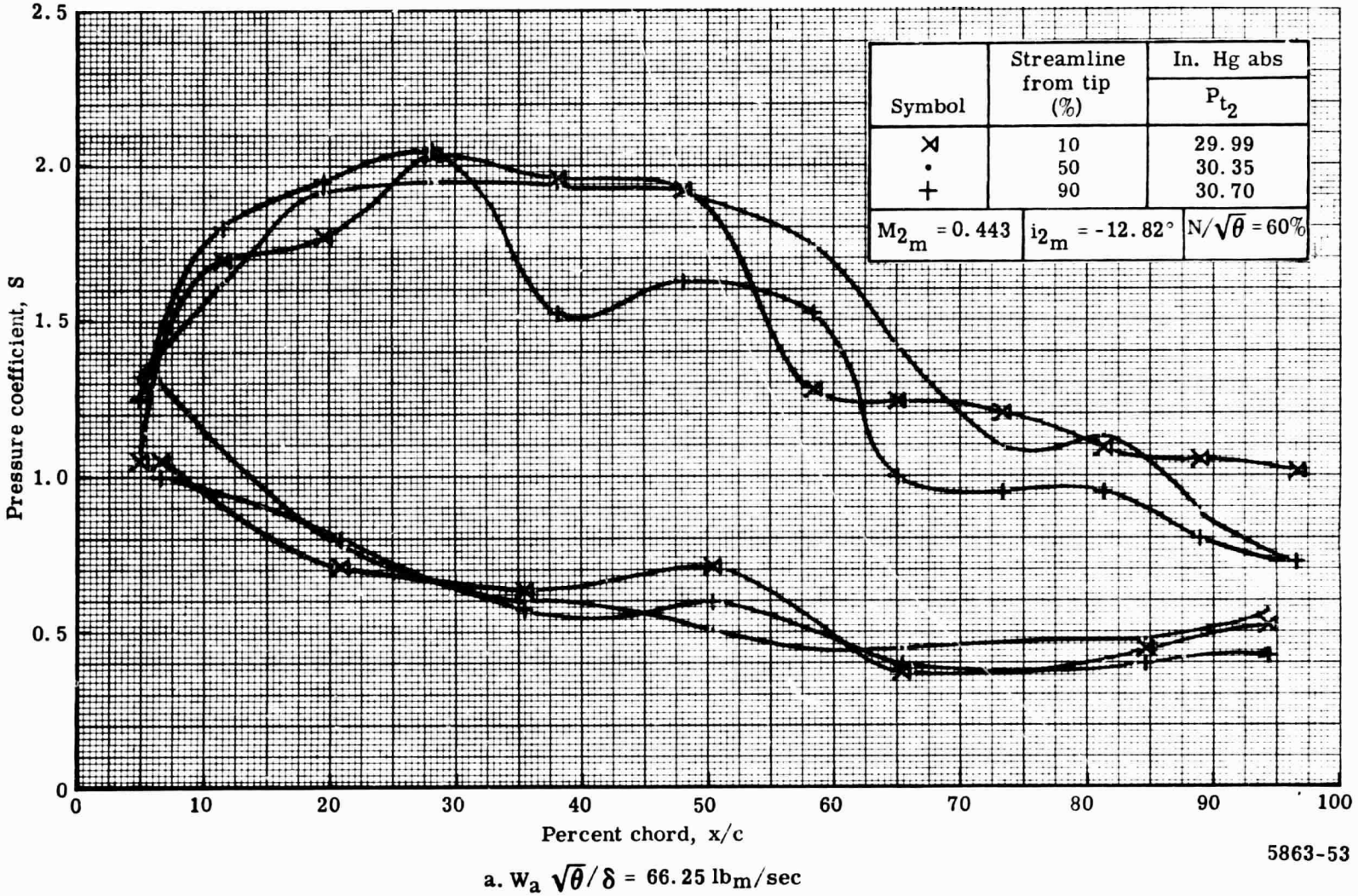

a. $W_a \sqrt{\theta}/\delta$ = 66.25 lb_m/sec

Figure 26. Stator static pressure distribution at 60% speed with optimum wall bleed.

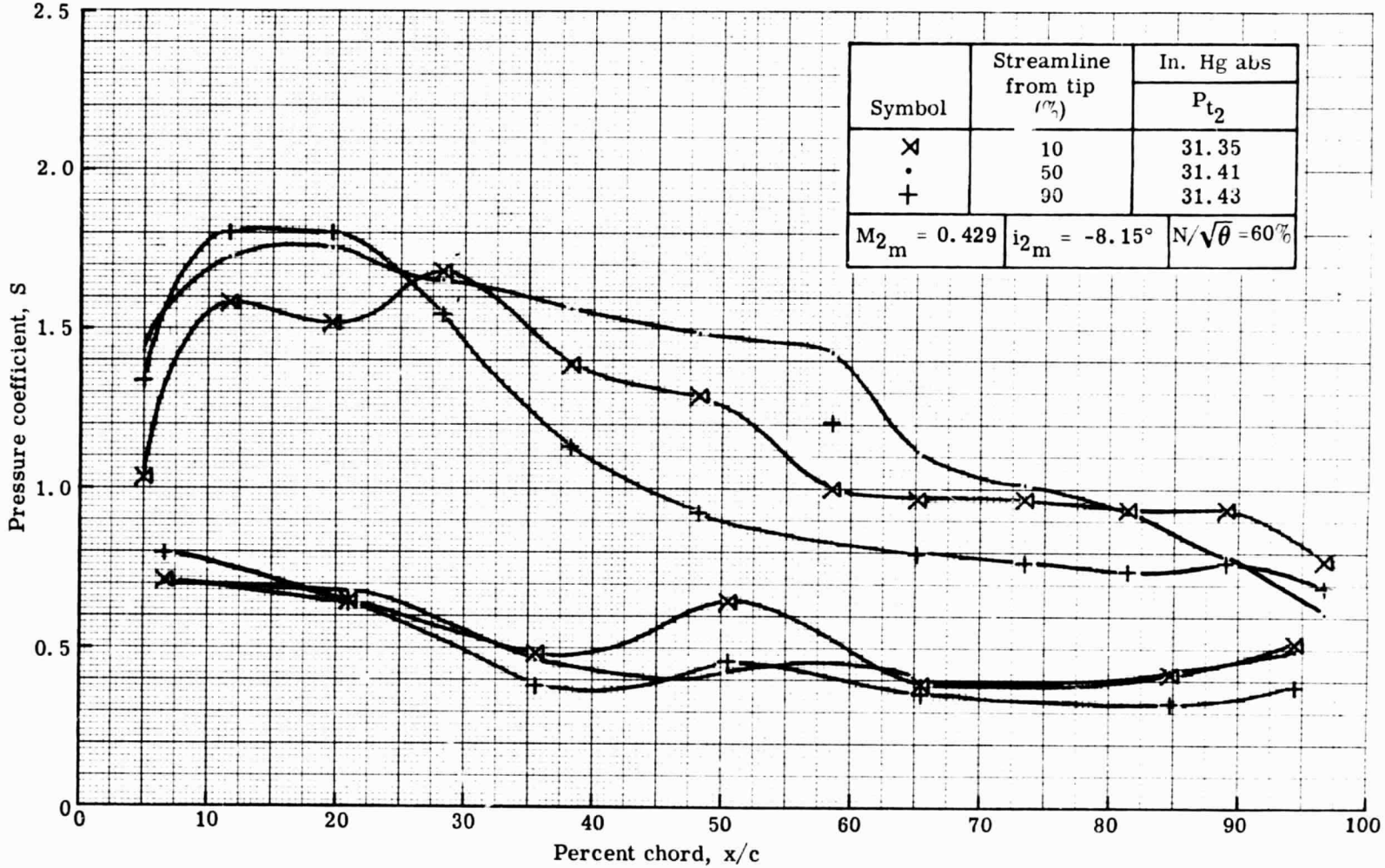

b. $W_a \sqrt{\theta}/\delta$ = 61.17 lb_m/sec

5863-54

Figure 26. Stator static pressure distribution at 60% speed with optimum wall bleed.

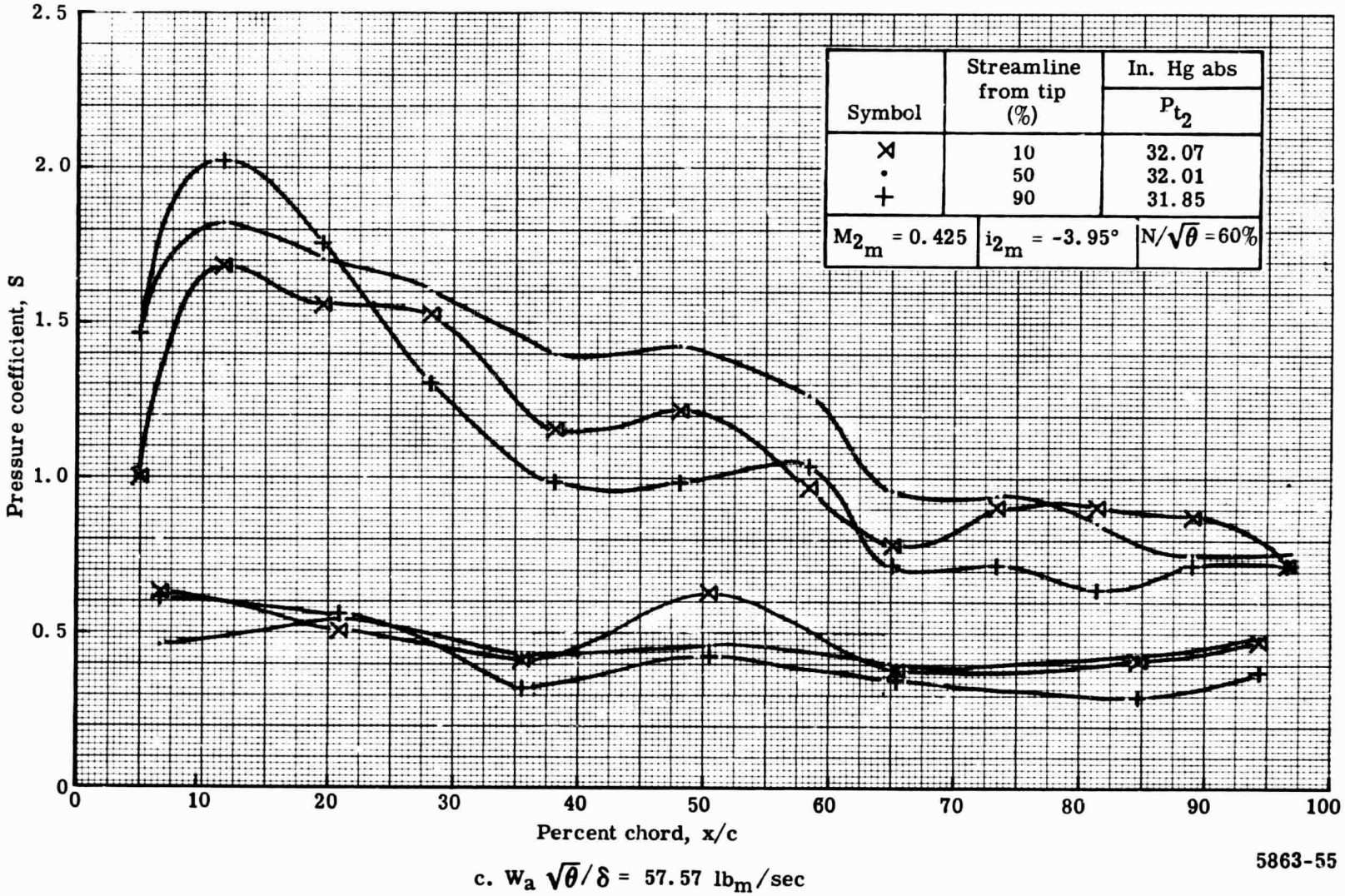

c. $W_a \sqrt{\theta}/\delta$ = 57.57 lb_m/sec

Figure 26. Stator static pressure distribution at 60% speed with optimum wall bleed.

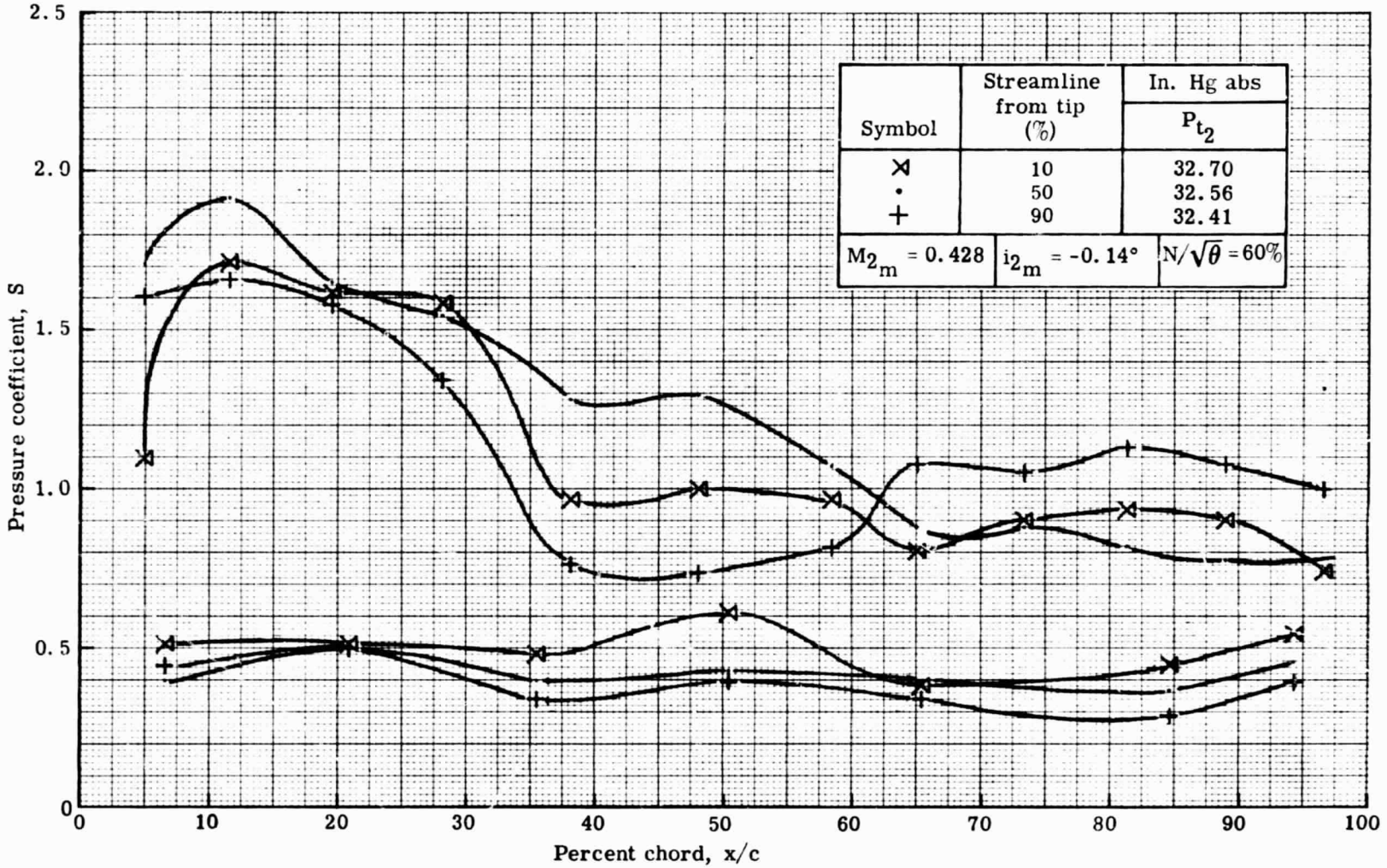

d. $W_a \sqrt{\theta}/\delta$ = 52.97 lb_m/sec

5863-56

Figure 26. Stator static pressure distribution at 60% speed with optimum wall bleed.

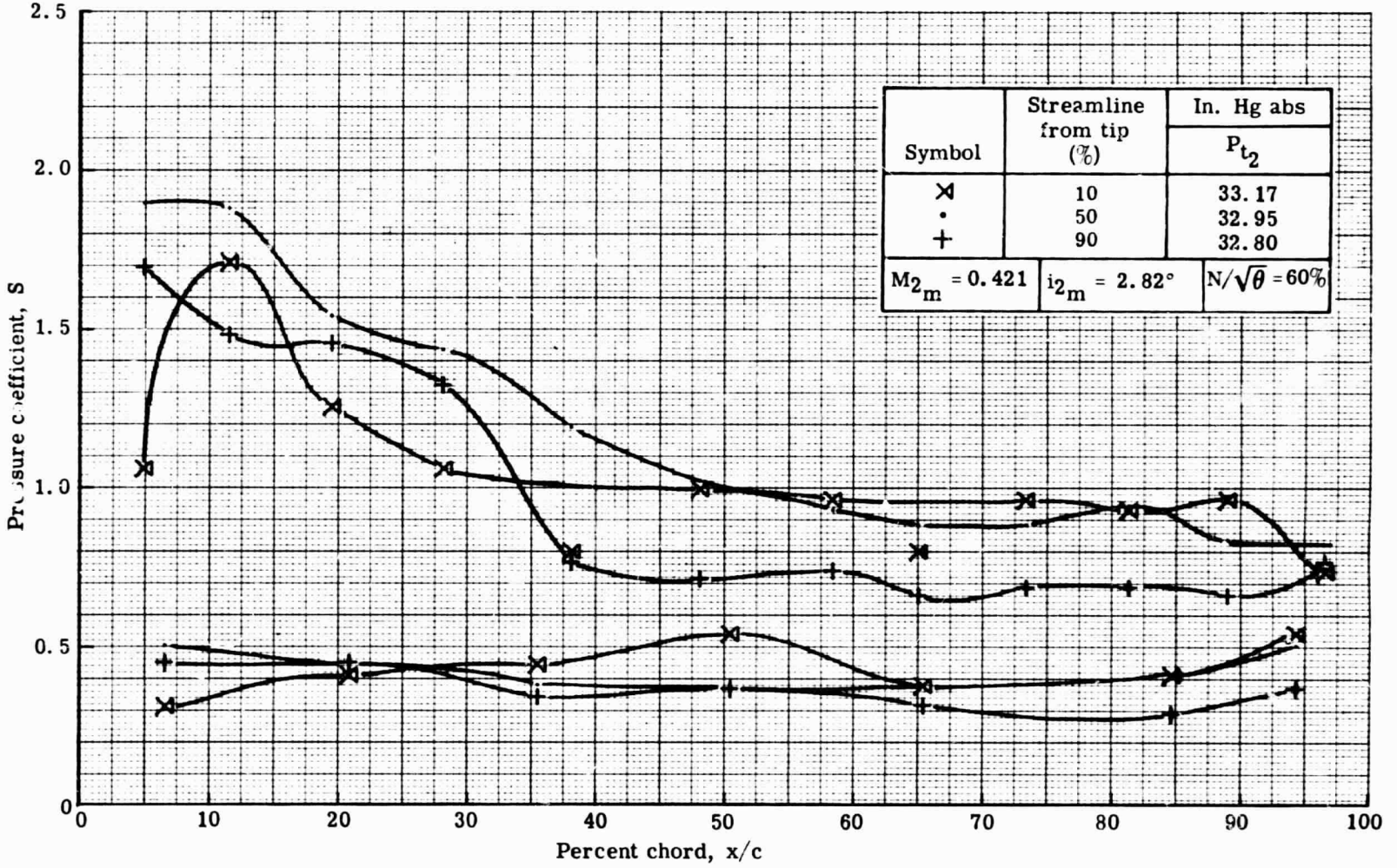

e. $W_a \sqrt{\theta}/\delta$ = 48.76 lb_m/sec

5863-57

Figure 26. Stator static pressure distribution at 60% speed with optimum wall bleed.

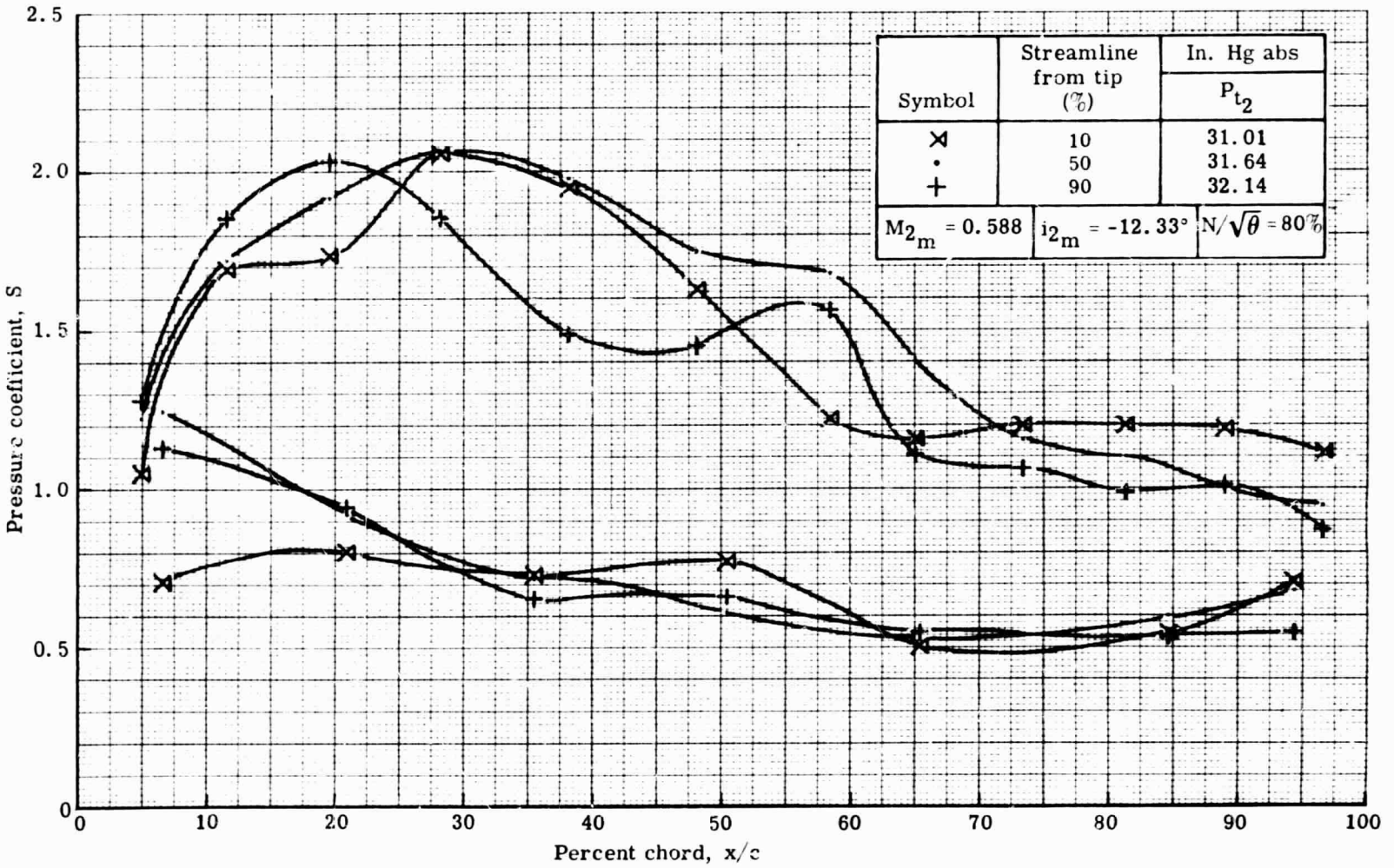

a. $W_a \sqrt{\theta}/\delta$ = 84.27 lb_m/sec

5863-58

Figure 27. Stator static pressure distribution at 80% speed with optimum wall bleed.

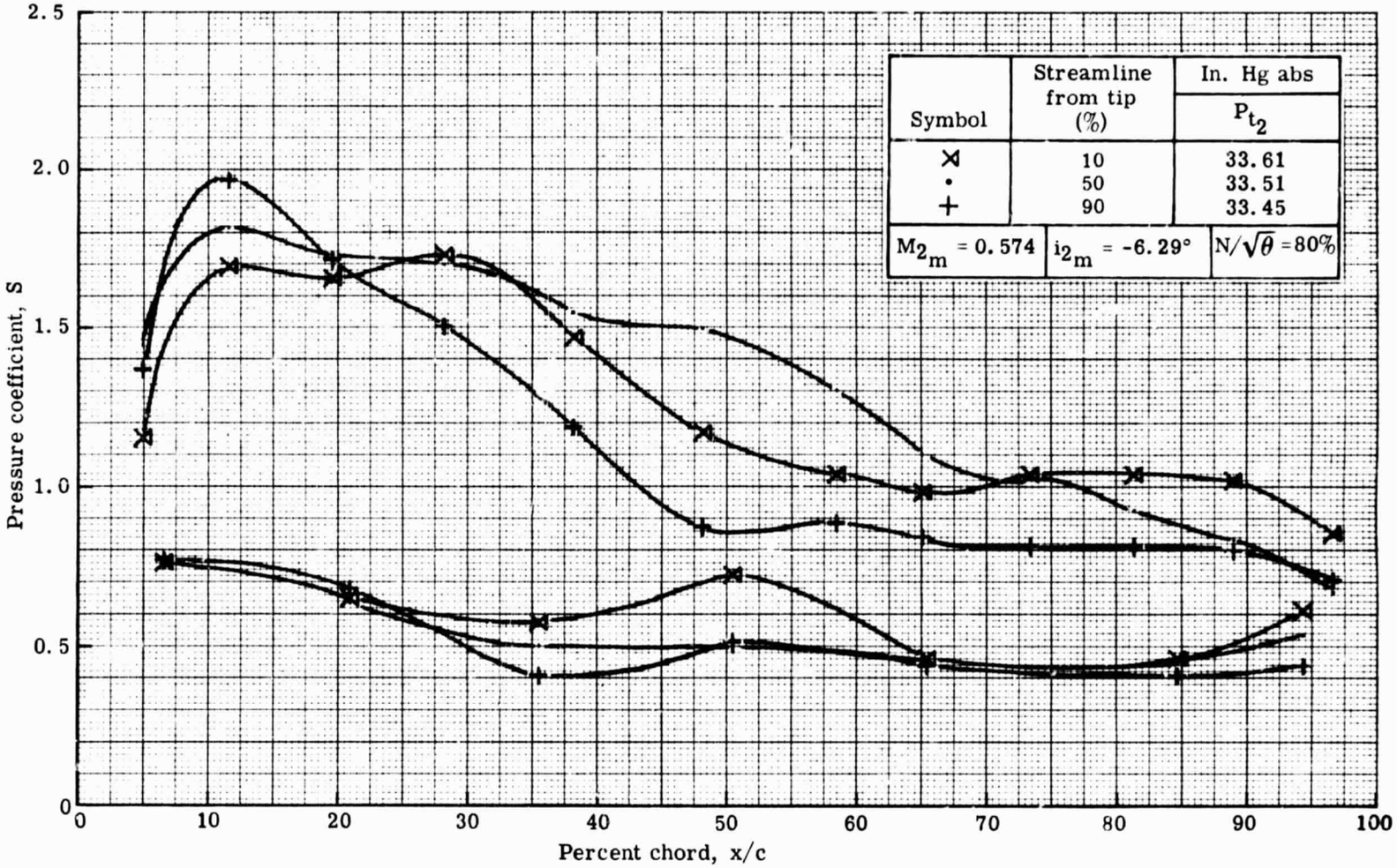

b. $W_a \sqrt{\theta}/\delta$ = 79.51 lb_m/sec

5863-59

Figure 27. Stator static pressure distribution at 80% speed with optimum wall bleed.

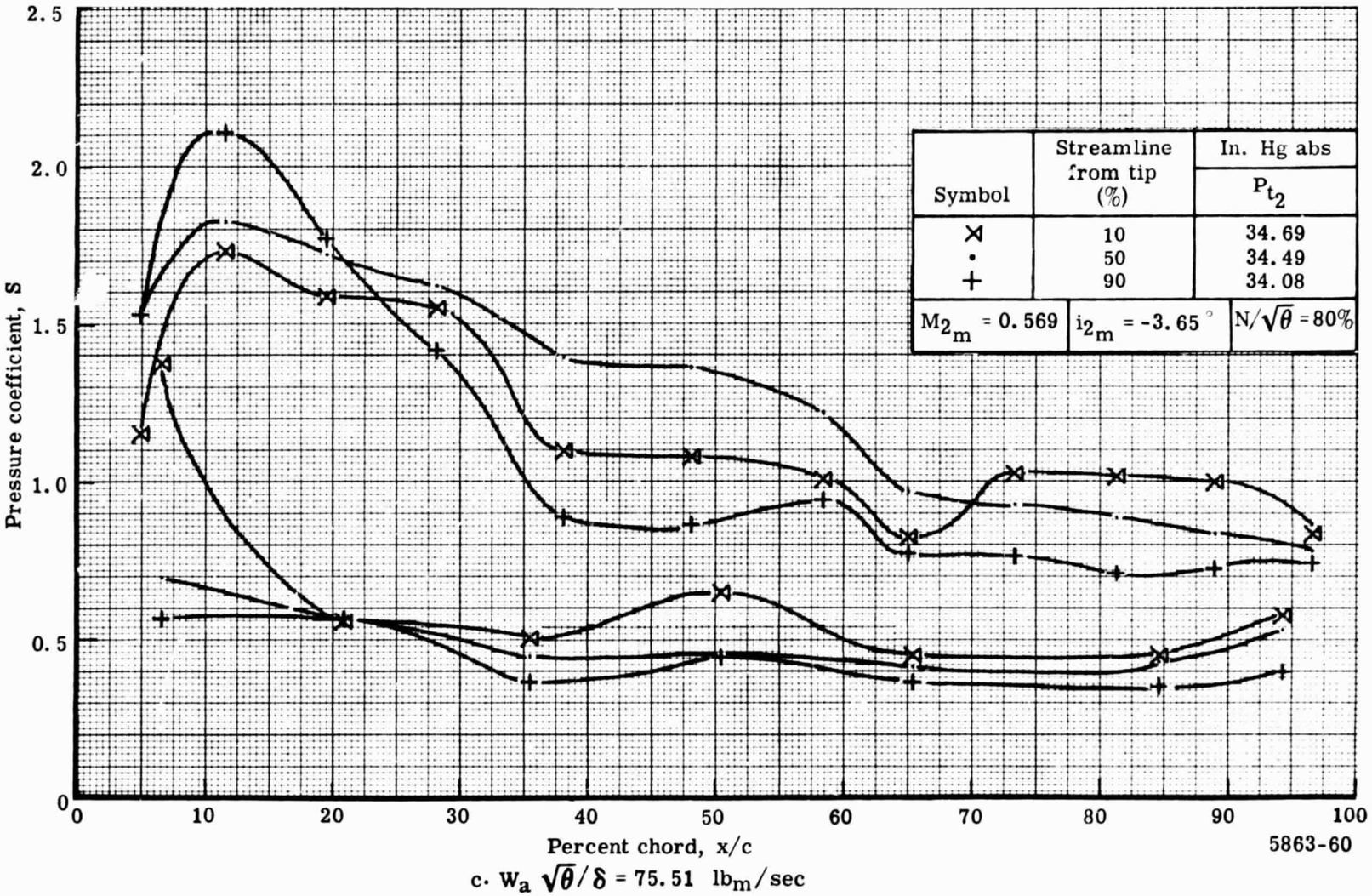

Figure 27. Stator static pressure distribution at 80% speed with optimum wall bleed.

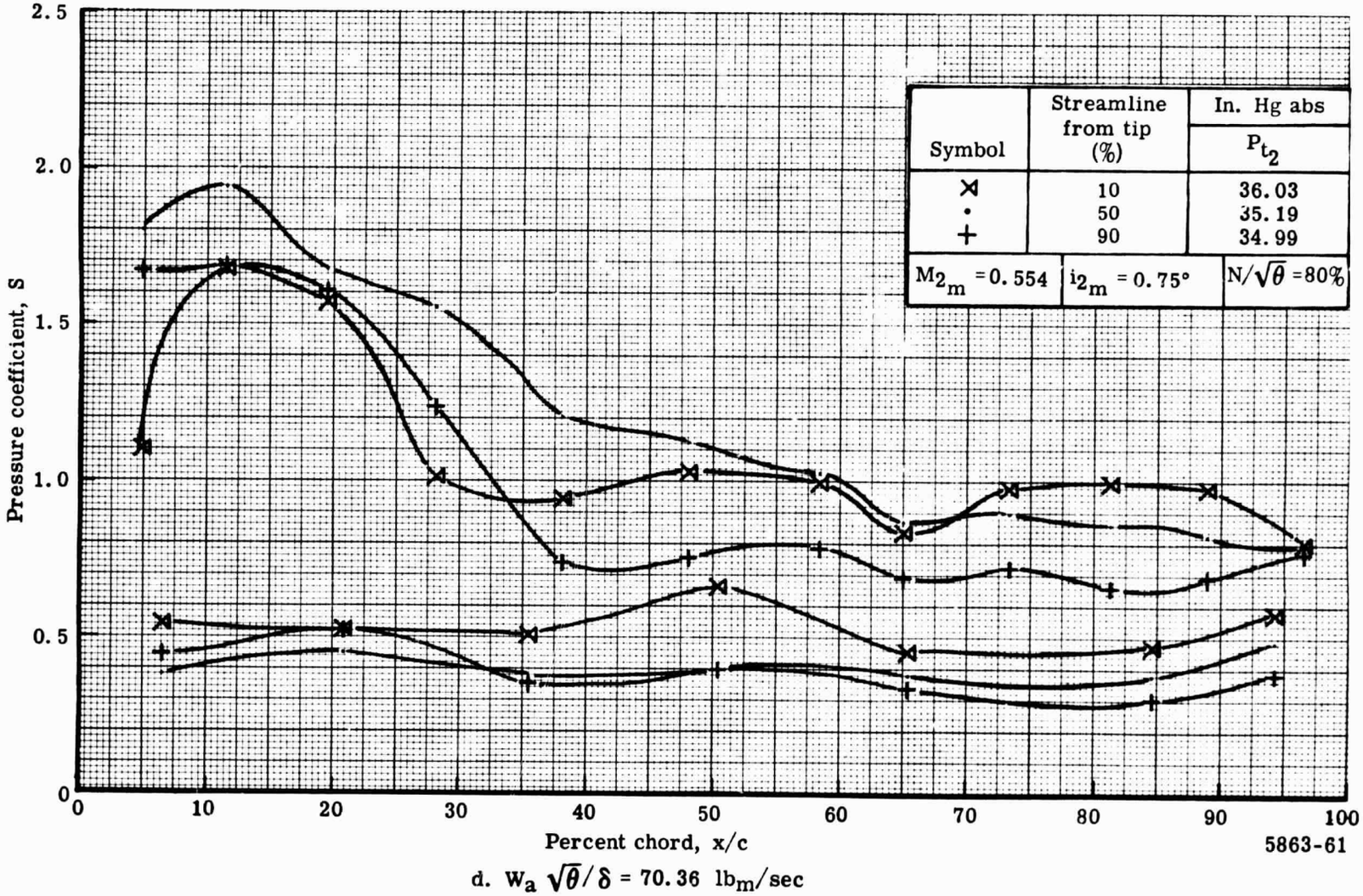

d. $W_a \sqrt{\theta}/\delta$ = 70.36 lb_m/sec

Figure 27. Stator static pressure distribution at 80% speed with optimum wall bleed.

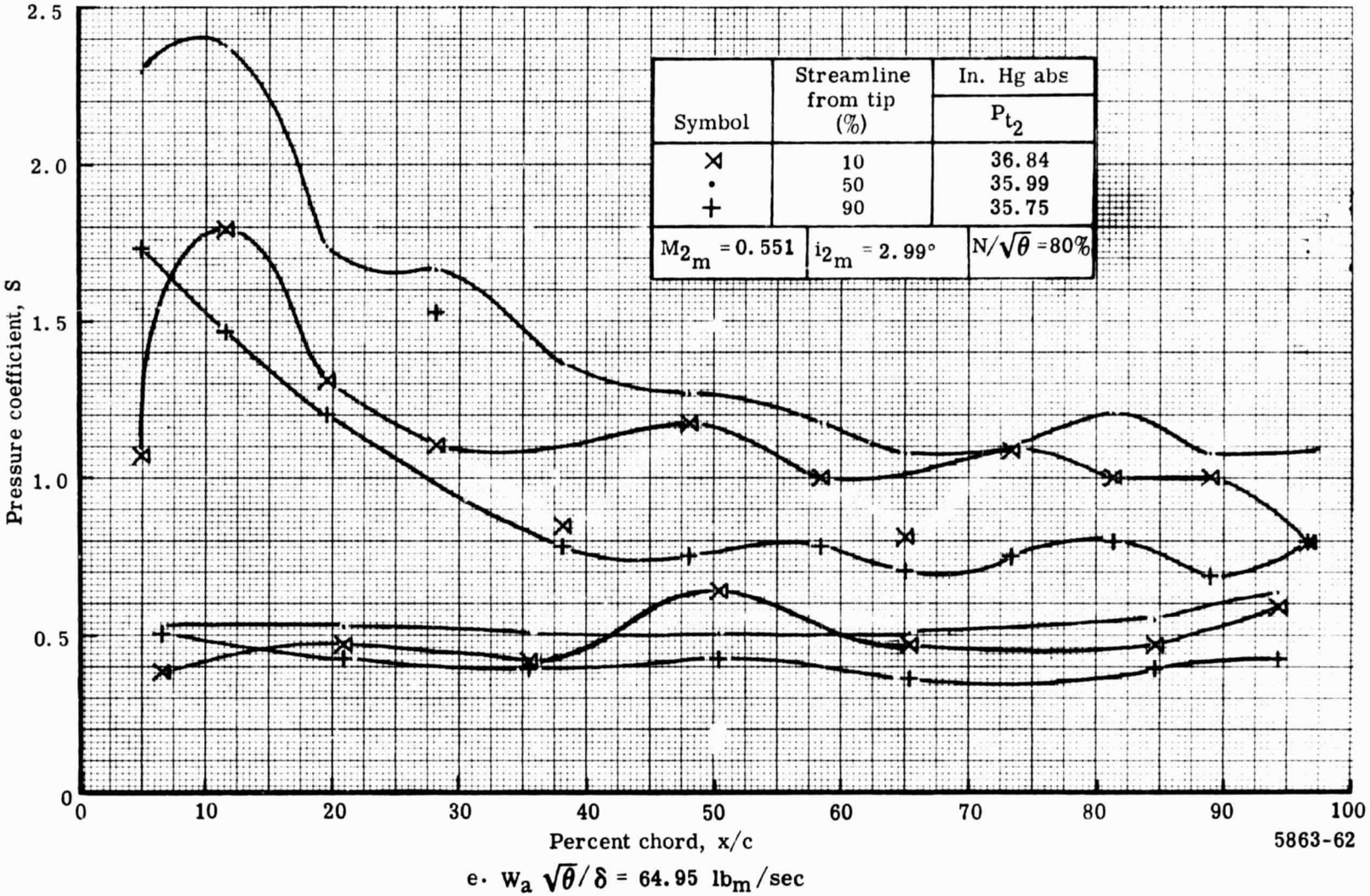

Figure 27. Stator static pressure distribution at 80% speed with optimum wall bleed.

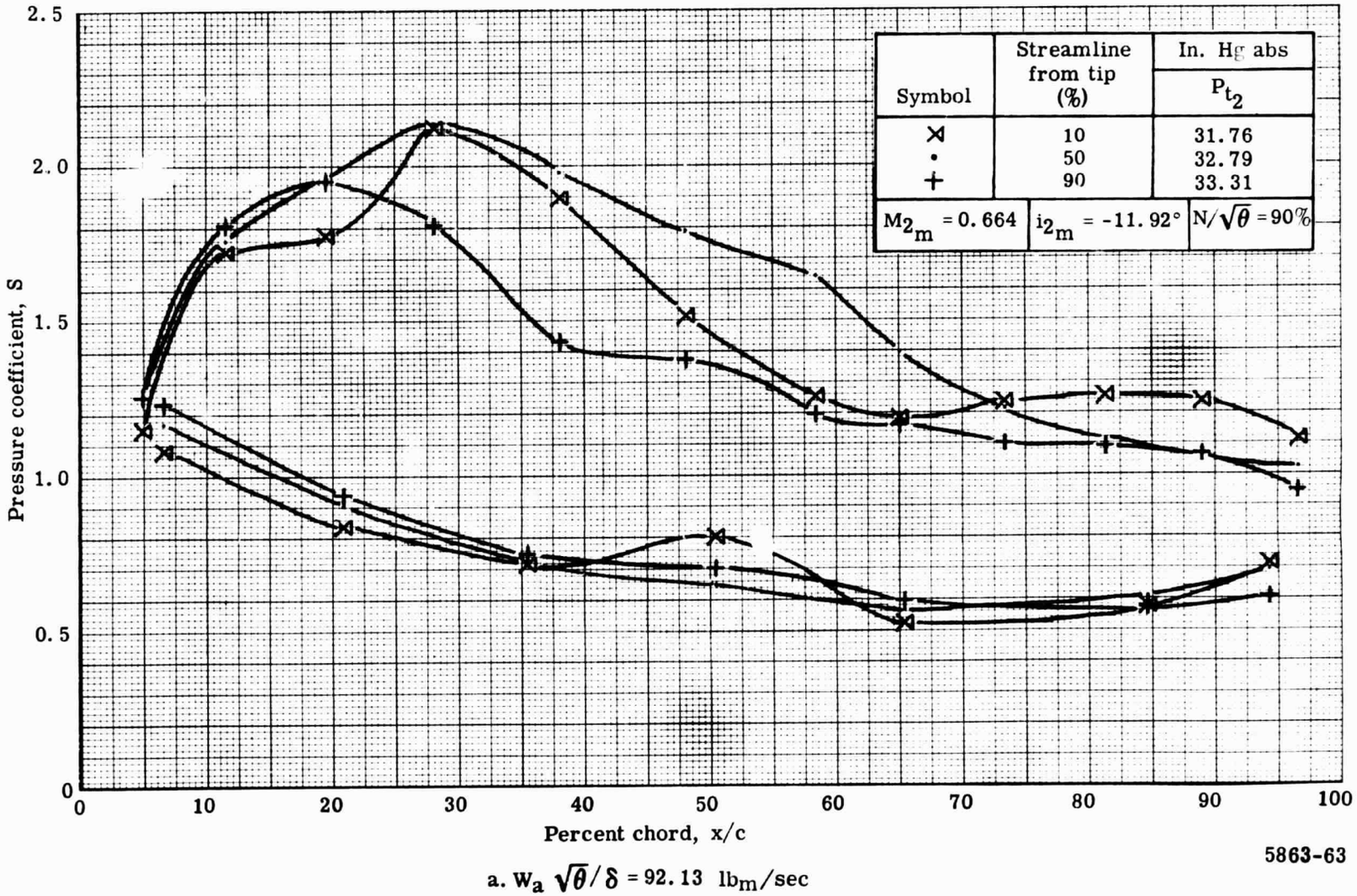

a. $W_a \sqrt{\theta}/\delta$ = 92.13 lb_m/sec

Figure 28. Stator static pressure distribution at 90% speed with optimum wall bleed.

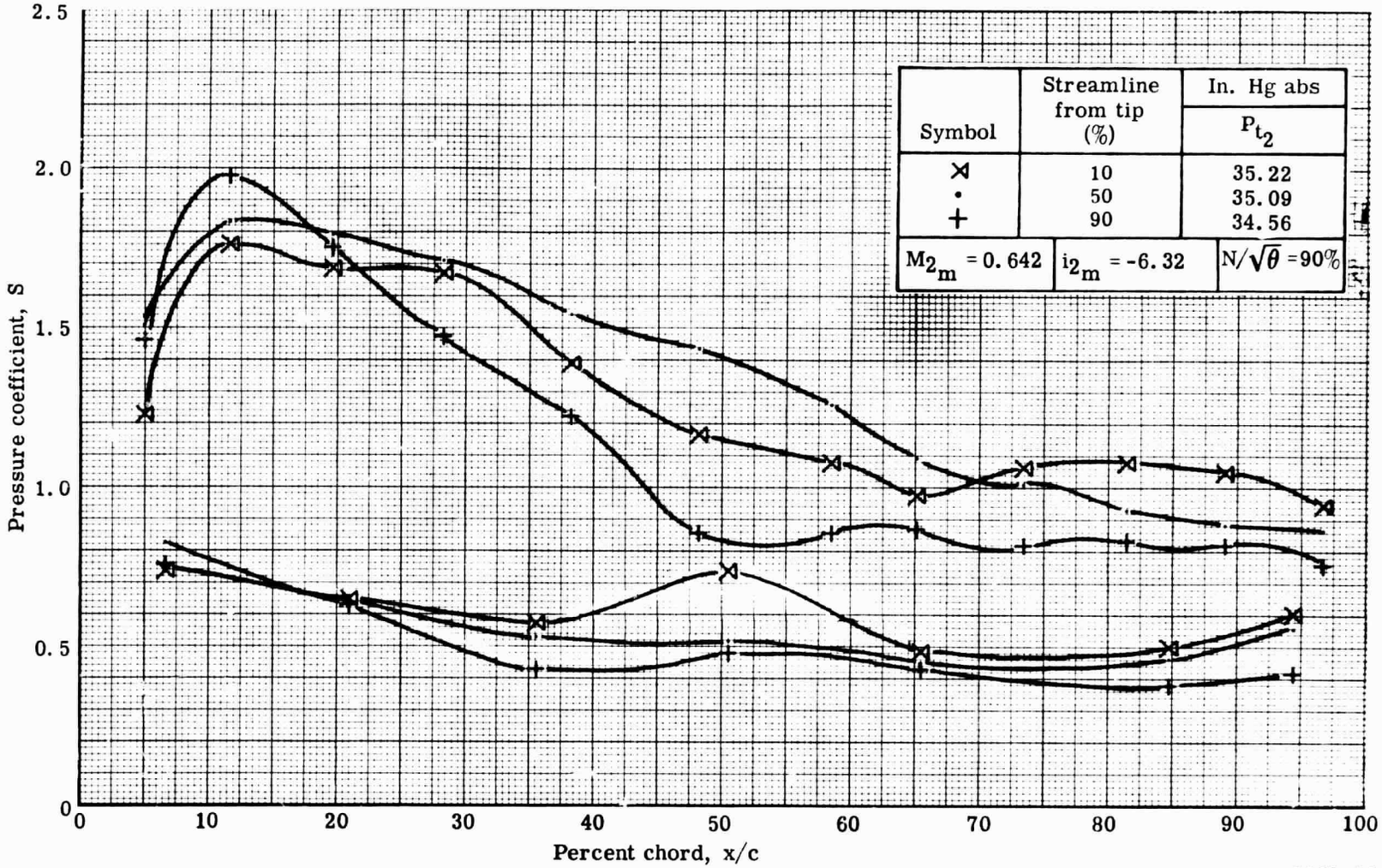

b. $W_a \sqrt{\theta}/\delta$ = 87.50 lb_m/sec

Figure 28. Stator static pressure distribution at 90% speed with optimum wall bleed.

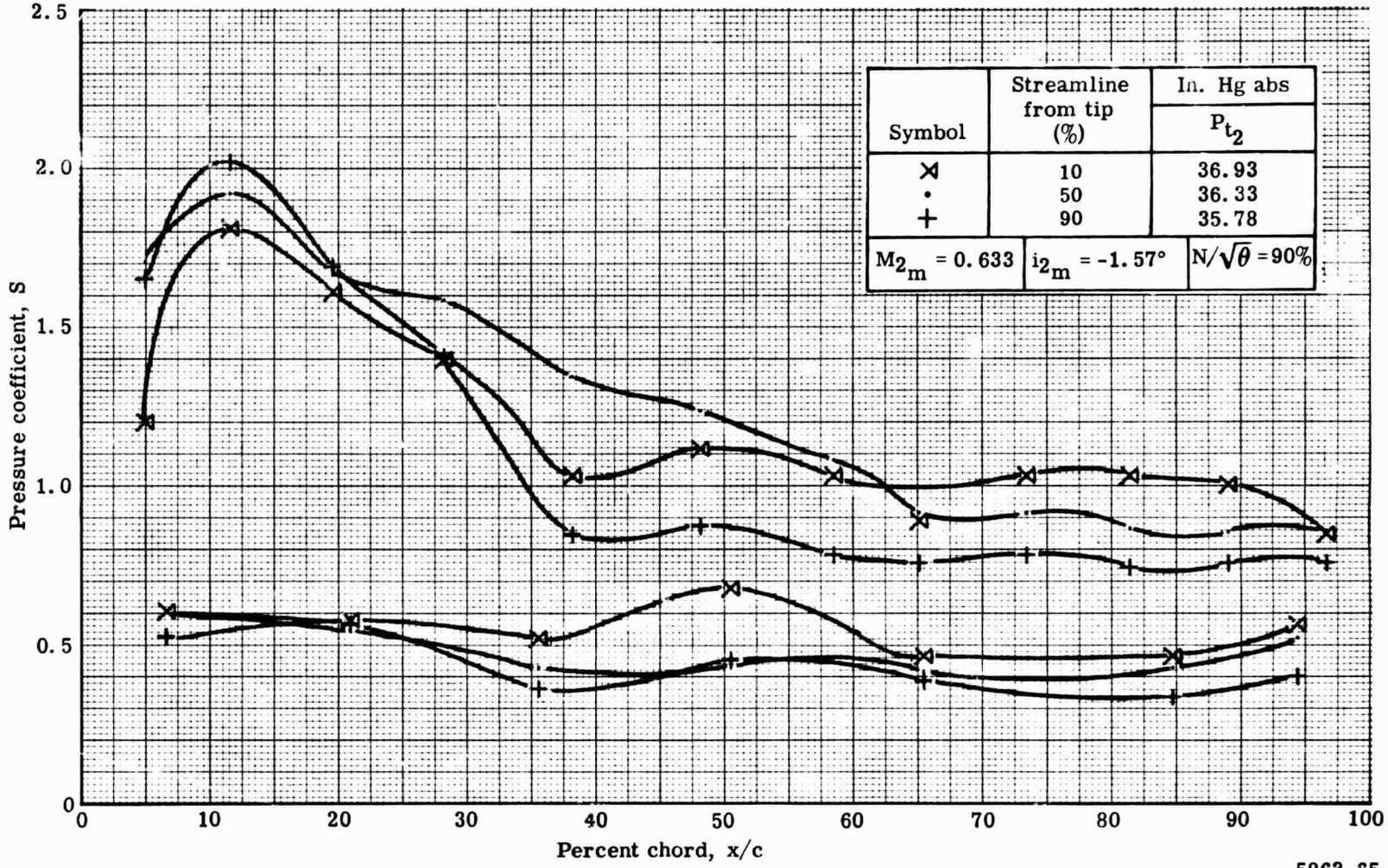

c. $W_a \sqrt{\theta}/\delta$ = 82.70 lb_m/sec

Figure 28. Stator static pressure distribution at 90% speed with optimum wall bleed.

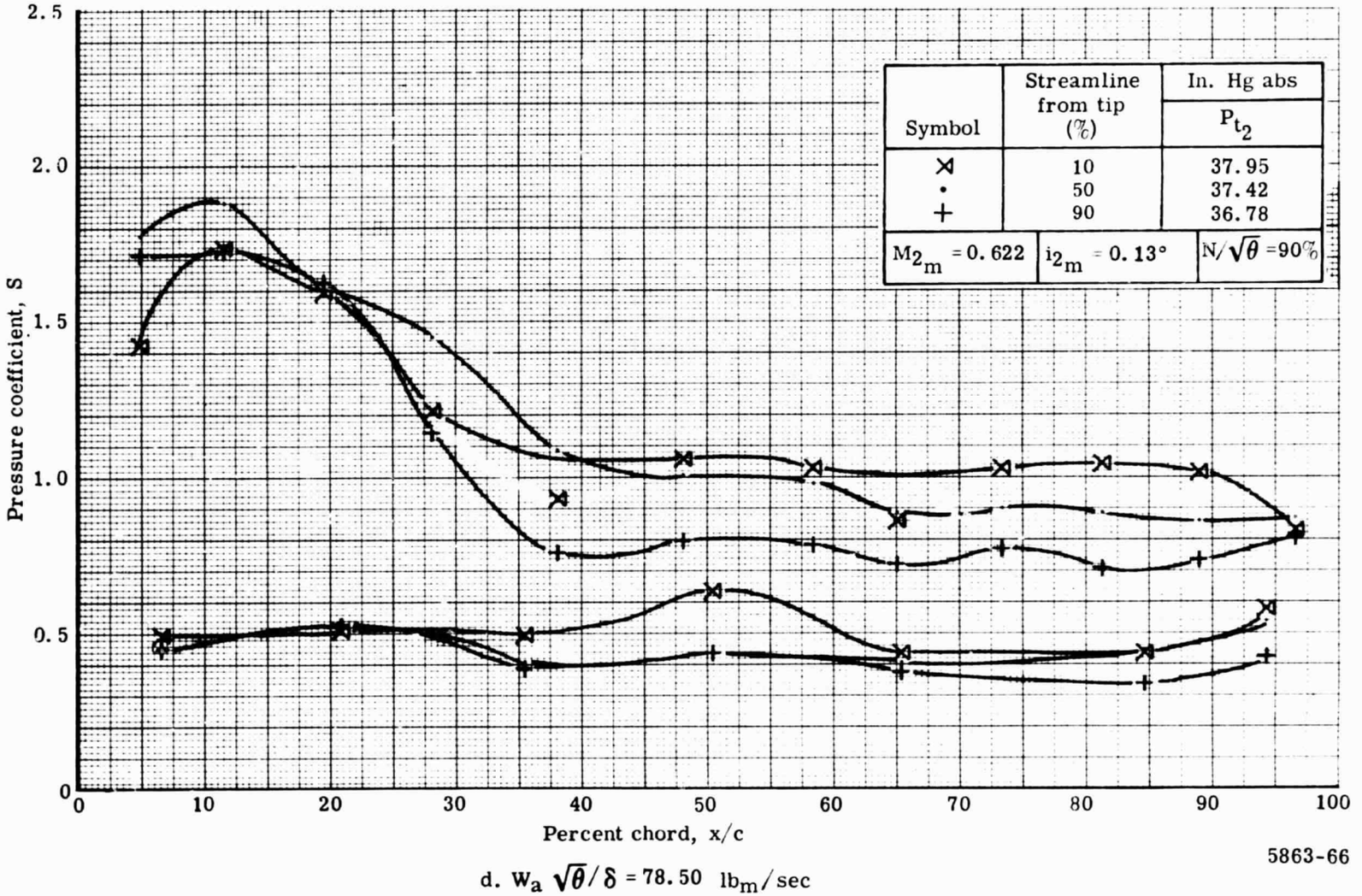

d. $W_a \sqrt{\theta}/\delta$ = 78.50 lb_m/sec

Figure 28. Stator static pressure distribution at 90% speed with optimum wall bleed.

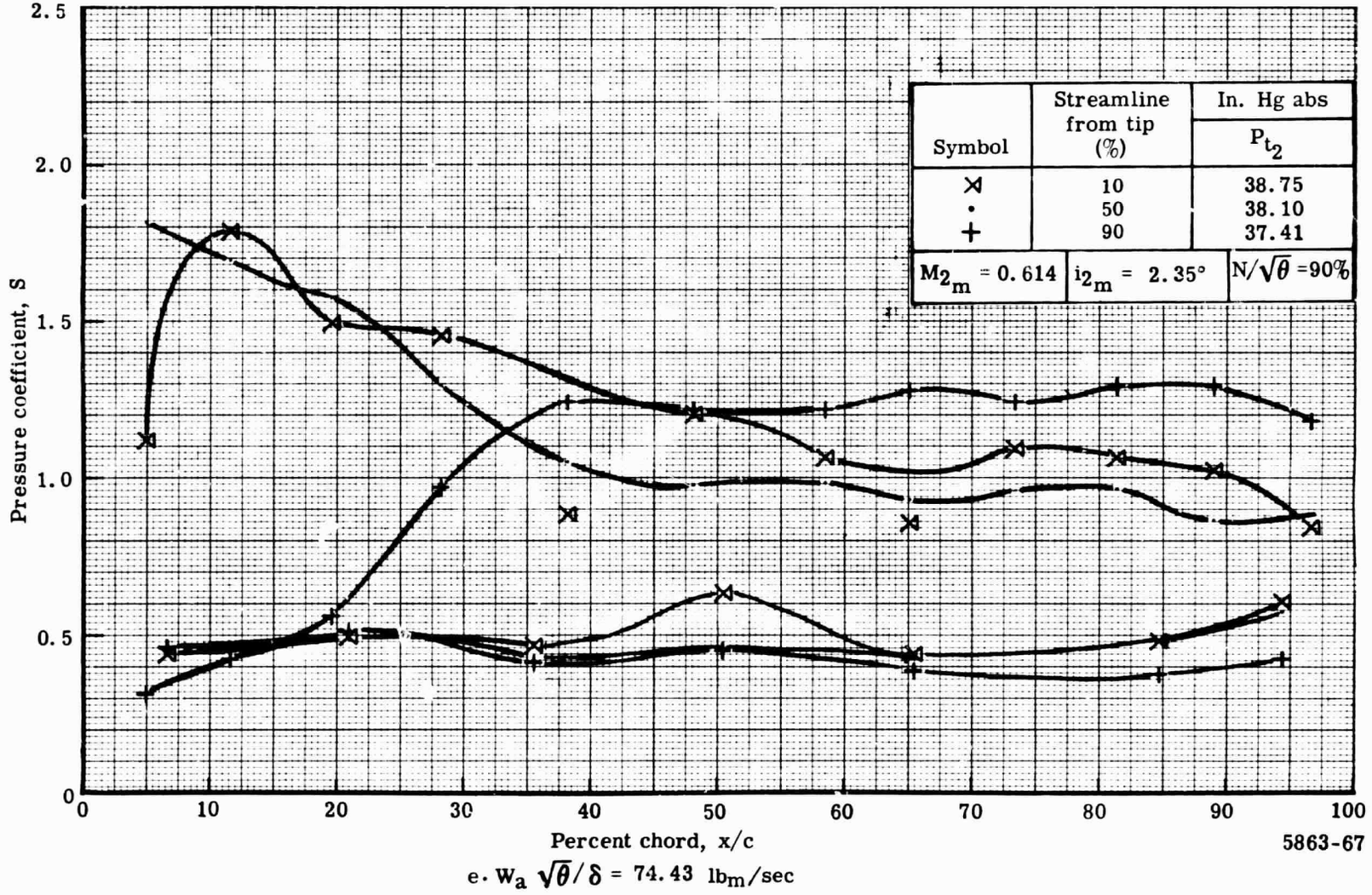

Figure 28. Stator static pressure distribution at 90% speed with optimum wall bleed.

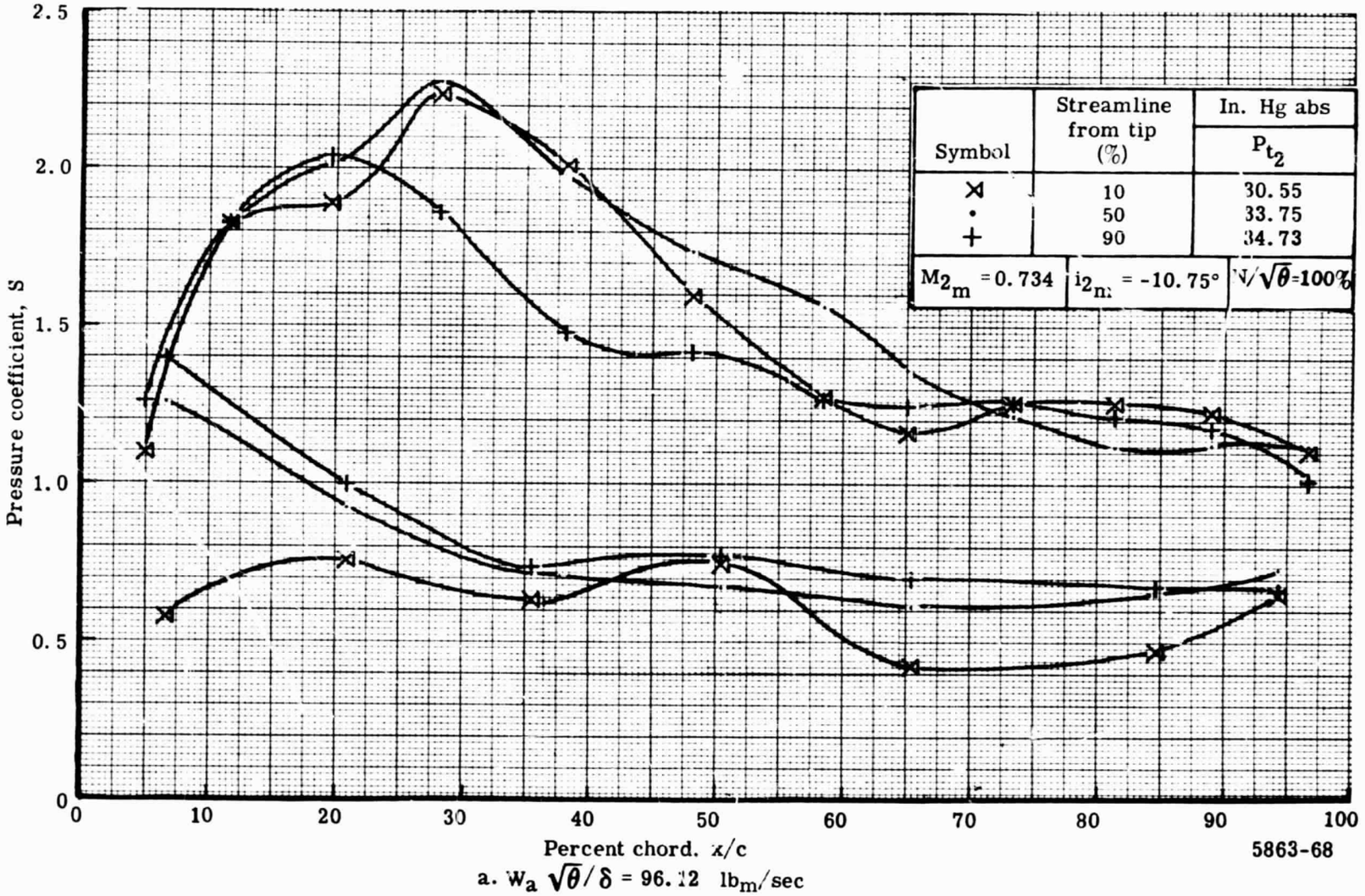

Figure 29. Stator static pressure distribution at 100% speed with optimum wall bleed.

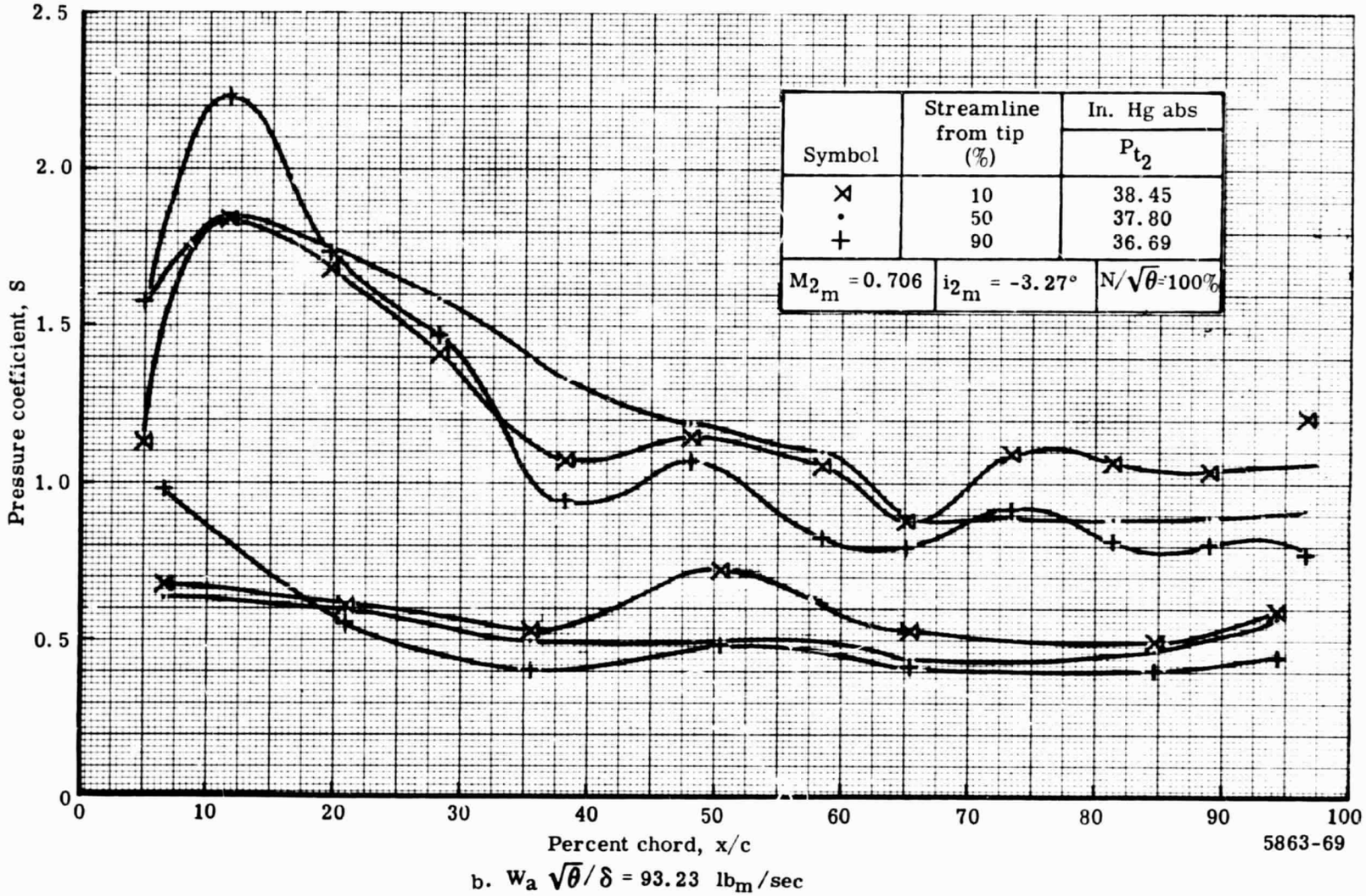

b. $W_a \sqrt{\theta}/\delta$ = 93.23 lb_m/sec

Figure 29. Stator static pressure distribution at 100% speed with optimum wall bleed.

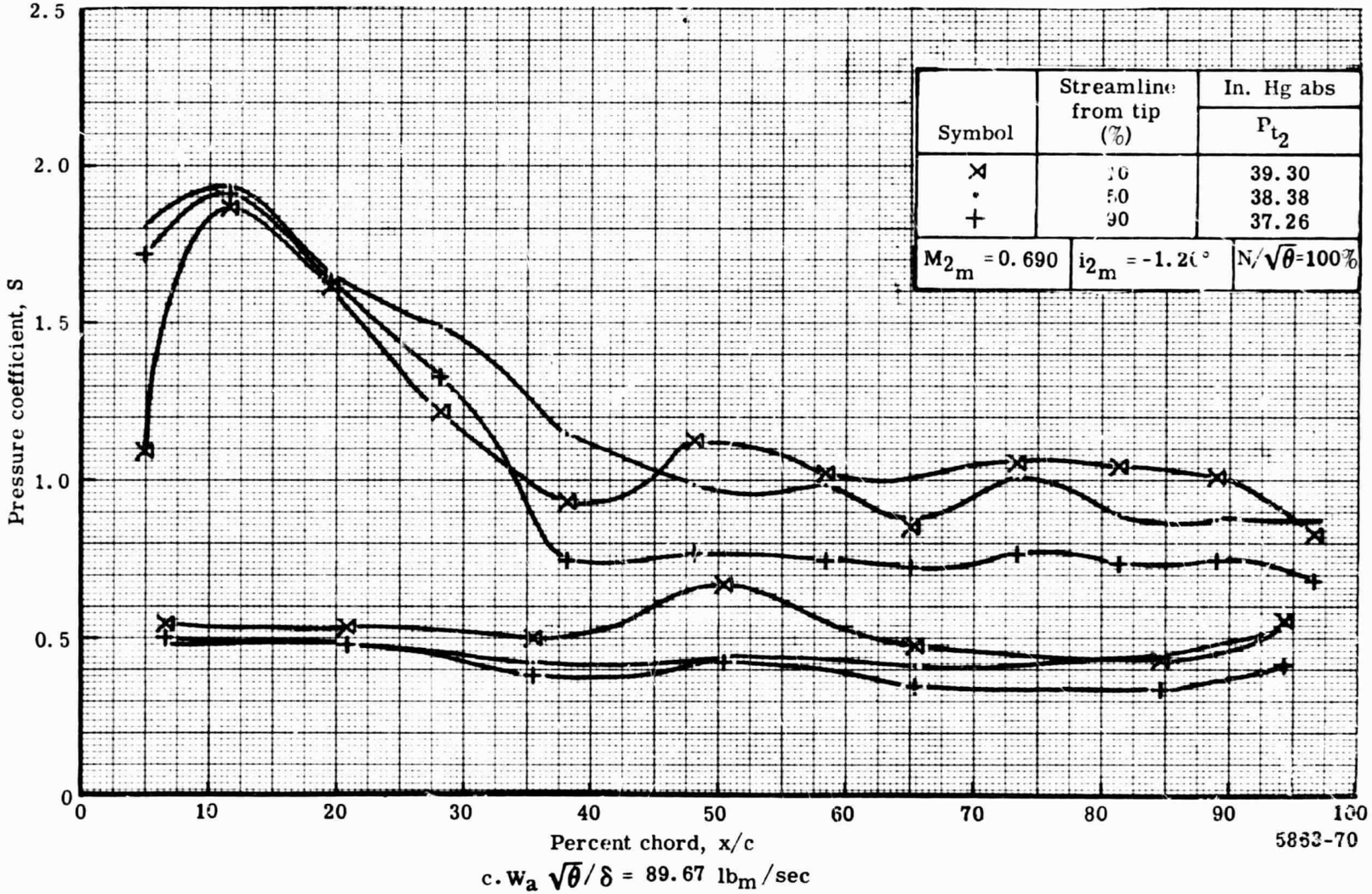

Figure 29. Stator static pressure distribution at 100% speed with optimum wall bleed.

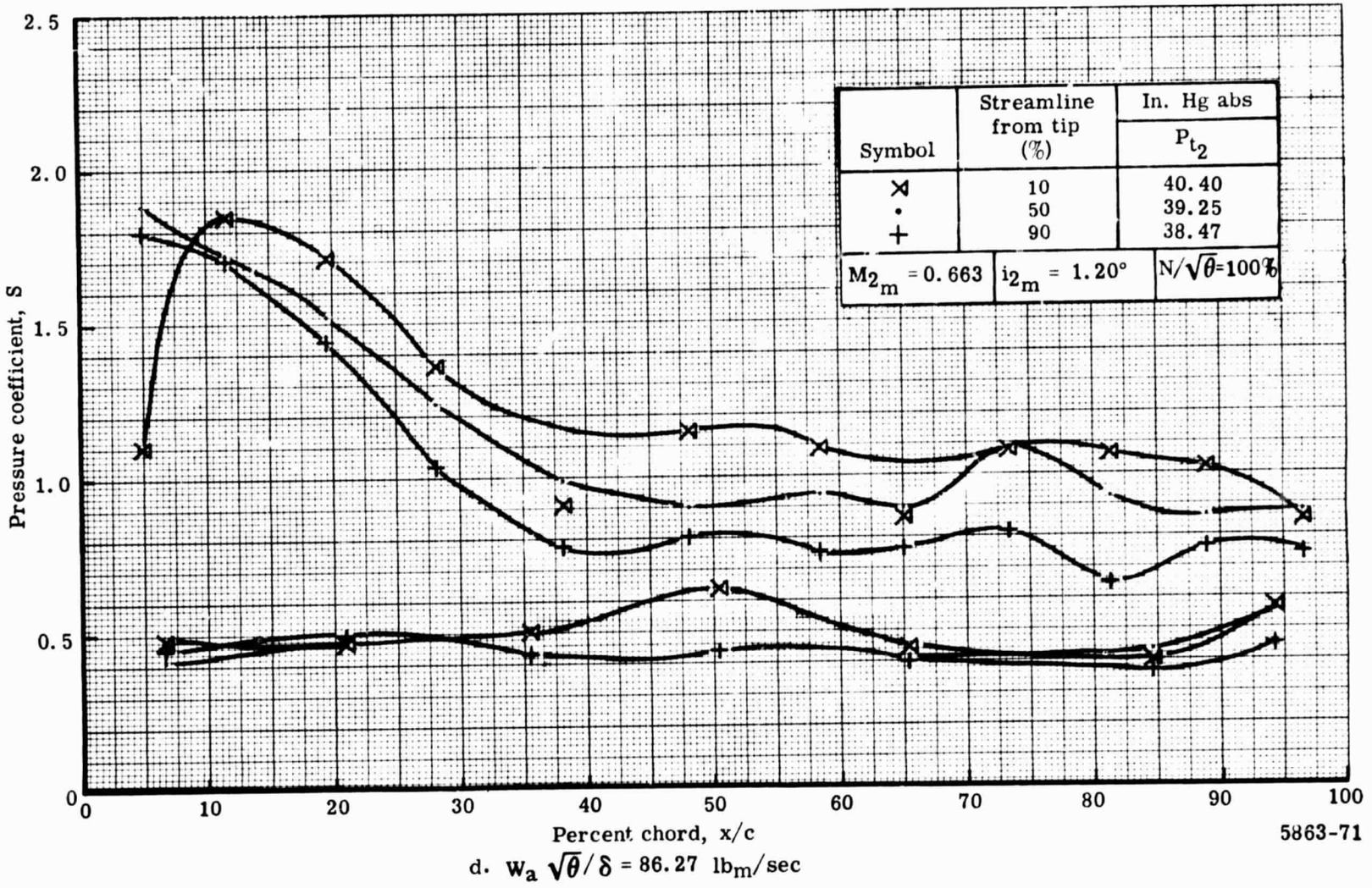

Figure 29. Stator static pressure distribution at 100% speed with optimum wall bleed.

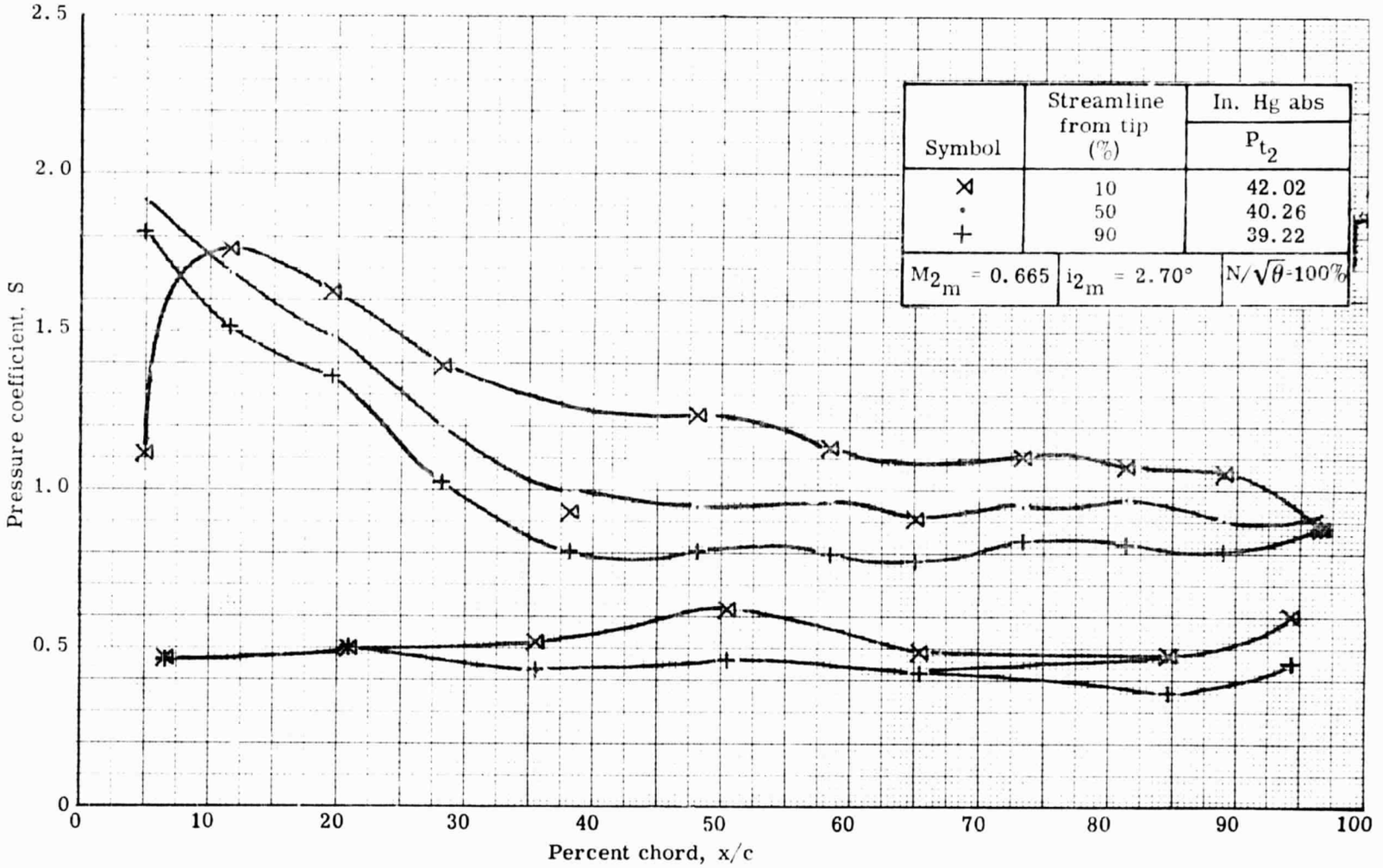

Figure 29. Stator static pressure distribution at 100% speed with optimum wall bleed.

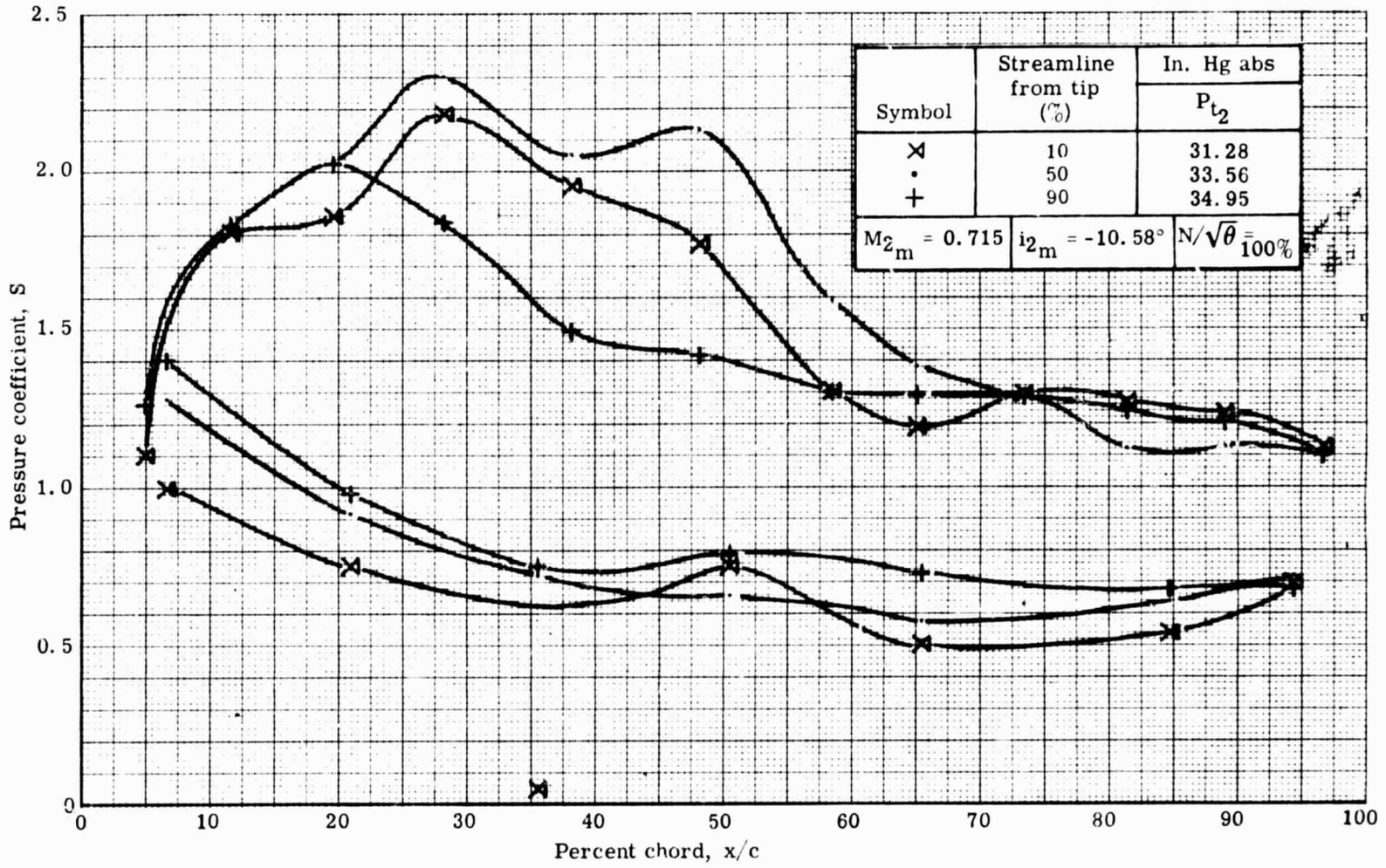

a. $W_a \sqrt{\theta}/\delta$ = 97.01 lb_m/sec

5863-77

Figure 30. Stator static pressure distribution at 100% speed with mean wall bleed.

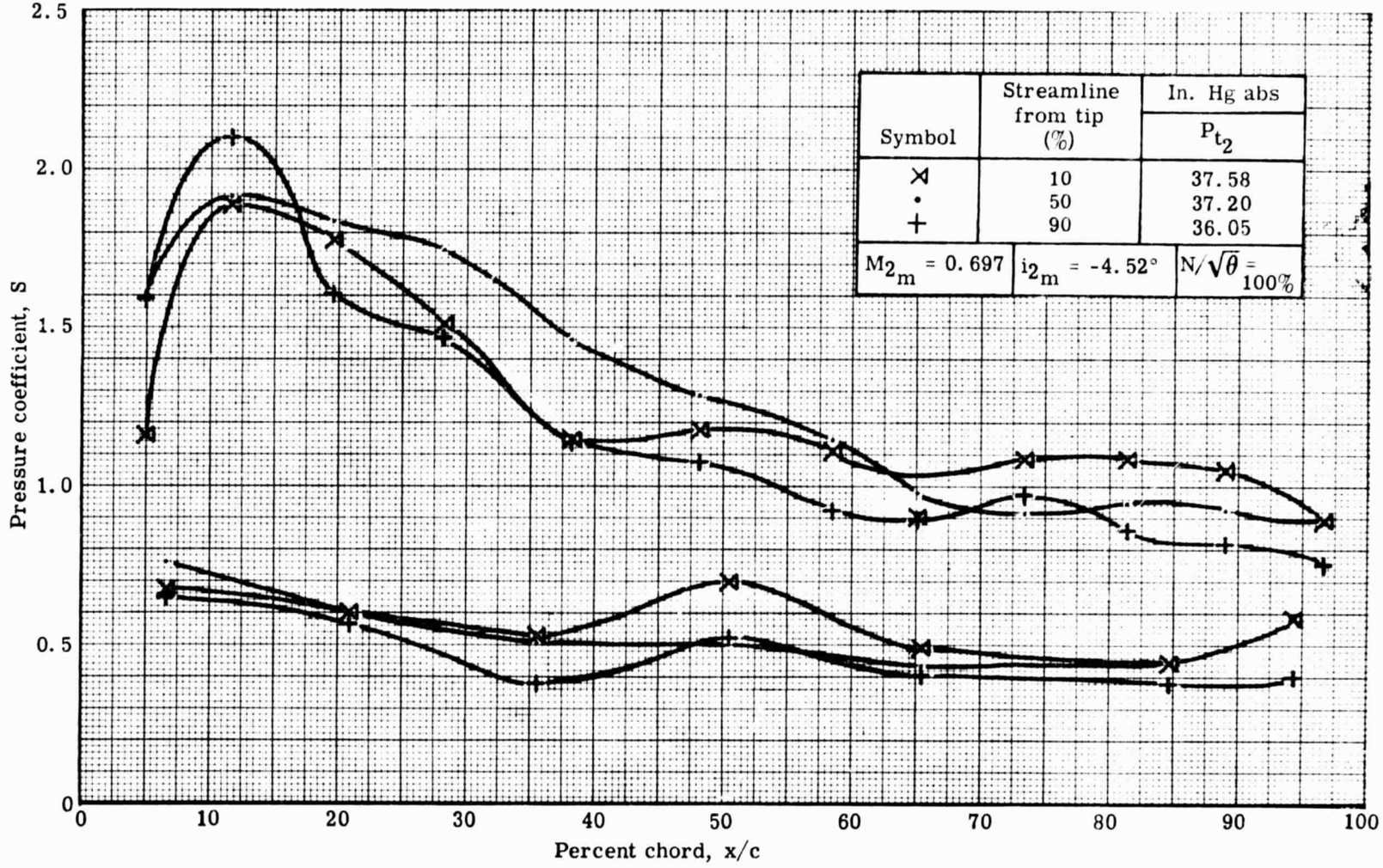

b. $W_a \sqrt{\theta}/\delta$ = 93.74 lb_m/sec

5863-78

Figure 30. Stator static pressure distribution at 100% speed with mean wall bleed.

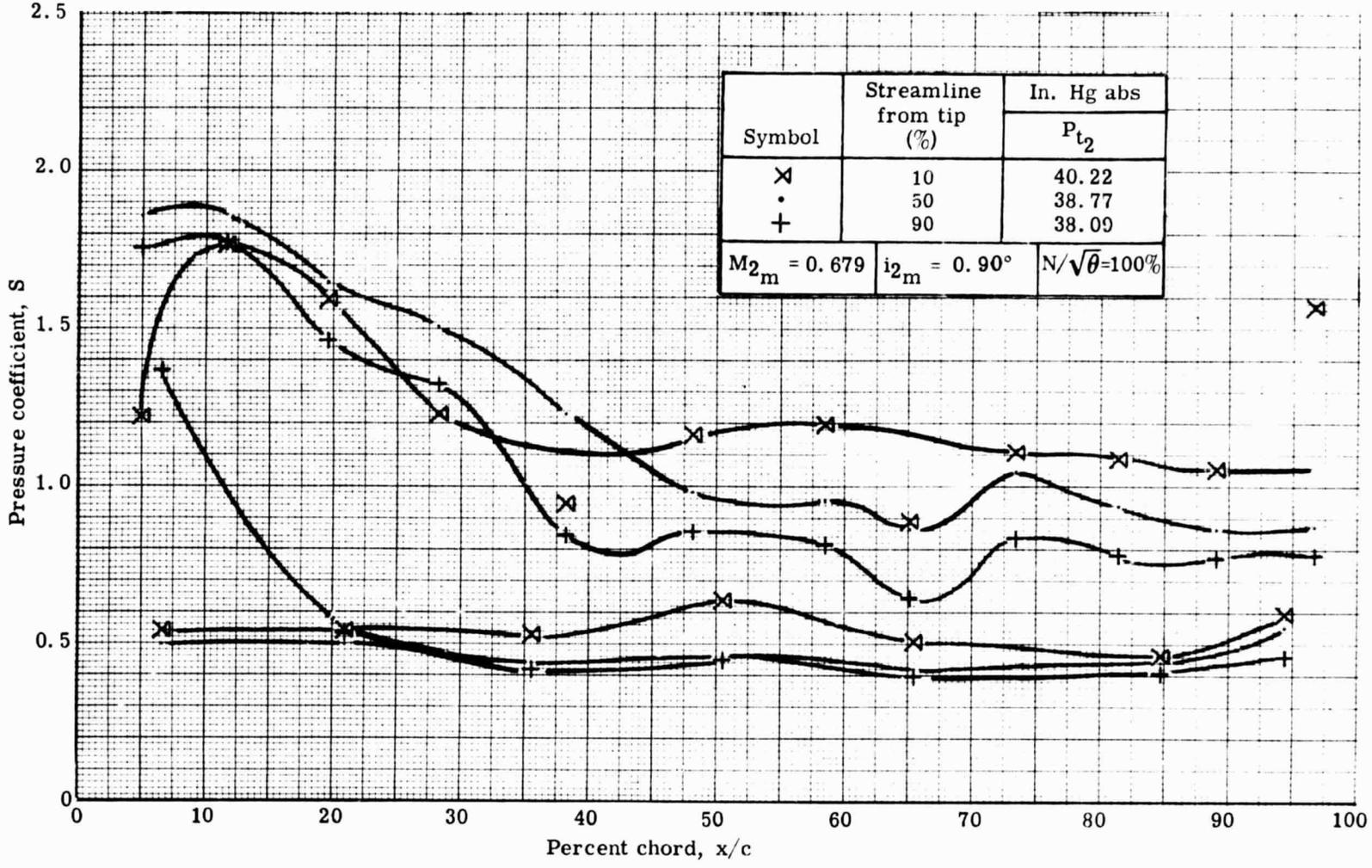

c. $W_a \sqrt{\theta}/\delta$ = 87.85 lb_m/sec

5863-79

Figure 30. Stator static pressure distribution at 100% speed with mean wall bleed.

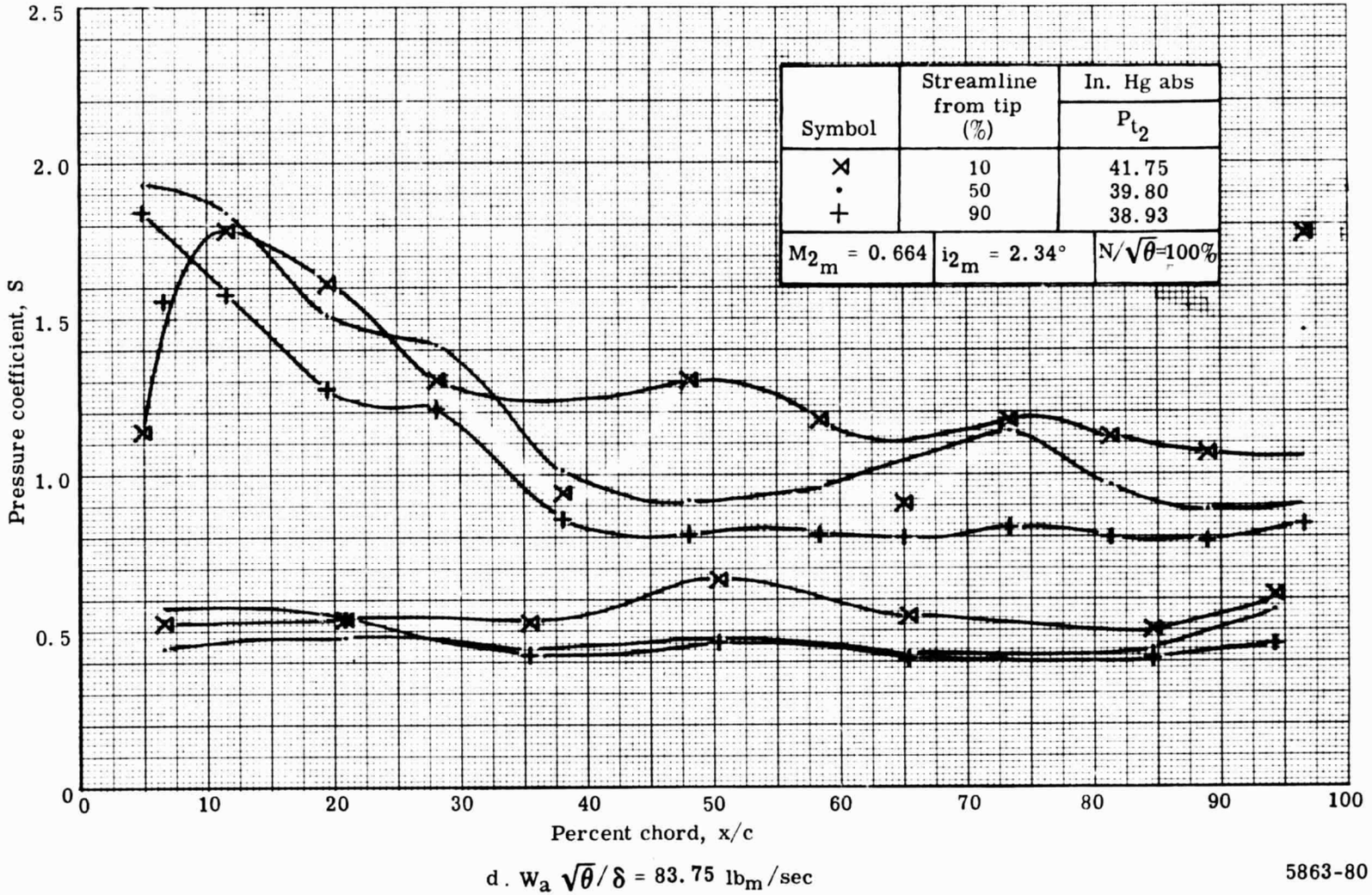

Figure 30. Stator static pressure distribution at 100% speed with mean wall bleed.

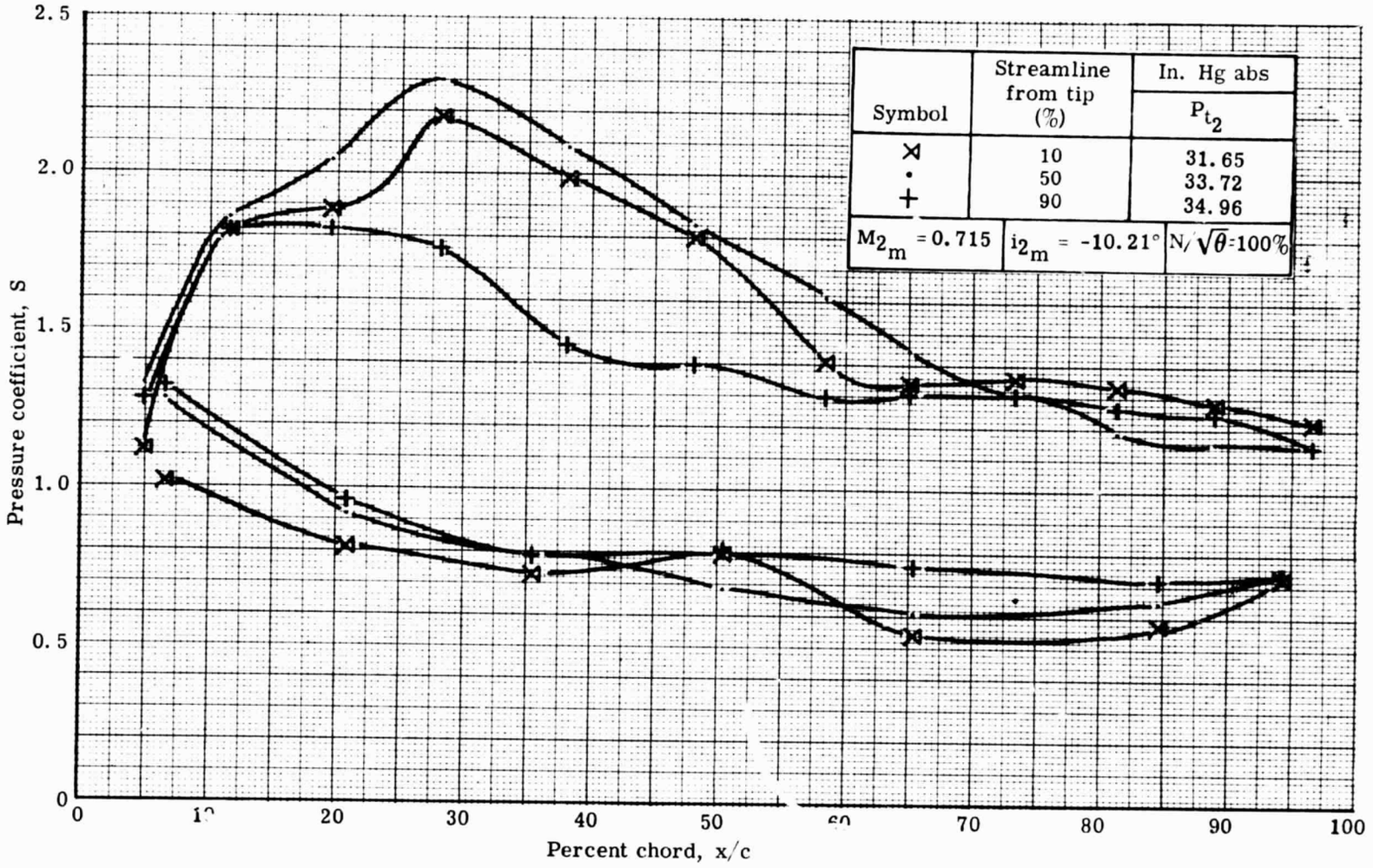

a. $W_a \sqrt{\theta}/\delta$ = 96.46 lb_m/sec

5863-73

Figure 31. Stator static pressure distribution at 100% speed with minimum wall bleed.

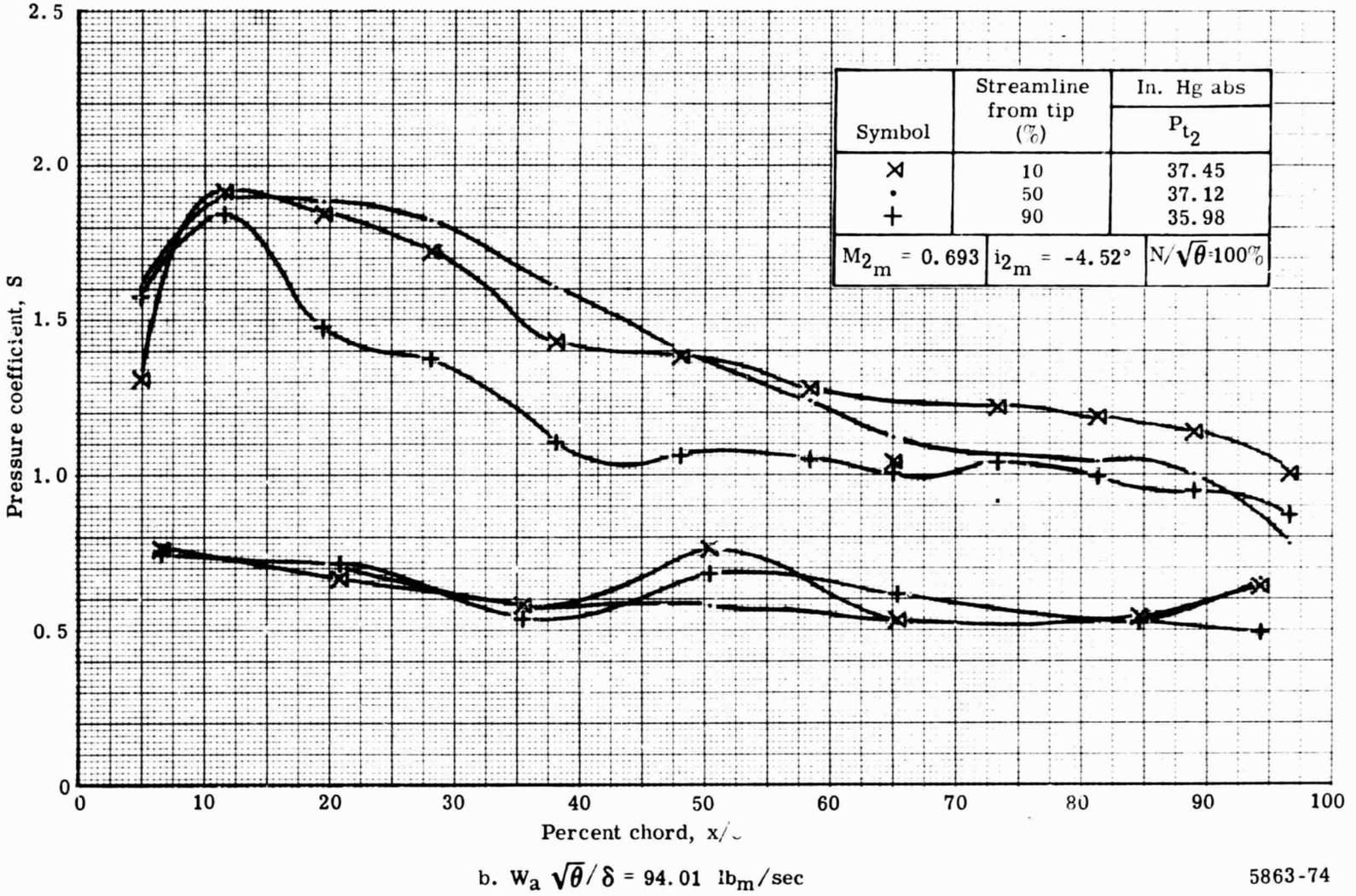

b. $W_a \sqrt{\theta}/\delta$ = 94.01 lb_m/sec

5863-74

Figure 31. Stator static pressure distribution at 100% speed with minimum wall bleed.

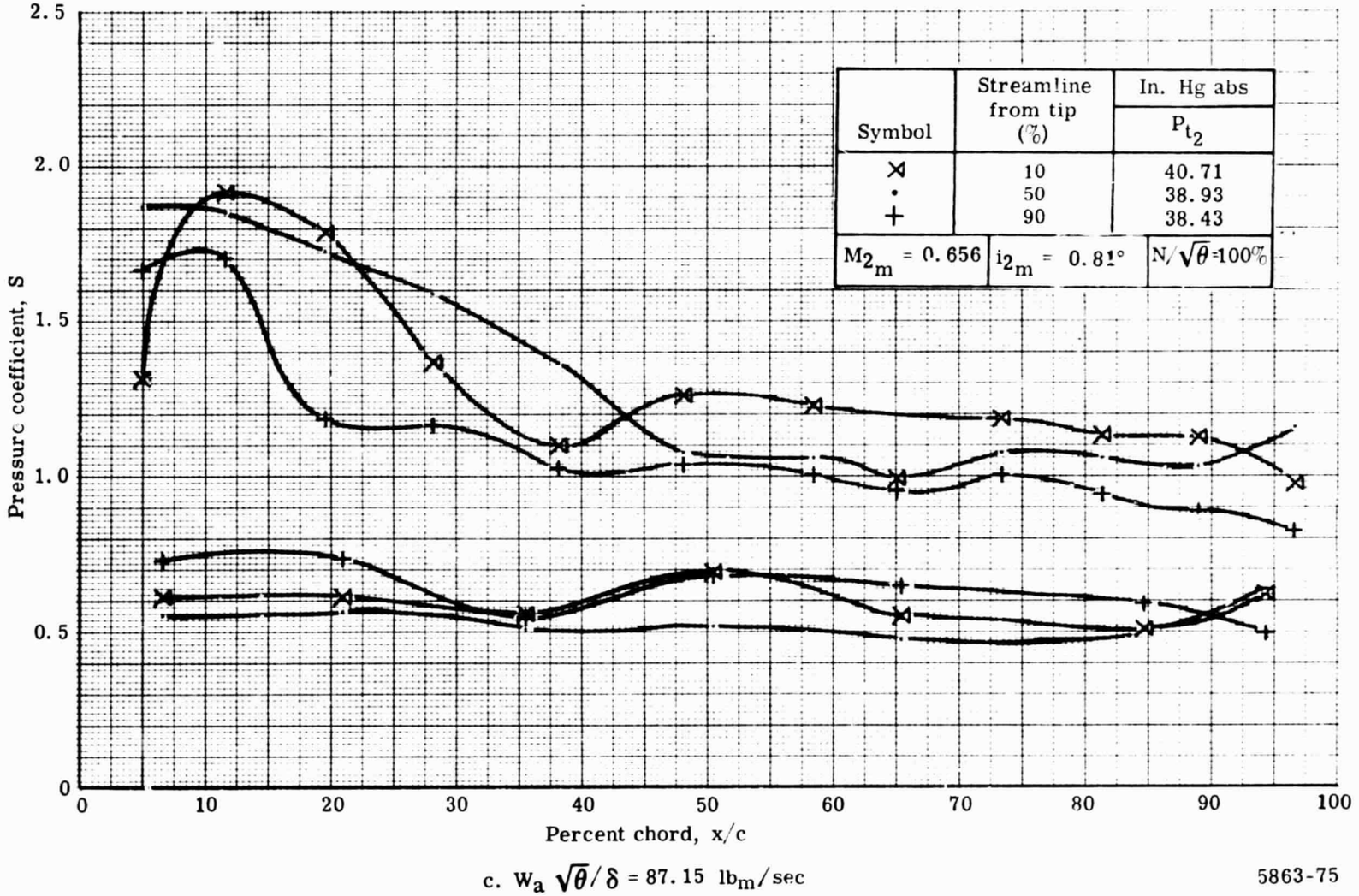

Figure 31. Stator static pressure distribution at 100% speed with minimum wall bleed.

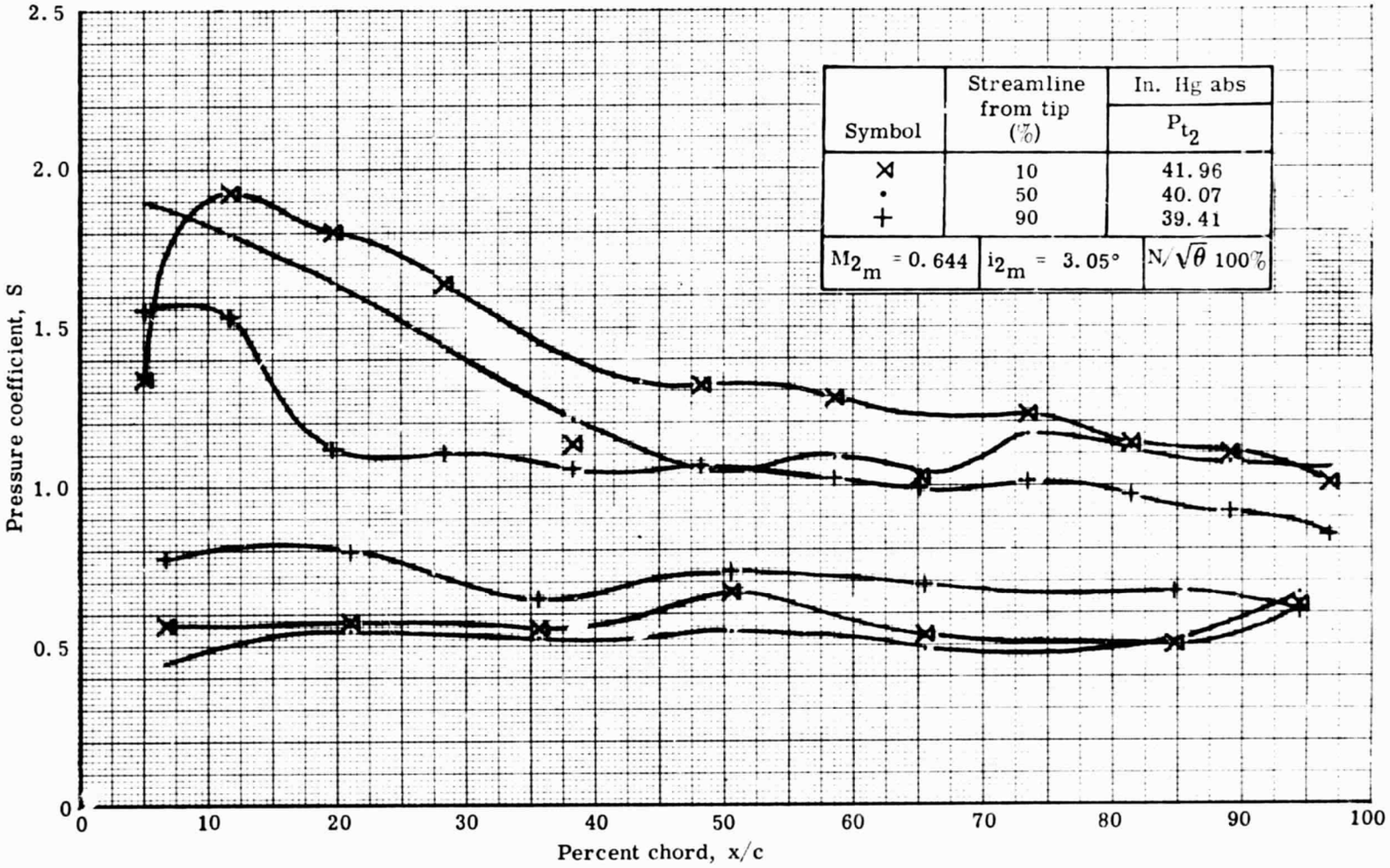

d. $W_a \sqrt{\theta}/\delta$ = 83.50 lb_m/sec

5863-76

Figure 31. Stator static pressure distribution at 100% speed with minimum wall bleed.

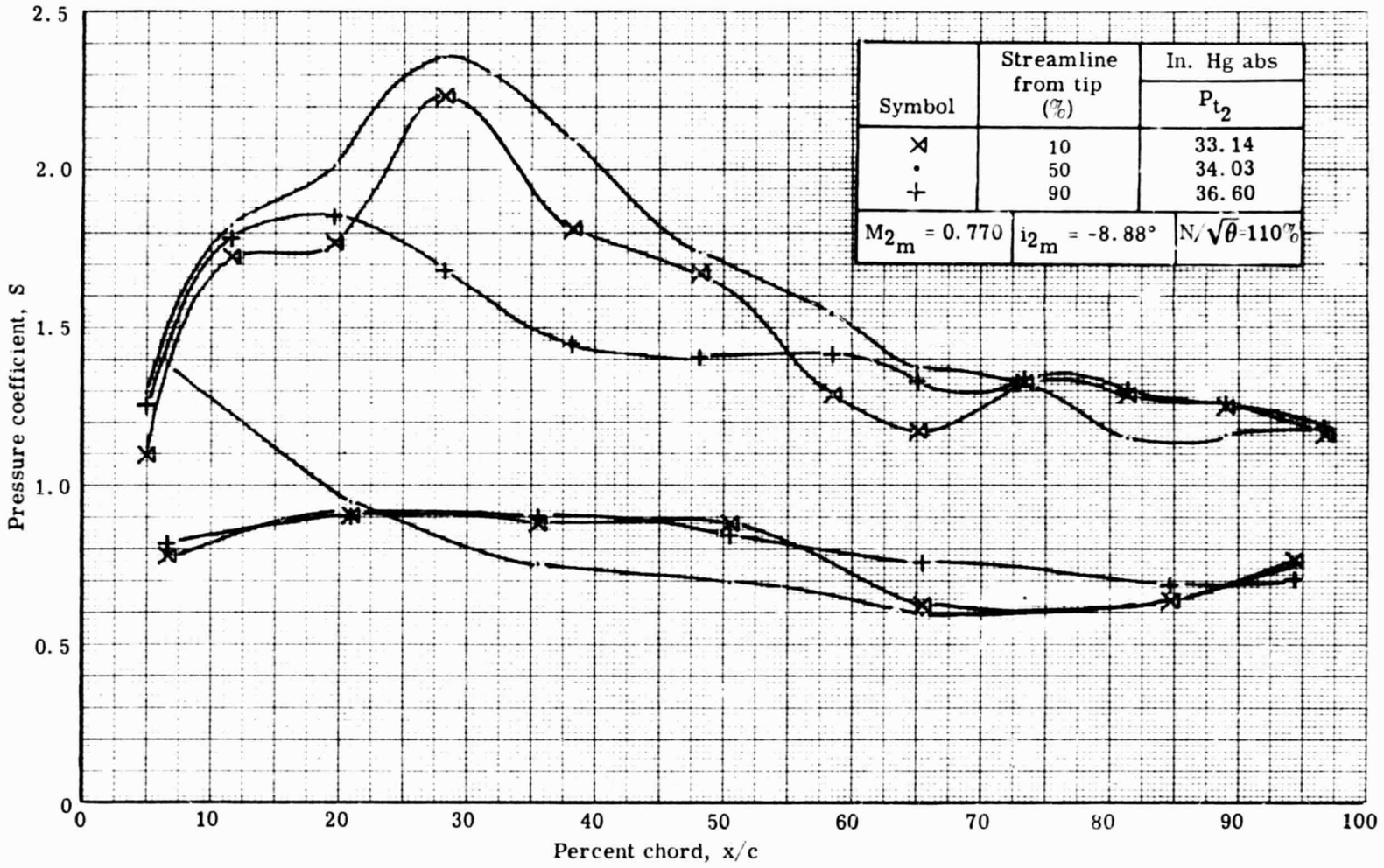

a. $W_a \sqrt{\theta}/\delta$ = 100.38 lb_m/sec

5863-81

Figure 32. Stator static pressure distribution at 110% speed with optimum wall bleed.

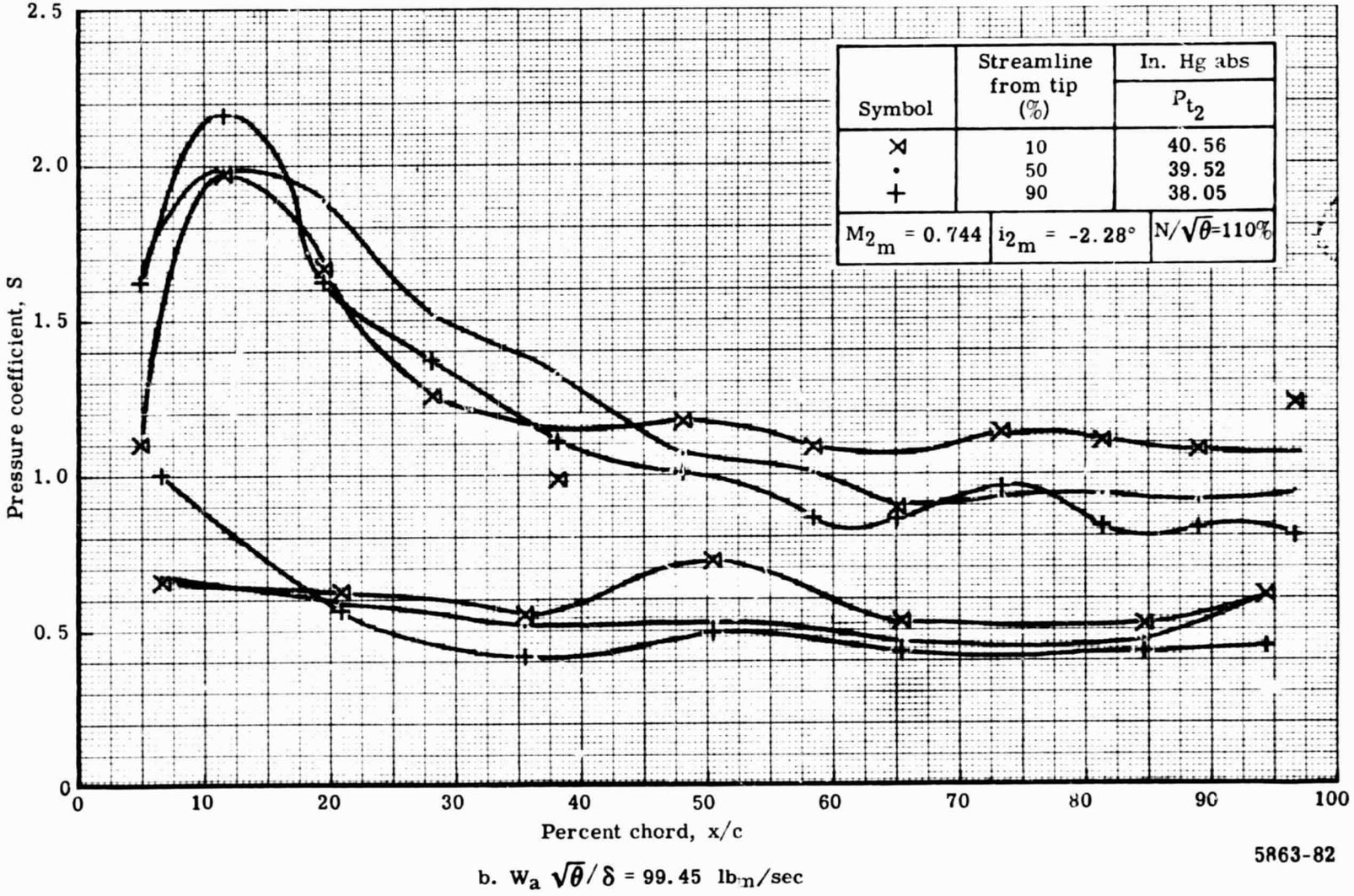

b. $W_a \sqrt{\theta}/\delta$ = 99.45 lb$_m$/sec

Figure 32. Stator static pressure distribution at 110% speed with optimum wall bleed.

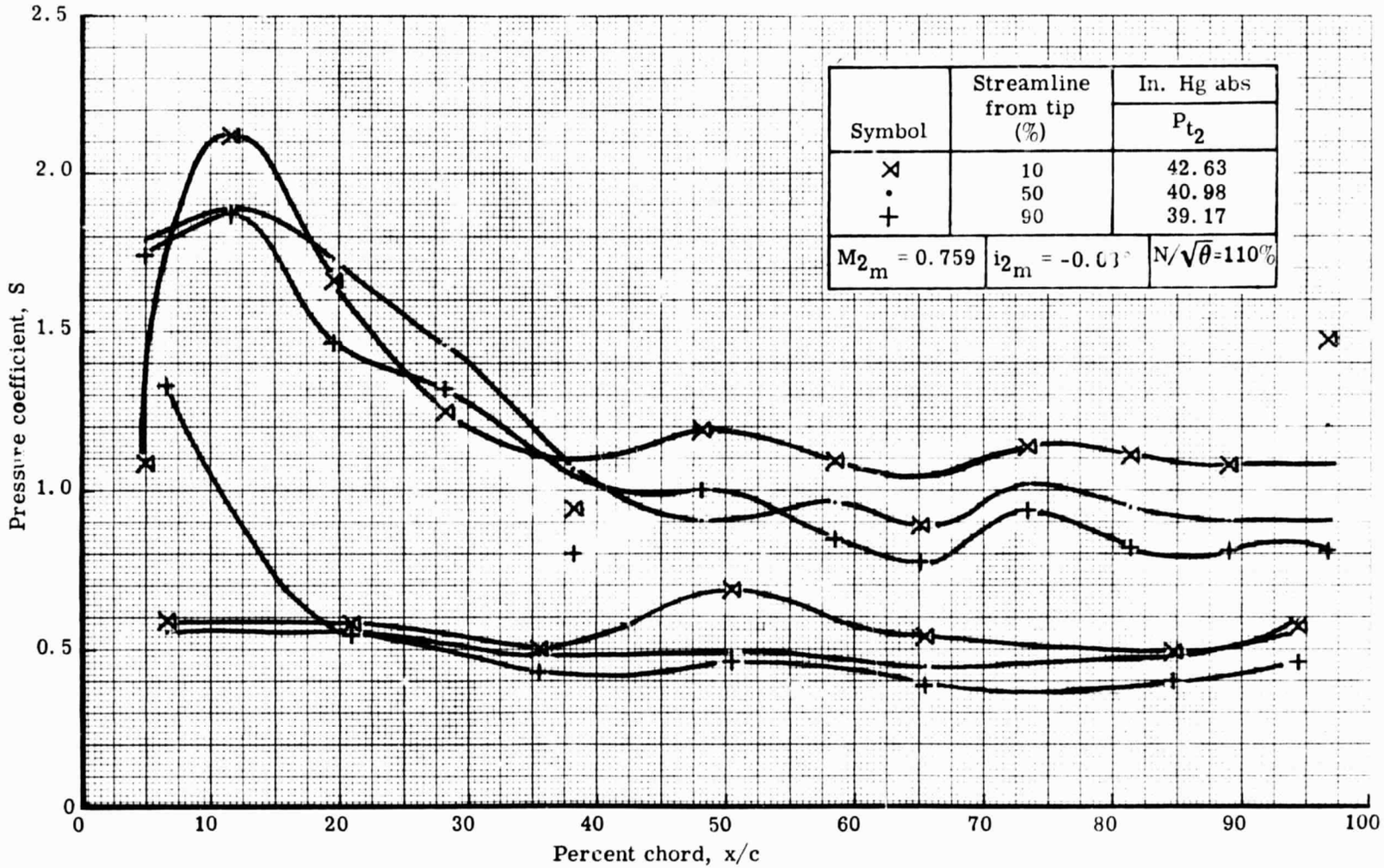

Figure 32. Stator static pressure distribution at 110% speed with optimum wall bleed.

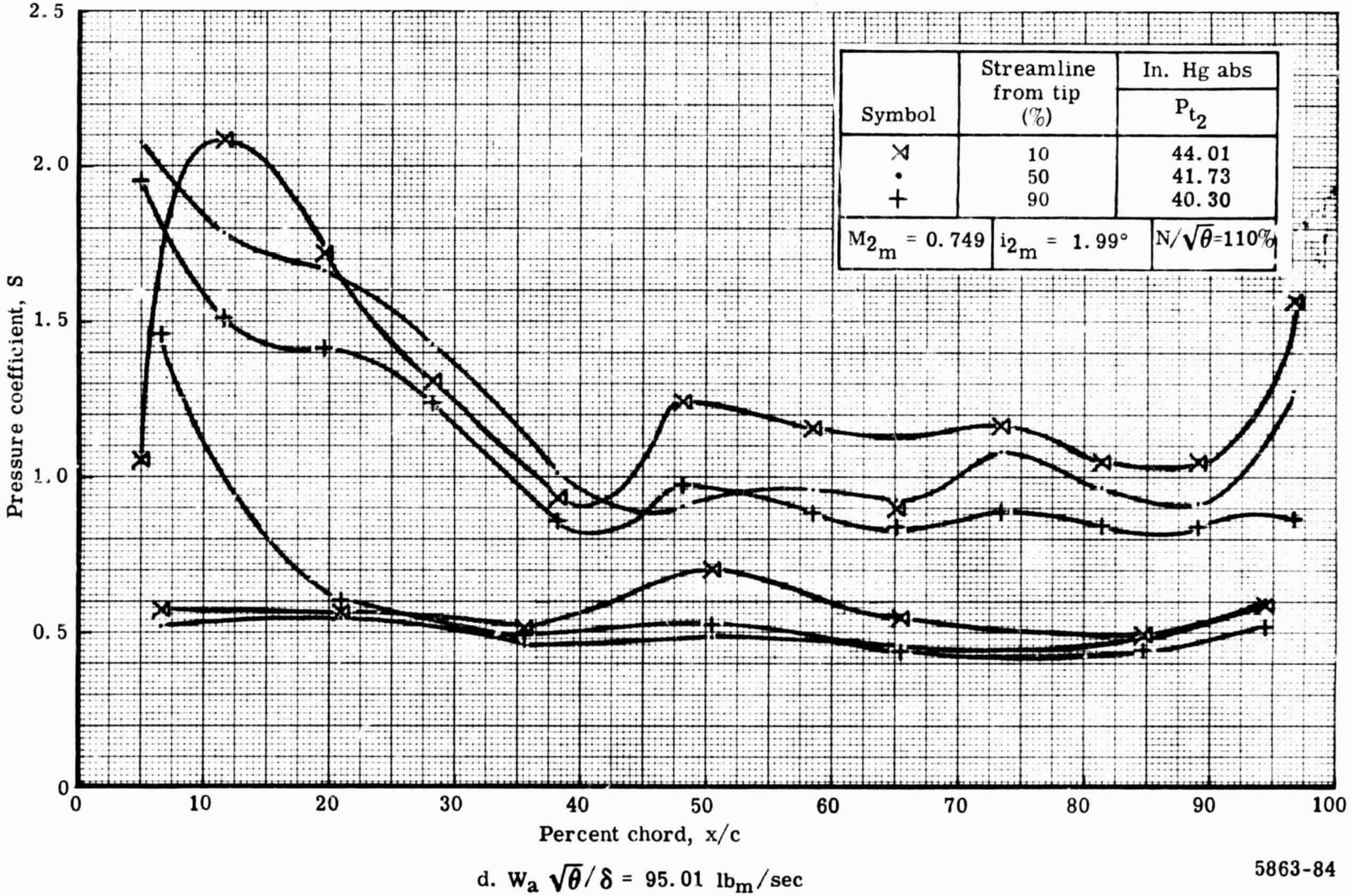

Figure 32. Stator static pressure distribution at 110% speed with optimum wall bleed.

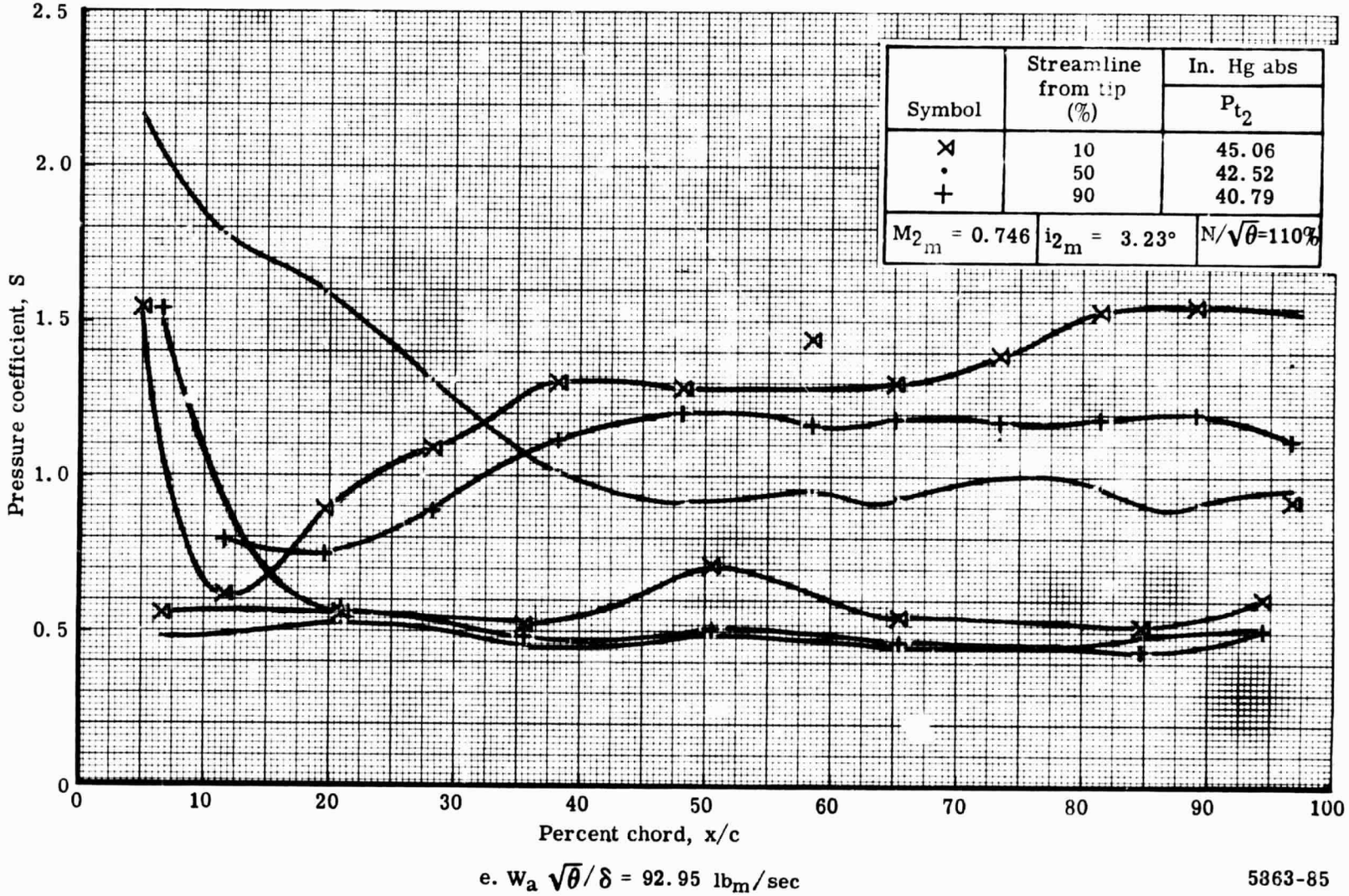

Figure 32. Stator static pressure distribution at 110% speed with optimum wall bleed.

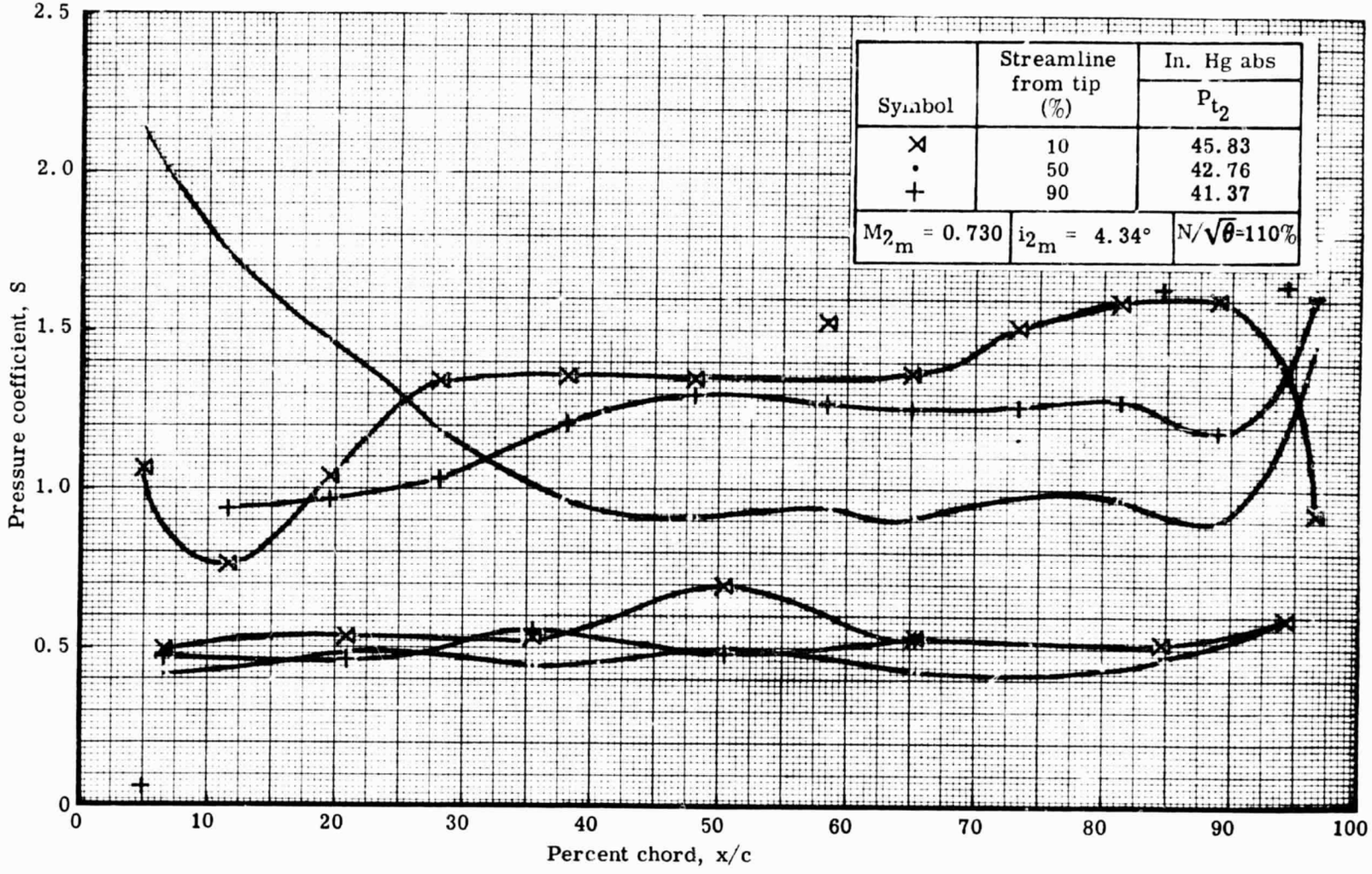

f. $W_a \sqrt{\theta}/\delta$ = 90.80 lb_m/sec

5863-86

Figure 32. Stator static pressure distribution at 110% speed with optimum wall bleed.

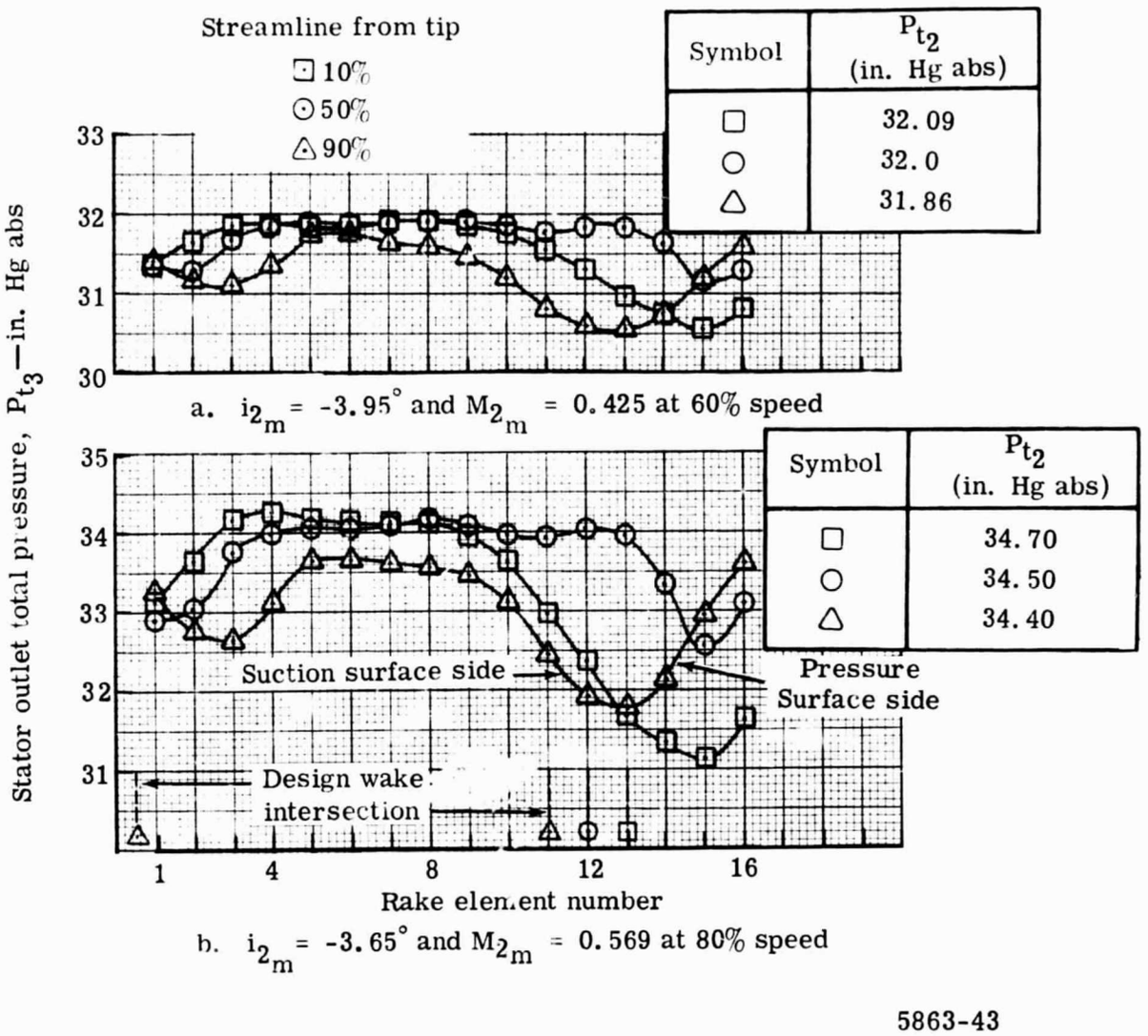

Figure 33. Stator wake surveys with optimum wall bleed.

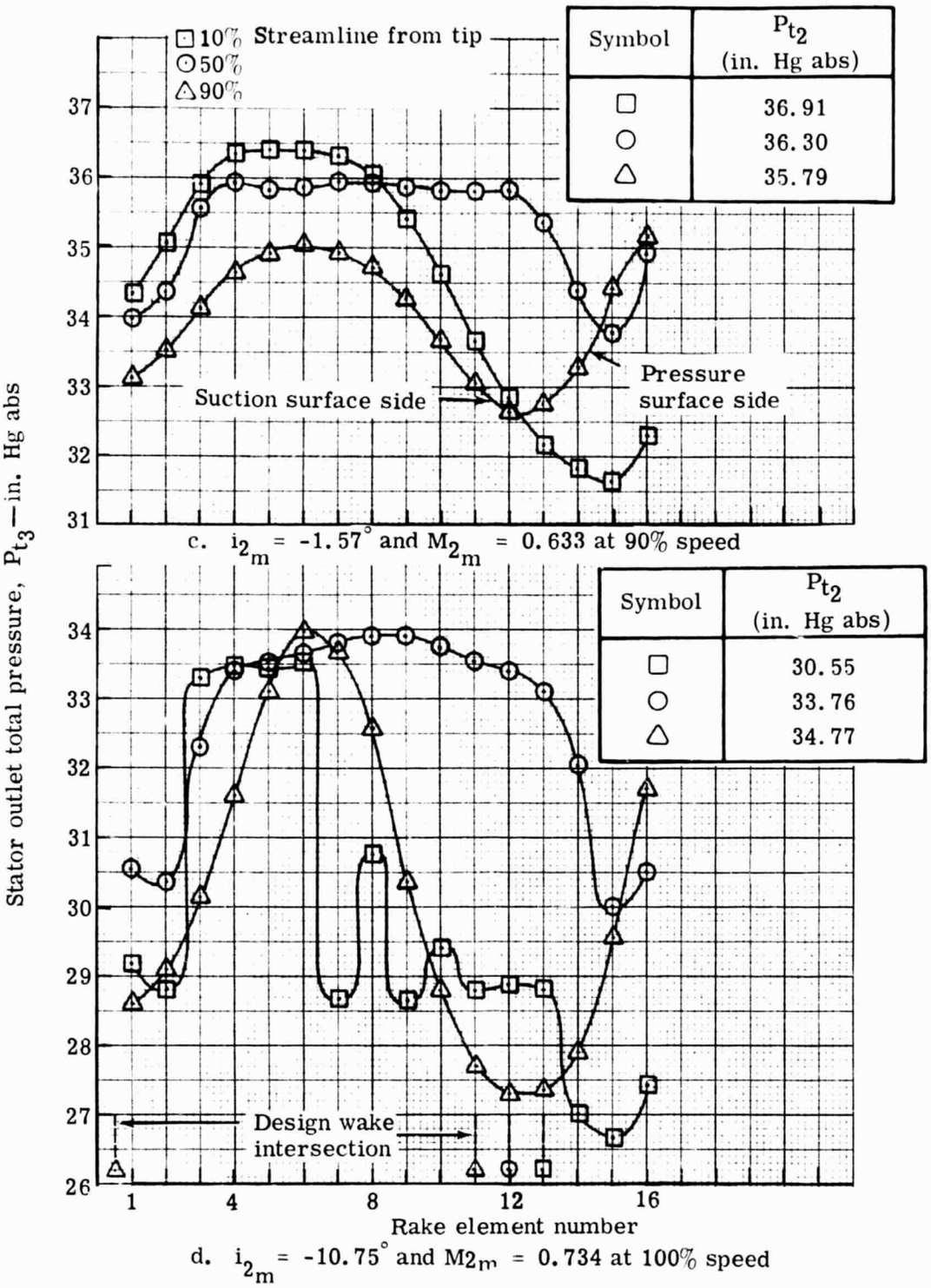

Figure 33. Stator wake surveys with optimum wall bleed.

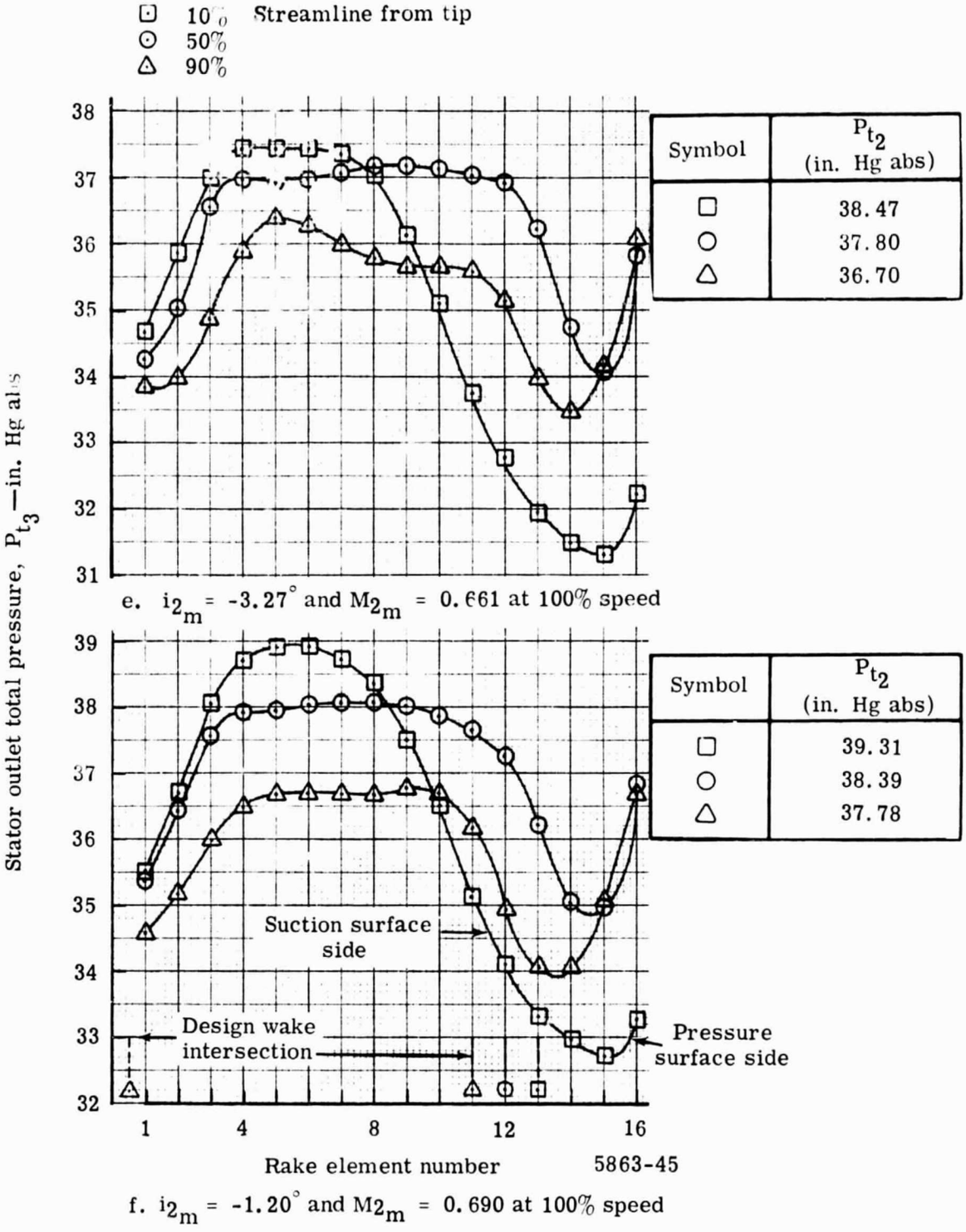

Figure 33. Stator wake surveys with optimum wall bleed.

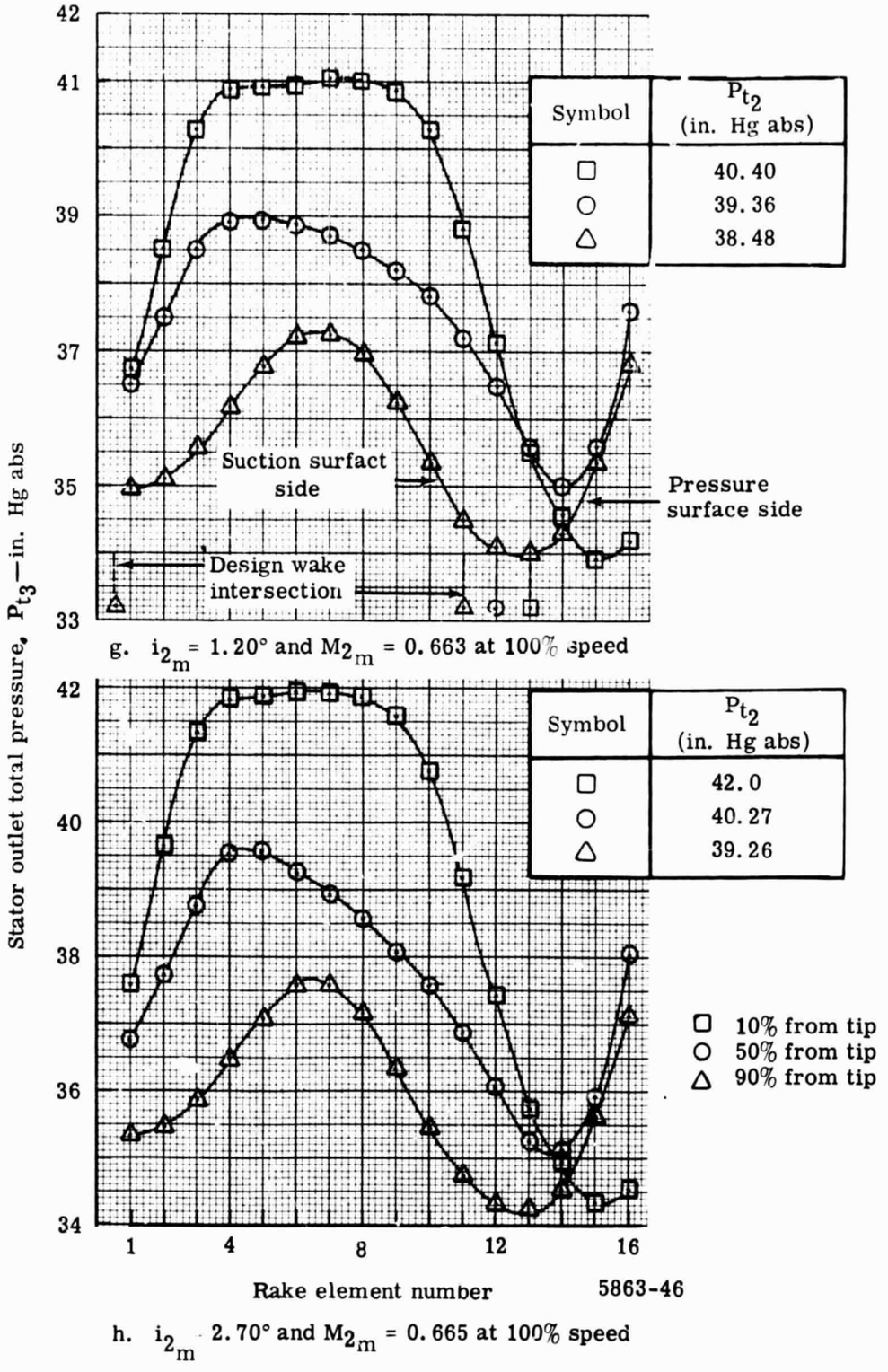

Figure 33. Stator wake surveys with optimum wall bleed.

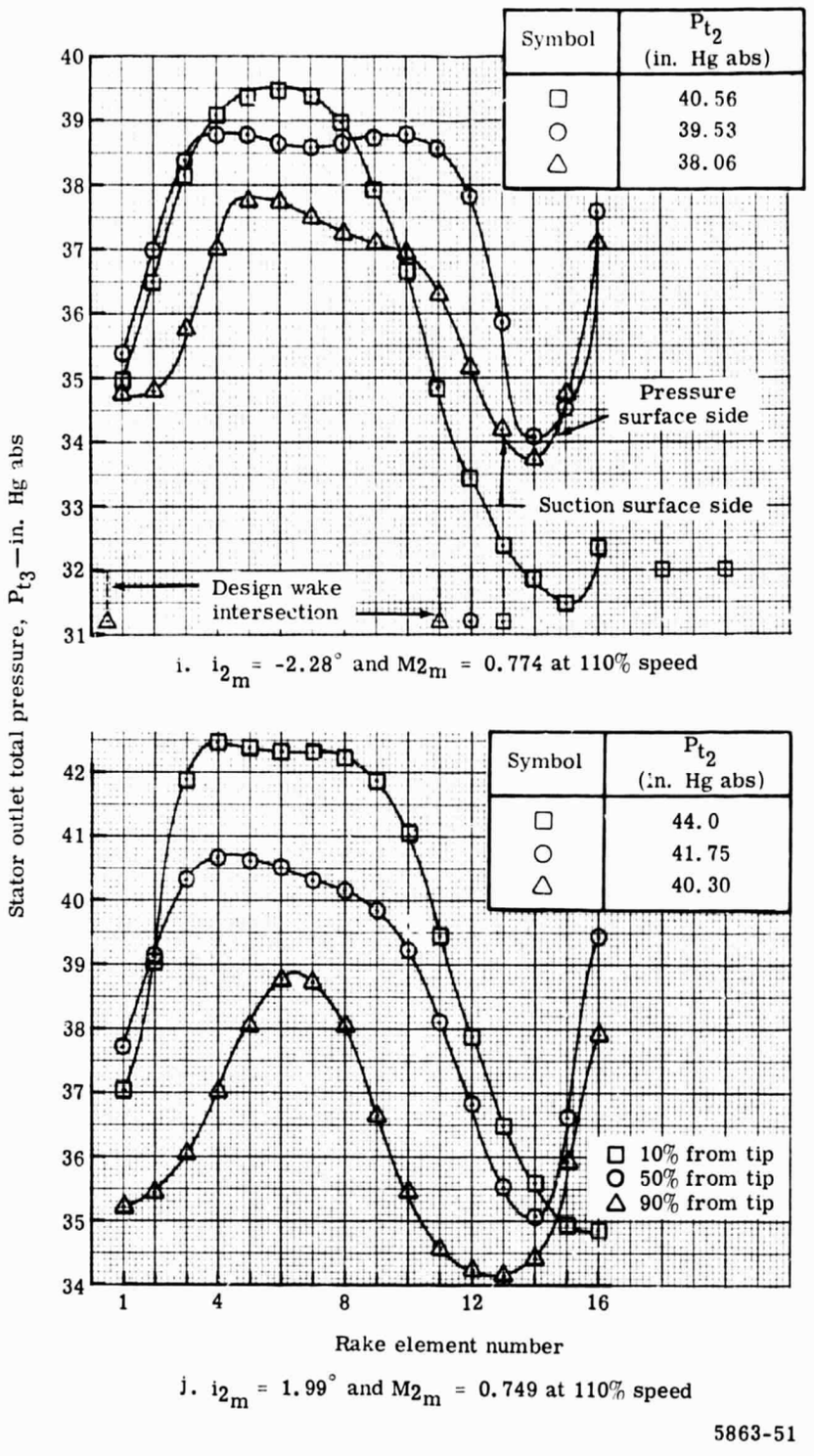

Figure 33. Stator wake surveys with optimum wall bleed

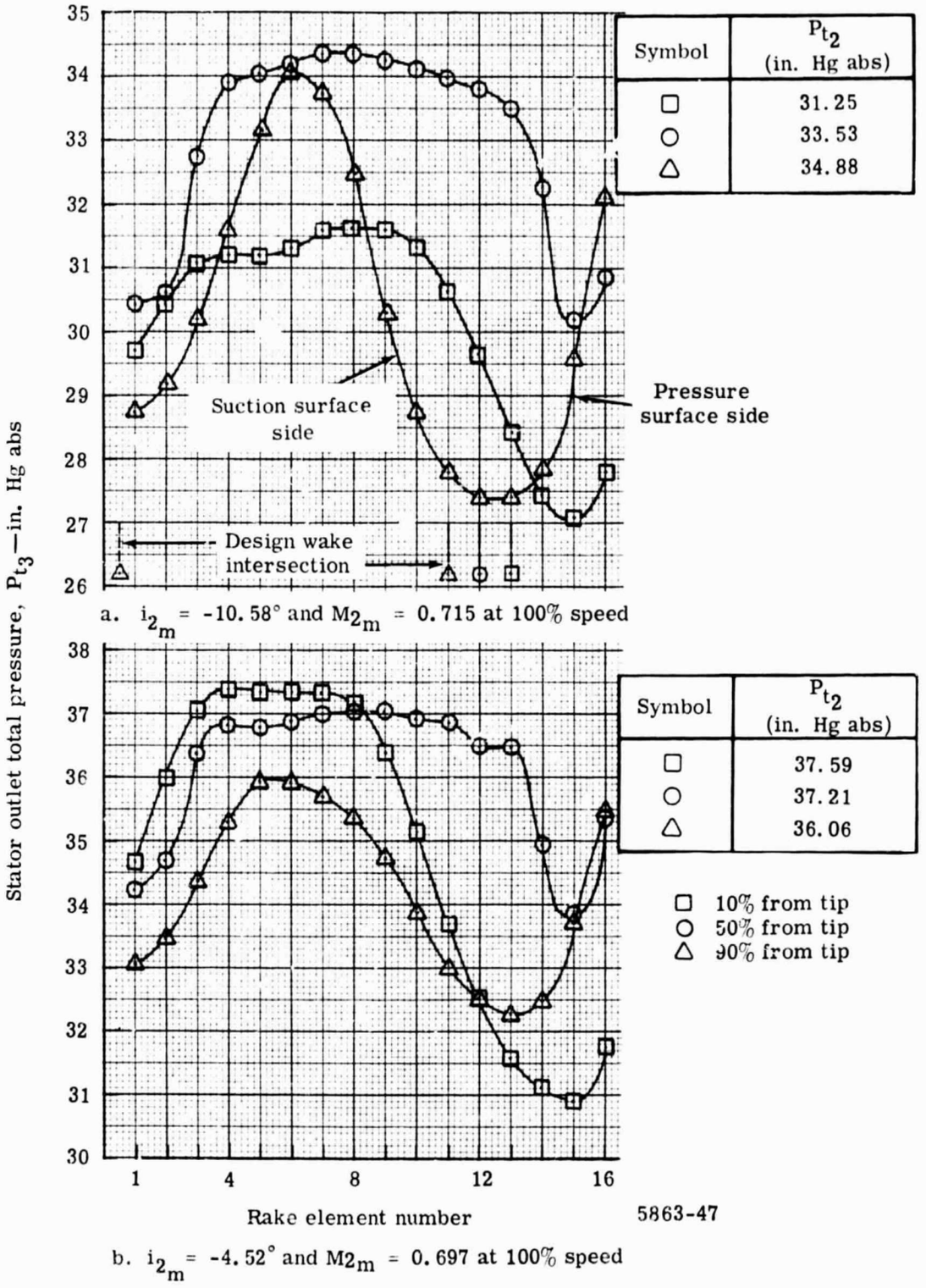

Figure 34. Stator wake surveys with mean wall bleed.

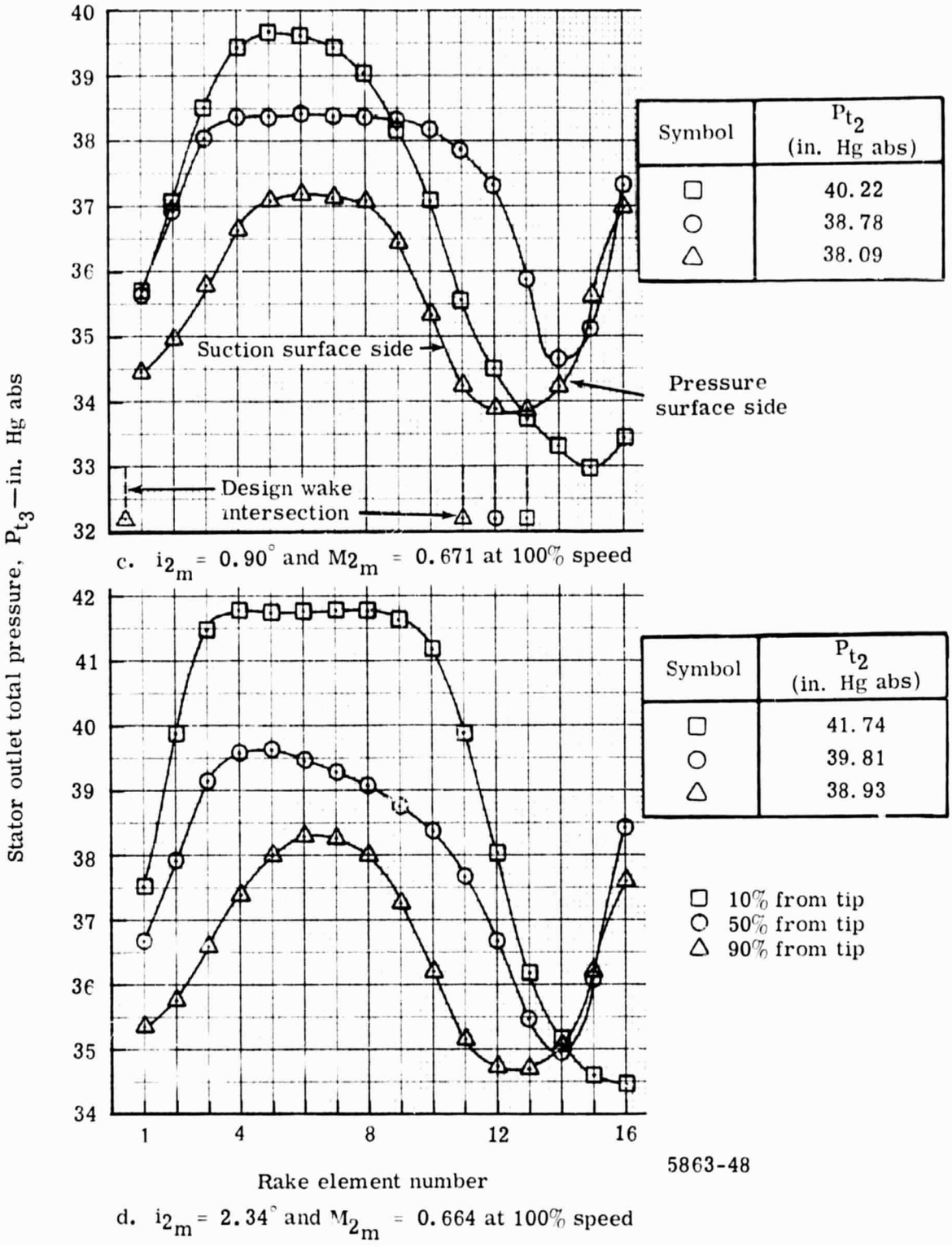

Figure 34. Stator wake surveys with mean wall bleed.

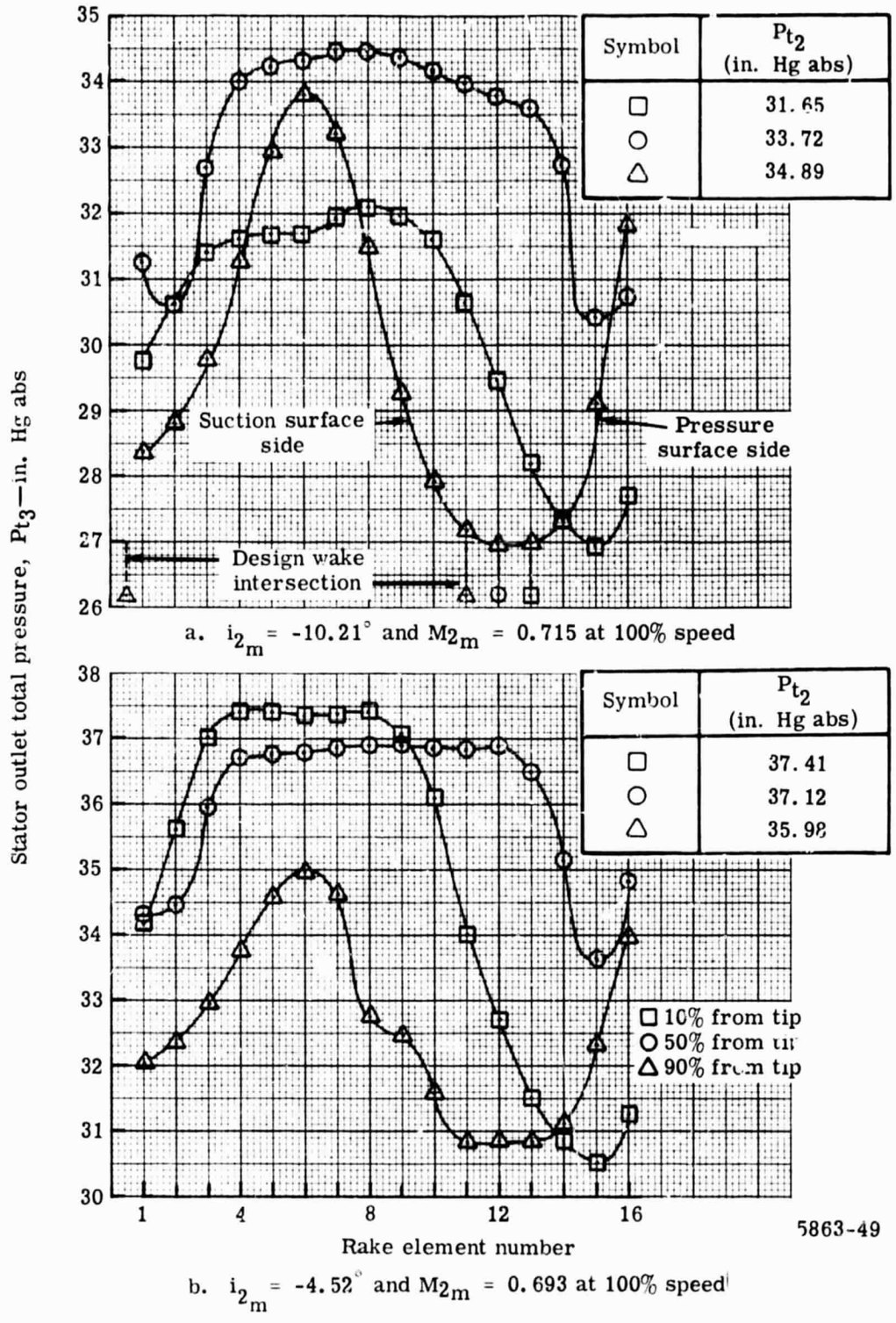

Figure 35. Stator wake surveys with minimum wall bleed.

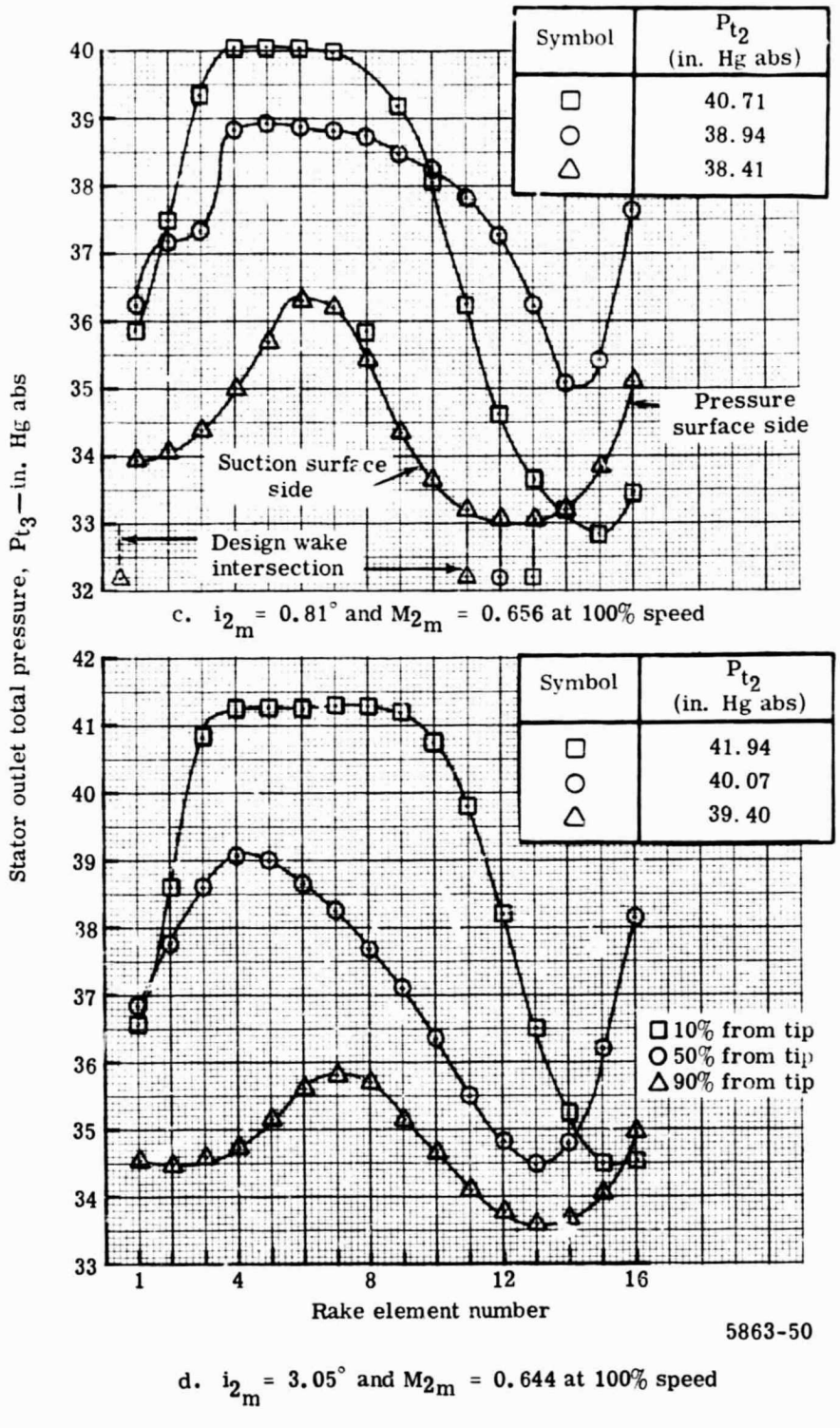

Figure 35. Stator wake surveys with minimum wall bleed.

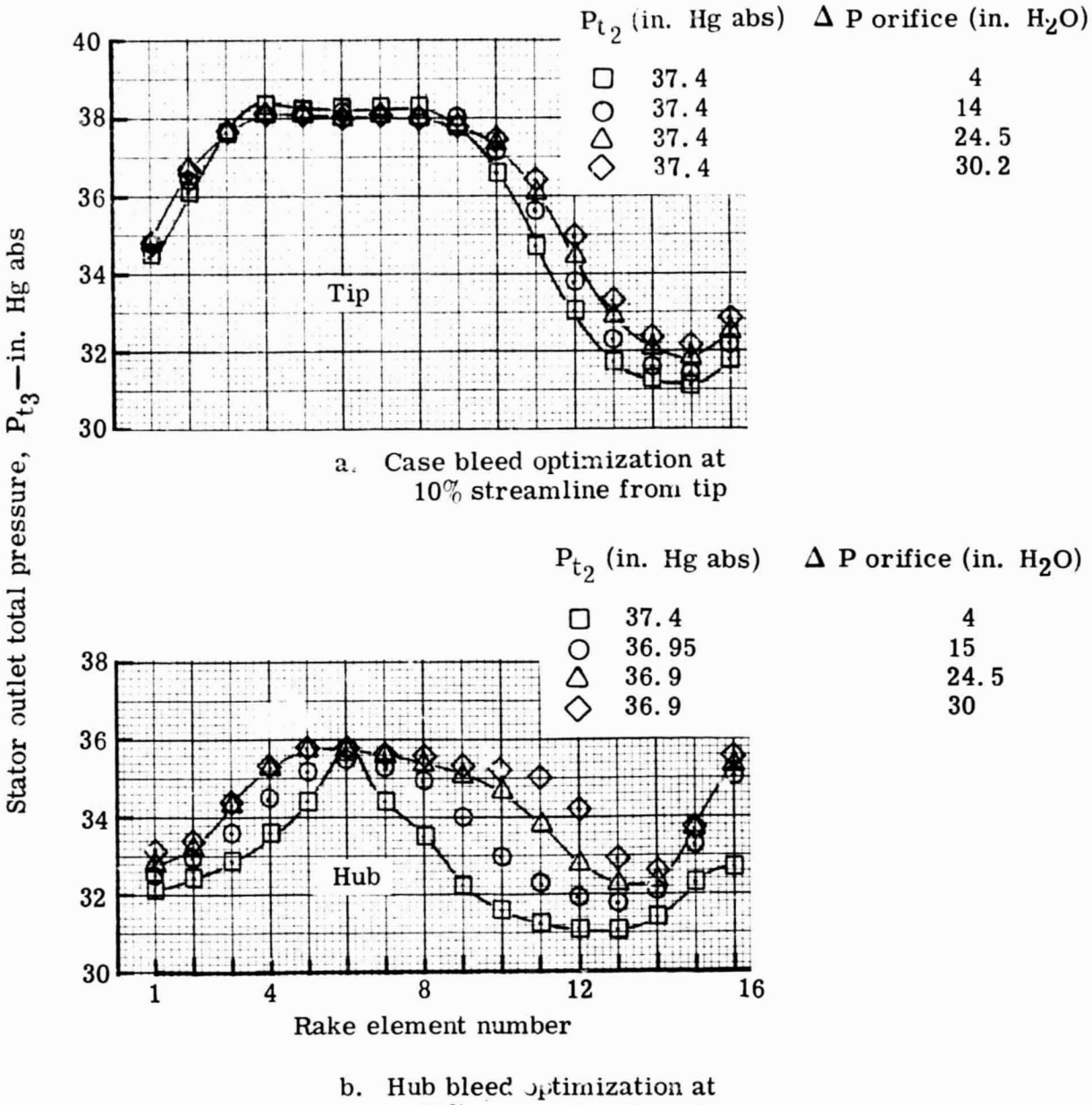

Figure 36. Variation in stator wake at 10 and 90% streamlines from tip during wall bleed optimization.

Table I.

Blade and vane geometry summary.

Blade row	Exit radius (in.)	κ_1 (degrees)	κ_2 (degrees)	ϕ ($\kappa_1 - \kappa_2$)	c (in.)	$\frac{\bar{\sigma}}{\quad}$	t/c	$\delta°$ (degrees)	i_{des} (degrees)	α_{des} (degrees)	n
Design inlet guide vane (63-006 series)	10.49	—	—	—	2.733	1.41	0.06	—	—	17.80	34
	11.51	—	—	—	2.733	1.29	0.06	—	—	16.25	
	12.53	—	—	—	2.733	1.18	0.06	—	—	15.16	
	13.54	—	—	—	2.733	1.09	0.06	—	—	14.36	
	14.58	—	—	—	2.733	1.02	0.06	—	—	13.30	
Rotor blade (double circular arc)	10.97	43.1	9.1	34.0	2.875	1.89	0.078	7.81	0	—	45
	11.86	49.2	21.0	28.2	2.875	1.74	0.052	7.38	0	—	
	12.76	53.4	31.2	22.2	2.875	1.61	0.039	6.34	0	—	
	13.65	56.7	39.1	17.6	2.875	1.51	0.033	5.52	0	—	
	14.54	59.6	44.4	15.2	2.875	1.42	0.032	4.85	0	—	
Stator blade $0.75\ D_{f_H}$ (65 series-circular arc meanline)	11.02	56.16	-17.80	73.96	3.0	1.65	0.10	17.82	-3	—	38
	11.94	54.15	-17.70	71.85	3.0	1.52	0.10	17.70	-3	—	
	12.84	52.74	-17.75	70.49	3.0	1.41	0.10	17.74	-3	—	
	13.71	52.12	-18.05	70.17	3.0	1.32	0.10	18.06	-3	—	
	14.58	50.09	-18.96	69.05	3.0	1.24	0.10	19.03	-3	—	

Table II.

Rotor incidence at minimum and maximum flow for flow generation rotor and complete stage.

Corrected speed (%)	Streamline from tip (%)	Flow generation rotor test		Complete stage test	
		i_{max} (stall) (degrees)	i_{min} (choke) (degrees)	i_{max} (stall) (degrees)	i_{min} (choke) (degrees)
60	10	6.2	- 8.0	5.26	-5.49
	50	6.0	-12.0	6.51	-5.02
	90	7.6	-13.0	8.62	-6.25
80	10	5.4	- 8.0	5.64	-3.22
	50	5.4	- 7.5	6.16	-5.02
	90	8.0	- 8.0	7.19	-5.51
100	10	4.0	- 3.0	4.16	-5.88
	50	4.0	- 4.3	4.20	-3.83
	90	4.7	- 5.0	5.84	-1.54

Table III.

Rotating stall results for complete stage test.

Corrected speed (%)	Corrected airflow (lb_m/sec)	Number of stall cells at streamline from tip		Rotative cell speed (% rpm)	Stall cell frequency (cps)	Comment
		10%	90%			
60	47.39 35.11 43.82	1 1 1	1 1 1	40 27 31	33 22 35.5	Hysteresis points were not dictated by stress considerations
60	43.77	1	1	45	37	Stresses 9.41 cps; stall abrupt, however, there were no high stress problems
80	61.47	1 1	1 1	45 47	52 55	Abrupt stall; stresses were above steady state limit
90	72.08	1	1	44	55	Abrupt stall; stresses were approaching the transient limit
100	79.33	1 1	1 1	46 45	64 62	Stress limited, abrupt stall; maximum stresses observed were with wall bleed at optimum rate
100	79.71	5 6	5 6	44 42	300 350	Stress limited, abrupt stall; stresses were above the steady state limit; wall bleed held at minimum rate
100	80.81	1	1	46	64	Wall bleed at mean rate; stress limited, abrupt stall
100	83.75	2	2	40	110	Intermittent stall; stresses above steady-state limit; wall bleed at mean rate
110	86.57	1	1	44	67	Abrupt stall observed with stresses of 13,500 psi which were above the steady-state limit

Table IVa.

Blade element performance for complete stage.

PERCENT DESIGN SPEED = 59.74

CORRECTED WEIGHT FLOW = 66.25

CORRECTED ROTOR SPEED = 5014.92

PRESSURE RATIO = 1.0718

ADIABATIC EFFICIENCY = 86.8524

Optimum Bleed

ROTOR 1

STATION 1 - STATION 2

	10	30	50	70	90
DIA 1	29.150	27.080	25.060	23.020	20.938
DIA 2	29.088	27.302	25.516	23.730	21.944
BETA 1	19.021	21.559	22.850	24.764	27.244
BETA 2	34.558	36.462	39.879	40.664	42.485
BETA(PR) 1	56.109	52.581	48.675	43.986	38.748
BETA(PR) 2	47.642	40.981	32.763	24.924	15.669
V 1	364.63	370.87	378.27	385.30	388.50
V 2	428.88	457.82	487.40	518.16	539.26
VZ 1	344.72	344.92	348.58	349.87	345.40
VZ 2	353.20	368.20	374.03	393.04	397.68
V-THETA 1	118.84	136.28	146.89	161.39	177.85
V-THETA 2	243.27	272.08	312.51	337.65	364.23
V(PR) 1	618.2	567.7	527.9	486.3	442.9
V(PR) 2	524.2	487.7	444.8	431.0	413.0
VTHETA PR1	513.2	450.8	396.4	337.7	277.2
VTHETA PR2	387.4	319.9	240.7	176.8	111.5
U 1	632.00	587.12	543.32	496.10	455.04
U 2	630.66	591.93	553.21	514.49	475.77
M 1	0.3334	0.3393	0.3462	0.3528	0.3558
M 2	0.3880	0.4152	0.4429	0.4715	0.4914
M(PR) 1	0.5653	0.5193	0.4832	0.4453	0.4056
M(PR) 2	0.4742	0.4424	0.4042	0.3922	0.3764
TURN(PR)	8.466	11.601	15.912	19.762	23.079
LOSS COEF.	0.0881	0.0537	0.0474	0.0608	0.0600
DFAC	0.2237	0.2170	0.2479	0.2076	0.1648
EFFP	0.8318	0.9098	0.9329	0.9311	0.9443
EFF	0.8298	0.9087	0.9320	0.9301	0.9435
LOSS PARA.	0.0209	0.0134	0.0122	0.0157	0.0151
INCID	-3.49	-4.32	-5.02	-5.81	-6.25
DEV	2.542	2.181	1.963	3.524	6.969

CORRECTED WEIGHT FLOW

UPSTREAM OF ROTOR	66.25
UPSTREAM OF STATOR	66.25
DOWNSTREAM OF STATOR	62.73

STATOR 1

STATION 2 - STATION 3

	10	30	50	70	90
DIA 3	29.164	27.422	25.672	23.874	22.034
BETA 2	34.558	36.462	39.879	40.664	42.485
BETA 3	-5.306	-5.306	-6.005	-5.656	-5.831
V 2	428.88	457.82	487.40	518.16	539.26
V 3	314.03	324.73	342.27	356.60	337.83
VZ 2	353.20	368.20	374.03	393.04	397.68
VZ 3	312.68	323.34	340.39	354.86	336.08
V-THETA 2	243.27	272.08	312.51	337.65	364.22
V-THETA 3	-29.04	-30.03	-35.81	-35.14	-34.32
M 2	0.3880	0.4152	0.4429	0.4715	0.4914
M 3	0.2822	0.2922	0.3081	0.3211	0.3036
TURN	39.864	41.769	45.885	46.321	48.316
LOSS COEF.	0.0309	0.0367	0.0302	0.0430	0.1033
DFAC	0.5228	0.5393	0.5490	0.5471	0.5968
LOSS PARA.	0.0123	0.0138	0.0106	0.0140	0.0310
INCID	-17.52	-15.68	-12.82	-13.34	-13.46
DEV	13.454	12.734	11.745	12.024	11.969

Table IVb.

Blade element performance for complete stage.

PERCENT DESIGN SPEED = 59.97

CORRECTED WEIGHT FLOW = 61.17

CORRECTED ROTOR SPEED = 5017.33

PRESSURE RATIO = 1.1145

ADIABATIC EFFICIENCY = 89.7287

OPTIMUM BLEED

ROTOR 1

STATION 1 - STATION 2

	10	30	50	70	90
DIA 1	29.153	27.080	25.060	23.020	20.988
DIA 2	29.088	27.302	25.516	23.730	21.944
BETA 1	19.023	21.558	22.652	23.993	25.079
BETA 2	40.374	42.131	44.552	45.997	47.376
BETA(PR) 1	58.589	55.212	51.928	48.052	43.244
BETA(PR) 2	46.982	41.168	33.231	24.588	15.920
V 1	337.03	343.90	347.34	350.40	356.48
V 2	430.45	448.39	473.18	495.75	511.84
VZ 1	318.62	319.85	320.55	320.21	322.97
VZ 2	327.93	332.53	337.20	344.40	346.61
V-THETA 1	109.85	126.36	133.77	142.52	151.10
V-THETA 2	278.83	300.79	331.96	356.59	376.62
V(PR) 1	611.4	560.6	519.8	479.0	443.2
V(PR) 2	480.7	441.7	403.1	378.7	360.4
VTHETA PR1	521.8	460.4	409.2	356.3	303.7
VTHETA PR2	351.4	290.8	220.9	157.6	98.9
U 1	631.62	586.77	543.00	498.79	454.77
U 2	630.27	591.58	552.88	514.18	475.48
M 1	0.3080	0.3145	0.3177	0.3206	0.3262
M 2	0.3884	0.4056	0.4286	0.4497	0.4650
M(PR) 1	0.5589	0.5126	0.4754	0.4382	0.4056
M(PR) 2	0.4337	0.3996	0.3652	0.3435	0.3274
TURN(PR)	11.607	14.044	18.697	23.464	27.324
LOSS COEF.	0.0617	0.0338	0.0407	0.0529	0.0729
DFAC	0.3120	0.3119	0.3356	0.3272	0.3071
EFFP	0.9089	0.9550	0.9538	0.9494	0.9390
EFF	0.9074	0.9542	0.9530	0.9485	0.9380
LOSS PARA.	0.0148	0.0084	0.0105	0.0137	0.0182
INCID	-1.01	-1.69	-1.77	-1.75	-1.76
DEV	1.882	2.368	2.431	3.888	7.220

CORRECTED WEIGHT FLOW

UPSTREAM OF ROTOR	61.17
UPSTREAM OF STATOR	61.17
DOWNSTREAM OF STATOR	57.52

STATOR 1

STATION 2 - STATION 3

	10	30	50	70	90
DIA 3	29.164	27.422	25.672	23.874	22.034
BETA 2	40.374	42.131	44.552	45.997	47.376
BETA 3	-5.831	-4.956	-5.481	-6.180	-6.005
V 2	430.45	448.39	473.18	495.75	511.84
V 3	289.54	305.38	310.24	312.20	302.92
VZ 2	327.93	332.53	337.20	344.40	346.61
VZ 3	288.04	304.24	308.82	310.39	301.26
V-THETA 2	278.93	300.79	331.96	356.59	376.62
V-THETA 3	-29.41	-26.38	-29.63	-33.61	-31.69
M 2	0.3884	0.4056	0.4286	0.4497	0.4650
M 3	0.2591	0.2739	0.2784	0.2802	0.2715
TURN	46.204	47.087	50.033	52.177	53.382
LOSS COEF.	0.1271	0.0609	0.0616	0.0654	0.0738
DFAC	0.6149	0.5939	0.6131	0.6276	0.6492
LOSS PARA.	0.0508	0.0229	0.0216	0.0213	0.0222
INCID	-11.71	-10.01	-8.15	-8.00	-8.57
DEV	13.129	13.084	12.269	11.500	11.795

Table IVc.

Blade element performance for complete stage.

PERCENT DESIGN SPEED = 60.02

CORRECTED WEIGHT FLOW = 57.57

CORRECTED ROTOR SPEED = 5021.55

PRESSURE RATIO = 1.1262

ADIABATIC EFFICIENCY = 87.7723

OPTIMUM BLEED

ROTOR 1

STATION 1 - STATION 2

	10	30	50	70	90
DIA 1	29.150	27.080	25.060	23.020	20.988
DIA 2	29.088	27.302	25.516	23.730	21.944
BETA 1	19.965	21.736	22.959	24.050	24.957
BETA 2	44.009	46.114	48.749	50.420	51.196
BETA(PR) 1	60.873	58.632	54.262	51.067	45.876
BETA(PR) 2	46.616	41.500	32.865	24.358	15.479
V 1	312.65	310.11	325.54	324.65	327.50
V 2	433.39	443.89	469.88	485.93	499.53
VZ 1	295.68	288.06	299.75	296.47	296.92
VZ 2	311.71	307.72	309.82	309.62	313.03
V-THETA 1	101.62	114.84	126.99	132.31	138.19
V-THETA 2	301.11	319.92	353.27	374.52	389.28
V(PR) 1	607.5	553.4	513.2	471.8	434.4
V(PR) 2	453.8	410.9	368.9	339.9	324.8
VTHETA PR1	530.6	472.5	416.6	367.0	317.0
VTHETA PR2	329.8	272.2	200.2	140.2	86.7
U 1	632.25	587.36	543.54	499.30	455.22
U 2	630.91	592.17	553.43	514.70	475.96
M 1	0.2853	0.2830	0.2973	0.2965	0.2991
M 2	0.3899	0.4003	0.4246	0.4399	0.4525
M(PR) 1	0.5544	0.5050	0.4687	0.4308	0.3967
M(PR) 2	0.4083	0.3705	0.3333	0.3077	0.2943
TURN(PR)	14.257	17.132	21.397	26.709	31.398
LOSS COEF.	0.0677	0.0349	0.0420	0.0255	0.0701
DFAC	0.3695	0.3770	0.4106	0.4162	0.3903
EFFP	0.9140	0.9604	0.9580	0.9782	0.9475
EFF	0.9123	0.9597	0.9572	0.9778	0.9465
LOSS PARA.	0.0164	0.0086	0.0108	0.0066	0.0175
INCID	1.27	1.73	0.56	1.27	1.88
DEV	1.515	2.700	2.065	3.658	6.778

CORRECTED WEIGHT FLOW

UPSTREAM OF ROTOR	57.57
UPSTREAM OF STATOR	57.57
DOWNSTREAM OF STATOR	53.84

STATOR 1

STATION 2 - STATION 3

	10	30	50	70	90
DIA 3	29.164	27.422	25.672	23.874	22.034
BETA 2	44.009	46.114	48.749	50.420	51.196
BETA 3	-4.255	-4.781	-5.481	-5.306	-6.529
V 2	433.39	443.89	469.88	485.93	499.53
V 3	285.15	293.03	296.34	282.17	260.70
VZ 2	311.71	307.72	309.82	309.62	313.03
VZ 3	284.36	292.01	294.98	280.96	259.01
V-THETA 2	301.11	319.92	353.27	374.52	389.28
V-THETA 3	-21.16	-24.42	-28.31	-26.09	-29.64
M 2	0.3899	0.4003	0.4246	0.4399	0.4526
M 3	0.2544	0.2620	0.2651	0.2523	0.2329
TURN	48.264	50.895	54.230	55.726	57.725
LOSS COEF.	0.1284	0.0547	0.0626	0.0791	0.0978
DFAC	0.6407	0.6321	0.6549	0.6889	0.7315
LOSS PARA.	0.0514	0.0206	0.0219	0.0258	0.0294
INCID	-8.07	-6.03	-3.95	-3.58	-4.75
DEV	14.705	13.259	12.269	12.374	11.271

Table IVd.

Blade element performance for complete stage.

PERCENT DESIGN SPEED = 59.94

CORRECTED WEIGHT FLOW = 52.97

CORRECTED ROTOR SPEED = 5014.92

PRESSURE RATIO = 1.1438

ADIABATIC EFFICIENCY = 89.8999

OPTIMUM BLEED

ROTOR 1

STATION 1 - STATION 2

	10	30	50	70	90
DIA 1	29.150	27.080	25.060	23.020	20.988
DIA 2	29.098	27.302	25.516	23.730	21.944
BETA 1	18.929	20.192	22.748	24.670	25.855
BETA 2	48.574	50.004	52.560	52.480	53.367
BETA(PR) 1	62.856	60.028	56.927	53.937	49.455
BETA(PR) 2	45.334	39.398	31.474	23.397	13.341
V 1	291.27	297.58	301.32	299.65	305.73
V 2	444.28	457.35	474.29	486.81	503.90
VZ 1	275.52	279.29	277.88	277.30	275.17
VZ 2	293.96	293.96	288.33	296.48	300.67
V-THETA 1	94.49	102.71	116.51	125.07	133.33
V-THETA 2	333.13	350.37	376.59	386.11	404.37
V(PR) 1	603.9	559.1	509.2	462.6	423.2
V(PR) 2	418.2	380.4	338.1	323.0	309.0
VTHETA PR1	537.4	484.3	426.7	373.9	321.6
VTHETA PR2	297.4	241.4	176.5	128.3	71.7
U 1	631.87	587.00	543.22	499.00	454.05
U 2	630.53	591.81	553.10	514.39	475.67
M 1	0.2654	0.2712	0.2746	0.2731	0.2787
M 2	0.3986	0.4116	0.4276	0.4396	0.4553
M(PR) 1	0.5502	0.5095	0.4641	0.4216	0.3859
M(PR) 2	0.3752	0.3423	0.3048	0.2917	0.2792
TURN(PR)	17.522	20.630	25.453	30.541	36.114
LOSS COEF.	0.0890	0.0412	0.0377	0.0216	0.0944
DFAC	0.4477	0.4629	0.4868	0.4525	0.4239
EFFP	0.9013	0.9574	0.9666	0.9841	0.9809
EFF	0.8992	0.9565	0.9640	0.9837	0.9387
LOSS PARA.	0.0221	0.0105	0.0099	0.0056	0.0232
INCID	3.25	3.13	3.23	4.14	4.45
DEV	0.234	0.598	0.674	2.497	4.641

CORRECTED WEIGHT FLOW

UPSTREAM OF ROTOR	52.97
UPSTREAM OF STATOR	52.97
DOWNSTREAM OF STATOR	49.15

STATOR 1

STATION 2 - STATION 3

	10	30	50	70	90
DIA 3	29.164	27.422	25.672	23.874	22.034
BETA 2	48.574	50.004	52.560	52.480	53.367
BETA 3	-10.079	-6.355	-4.255	-5.306	-5.306
V 2	444.28	457.35	474.29	486.81	503.90
V 3	283.00	300.93	291.01	265.43	226.20
VZ 2	293.96	293.96	288.33	296.48	300.67
VZ 3	278.63	299.08	290.21	264.29	225.24
V-THETA 2	333.13	350.37	376.59	386.11	404.37
V-THETA 3	-49.53	-33.31	-21.59	-24.55	-20.92
M 2	0.3986	0.4116	0.4276	.4396	0.4553
M 3	0.2516	0.2684	0.2596	0.2367	0.2014
TURN	58.653	56.359	5 6	57.786	58.674
LOSS COEF.	0.1320	0.0506	0. 26	0.0540	0.1554
DFAC	0.7049	0.6581	0. 316	0.7306	0.8061
LOSS PARA.	0.0522	0.0189	0.0219	0.0306	0.0468
INCID	-3.51	-2.14	-0.14	-1.52	-2.58
DEV	8.881	11.685	13.695	12.374	12.494

Table IVe.

Blade element performance for complete stage.

PERCENT DESIGN SPEED = 59.91

CORRECTED WEIGHT FLOW = 48.76

CORRECTED ROTOR SPEED = 5012.28

PRESSURE RATIO = 1.1525

ADIABATIC EFFICIENCY = 82.0855

OPTIMUM BLEED

ROTOR 1

STATION 1 - STATION 2

	10	30	50	70	90
DIA 1	29.153	27.080	25.060	23.020	20.988
DIA 2	29.088	27.302	25.516	23.730	21.944
BETA 1	19.024	21.095	22.647	24.757	25.742
BETA 2	54.808	53.510	55.515	56.517	55.988
BETA(PR) 1	55.860	53.215	60.207	57.351	53.624
BETA(PR) 2	46.581	39.960	32.100	22.788	12.227
V 1	259.24	265.63	271.80	271.56	274.39
V 2	441.73	454.09	468.57	482.23	500.23
VZ 1	245.08	247.83	250.84	246.60	247.03
VZ 2	254.57	270.04	265.30	266.04	279.81
V-THETA 1	84.50	95.60	104.66	113.72	119.22
V-THETA 2	360.99	365.07	386.23	402.20	414.65
V(PR) 1	599.3	569.9	504.8	457.1	416.5
V(PR) 2	370.4	352.3	313.2	288.6	284.3
VTHETA PR1	546.9	490.9	448.1	384.9	335.4
VTHETA PR2	263.2	226.3	166.4	111.8	60.6
U 1	631.36	586.53	542.78	498.50	454.58
U 2	630.02	591.34	552.65	513.97	475.33
M 1	0.2359	0.2418	0.2475	0.2472	0.2498
M 2	0.3947	0.4077	0.4214	0.4346	0.4515
M(PR) 1	0.5453	0.5005	0.4596	0.4162	0.3793
M(PR) 2	0.3309	0.3163	0.2817	0.2601	0.2584
TURN(PR)	19.279	23.254	28.107	34.563	41.308
LOSS COEF.	0.1846	0.0747	0.0858	0.0860	0.0914
DFAC	0.5454	0.5182	0.5447	0.5384	0.4844
EFFP	0.8258	0.9314	0.9307	0.9543	0.9467
EFF	0.8218	0.9298	0.9292	0.9533	0.9454
LOSS PARA.	0.0447	0.0189	0.0223	0.0173	0.0233
INCID	6.25	6.31	6.51	7.55	9.62
DEV	1.481	1.160	1.300	2.088	3.527

CORRECTED WEIGHT FLOW

UPSTREAM OF ROTOR	48.76
UPSTREAM OF STATOR	48.76
DOWNSTREAM OF STATOR	44.90

STATOR 1

STATION 2 - STATION 3

	10	30	50	70	90
DIA 3	29.154	27.422	25.672	23.874	22.034
BETA 2	54.808	53.510	55.515	56.517	55.988
BETA 3	-11.515	-13.679	-10.438	-7.934	-7.756
V 2	441.73	454.09	468.57	482.23	500.23
V 3	296.61	258.28	275.75	271.06	265.93
VZ 2	254.57	270.04	265.30	266.04	279.81
VZ 3	290.64	250.95	271.19	268.46	262.49
V-THETA 2	360.99	365.07	386.23	402.20	414.65
V-THETA 3	-59.21	-61.08	-49.96	-37.42	-35.89
M 2	0.3947	0.4077	0.4214	0.4346	0.4515
M 3	0.2627	0.2292	0.2452	0.2412	0.2365
TURN	66.324	67.189	65.953	64.451	63.744
LOSS COEF.	0.1089	0.1669	0.0923	0.0747	0.0745
DFAC	0.7106	0.7848	0.7388	0.7360	0.7405
LOSS PARA.	0.0428	0.0611	0.0319	0.0242	0.0223
INCID	2.73	1.37	2.82	2.52	0.04
DEV	7.445	4.361	7.312	9.746	10.044

Table IVf.

Blade element performance for complete stage.

PERCENT DESIGN SPEED = 79.89

CORRECTED WEIGHT FLOW = 84.27

CORRECTED ROTOR SPEED = 6684.70

PRESSURE RATIO = 1.1575

ADIABATIC EFFICIENCY = 82.6912

Optimum Bleed

ROTOR 1

STATION 1 - STATION 2

	10	30	50	70	90
DIA 1	29.150	27.080	25.060	23.020	20.988
DIA 2	29.089	27.302	25.516	23.730	21.944
BETA 1	20.707	21.921	23.988	25.012	25.793
BETA 2	36.145	37.796	40.365	42.249	43.638
BETA(PR) 1	56.378	52.772	48.678	43.975	38.493
BETA(PR) 2	47.381	40.699	33.013	23.8[illegible]	15.012
V 1	489.36	501.90	512.24	524.33	526.93
V 2	585.78	624.34	659.86	701.50	722.30
VZ 1	457.74	465.61	468.00	475.35	474.44
VZ 2	473.03	493.35	[illegible].76	519.27	522.74
V-THETA 1	173.03	187.37	[illegible].25	221.78	229.29
V-THETA 2	345.51	392.62	427.36	4 1.65	438.44
V(PR) 1	826.7	769.7	708.8	660.4	614.8
V(PR) 2	698.5	650.6	599.6	567.8	543.8
VTHETA PR1	688.4	612.9	532.3	458.5	390.9
VTHETA PR2	514.1	424.2	326.7	229.6	150.0
U 1	851.41	800.24	740.55	680.27	620.22
U 2	859.58	806.80	754.02	701.25	644.47
M 1	0.4412	0.4530	0.4627	0.4743	0.4766
M 2	0.5185	0.5552	0.5882	0.6276	0.6470
M(PR) 1	0.7453	0.6946	0.6402	0.5972	0.5550
M(PR) 2	0.6184	0.5786	0.5345	0.5079	0.4872
TURN(PR)	8.997	12.097	15.665	20.113	23.477
LOSS COEF.	0.0815	0.0421	0.0491	0.0246	0.0474
DFAC	0.2293	0.2356	0.2431	0.2388	0.2174
EFFP	0.9575	0.9334	0.9355	0.9730	0.9550
EFF	0.8544	0.9319	0.9339	0.9723	0.9538
LOSS PARA.	0.0195	0.0105	0.0126	0.0064	0.0119
INCID	-3.22	-4.17	-5.02	-5.84	-5.51
DEV	2.281	1.888	2.213	3.152	7.313

CORRECTED WEIGHT FLOW

UPSTREAM OF ROTOR	84.27
UPSTREAM OF STATOR	84.27
DOWNSTREAM OF STATOR	81.03

STATOR 1

STATION 2 - STATION 3

	10	30	50	70	90
DIA 3	29.164	27.422	25.672	23.874	22.034
BETA 2	36.146	37.796	40.365	42.249	43.638
BETA 3	-9.005	-4.956	-5.481	-5.856	-5.306
V 2	585.78	624.34	659.86	701.50	722.30
V 3	426.70	466.56	484.66	498.10	430.53
VZ 2	473.03	493.35	502.76	519.27	522.74
VZ 3	421.44	464.81	482.45	495.67	428.69
V-THETA 2	345.51	382.62	427.36	471.65	498.46
V-THETA 3	-66.79	-40.31	-46.29	-49.09	-39.82
M 2	0.5185	0.5552	0.5882	0.6276	0.6470
M 3	0.3729	0.4098	0.4259	0.4376	0.3758
TURN	45.151	42.752	45.846	47.905	48.944
LOSS COEF.	0.1166	0.0552	0.0439	0.0703	0.1814
DFAC	0.5542	0.5080	0.5179	0.5327	0.6291
LOSS PARA.	0.0462	0.0207	0.0154	0.0229	0.0546
INCID	-15.93	-14.34	-12.33	-11.75	-12.31
DEV	9.955	13.084	12.269	12.024	12.494

Table IVg.

Blade element performance for complete stage.

PERCENT DESIGN SPEED = 80.00 *OPTIMUM BLEED*

CORRECTED WEIGHT FLOW = 79.51

CORRECTED ROTOR SPEED = 6693.23

PRESSURE RATIO = 1.2133

ADIABATIC EFFICIENCY = 91.2435

ROTOR 1

STATION 1 - STATION 2

	10	30	50	70	90
DIA 1	29.150	27.090	25.060	23.020	20.980
DIA 2	29.098	27.302	25.516	23.730	21.944
BETA 1	19.291	21.647	23.124	24.857	25.578
BETA 2	41.702	44.183	46.412	47.790	48.213
BETA(PR) 1	58.572	55.262	51.778	47.745	43.015
BETA(PR) 2	45.866	40.270	32.578	23.458	15.511
V 1	449.47	458.42	464.68	468.38	474.43
V 2	586.62	605.61	633.82	665.20	682.34
VZ 1	424.61	426.09	427.35	425.89	429.57
VZ 2	437.98	434.29	437.00	446.92	454.69
V-THETA 1	148.62	169.10	182.49	197.31	206.51
V-THETA 2	390.25	422.08	459.09	492.71	508.77
V(PR) 1	814.3	747.7	690.7	633.4	587.5
V(PR) 2	529.0	569.2	518.6	487.2	471.9
VTHETA PR1	694.9	614.5	542.6	468.8	401.8
VTHETA PR2	451.4	367.9	279.2	193.9	126.2
U 1	843.47	783.58	725.13	666.10	607.30
U 2	841.68	790.00	738.32	686.64	634.34
M 1	0.4139	0.4220	0.4279	0.4324	0.4394
M 2	0.5273	0.5464	0.5735	0.6035	0.6201
M(PR) 1	0.7491	0.6883	0.6361	0.5835	0.5414
M(PR) 2	0.5654	0.5136	0.4693	0.4420	0.4283
TURN(PR)	12.705	14.992	19.200	24.287	27.504
LOSS COEF.	0.0475	0.0316	0.0322	0.0374	0.0838
DFAC	0.3330	0.3476	0.3662	0.3541	0.3195
EFFP	0.9370	0.9620	0.9664	0.9670	0.9297
EFF	0.9350	0.9609	0.9653	0.9660	0.9274
LOSS PARA.	0.0117	0.0080	0.0093	0.0098	0.0225
INCID	-1.03	-1.64	-1.92	-2.05	-1.99
DEV	3.765	1.470	1.778	2.758	6.811

STATOR 1

STATION 2 - STATION 3

	10	30	50	70	90
DIA 3	29.164	27.422	25.672	23.874	22.034
BETA 2	41.702	44.183	46.412	47.790	48.213
BETA 3	-11.875	-7.052	-5.481	-4.956	-5.131
V 2	586.62	605.61	633.82	665.20	682.34
V 3	379.03	411.50	421.84	421.34	402.15
VZ 2	437.98	434.29	437.00	446.92	454.69
VZ 3	370.92	408.38	419.91	419.76	400.54
V-THETA 2	390.26	422.08	459.09	492.71	508.77
V-THETA 3	-78.00	-50.52	-40.29	-36.40	-35.97
M 2	0.5273	0.5464	0.5735	0.6035	0.6201
M 3	0.3358	0.3661	0.3758	0.3752	0.3572
TURN	53.577	51.235	51.894	52.746	53.344
LOSS COEF.	0.1913	0.0901	0.0657	0.0787	0.0848
DFAC	0.6745	0.6146	0.6115	0.6267	0.6518
LOSS PARA.	0.0752	0.0337	0.0230	0.0256	0.0255
INCID	-10.38	-7.96	-6.29	-6.21	-7.74
DEV	7.085	10.988	12.269	12.724	12.669

CORRECTED WEIGHT FLOW

UPSTREAM OF ROTOR	79.51
UPSTREAM OF STATOR	79.51
DOWNSTREAM OF STATOR	75.89

Table IVh.

Blade element performance for complete stage.

PERCENT DESIGN SPEED = 79.86 *OPTIMUM BLEED*

CORRECTED WEIGHT FLOW = 75.51

CORRECTED ROTOR SPEED = 6682.22

PRESSURE RATIO = 1.2360

ADIABATIC EFFICIENCY = 90.9348

ROTOR 1

STATION 1 - STATION 2

	10	30	50	70	90
DIA 1	29.150	27.980	25.060	23.020	20.938
DIA 2	29.089	27.302	25.516	23.730	21.944
BETA 1	19.203	21.196	23.230	24.492	25.303
BETA 2	44.733	47.013	49.050	50.661	52.086
BETA(PR) 1	61.014	57.891	54.293	50.566	46.203
BETA(PR) 2	45.624	39.937	32.178	24.147	14.823
V 1	414.22	423.59	432.89	437.31	442.60
V 2	587.85	605.77	631.45	648.37	666.39
VZ 1	391.17	394.94	397.86	397.96	400.14
VZ 2	417.61	413.03	413.85	411.01	409.48
V-THETA 1	136.24	153.15	170.60	181.29	189.17
V-THETA 2	413.73	443.12	476.92	501.46	525.74
V(PR) 1	807.2	743.0	68[illegible]	626.5	578.1
V(PR) 2	597.1	538.7	489.0	450.4	423.6
VTHETA PR1	706.1	629.4	553.5	483.9	417.3
VTHETA PR2	426.8	345.8	260.4	184.3	108.4
U 1	842.33	782.51	724.14	665.19	606.48
U 2	840.54	788.93	737.32	685.71	634.17
M 1	0.3799	0.3888	0.3976	0.4018	0.4069
M 2	0.5261	0.5444	0.5693	0.5861	0.6035
M(PR) 1	0.7404	0.6820	0.6261	0.5755	0.5314
M(PR) 2	0.5344	0.4841	0.4408	0.4072	0.3836
TURN(PR)	15.390	17.954	22.115	26.420	31.380
LOSS COEF.	0.0412	0.0152	0.0155	0.0187	0.0642
DFAC	0.3822	0.4010	0.4146	0.4170	0.4065
EFFP	0.9523	0.9843	0.9862	0.9851	0.9525
EFF	0.9505	0.9839	0.9857	0.9846	0.9509
LOSS PARA.	0.0102	0.0039	0.0040	0.0049	0.0167
INCID	1.41	0.99	0.59	0.77	1.20
DEV	0.524	1.137	1.378	3.4[illegible]	6.123

CORRECTED WEIGHT FLOW

UPSTREAM OF ROTOR	75.51
UPSTREAM OF STATOR	75.51
DOWNSTREAM OF STATOR	71.72

STATOR 1

STATION 2 - STATION 3

	10	30	50	70	90
DIA 3	29.164	27.422	25.672	23.874	22.034
BETA 2	44.733	47.013	49.050	50.661	52.086
BETA 3	-9.900	-6.878	-5.131	-5.656	-9.184
V 2	587.85	605.77	631.45	648.37	666.39
V 3	372.53	387.48	390.12	372.40	345.30
VZ 2	417.61	413.03	413.85	411.01	409.48
VZ 3	366.99	384.69	388.55	370.59	340.87
V-THETA 2	413.73	443.12	476.92	501.46	525.74
V-THETA 3	-64.05	-46.40	-34.89	-36.70	-55.11
M 2	0.5261	0.5444	0.5693	0.5861	0.6035
M 3	0.3282	0.3429	0.3456	0.3297	0.3052
TURN	54.633	53.890	54.181	56.317	61.270
LOSS COEF.	0.1725	0.1087	0.0911	0.0904	0.1064
DFAC	0.6927	0.6648	0.6672	0.6971	0.7452
LOSS PARA.	0.0682	0.0406	0.0319	0.0294	0.0317
INCID	-7.35	-5.13	-3.65	-3.34	-3.86
DEV	9.060	11.162	12.619	12.024	8.616

Table IVi.

Blade element performance for complete stage.

PERCENT DESIGN SPEED = 79.94 *OPTIMUM BLEED*

CORRECTED WEIGHT FLOW = 70.36

CORRECTED ROTOR SPEED = 6688.88

PRESSURE RATIO = 1.2574

ADIABATIC EFFICIENCY = 86.7177

ROTOR 1

STATION 1 - STATION 2

	10	30	50	70	90
DIA 1	29.150	27.080	25.060	23.020	20.988
DIA 2	29.088	27.302	25.516	23.730	21.944
BETA 1	19.200	21.436	22.660	25.312	26.157
BETA 2	49.112	51.016	53.450	54.987	55.811
BETA(PR) 1	62.299	59.809	56.809	53.249	49.095
BETA(PR) 2	44.644	39.773	33.469	22.693	13.244
V 1	396.44	398.71	402.67	406.63	411.30
V 2	600.13	607.24	616.79	648.42	661.79
VZ 1	374.39	371.13	371.58	367.59	369.18
VZ 2	392.84	382.02	367.31	372.04	371.88
V-THETA 1	130.38	145.71	155.13	173.85	181.37
V-THETA 2	453.69	472.02	495.49	531.07	547.42
V(PR) 1	805.4	738.0	690.4	614.4	563.7
V(PR) 2	552.1	497.0	440.3	403.3	382.1
VTHETA PR1	713.1	637.9	570.0	492.2	426.0
VTHETA PR2	388.0	318.0	242.8	155.6	87.5
U 1	843.47	783.58	725.13	666.10	607.33
U 2	841.68	790.00	738.32	686.64	634.94
M 1	0.3631	0.3652	0.3689	0.3726	0.3770
M 2	0.5348	0.5433	0.5535	0.5835	0.5968
M(PR) 1	0.7376	0.6759	0.6234	0.5630	0.5147
M(PR) 2	0.4920	0.4447	0.3952	0.3629	0.3445
TURN(PR)	17.655	20.035	23.431	30.556	35.849
LOSS COEF.	0.0761	0.0472	0.0421	0.0509	0.0908
DFAC	0.4568	0.4695	0.5004	0.4993	0.4784
EFFP	0.9215	0.9552	0.9636	0.9637	0.9428
EFF	0.9185	0.9534	0.9623	0.9624	0.9409
LOSS PARA.	0.0191	0.0120	0.0108	0.0133	0.0237
INCID	2.70	2.91	3.20	3.45	4.00
DEV	-0.456	0.973	2.669	1.993	4.544

CORRECTED WEIGHT FLOW

UPSTREAM OF ROTOR	70.36
UPSTREAM OF STATOR	70.36
DOWNSTREAM OF STATOR	64.43

STATOR 1

STATION 2 - STATION 3

	10	30	50	70	90
DIA 3	29.164	27.422	25.672	23.874	22.034
BETA 2	49.112	51.016	53.450	54.587	55.811
BETA 3	-18.020	-10.438	-4.956	-4.956	-6.878
V 2	600.13	607.24	616.79	648.42	661.79
V 3	354.88	373.85	371.08	322.20	278.10
VZ 2	392.84	382.02	367.31	372.04	371.88
VZ 3	337.47	367.66	369.69	321.00	276.10
V-THETA 2	453.69	472.02	495.49	531.07	547.42
V-THETA 3	-109.78	-67.73	-32.06	-27.84	-33.30
M 2	0.5348	0.5433	0.5535	0.5835	0.5968
M 3	0.3106	0.3288	0.3268	0.2834	0.2441
TURN	67.132	61.453	58.406	59.943	62.688
LOSS COEF.	0.2146	0.1120	0.0565	0.1509	0.1652
DFAC	0.7857	0.7193	0.6991	0.7850	0.8449
LOSS PARA.	0.0820	0.0415	0.0198	0.0492	0.0496
INCID	-2.97	-1.12	0.75	0.99	-0.14
DEV	0.940	7.602	12.794	12.724	10.922

Table IVj.

Blade element performance for complete stage.

PERCENT DESIGN SPEED = 79.90

CORRECTED WEIGHT FLOW = 64.95

CORRECTED ROTOR SPEED = 6685.57

PRESSURE RATIO = 1.2774

ADIABATIC EFFICIENCY = 82.9182

OPTIMUM BLEED

ROTOR 1

STATION 1 - STATION 2

	10	30	50	70	90
DIA 1	29.153	27.080	25.060	23.020	20.988
DIA 2	29.089	27.302	25.516	23.730	21.944
BETA 1	19.927	21.914	22.895	25.070	25.669
BETA 2	53.623	53.744	55.691	56.632	56.750
BETA(PR) 1	65.236	62.496	59.865	56.157	52.189
BETA(PR) 2	45.187	40.325	33.426	23.838	12.741
V 1	354.36	363.38	366.75	375.12	380.60
V 2	599.93	603.45	615.90	636.47	660.70
VZ 1	333.15	337.12	337.86	339.78	343.04
VZ 2	355.82	356.88	347.16	350.06	362.26
V-THETA 1	120.79	135.62	142.68	158.95	164.86
V-THETA 2	483.02	486.61	508.74	531.55	552.54
V(PR) 1	795.3	730.0	673.0	610.1	559.6
V(PR) 2	504.9	468.1	416.0	382.7	371.4
VTHETA PR1	722.2	647.5	582.0	506.7	442.1
VTHETA PR2	358.2	302.9	229.1	154.7	82.0
U 1	842.96	783.10	724.69	665.70	606.93
U 2	841.17	789.52	737.87	686.23	634.58
M 1	0.3237	0.3321	0.3353	0.3431	0.3482
M 2	0.5309	0.5384	0.5511	0.5712	0.5948
M(PR) 1	0.7265	0.6672	0.6152	0.5580	0.5120
M(PR) 2	0.4467	0.4174	0.3722	0.3435	0.3344
TURN(PR)	20.043	22.171	26.439	32.319	39.428
LOSS COEF.	0.1759	0.0587	0.0601	0.0740	0.0794
DFAC	0.5266	0.5145	0.5427	0.5367	0.5038
EFFP	0.8447	0.9494	0.9524	0.9495	0.9531
EFF	0.8382	0.9464	0.9506	0.9476	0.9513
LOSS PARA.	0.0437	0.0148	0.0154	0.0192	0.0207
INCID	5.64	5.60	6.16	6.36	7.19
DEV	0.087	1.525	2.626	3.138	4.041

CORRECTED WEIGHT FLOW

UPSTREAM OF ROTOR	64.95
UPSTREAM OF STATOR	64.95
DOWNSTREAM OF STATOR	60.95

STATOR 1

STATION 2 - STATION 3

	10	30	50	70	90
DIA 3	29.164	27.422	25.672	23.874	22.034
BETA 2	53.623	53.744	55.691	56.632	56.750
BETA 3	-10.976	-10.617	-19.460	-23.960	-11.335
V 2	599.93	603.45	615.90	636.47	660.70
V 3	411.25	338.50	354.32	356.90	345.27
VZ 2	355.82	356.88	347.16	350.06	362.26
VZ 3	403.72	332.71	334.07	326.14	338.53
V-THETA 2	483.02	486.61	508.74	531.55	552.54
V-THETA 3	-78.30	-62.37	-118.04	-144.94	-67.86
M 2	0.5308	0.5384	0.5511	0.5712	0.5948
M 3	0.3588	0.2958	0.3107	0.3135	0.3033
TURN	64.599	64.361	75.151	80.592	68.085
LOSS COEF.	0.1379	0.2092	0.1138	0.0847	0.0887
DFAC	0.6903	0.7818	0.7826	0.7868	0.7611
LOSS PARA.	0.0544	0.0775	0.0377	0.0253	0.0263
INCID	1.54	1.60	2.99	2.63	0.80
DEV	7.984	7.423	-1.710	-6.280	6.465

Table IVk.

Blade element performance for complete stage.

PERCENT DESIGN SPEED = 89.97

CORRECTED WEIGHT FLOW = 92.13

CORRECTED ROTOR SPEED = 7328.04

PRESSURE RATIO = 1.1940

ADIABATIC EFFICIENCY = 76.7506

OPTIMUM BLEED

ROTOR 1

STATION 1 - STATION 2

	10	30	50	70	90
DIA 1	29.150	27.080	25.060	23.020	20.990
DIA 2	29.088	27.302	25.516	23.730	21.944
BETA 1	20.467	21.924	23.679	25.883	28.674
BETA 2	36.151	38.169	40.783	42.369	43.399
BETA(PR) 1	55.645	52.236	48.333	44.364	39.152
BETA(PR) 2	47.844	40.505	32.876	24.621	16.669
V 1	554.09	563.67	572.75	581.42	588.02
V 2	641.87	692.26	730.20	766.35	793.17
VZ 1	519.11	522.91	524.53	533.67	529.94
VZ 2	518.29	544.25	552.91	566.19	576.31
V-THETA 1	193.75	210.47	230.02	230.75	254.81
V-THETA 2	378.65	427.80	476.96	516.45	544.97
V(PR) 1	919.9	853.8	789.0	746.5	693.4
V(PR) 2	772.2	715.8	658.3	622.8	601.6
VTHETA PR1	759.4	675.0	589.4	522.0	431.5
VTHETA PR2	572.5	464.9	357.4	259.5	172.4
U 1	953.15	885.47	819.42	752.71	686.27
U 2	951.13	892.73	834.33	775.93	717.53
M 1	0.5117	0.5210	0.5299	0.5384	0.5449
M 2	0.5776	0.6268	0.6639	0.6995	0.7261
M(PR) 1	0.8495	0.7893	0.7300	0.6912	0.6332
M(PR) 2	0.6949	0.6481	0.5986	0.5685	0.5537
TURN(PR)	7.801	11.731	15.457	19.743	22.483
LOSS COEF.	0.1249	0.0712	0.0492	0.0302	0.0253
DFAC	0.2322	0.2429	0.2558	0.2656	0.2183
EFFP	0.7906	0.8935	0.9363	0.9657	0.9759
EFF	0.7851	0.8904	0.9344	0.9645	0.9751
LOSS PARA.	0.0296	0.0179	0.0127	0.0078	0.0063
INCID	-3.96	-4.66	-5.37	-5.44	-5.85
DEV	2.744	1.705	2.076	3.921	7.949

CORRECTED WEIGHT FLOW

UPSTREAM OF ROTOR	92.13
UPSTREAM OF STATOR	92.13
DOWNSTREAM OF STATOR	89.03

STATOR 1

STATION 2 - STATION 3

	10	30	50	70	90
DIA 3	29.164	27.422	25.672	23.874	22.034
BETA 2	36.151	38.169	40.783	42.369	43.399
BETA 3	-10.079	-5.481	-5.656	-5.306	-9.542
V 2	641.87	692.26	730.20	766.35	793.17
V 3	466.20	512.40	535.83	538.34	462.85
VZ 2	518.29	544.25	552.91	566.19	576.31
VZ 3	459.00	510.06	533.22	536.03	456.44
V-THETA 2	378.65	427.80	476.96	516.45	544.97
V-THETA 3	-81.59	-48.94	-52.81	-49.79	-76.72
M 2	0.5776	0.6268	0.6639	0.6995	0.7261
M 3	0.4126	0.4561	0.4777	0.4796	0.4095
TURN	46.230	43.650	46.439	47.675	52.941
LOSS COEF.	0.1297	0.0923	0.0699	0.0923	0.2148
DFAC	0.5617	0.5193	0.5213	0.5391	0.5833
LOSS PARA.	0.0513	0.0346	0.0244	0.0301	0.0640
INCID	-15.94	-13.97	-11.92	-11.63	-12.55
DEV	8.88.	12.559	12.094	12.374	8.258

Table IVl.

Blade element performance for complete stage.

PERCENT DESIGN SPEED = 90.04 *OPTIMUM BLEED*

CORRECTED WEIGHT FLOW = 87.50

CORRECTED ROTOR SPEED = 7532.48

PRESSURE RATIO = 1.2723

ADIABATIC EFFICIENCY = 88.5946

ROTOR 1

STATION 1 - STATION 2

	10	30	50	70	90
DIA 1	29.160	27.040	25.060	23.020	20.988
DIA 2	27.048	27.302	25.516	23.730	21.944
BETA 1	19.649	21.284	23.753	25.205	25.439
BETA 2	42.795	43.669	46.379	48.211	49.882
BETA(PR) 1	58.363	54.971	51.208	47.034	42.458
BETA(PR) 2	46.021	40.625	32.923	24.188	16.523
V 1	510.84	522.96	531.29	538.40	546.18
V 2	660.25	680.58	712.34	742.17	750.21
VZ 1	481.10	487.29	486.28	487.14	493.23
VZ 2	484.47	492.29	491.43	494.57	483.41
V-THETA 1	171.77	189.83	214.00	229.29	234.61
V-THETA 2	446.57	469.94	515.68	553.37	573.70
V(PR) 1	917.2	848.9	776.2	714.7	658.5
V(PR) 2	697.7	648.6	585.5	542.2	504.2
VTHETA PR1	780.9	695.2	605.0	523.0	451.3
VTHETA PR2	502.1	422.3	318.2	232.1	143.4
U 1	952.64	884.99	818.98	752.31	685.90
U 2	930.67	892.25	833.88	775.51	717.15
M 1	0.4705	0.4822	0.4902	0.4971	0.5046
M 2	0.5835	0.6106	0.6619	0.6714	0.6803
M(PR) 1	0.8447	0.7827	0.7162	0.6599	0.6177
M(PR) 2	0.6229	0.5820	0.5276	0.4905	0.4572
TURN(PR)	12.342	14.346	18.265	22.844	25.930
LOSS COEF.	0.0568	0.0399	0.0245	0.0165	0.0564
DFAC	0.3465	0.3421	0.3591	0.3610	0.3657
EFFP	0.9295	0.9541	0.9757	0.9861	0.9538
EFF	0.9257	0.9523	0.9747	0.9855	0.9521
LOSS PARA.	0.0139	0.0100	0.0063	0.0043	0.0141
INCID	-1.24	-1.93	-2.49	-2.77	-2.54
DEV	3.921	1.825	2.123	3.488	7.828

CORRECTED WEIGHT FLOW

UPSTREAM OF ROTOR	87.50
UPSTREAM OF STATOR	87.50
DOWNSTREAM OF STATOR	83.86

STATOR 1

STATION 2 - STATION 3

	10	30	50	70	90
DIA 3	29.164	27.422	25.672	23.874	22.034
BETA 2	42.796	43.669	46.379	48.211	49.882
BETA 3	-12.950	-6.878	-5.131	-5.481	-10.258
V 2	660.25	680.58	712.34	742.17	750.21
V 3	429.93	447.18	463.90	458.05	429.08
VZ 2	484.47	492.29	491.43	494.57	483.41
VZ 3	418.98	443.96	462.04	455.96	422.22
V-THETA 2	446.57	469.94	515.68	553.37	573.70
V-THETA 3	-96.39	-53.55	-41.49	-43.75	-76.41
M 2	0.5835	0.6106	0.6619	0.6714	0.6803
M 3	0.3767	0.3936	0.4093	0.4040	0.3779
TURN	55.753	50.547	51.510	53.692	60.140
LOSS COEF.	0.1850	0.1184	0.0877	0.0930	0.0758
DFAC	0.6803	0.6328	0.6238	0.6459	0.6899
LOSS PARA.	0.0724	0.0443	0.0307	0.0303	0.0228
INCID	-5.28	-6.47	-6.32	-5.79	-6.07
DEV	6.004	11.162	12.619	12.199	7.542

Table IVm.

Blade element performance for complete stage.

PERCENT DESIGN SPEED = 89.90 *Optimum Bleed*

CORRECTED WEIGHT FLOW = 82.70

CORRECTED ROTOR SPEED = 7522.33

PRESSURE RATIO = 1.3084

ADIABATIC EFFICIENCY = 88.2594

ROTOR 1

STATION 1 - STATION 2

	10	30	50	70	90
DIA 1	29.150	27.080	25.040	23.020	20.980
DIA 2	29.089	27.302	25.516	23.730	21.944
BETA 1	19.652	21.469	23.769	25.265	26.098
BETA 2	46.414	48.869	51.132	51.586	52.622
BETA(PR) 1	60.457	57.431	54.028	50.011	45.555
BETA(PR) 2	45.115	39.607	32.637	23.304	15.394
V 1	475.93	484.59	491.26	498.95	505.06
V 2	659.82	686.38	705.07	730.98	744.24
VZ 1	448.21	450.96	449.59	451.22	453.57
VZ 2	461.80	451.49	442.45	454.19	451.81
V-THETA 1	160.06	177.36	198.00	212.95	222.18
V-THETA 2	485.18	516.98	548.96	572.75	591.41
V(PR) 1	909.0	837.7	765.4	702.1	647.7
V(PR) 2	654.4	586.0	525.4	494.8	468.6
VTHETA PR1	790.8	706.0	619.4	538.0	462.4
VTHETA PR2	463.7	373.6	283.4	201.3	124.4
U 1	950.86	883.34	817.45	750.90	684.62
U 2	948.84	890.58	832.32	774.06	715.31
M 1	0.4373	0.4456	0.4520	0.4593	0.4652
M 2	0.5955	0.6136	0.6326	0.6583	0.6719
M(PR) 1	0.8352	0.7703	0.7042	0.6464	0.5966
M(PR) 2	0.5815	0.5259	0.4714	0.4474	0.4231
TURN(PR)	15.341	17.824	21.391	26.107	30.161
LOSS COEF.	0.0585	0.0233	0.0232	0.0253	0.0674
DFAC	0.4070	0.4314	0.4482	0.4286	0.4124
EFFP	0.9363	0.9766	0.9798	0.9807	0.9525
EFF	0.9340	0.9755	0.9789	0.9798	0.9507
LOSS PARA.	0.0146	0.0060	0.0060	0.0064	0.0171
INCID	0.46	0.53	0.33	0.21	0.55
DEV	0.015	0.807	1.837	3.204	6.694

CORRECTED WEIGHT FLOW

UPSTREAM OF ROTOR	82.70
UPSTREAM OF STATOR	82.70
DOWNSTREAM OF STATOR	78.92

STATOR 1

STATION 2 - STATION 3

	10	30	50	70	90
DIA 3	29.164	27.422	25.672	23.874	22.034
BETA 2	46.414	48.869	51.132	51.586	52.622
BETA 3	-13.760	-7.400	-4.781	-5.406	-9.184
V 2	659.82	686.38	705.07	730.98	744.24
V 3	432.30	401.55	426.56	413.37	335.41
VZ 2	461.80	451.49	442.45	454.19	451.81
VZ 3	386.46	398.20	425.07	411.60	334.11
V-THETA 2	485.18	516.98	548.96	572.75	591.41
V-THETA 3	-116.38	-51.72	-35.55	-38.23	-53.53
M 2	0.5955	0.6136	0.6326	0.6583	0.6719
M 3	0.3510	0.3308	0.3740	0.3624	0.2928
TURN	63.174	56.269	55.913	56.892	61.800
LOSS COEF.	0.2003	0.1556	0.0813	0.0913	0.1527
DFAC	0.7581	0.7272	0.6865	0.7078	0.8111
LOSS PARA.	0.0770	0.0581	0.0285	0.0297	0.0455
INCID	-5.67	-3.27	-1.57	-2.41	-3.33
DEV	2.200	10.640	12.969	12.374	8.816

Table IVn.

Blade element performance for complete stage.

PERCENT DESIGN SPEED = 89.87

CORRECTED WEIGHT FLOW = 78.50

CORRECTED ROTOR SPEED = 7519.79

PRESSURE RATIO = 1.3355

ADIABATIC EFFICIENCY = 87.9055

OPTIMUM BLEED

ROTOR 1

STATION 1 - STATION 2

	10	30	50	70	90
DIA 1	29.150	27.080	25.060	23.020	20.988
DIA 2	29.088	27.302	25.516	23.730	21.944
BETA 1	19.543	21.738	23.195	25.970	25.545
BETA 2	48.872	51.670	52.834	54.315	56.163
BETA(PR) 1	62.505	59.674	56.475	52.653	48.858
BETA(PR) 2	46.332	40.541	33.413	25.298	14.510
V 1	441.37	449.20	457.01	462.73	465.72
V 2	655.13	674.48	693.37	708.09	731.31
VZ 1	415.89	417.26	420.07	416.00	420.19
VZ 2	430.91	418.31	418.89	411.03	407.21
V-THETA 1	147.79	166.37	180.00	202.63	200.83
V-THETA 2	493.47	529.10	552.53	576.58	607.45
V(PR) 1	900.9	826.4	760.6	685.8	638.7
V(PR) 2	524.1	550.5	501.8	454.6	420.6
VTHETA PR1	799.1	713.3	634.1	545.2	481.9
VTHETA PR2	451.4	357.9	276.3	194.3	105.4
U 1	946.92	879.68	814.06	747.79	681.79
U 2	944.90	886.89	828.97	770.85	712.84
M 1	0.4061	0.4135	0.4210	0.4264	0.4293
M 2	0.5813	0.6022	0.6221	0.6373	0.6600
M(PR) 1	0.8288	0.7607	0.7006	0.6319	0.5887
M(PR) 2	0.5537	0.4914	0.4502	0.4092	0.3794
TURN(PR)	16.173	19.133	23.063	27.355	34.348
LOSS COEF.	0.0909	0.0461	0.0202	0.0362	0.0615
DFAC	0.4433	0.4759	0.4845	0.4824	0.4845
EFFP	0.9099	0.9580	0.9837	0.9741	0.9605
EFF	0.9055	0.9560	0.9829	0.9730	0.9589
LOSS PARA.	0.0221	0.0116	0.0052	0.0093	0.0155
INCID	2.91	2.77	2.78	2.85	3.84
DEV	1.232	1.741	2.613	4.598	5.810

CORRECTED WEIGHT FLOW

UPSTREAM OF ROTOR	78.50
UPSTREAM OF STATOR	78.50
DOWNSTREAM OF STATOR	74.52

STATOR 1

STATION 2 - STATION 3

	10	30	50	70	90
DIA 3	29.164	27.422	25.672	23.874	22.034
BETA 2	48.872	51.670	52.834	54.515	56.163
BETA 3	-17.840	-15.128	-5.656	-5.481	-6.529
V 2	655.13	674.48	693.37	708.09	731.31
V 3	420.49	387.20	419.88	403.59	357.25
VZ 2	430.91	418.31	418.89	411.03	407.21
VZ 3	400.28	373.79	417.83	401.74	354.94
V-THETA 2	493.47	529.10	552.53	576.58	607.45
V-THETA 3	-128.82	-101.05	-41.38	-38.55	-40.62
M 2	0.5813	0.6022	0.6221	0.6373	0.6600
M 3	0.3660	0.3379	0.3680	0.3541	0.3125
TURN	66.712	66.798	58.490	59.997	62.692
LOSS COEF.	0.1559	0.1735	0.0892	0.0696	0.1161
DFAC	0.7396	0.7779	0.6956	0.7147	0.7792
LOSS PARA.	0.0596	0.0631	0.0312	0.0226	0.0349
INCID	-3.21	-0.47	0.13	0.52	0.21
DEV	1.120	2.912	12.094	12.199	11.271

Table IVc.

Blade element performance for complete stage.

PERCENT DESIGN SPEED = 89.90 *Optimum Bleed*

CORRECTED WEIGHT FLOW = 74.43

CORRECTED ROTOR SPEED = 7521.53

PRESSURE RATIO = 1.3515

ADIABATIC EFFICIENCY = 82.9921

ROTOR 1

STATION 1 - STATION 2

	10	30	50	70	90
DIA 1	29.150	27.090	25.060	23.020	20.988
DIA 2	29.089	27.302	25.516	23.730	21.944
BETA 1	19.292	21.860	22.895	24.953	25.130
BETA 2	52.917	53.922	55.050	56.986	57.632
BETA(PR) 1	64.013	61.650	58.823	55.236	51.841
BETA(PR) 2	47.159	42.213	34.079	25.680	14.772
V 1	417.98	420.52	425.98	432.83	432.49
V 2	652.74	660.84	686.79	700.63	723.30
VZ 1	394.41	390.29	392.42	397.3	391.55
VZ 2	393.58	389.16	393.44	38..3	387.22
V-THETA 1	138.06	156.57	165.73	182.60	193.67
V-THETA 2	520.74	534.10	562.92	587.51	610.92
V(PR) 1	900.1	821.9	758.0	688.2	633.7
V(PR) 2	578.8	525.4	475.0	423.6	400.5
VTHETA PR1	809.1	723.3	648.6	565.4	498.3
VTHETA PR2	424.4	35..0	266.2	183.6	102.1
U 1	947.17	879.91	814.28	747.99	681.96
U 2	945.16	887.13	829.09	771.06	713.03
M 1	0.3838	0.3863	0.3914	0.3979	0.3976
M 2	0.5763	0.5879	0.6139	0.6284	0.6507
M(PR) 1	0.8267	0.7550	0.6966	0.6328	0.5826
M(PR) 2	0.5110	0.4674	0.4246	0.3799	0.3603
TURN(PR)	16.853	19.438	24.744	29.556	37.069
LOSS COEF.	0.1390	0.0646	0.0416	0.0534	0.0677
DFAC	0.5076	0.5094	0.5281	0.5422	0.5309
EFFP	0.8715	0.9435	0.9676	0.9632	0.9591
EFF	0.8651	0.9407	0.9660	0.9615	0.9572
LOSS PARA.	0.0333	0.0158	0.0106	0.0137	0.0170
INCID	4.41	4.75	5.12	5.44	6.96
DEV	2.459	3.413	3.279	4.980	6.072

CORRECTED WEIGHT FLOW

UPSTREAM OF ROTOR	74.43
UPSTREAM OF STATOR	74.43
DOWNSTREAM OF STATOR	70.40

STATOR 1

STATION 2 - STATION 3

	10	30	50	70	90
DIA 3	29.164	27.422	25.672	23.874	22.034
BETA 2	52.917	53.922	55.050	56.986	57.632
BETA 3	-12.235	-12.235	-11.515	-11.875	-16.036
V 2	652.74	660.84	686.79	700.63	723.30
V 3	486.85	427.55	401.26	352.36	337.76
VZ 2	393.58	389.16	393.44	381.73	387.22
VZ 3	475.79	418.23	393.19	344.82	324.62
V-THETA 2	520.74	534.10	562.92	587.51	610.92
V-THETA 3	-103.18	-90.69	-80.10	-72.51	-93.31
M 2	0.5763	0.5879	0.6139	0.6284	0.6507
M 3	0.4232	0.3729	0.3500	0.3069	0.2943
TURN	65.153	66.157	66.565	68.861	73.668
LOSS COEF.	0.0603	0.1186	0.1489	0.1712	0.1618
DFAC	0.6380	0.7086	0.7450	0.8051	0.8272
LOSS PARA.	0.0237	0.0437	0.0513	0.0548	0.0470
INCID	0.84	1.78	2.35	2.99	1.68
DEV	6.725	5.805	6.235	5.805	1.764

Table IVp.

Blade element performance for complete stage.

PERCENT DESIGN SPEED = 99.92

CORRECTED WEIGHT FLOW = 96.12

CORRECTED ROTOR SPEED = 8360.39

PRESSURE RATIO = 1.2475

ADIABATIC EFFICIENCY = 76.0833

OPTIMUM BLEED

ROTOR 1

STATION 1 - STATION 2

	10	30	50	70	90
DIA 1	29.153	27.080	25.060	23.020	20.989
DIA 2	29.089	27.302	25.516	23.730	21.944
BETA 1	20.766	22.166	23.438	25.316	25.438
BETA 2	37.250	40.477	41.954	43.161	44.065
BETA(PR) 1	53.716	50.249	49.869	47.832	43.460
BETA(PR) 2	53.086	41.520	32.817	24.749	16.276
V 1	661.91	671.59	623.45	596.97	603.72
V 2	645.93	763.20	821.67	859.86	896.20
VZ 1	618.91	621.96	572.01	539.64	545.19
VZ 2	514.16	580.54	611.06	627.21	643.97
V-THETA 1	234.68	253.38	247.98	255.27	259.32
V-THETA 2	390.97	495.43	549.31	588.20	623.28
V(PR) 1	1045.8	972.7	887.5	803.9	751.1
V(PR) 2	956.1	775.4	727.1	690.6	670.9
VTHETA PR1	843.3	747.8	678.5	595.8	516.6
VTHETA PR2	684.5	514.0	394.1	289.1	188.9
U 1	1077.72	1001.19	926.51	851.09	775.96
U 2	1075.43	1009.40	943.37	877.33	811.30
M 1	0.6064	0.6160	0.5688	0.5432	0.5497
M 2	0.5659	0.6776	0.7336	0.7714	0.8077
M(PR) 1	0.9542	0.8921	0.8097	0.7315	0.6839
M(PR) 2	0.7498	0.6884	0.6492	0.6196	0.6045
TURN(PR)	0.629	8.730	17.052	23.083	27.183
LOSS COEF.	0.3495	0.2320	0.1028	-0.0027	-0.0479
DFAC	0.2349	0.2822	0.2790	0.2492	0.2208
EFFP	0.4014	0.6518	0.8764	1.0032	1.0432
EFF	0.3917	0.6427	0.8718	1.0033	1.0451
LOSS PARA.	0.0743	0.0573	0.0265	-0.0006	-0.0120
INCID	-5.88	-6.65	-3.83	-1.97	-1.54
DEV	7.985	2.720	2.017	4.049	7.574

CORRECTED WEIGHT FLOW

UPSTREAM OF ROTOR	96.12
UPSTREAM OF STATOR	96.12
DOWNSTREAM OF STATOR	93.14

STATOR 1

STATION 2 - STATION 3

	10	30	50	70	90
DIA 3	29.164	27.422	25.672	23.874	22.034
BETA 2	37.250	40.477	41.954	43.161	44.065
BETA 3	-10.258	-5.481	-4.080	-6.180	-15.128
V 2	645.93	763.20	821.67	859.86	896.20
V 3	496.39	656.98	821.59	607.27	524.29
VZ 2	514.16	580.54	611.06	627.21	643.97
VZ 3	488.46	653.97	620.01	603.74	506.12
V-THETA 2	390.97	495.43	549.31	588.20	623.28
V THETA 3	-88.40	-62.75	-44.22	-65.37	-136.83
M 2	0.5658	0.6776	0.7336	0.7714	0.8077
M 3	0.4296	0.5771	0.5420	0.5291	0.4529
TURN	47.508	45.558	46.033	49.342	59.192
LOSS COEF.	-0.0765	-0.1465	0.0602	0.1219	0.2566
DFAC	0.5296	0.4147	0.4975	0.5423	0.6712
LOSS PARA.	-0.0302	-0.0550	0.0211	0.0396	0.0749
INCID	-14.83	-11.66	-10.75	-10.84	-11.89
DEV	8.702	12.559	13.670	11.500	2.672

Table IVq.

Blade element performance for complete stage.

PERCENT DESIGN SPEED = 99.96

CORRECTED WEIGHT FLOW = 93.23

CORRECTED ROTOR SPEED = 4363.01

PRESSURE RATIO = 1.3594

ADIABATIC EFFICIENCY = 87.1155

Optimum Bleed

ROTOR 1

STATION 1 - STATION 2

	10	30	50	70	90
DIA 1	29.150	27.080	25.060	23.020	20.999
DIA 2	29.088	27.302	25.516	23.730	21.944
BETA 1	20.405	22.420	24.797	25.804	25.983
BETA 2	45.752	47.638	49.433	50.924	52.175
BETA(PR) 1	58.326	55.091	51.583	47.469	43.644
BETA(PR) 2	45.191	39.255	32.666	24.051	16.553
V 1	570.00	579.71	586.43	593.15	591.11
V 2	749.79	796.19	792.02	814.44	824.33
VZ 1	534.73	535.84	534.49	534.00	531.35
VZ 2	522.48	516.27	515.08	515.53	505.56
V-THETA 1	198.73	221.09	241.30	258.14	254.36
V-THETA 2	536.37	566.13	601.65	636.14	651.18
V(PR) 1	1017.4	936.4	860.2	790.3	734.6
V(PR) 2	741.4	672.5	611.9	565.6	527.4
VTHETA PR1	465.9	767.9	673.9	582.5	507.4
VTHETA PR2	329.0	431.0	330.2	230.5	150.3
U 1	1084.81	969.01	915.24	840.74	784.57
U 2	1052.35	937.12	931.89	856.67	801.44
M 1	0.5243	0.5337	0.5402	0.5468	0.5449
M 2	0.6807	0.6801	0.7064	0.7336	0.7337
M(PR) 1	0.9358	0.8621	0.7924	0.7285	0.6773
M(PR) 2	0.6541	0.5970	0.5457	0.5064	0.4737
TURN(PR)	13.135	15.235	18.917	23.439	27.134
LOSS COEF.	0.0545	0.0357	0.0316	0.0473	0.1001
DFAC	0.3891	0.4005	0.4112	0.4104	0.4043
EFFP	0.9362	0.9640	0.9716	0.9824	0.9837
EFF	0.9327	0.9621	0.9702	0.9805	0.9836
LOSS PARA.	0.0146	0.0097	0.0082	0.0123	0.0225
INCID	-1.27	-1.81	-2.12	-2.31	-1.41
DEV	0.091	1.055	1.366	3.351	7.853

CORRECTED WEIGHT FLOW

UPSTREAM OF ROTOR	93.23
UPSTREAM OF STATOR	93.23
DOWNSTREAM OF STATOR	89.64

STATOR 1

STATION 2 - STATION 3

	10	30	50	70	90
DIA 3	29.184	27.442	25.672	23.874	22.034
BETA 2	45.752	47.638	49.433	50.924	52.175
BETA 3	-11.515	-5.306	-4.781	-4.721	-18.620
V 2	748.78	788.15	792.02	819.44	824.39
V 3	452.20	458.31	460.71	475.62	426.46
VZ 2	522.48	516.27	515.08	515.53	505.56
VZ 3	443.10	456.34	489.00	488.79	405.54
V-THETA 2	536.37	566.13	601.65	636.14	651.18
V-THETA 3	-90.27	-94.38	-40.90	-80.31	-131.92
M 2	0.6807	0.6801	0.7064	0.7336	0.7337
M 3	0.3985	0.3961	0.4261	0.4129	0.3691
TURN	57.267	52.944	54.214	60.645	70.195
LOSS COEF.	0.2422	0.1767	0.1032	0.1065	0.1007
DFAC	0.7322	0.7011	0.6857	0.7055	0.7457
LOSS PARA.	0.0931	0.0663	0.0362	0.0343	0.0289
INCID	-6.13	-4.50	-3.27	-3.08	-3.77
DEV	7.445	12.734	12.569	7.559	-0.220

Table IVr.

Blade element performance for complete stage.

PERCENT DESIGN SPEED = 99.71

CORRECTED WEIGHT FLOW = 89.67

CORRECTED ROTOR SPEED = 8342.53

PRESSURE RATIO = 1.3982

ADIABATIC EFFICIENCY = 87.7467

Optimum Bleed

ROTOR 1

STATION 1 - STATION 2

	10	30	50	70	90
DIA 1	29.150	27.080	25.060	23.020	20.988
DIA 2	29.088	27.302	25.516	23.730	21.944
BETA 1	20.286	22.386	24.356	25.801	25.142
BETA 2	46.472	48.771	51.497	53.189	54.430
BETA(PR) 1	57.282	58.989	58.752	49.697	45.915
BETA(PR) 2	43.824	40.749	33.587	26.143	16.776
V 1	544.04	539.36	544.12	552.64	554.73
V 2	728.96	743.24	765.61	778.91	797.47
VZ 1	510.29	498.71	495.69	497.55	502.14
VZ 2	502.04	489.85	476.63	466.70	463.38
V-THETA 1	188.62	205.42	224.40	240.54	255.59
V-THETA 2	528.52	556.98	599.14	623.62	648.66
V(PR) 1	999.0	915.4	838.3	759.2	721.8
V(PR) 2	720.4	646.6	572.8	517.9	484.5
VTHETA PR1	858.8	767.6	676.1	586.6	518.5
VTHETA PR2	516.7	422.1	317.7	227.1	139.4
U 1	1047.44	973.06	900.47	827.17	754.16
U 2	1045.21	931.03	916.86	852.68	799.51
M 1	0.5054	0.5013	0.5065	0.5149	0.5159
M 2	0.6503	0.6664	0.6895	0.7048	0.7240
M(PR) 1	0.9299	0.8517	0.7804	0.7166	0.6725
M(PR) 2	0.6427	0.5797	0.5158	0.4704	0.4397
TURN(PR)	13.458	15.241	20.065	23.554	29.183
LOSS COEF.	0.0477	0.0204	0.0173	0.0173	0.0342
DFAC	0.3996	0.4183	0.4478	0.4562	0.4654
EFFP	0.9502	0.9807	0.9859	0.9871	0.9725
EFF	0.9474	0.9797	0.9852	0.9865	0.9716
LOSS PARA.	0.0117	0.0052	0.0044	0.0044	0.0085
INCID	-0.82	0.09	0.65	-0.10	0.81
DEV	0.724	1.949	2.887	5.443	8.076

CORRECTED WEIGHT FLOW

UPSTREAM OF ROTOR	89.67
UPSTREAM OF STATOR	89.67
DOWNSTREAM OF STATOR	85.66

STATOR 1

STATION 2 - STATION 3

	10	30	50	70	90
DIA 3	29.164	27.422	25.672	23.874	22.034
BETA 2	46.472	48.771	51.497	53.189	54.430
BETA 3	-13.036	-6.665	-4.430	-7.756	-14.564
V 2	728.96	743.24	765.61	778.91	797.47
V 3	458.33	435.56	474.30	450.33	403.62
VZ 2	502.04	489.85	476.63	466.70	463.38
VZ 3	440.71	433.16	472.38	446.21	392.55
V-THETA 2	528.52	556.98	599.14	623.62	648.66
V-THETA 3	-126.67	-45.57	-36.64	-50.78	-102.13
M 2	0.6503	0.6664	0.6895	0.7048	0.7240
M 3	0.3976	0.3754	0.4155	0.3947	0.3542
TURN	62.303	54.776	55.927	60.946	69.014
LOSS COEF.	0.1869	0.1055	0.0774	0.0618	0.0844
DFAC	0.7319	0.7205	0.6725	0.7092	0.7756
LOSS PARA.	0.0728	0.0420	0.0271	0.0200	0.0247
INCID	-5.61	-3.37	-1.20	-0.81	-1.52
DEV	2.924	12.035	13.320	7.924	3.216

Table IVs.

Blade element performance for complete stage.

PERCENT DESIGN SPEED = 99.89

CORRECTED WEIGHT FLOW = 86.27

CORRECTED ROTOR SPEED = 9357.45

PRESSURE RATIO = 1.4239

ADIABATIC EFFICIENCY = 84.4486

Optimum Bleed

ROTOR 1

STATION 1 - STATION 2

	10	30	50	70	90
DIA 1	29.150	27.090	25.060	23.020	20.998
DIA 2	29.098	27.302	25.516	23.730	21.944
BETA 1	20.466	22.472	23.815	25.043	26.040
BETA 2	49.435	51.500	53.809	56.196	57.338
BETA(PR) 1	61.798	59.155	55.874	52.099	48.076
BETA(PR) 2	47.642	41.774	36.267	26.762	16.939
V 1	500.33	505.07	514.28	520.02	524.71
V 2	710.75	733.99	740.40	768.35	784.86
VZ 1	468.75	466.72	470.49	467.22	471.45
VZ 2	462.21	456.92	436.26	427.47	423.57
V-THETA 1	174.94	193.05	207.66	228.32	230.35
V-THETA 2	539.94	574.42	598.23	636.45	660.75
V(PR) 1	991.9	910.3	838.6	760.6	705.5
V(PR) 2	686.0	612.7	541.1	478.8	442.8
VTHETA PR1	874.2	781.5	694.2	600.2	525.0
VTHETA PR2	506.9	406.2	320.1	215.6	129.1
U 1	1049.09	974.59	901.89	828.48	755.35
U 2	1046.86	982.58	918.31	854.03	789.75
M 1	0.4640	0.4686	0.4775	0.4831	0.4877
M 2	0.6304	0.6551	0.6633	0.6922	0.7089
M(PR) 1	0.9199	0.8445	0.7787	0.7046	0.6558
M(PR) 2	0.6084	0.5468	0.4848	0.4313	0.4000
TURN(PR)	14.156	17.381	19.607	25.338	31.137
LOSS COEF.	0.0502	0.0131	0.0296	0.0040	0.0531
DFAC	0.4389	0.4623	0.4917	0.5142	0.5186
EFFP	0.9514	0.9891	0.9762	0.9980	0.9659
EFF	0.9485	0.9884	0.9749	0.9979	0.9641
LOSS PARA.	0.0119	0.0032	0.0073	0.0010	0.0132
INCID	2.20	2.26	2.17	2.30	3.08
DEV	2.542	2.974	5.467	6.062	8.239

STATOR 1

STATION 2 - STATION 3

	10	30	50	70	90
DIA 3	29.164	27.422	25.672	23.874	22.034
BETA 2	49.435	51.500	53.899	56.196	57.338
BETA 3	-14.584	-8.827	-5.656	-7.934	-10.218
V 2	710.75	733.99	740.40	768.35	784.86
V 3	529.88	480.05	453.16	385.81	335.91
VZ 2	462.21	456.92	436.26	427.47	423.57
VZ 3	512.81	474.37	450.96	382.12	322.54
V-THETA 2	539.94	574.42	598.23	638.45	660.75
V-THETA 3	-133.42	-73.66	-44.66	-53.26	-93.82
M 2	0.6304	0.6551	0.6633	0.6922	0.7089
M 3	0.4596	0.4177	0.3950	0.3353	0.2911
TURN	64.019	60.326	59.555	64.130	73.556
LOSS COEF.	0.0698	0.1438	0.1165	0.1938	0.1993
DFAC	0.6350	0.6787	0.6933	0.7523	0.8625
LOSS PARA.	0.0271	0.0536	0.0408	0.0628	0.0578
INCID	-2.64	-0.84	1.20	2.20	1.39
DEV	4.376	9.213	12.094	9.746	1.582

CORRECTED WEIGHT FLOW

UPSTREAM OF ROTOR	86.27
UPSTREAM OF STATOR	86.27
DOWNSTREAM OF STATOR	82.15

Table IVt.

Blade element performance for complete stage.

PERCENT DESIGN SPEED = 99.92

CORRECTED WEIGHT FLOW = 82.61

CORRECTED ROTOR SPEED = 8360.14

PRESSURE RATIO = 1.4335

ADIABATIC EFFICIENCY = 80.6706

Optimum Bleed

ROTOR 1

STATION 1 - STATION 2

	10	30	50	70	90
DIA 1	29.160	27.080	25.060	23.020	20.980
DIA 2	29.088	27.302	25.516	23.730	21.944
BETA 1	19.739	22.113	23.949	25.340	26.530
BETA 2	52.914	52.832	55.403	58.276	59.151
BETA(PR) 1	63.760	61.105	57.808	54.671	50.845
BETA(PR) 2	46.146	41.135	35.882	27.431	18.209
V 1	471.48	478.96	489.01	492.55	493.52
V 2	741.76	749.20	751.62	767.70	791.60
VZ 1	443.77	443.73	446.91	441.42	441.34
VZ 2	447.29	452.63	426.77	403.67	405.91
V-THETA 1	159.24	190.50	198.60	219.55	220.83
V-THETA 2	591.73	597.02	618.71	653.00	679.61
V(PR) 1	1003.7	918.3	840.9	759.6	699.0
V(PR) 2	645.6	601.0	526.7	454.8	422.7
VTHETA PR1	900.3	804.0	712.4	618.2	542.0
VTHETA PR2	465.5	395.3	309.7	209.5	118.0
U 1	1059.53	984.29	910.86	836.72	762.85
U 2	1057.27	992.36	927.44	862.52	797.61
M 1	0.4319	0.4390	0.4486	0.4520	0.4529
M 2	0.6476	0.6596	0.6650	0.6823	0.7047
M(PR) 1	0.9194	0.8417	0.7714	0.6970	0.6414
M(PR) 2	0.5637	0.5291	0.4660	0.4042	0.3763
TURN(PR)	17.614	19.970	22.015	27.039	34.636
LOSS COEF.	0.1025	0.0432	0.0426	0.0401	0.1203
DFAC	0.5095	0.4924	0.5209	0.5541	0.5532
EFFP	0.9105	0.9647	0.9676	0.9733	0.9297
EFF	0.9047	0.9625	0.9657	0.9719	0.9259
LOSS PARA.	0.0251	0.0107	0.0106	0.0101	0.0301
INCID	4.16	4.21	4.20	4.67	5.84
DEV	1.046	2.335	5.082	6.731	7.509

CORRECTED WEIGHT FLOW

UPSTREAM OF ROTOR	82.61
UPSTREAM OF STATOR	82.61
DOWNSTREAM OF STATOR	78.46

STATOR 1

STATION 2 - STATION 3

	10	30	50	70	90
DIA 3	29.164	27.422	25.672	23.874	22.034
BETA 2	52.914	52.832	55.403	58.276	59.151
BETA 3	-13.860	-12.956	-10.976	-12.776	-20.000
V 2	741.76	749.20	751.62	767.70	791.60
V 3	544.91	484.83	432.63	369.01	316.47
VZ 2	447.29	452.63	426.77	403.67	405.91
VZ 3	529.05	472.49	424.72	359.88	297.38
V-THETA 2	591.73	597.02	618.71	653.00	679.61
V-THETA 3	-130.53	-108.70	-82.37	-81.60	-108.24
M 2	0.6476	0.6596	0.6650	0.6823	0.7047
M 3	0.4662	0.4160	0.3718	0.3162	0.2710
TURN	66.774	65.789	66.379	71.052	79.151
LOSS COEF.	0.1396	0.1865	0.1886	0.2171	0.2330
DFAC	0.6564	0.7078	0.7524	0.8322	0.9009
LOSS PARA.	0.0544	0.0685	0.0651	0.0693	0.0662
INCID	0.83	0.69	2.70	4.28	3.20
DEV	5.100	5.084	6.774	4.904	-2.200

Table IVu.

Blade element performance for complete stage.

PERCENT DESIGN SPEED = 79.93

CORRECTED WEIGHT FLOW = 96.46

CORRECTED ROTOR SPEED = 8361.12

PRESSURE RATIO = 1.2299

ADIABATIC EFFICIENCY = 83.4738

Minimum Bleed

ROTOR 1

STATION 1 - STATION 2

	10	30	50	70	90
DIA 1	29.150	27.080	25.060	23.020	20.988
DIA 2	29.088	27.302	25.516	23.730	21.944
BETA 1	20.408	22.172	24.473	25.744	25.438
BETA 2	36.705	39.452	42.489	44.474	44.658
BETA(PR) 1	56.795	53.538	49.791	45.436	40.854
BETA(PR) 2	51.326	41.527	34.220	24.752	16.752
V 1	589.89	598.25	605.50	614.76	624.59
V 2	655.19	745.53	780.99	830.29	862.09
VZ 1	552.85	554.02	551.10	553.76	564.03
VZ 2	525.28	575.67	575.91	592.47	613.22
V-THETA 1	205.60	225.78	250.83	267.04	268.29
V-THETA 2	391.60	473.74	527.52	581.70	605.94
V(PR) 1	1009.3	932.2	853.7	789.2	745.7
V(PR) 2	940.6	769.0	696.5	652.4	640.4
VTHETA PR1	844.4	749.8	651.9	562.2	487.8
VTHETA PR2	656.3	509.8	391.7	273.2	184.6
U 1	1050.11	975.54	902.77	829.28	756.08
U 2	1047.88	983.54	919.20	854.86	790.52
M 1	0.5514	0.5597	0.5669	0.5762	0.5860
M 2	0.5922	0.6797	0.7148	0.7639	0.7962
M(PR) 1	0.9435	0.8722	0.7993	0.7396	0.6996
M(PR) 2	0.7598	0.7010	0.6374	0.6002	0.5915
TURN(PR)	5.460	12.011	15.571	20.683	24.102
LOSS COEF.	0.1791	0.1049	0.0980	0.0624	0.0496
DFAC	0.2329	0.2601	0.2776	0.2774	0.2471
EFFP	0.6933	0.8514	0.8813	0.9365	0.9550
EFF	0.6852	0.8463	0.8770	0.9340	0.9532
LOSS PARA.	0.0395	0.0259	0.0249	0.0161	0.0124
INCID	-2.81	-3.36	-3.91	-4.36	-4.15
DEV	6.226	2.727	3.420	4.052	8.052

CORRECTED WEIGHT FLOW

UPSTREAM OF ROTOR	96.46
UPSTREAM OF STATOR	96.46
DOWNSTREAM OF STATOR	95.03

STATOR 1

STATION 2 - STATION 3

	10	30	50	70	90
DIA 3	29.164	27.422	25.672	23.874	22.034
BETA 2	36.705	39.452	42.489	44.474	44.658
BETA 3	-14.403	-4.606	-4.080	-7.534	-27.380
V 2	655.19	745.53	780.99	830.29	862.09
V 3	505.95	576.51	633.80	612.42	497.97
VZ 2	525.28	575.67	575.91	592.47	613.22
VZ 3	490.05	574.65	632.19	606.56	442.19
V-THETA 2	391.60	473.74	527.52	581.70	605.94
V-THETA 3	-125.85	-46.29	-45.09	-84.54	-229.01
M 2	0.5922	0.6797	0.7148	0.7639	0.7962
M 3	0.4495	0.5153	0.5680	0.5485	0.4402
TURN	51.108	44.058	46.568	52.409	72.038
LOSS COEF.	0.0870	0.1091	0.0062	0.1244	0.3087
DFAC	0.5450	0.4855	0.4463	0.5248	0.7150
LOSS PARA.	0.0339	0.0410	0.0022	0.0403	0.0828
INCID	-15.38	-12.69	-10.21	-9.53	-11.29
DEV	4.557	13.434	13.670	9.746	-9.580

Table IVv.

Blade element performance for complete stage.

PERCENT DESIGN SPEED = 99.93

CORRECTED WEIGHT FLOW = 94.01

CORRECTED ROTOR SPEED = 9361.41

PRESSURE RATIO = 1.3480

ADIABATIC EFFICIENCY = 84.6860

Minimum Bleed

ROTOR 1

STATION 1 - STATION 2

	10	30	50	70	90
DIA 1	29.150	27.080	25.060	23.020	20.988
DIA 2	29.088	27.302	25.516	23.730	21.944
BETA 1	21.007	22.405	24.180	25.627	25.800
BETA 2	43.936	45.835	48.181	49.088	52.566
BETA(PR) 1	58.082	55.074	51.416	47.352	42.937
BETA(PR) 2	46.837	41.230	34.354	26.669	18.729
V 1	565.49	572.19	581.36	587.65	594.03
V 2	716.98	740.74	765.44	788.23	790.50
VZ 1	527.91	529.00	530.36	529.84	534.91
VZ 2	516.31	516.10	510.38	516.22	480.51
V-THETA 1	202.72	218.10	238.12	254.16	258.54
V-THETA 2	497.48	531.36	570.44	595.68	627.70
V(PR) 1	998.5	924.0	850.4	782.1	730.5
V(PR) 2	754.8	686.2	618.2	577.7	507.4
VTHETA PR1	847.5	757.6	664.8	575.2	497.6
VTHETA PR2	550.5	452.3	348.9	259.3	162.9
U 1	1050.24	975.64	902.48	825.38	756.17
U 2	1048.00	983.66	919.31	854.96	790.61
M 1	0.5273	0.5339	0.5429	0.5491	0.5555
M 2	0.6430	0.6678	0.6934	0.7161	0.7194
M(PR) 1	0.9310	0.8621	0.7942	0.7308	0.6831
M(PR) 2	0.6769	0.6187	0.5500	0.5248	0.4618
TURN(PR)	11.245	13.843	17.062	20.682	24.203
LOSS COEF.	0.0285	0.0054	-0.0073	0.0160	0.0779
DFAC	0.3490	0.3663	0.3870	0.3761	0.4249
EFFP	0.9665	0.9950	1.0083	0.9870	0.9375
EFF	0.9648	0.9948	1.0087	0.9863	0.9349
LOSS PARA.	0.0069	0.0013	-0.0019	0.0041	0.0192
INCID	-1.52	-1.63	-2.28	-2.45	-2.06
DEV	1.737	2.430	3.554	5.969	10.029

CORRECTED WEIGHT FLOW

UPSTREAM OF ROTOR 94.01

UPSTREAM OF STATOR 94.01

DOWNSTREAM OF STATOR 92.29

STATOR 1

STATION 2 - STATION 3

	10	30	50	70	90
DIA 3	29.164	27.422	25.672	23.874	22.034
BETA 2	43.936	45.835	48.181	49.088	52.566
BETA 3	-11.515	-4.255	-6.005	-3.184	-35.120
V 2	716.98	740.74	765.44	788.23	790.50
V 3	528.25	539.62	548.22	473.80	383.30
VZ 2	516.31	516.10	510.38	516.22	480.51
VZ 3	517.62	538.14	545.21	467.73	313.52
V-THETA 2	497.48	531.36	570.44	595.68	627.70
V-THETA 3	-105.45	-40.04	-57.36	-75.62	-220.51
M 2	0.6430	0.6678	0.6934	0.7161	0.7194
M 3	0.4637	0.4762	0.4851	0.4169	0.3351
TURN	55.451	50.090	54.186	53.272	87.686
LOSS COEF.	0.1352	0.1016	0.0675	0.1704	0.2277
DFAC	0.6309	0.5022	0.5722	0.6774	0.8393
LOSS PARA.	0.0532	0.0383	0.0236	0.0550	0.0563
INCID	-8.14	-6.31	-4.52	-4.91	-5.38
DEV	7.445	13.785	11.745	8.496	-17.320

Table IVw.

Blade element performance for complete stage.

PERCENT DESIGN SPEED = 99.93

CORRECTED WEIGHT FLOW = 87.15

CORRECTED ROTOR SPEED = 8361.50

PRESSURE RATIO = 1.3972

ADIABATIC EFFICIENCY = 82.1879

Minimum Blade

ROTOR 1

STATION 1 - STATION 2

	10	30	50	70	90
DIA 1	29.150	27.080	25.060	23.020	20.988
DIA 2	29.088	27.302	25.516	23.730	21.944
BETA 1	20.047	22.115	23.757	25.806	25.743
BETA 2	47.673	50.300	53.507	54.868	56.869
BETA(PR) 1	61.518	58.301	55.271	51.861	48.051
BETA(PR) 2	45.569	41.059	37.235	29.137	18.494
V 1	517.72	531.64	535.75	536.11	538.26
V 2	751.39	758.64	748.47	767.80	792.39
VZ 1	486.36	492.53	490.35	482.65	484.43
VZ 2	505.96	484.60	445.14	441.83	433.08
V-THETA 1	177.47	200.15	215.84	233.38	233.78
V-THETA 2	555.51	583.70	601.72	627.93	663.57
V(PR) 1	1019.9	937.3	860.7	781.5	725.3
V(PR) 2	722.7	642.7	559.1	505.8	456.7
VTHETA PR1	896.4	797.5	707.4	614.7	539.4
VTHETA PR2	516.1	422.1	338.3	246.3	144.9
U 1	1073.90	997.64	923.23	848.07	773.21
U 2	1071.62	1005.62	940.02	874.23	808.43
M 1	0.4695	0.4827	0.4866	0.4870	0.4890
M 2	0.6517	0.6619	0.6558	0.6754	0.6991
M(PR) 1	0.9249	0.8510	0.7818	0.7099	0.6583
M(PR) 2	0.6269	0.5607	0.4899	0.4450	0.4029
TURN(PR)	15.949	17.242	18.036	22.724	29.556
LOSS COEF.	0.0722	0.0496	0.0410	0.0251	0.0422
DFAC	0.4228	0.4465	0.4820	0.4867	0.5120
EFFP	0.9310	0.9556	0.9653	0.9818	0.9726
EFF	0.9268	0.9530	0.9635	0.9809	0.9712
LOSS PARA.	0.0178	0.0124	0.0100	0.0062	0.0104
INCID	1.92	1.40	1.57	2.06	3.05
DEV	0.469	2.259	6.435	8.437	9.794

CORRECTED WEIGHT FLOW

UPSTREAM OF ROTOR 87.15

UPSTREAM OF STATOR 87.15

DOWNSTREAM OF STATOR 85.34

STATOR 1

STATION 2 - STATION 3

	10	30	50	70	90
DIA 3	29.154	27.422	25.672	23.874	22.034
BETA 2	47.673	50.300	53.507	54.868	56.869
BETA 3	-7.226	-4.430	-1.721	-20.360	-33.720
V 2	751.39	758.64	748.47	767.80	792.39
V 3	514.60	539.72	517.82	374.80	315.66
VZ 2	505.96	484.60	445.14	441.83	433.08
VZ 3	510.57	538.11	510.39	351.39	246.28
V-THETA 2	555.51	583.70	601.72	627.93	663.57
V-THETA 3	-64.74	-41.69	-87.43	-130.40	-137.45
M 2	0.6517	0.6619	0.6558	0.6754	0.6991
M 3	0.4364	0.4617	0.4436	0.3183	0.2674
TURN	54.899	54.730	63.228	75.228	95.589
LOSS COEF.	0.2349	0.1376	0.0756	0.2646	0.3054
DFAC	0.6466	0.5952	0.6319	0.8348	0.9299
LOSS PARA.	0.0936	0.0517	0.0262	0.0811	0.0720
INCID	-4.41	-1.84	0.81	0.87	0.92
DEV	11.734	13.610	8.029	-2.680	-20.920

Table IVx.

Blade element performance for complete stage.

PERCENT DESIGN SPEED = 100.04

CORRECTED WEIGHT FLOW = 83.50

CORRECTED ROTOR SPEED = 8370.58

PRESSURE RATIO = 1.4159

ADIABATIC EFFICIENCY = 78.2805

Minimum Bleed

ROTOR 1

STATION 1 - STATION 2

	10	30	50	70	90
DIA 1	29.150	27.080	25.060	23.020	20.989
DIA 2	29.088	27.302	25.516	23.730	21.944
BETA 1	20.286	22.360	23.937	25.447	25.622
BETA 2	50.242	52.383	55.753	57.632	60.492
BETA(PR) 1	63.122	60.555	57.557	54.333	50.431
BETA(PR) 2	45.938	41.579	38.466	30.141	19.700
V 1	489.7	495.14	501.73	503.41	508.47
V 2	751.02	755.62	739.42	758.03	773.87
VZ 1	459.29	457.91	458.58	454.57	458.47
VZ 2	480.31	461.22	416.11	405.81	381.15
V-THETA 1	169.77	188.36	203.57	216.31	219.87
V-THETA 2	577.35	598.53	611.22	640.26	673.49
V(PR) 1	1015.9	931.5	854.8	779.6	719.7
V(PR) 2	690.7	616.6	531.5	469.3	404.9
VTHETA PR1	906.2	811.2	721.4	633.4	554.8
VTHETA PR2	496.3	409.2	330.6	235.6	136.5
U 1	1075.94	999.53	924.98	849.68	774.68
U 2	1073.65	1007.73	941.81	875.88	809.96
M 1	0.4427	0.4478	0.4540	0.4556	0.4604
M 2	0.6472	0.6558	0.6442	0.6629	0.6784
M(PR) 1	0.9184	0.8424	0.7735	0.7056	0.6516
M(PR) 2	0.5952	0.5351	0.4630	0.4104	0.3549
TURN(PR)	17.183	18.976	19.091	24.192	30.731
LOSS COEF.	0.1030	0.0460	0.0433	0.0317	0.0623
DFAC	0.4624	0.4805	0.5185	0.5430	0.5889
EFFP	0.9087	0.9621	0.9662	0.9786	0.9620
EFF	0.9029	0.9597	0.9643	0.9774	0.9599
LOSS PARA.	0.0253	0.0113	0.0104	0.0078	0.0153
INCID	3.52	3.66	3.86	4.53	5.43
DEV	0.838	2.779	7.666	9.441	11.000

CORRECTED WEIGHT FLOW

UPSTREAM OF ROTOR	83.50
UPSTREAM OF STATOR	83.50
DOWNSTREAM OF STATOR	81.65

STATOR 1

STATION 2 - STATION 3

	10	30	50	70	90
DIA 3	29.164	27.422	25.672	23.874	22.034
BETA 2	50.242	52.383	55.753	57.632	60.492
BETA 3	-7.400	-5.831	-12.055	-32.560	-41.780
V 2	751.02	755.62	739.42	758.03	773.87
V 3	576.24	556.07	457.31	299.10	260.73
VZ 2	480.31	461.22	416.11	405.81	381.16
VZ 3	571.44	553.20	447.22	250.96	194.43
V-THETA 2	577.35	598.53	611.22	640.26	673.49
V-THETA 3	-74.22	-56.49	-95.51	-162.72	-173.72
M 2	0.6472	0.6558	0.6442	0.6629	0.6784
M 3	0.4877	0.4736	0.3881	0.2519	0.2198
TURN	57.642	58.214	67.808	90.592	102.272
LOSS COEF.	0.1885	0.1746	0.2406	0.4280	0.4097
DFAC	0.5811	0.5507	0.7176	0.9518	0.9938
LOSS PARA.	0.0751	0.0655	0.0827	0.1174	0.0923
INCID	-1.84	0.24	3.05	3.63	4.54
DEV	11.560	12.209	5.695	-15.280	-23.980

Table IVy.

Blade element performance for complete stage.

MEAN BLEED

PERCENT DESIGN SPEED = 99.94

CORRECTED WEIGHT FLOW = 97.01

CORRECTED ROTOR SPEED = 8362.00

PRESSURE RATIO = 1.2293

ADIABATIC EFFICIENCY = 89.4006

ROTOR 1

STATION 1 - STATION 2

	10	30	50	70	90
DIA 1	29.150	27.080	25.060	23.020	20.999
DIA 2	29.088	27.302	25.516	23.730	21.944
BETA 1	20.227	22.172	24.056	25.325	25.443
BETA 2	36.978	39.279	42.122	43.298	44.109
BETA(PR) 1	56.886	53.548	49.653	45.257	40.843
BETA(PR) 2	52.040	41.666	34.289	25.156	16.665
V 1	589.64	599.26	610.09	620.17	625.55
V 2	645.93	745.44	782.83	833.52	869.47
VZ 1	553.28	554.95	557.10	560.57	564.97
VZ 2	516.69	577.03	580.63	606.63	624.30
V-THETA 1	203.87	226.16	248.69	265.26	268.79
V-THETA 2	387.63	471.94	525.06	571.62	605.17
V(PR) 1	1012.8	934.0	860.5	796.4	747.0
V(PR) 2	840.0	772.4	702.8	670.2	651.7
VTHETA PR1	848.3	751.3	655.8	565.6	488.8
VTHETA PR2	662.3	513.5	395.9	284.9	186.3
U 1	1052.15	977.43	904.52	830.89	757.54
U 2	1049.91	985.44	920.98	856.51	792.05
M 1	0.5501	0.5596	0.5704	0.5804	0.5859
M 2	0.5825	0.6784	0.7152	0.7660	0.8022
M(PR) 1	0.9448	0.8722	0.8045	0.7453	0.6936
M(PR) 2	0.7575	0.7030	0.6420	0.6159	0.6012
TURN(PR)	4.846	11.881	15.364	20.101	24.198
LOSS COEF.	0.1918	0.1128	0.1151	0.0696	0.0464
DFAC	0.2354	0.2570	0.2760	0.2585	0.2329
EFFP	0.6650	0.8383	0.8586	0.9273	0.9581
EFF	0.6566	0.8336	0.8537	0.9245	0.9564
LOSS PARA.	0.0416	0.0278	0.0292	0.0179	0.0116
INC D	-2.71	-3.35	-4.05	-4.54	-4.14
DEV	5.940	2.866	3.489	4.456	7.965

CORRECTED WEIGHT FLOW

UPSTREAM OF ROTOR	97.01
UPSTREAM OF STATOR	97.01
DOWNSTREAM OF STATOR	94.67

STATOR 1

STATION 2 - STATION 3

	10	30	50	70	90
DIA 3	29.164	27.422	25.672	23.874	22.034
BETA 2	36.678	39.279	42.122	43.298	44.109
BETA 3	-11.695	-4.781	-4.080	-7.226	-20.540
V 2	645.93	745.44	782.83	833.52	869.47
V 3	477.80	551.50	616.20	599.48	503.98
VZ 2	516.69	577.03	580.63	606.63	624.30
VZ 3	467.88	549.58	614.63	594.72	471.94
V-THETA 2	387.63	471.94	525.06	571.62	605.17
V-THETA 3	-56.85	-45.97	-43.84	-75.40	-176.83
M 2	0.5825	0.6784	0.7152	0.7660	0.8022
M 3	0.4230	0.4915	0.5505	0.5353	0.4454
TURN	43.573	44.060	46.202	50.524	64.649
LOSS COEF.	0.0755	0.1162	0.0906	0.1117	0.2716
DFAC	0.5615	0.5220	0.4684	0.5346	0.6921
LOSS PARA.	0.0257	0.0436	0.0302	0.0362	0.0768
INCID	-15.20	-12.66	-10.58	-10.70	-11.64
DEV	7.265	13.259	13.670	10.454	-2.740

Table IVz.

Blade element performance for complete stage.

PERCENT DESIGN SPEED = 99.88

CORRECTED WEIGHT FLOW = 93.74

CORRECTED ROTOR SPEED = 8356.60

PRESSURE RATIO = 1.3554

ADIABATIC EFFICIENCY = 95.9968

MEAN BLEED

ROTOR 1

STATION 1 - STATION 2

	10	30	50	70	90
DIA 1	29.150	27.080	25.060	23.020	20.998
DIA 2	29.088	27.302	25.516	23.730	21.944
BETA 1	19.829	22.292	24.352	25.564	25.805
BETA 2	43.494	46.290	48.182	49.886	52.030
BETA(PR) 1	53.314	55.099	51.434	47.378	43.153
BETA(PR) 2	46.799	40.933	33.885	25.510	17.900
V 1	554.15	572.51	581.14	587.96	591.56
V 2	718.04	744.63	771.20	798.05	801.66
VZ 1	530.70	529.72	529.44	530.40	532.57
VZ 2	520.90	514.55	514.21	514.20	493.22
V-THETA 1	191.37	217.17	239.63	253.71	257.51
V-THETA 2	494.21	538.25	574.75	610.32	631.98
V(PR) 1	1010.4	925.8	849.2	783.3	730.0
V(PR) 2	760.9	681.1	619.4	569.7	518.3
VTHETA PR1	859.8	759.3	664.0	576.4	499.3
VTHETA PR2	554.7	446.2	345.3	245.4	159.3
U 1	1051.13	976.48	903.65	830.08	786.81
U 2	1048.89	984.49	920.09	855.69	791.28
M 1	0.5251	0.5334	0.5419	0.5486	0.5522
M 2	0.6426	0.6701	0.6971	0.7242	0.7291
M(PR) 1	0.9405	0.8625	0.7919	0.7309	0.6814
M(PR) 2	0.6810	0.6129	0.5599	0.5170	0.4714
TURN(PR)	11.515	14.166	17.549	21.868	25.253
LOSS COEF.	0.0269	0.0065	0.0054	0.0161	0.0695
DFAC	0.3533	0.3759	0.3857	0.3927	0.4113
EFFP	0.9686	0.9939	0.9958	0.9871	0.9454
EFF	0.9670	0.9936	0.9955	0.9865	0.9429
LOSS PARA.	0.0065	0.0016	0.0014	0.0041	0.0177
INCID	-1.29	-1.80	-2.27	-2.42	-1.85
DEV	1.699	2.133	3.085	4.810	9.200

STATOR 1

STATION 2 - STATION 3

	10	30	50	70	90
DIA 3	29.164	27.422	25.672	23.874	22.034
BETA 2	43.494	46.290	48.182	49.886	52.030
BETA 3	-11.515	-4.606	-4.781	-10.479	-21.440
V 2	718.04	744.63	771.20	798.05	801.66
V 3	476.85	483.65	505.56	481.52	410.17
VZ 2	520.90	514.55	514.21	514.20	493.22
VZ 3	467.25	482.09	505.80	474.09	331.78
V-THETA 2	494.21	538.25	574.75	610.32	631.98
V-THETA 3	-95.19	-38.84	-42.14	-84.27	-149.93
M 2	0.6426	0.6701	0.6971	0.7242	0.7291
M 3	0.4159	0.4240	0.4456	0.4233	0.3588
TURN	55.009	50.655	52.963	59.955	73.470
LOSS COEF.	0.1638	0.1255	0.0664	0.0874	0.1097
DFAC	0.6636	0.6425	0.6257	0.6812	0.7830
LOSS PARA.	0.0645	0.0471	0.0233	0.0281	0.0308
INCID	-6.59	-5.85	-4.52	-4.11	-3.62
DEV	7.445	13.434	12.569	7.601	-3.640

CORRECTED WEIGHT FLOW

UPSTREAM OF ROTOR	93.74
UPSTREAM OF STATOR	93.74
DOWNSTREAM OF STATOR	90.81

Table IVaa.

Blade element performance for complete stage.

PERCENT DESIGN SPEED = 99.98

CORRECTED WEIGHT FLOW = 87.35

CORRECTED ROTOR SPEED = 8357.16

PRESSURE RATIO = 1.4072

ADIABATIC EFFICIENCY = 85.7158

MEAN BLEED

ROTOR 1

STATION 1 - STATION 2

	10	30	50	70	90
DIA 1	29.150	27.080	25.060	23.020	20.998
DIA 2	29.084	27.302	25.516	23.730	21.944
BETA 1	21.048	22.964	24.857	25.745	25.889
BETA 2	49.348	51.131	53.596	55.103	56.839
BETA(PR) 1	60.884	57.893	54.728	51.958	47.125
BETA(PR) 2	43.417	40.301	34.560	25.835	15.415
V 1	524.19	533.36	539.29	545.20	548.38
V 2	749.72	762.15	769.31	791.42	817.15
VZ 1	489.22	491.09	491.29	491.09	491.64
VZ 2	486.41	478.28	456.56	452.77	456.13
V-THETA 1	188.25	208.10	222.41	236.82	234.57
V-THETA 2	558.80	593.40	619.18	649.11	676.64
V(PR) 1	1305.4	924.1	850.8	779.6	722.4
V(PR) 2	595.8	527.1	554.4	503.0	475.2
VTHETA PR1	476.4	782.8	594.6	605.5	529.4
VTHETA PR2	495.5	405.6	314.5	219.2	126.3
U 1	1066.65	990.91	915.99	842.34	767.99
U 2	1064.38	999.03	933.68	854.32	803.97
M 1	0.4784	0.4875	0.4932	0.4989	0.5000
M 2	0.6549	0.6701	0.6792	0.7020	0.7276
M(PR) 1	0.9163	0.8447	0.7791	0.7134	0.6611
M(PR) 2	0.6079	0.5514	0.4895	0.4462	0.4231
TURN(PR)	15.467	17.597	20.167	25.123	31.709
LOSS COEF.	0.0533	0.0377	0.0448	0.0444	0.0585
DFAC	0.4422	0.4561	0.4854	0.4855	0.4875
EFFP	0.9379	0.9466	0.9634	0.9575	0.9614
EFF	0.9341	0.9447	0.9614	0.9557	0.9593
LOSS PARA.	0.0162	0.0095	0.0113	0.0114	0.0147
INCID	1.28	1.00	1.03	1.16	2.12
DEV	0.317	1.501	3.760	5.135	6.716

CORRECTED WEIGHT FLOW

UPSTREAM OF ROTOR	87.85
UPSTREAM OF STATOR	87.85
DOWNSTREAM OF STATOR	84.73

STATOR 1

STATION 2 - STATION 3

	10	30	50	70	90
DIA 3	29.164	27.422	25.672	23.874	22.034
BETA 2	49.348	51.131	53.596	55.103	56.839
BETA 3	-19.280	-9.878	-4.606	-9.542	-19.460
V 2	749.72	762.15	769.31	791.42	817.15
V 3	482.23	469.30	481.83	432.70	335.24
VZ 2	486.41	478.28	456.56	452.77	456.13
VZ 3	455.23	465.92	480.27	426.71	363.23
V-THETA 2	568.80	593.40	619.18	649.11	676.64
V-THETA 3	-159.24	-58.20	-38.69	-71.73	-126.34
M 2	0.6549	0.6701	0.6792	0.7020	0.7276
M 3	0.4108	0.4015	0.4144	0.3716	0.3300
TURN	68.628	58.069	58.202	64.645	75.359
LOSS COEF.	0.2124	0.1743	0.0840	0.1233	0.1531
DFAC	0.7457	0.7054	0.6744	0.7511	0.8262
LOSS PARA.	0.0605	0.0852	0.0294	0.0398	0.0436
INCID	-2.73	-1.61	0.90	1.10	-0.65
DEV	-0.320	11.162	13.144	8.138	-1.660

Table IVbb.

Blade element performance for complete stage.

PERCENT DESIGN SPEED = 99.93

CORRECTED WEIGHT FLOW = 83.75

CORRECTED ROTOR SPEED = 9501.29

PRESSURE RATIO = 1.4376

ADIABATIC EFFICIENCY = 83.0526

MEAN BLEED

STATOR 1

STATION 2 - STATION 3

	10	30	50	70	90
DIA 3	29.164	27.422	25.672	23.874	22.034
BETA 2	51.583	52.946	55.043	56.809	57.398
BETA 3	-14.584	-9.631	-8.827	-15.673	-25.480
V 2	750.39	752.96	754.07	774.74	797.85
V 3	559.05	473.91	467.47	423.54	382.95
VZ 2	466.28	453.71	432.06	424.12	429.88
VZ 3	541.04	467.23	461.93	407.79	342.77
V-THETA 2	587.94	600.92	618.02	648.34	672.14
V-THETA 3	-140.77	-76.29	-71.73	-114.42	-170.75
M 2	0.6532	0.6607	0.6645	0.6856	0.7088
M 3	0.4772	0.4050	0.4010	0.3627	0.3274
TURN	66.167	62.577	63.869	72.481	83.878
LOSS COEF.	0.1140	0.1960	0.1154	0.1393	0.1493
DFAC	0.6450	0.7110	0.7017	0.7753	0.8392
LOSS PARA.	0.0443	0.0706	0.0401	0.0439	0.0404
INCID	-0.50	0.81	2.34	2.81	1.45
DEV	4.376	8.409	8.923	2.007	-8.680

ROTOR 1

STATION 1 - STATION 2

	10	30	50	70	90
DIA 1	29.150	27.080	25.060	23.020	20.988
DIA 2	29.086	27.302	25.516	23.730	21.944
BETA 1	20.406	22.503	24.206	25.742	26.191
BETA 2	51.583	52.946	55.043	56.809	57.398
BETA(PR) 1	62.774	60.046	57.166	53.535	49.733
BETA(PR) 2	45.495	41.129	35.997	27.239	16.741
V 1	490.54	498.02	501.93	508.54	510.78
V 2	750.39	752.96	754.07	774.74	797.85
VZ 1	459.76	460.10	457.80	459.09	458.34
VZ 2	466.28	453.71	432.06	424.12	429.38
V-THETA 1	171.32	190.61	205.80	220.88	225.44
V-THETA 2	587.34	600.92	618.02	648.34	672.14
V(PR) 1	1004.9	921.5	844.3	770.8	709.1
V(PR) 2	965.2	802.4	534.0	477.0	448.9
VTHETA PR1	893.6	798.4	709.4	619.9	541.1
VTHETA PR2	474.4	396.2	313.9	218.3	129.3
U 1	1054.61	989.01	915.24	840.74	766.52
U 2	1062.35	997.12	931.89	866.67	801.44
M 1	0.4479	0.4550	0.4587	0.4650	0.4671
M 2	0.6532	0.6607	0.6645	0.6856	0.7088
M(PR) 1	0.9175	0.8418	0.7716	0.7048	0.6485
M(PR) 2	0.5790	0.5285	0.4706	0.4221	0.3988
TURN(PR)	17.279	18.917	21.169	26.296	32.992
LOSS COEF.	0.1078	0.0547	0.0590	0.0767	0.0980
DFAC	0.4851	0.4904	0.5112	0.5291	0.5182
EFFP	0.9047	0.9539	0.9540	0.9469	0.9399
EFF	0.8986	0.9512	0.9514	0.9440	0.9367
LOSS PARA.	0.0267	0.0136	0.0146	0.0194	0.0244
INCID	3.17	3.15	3.47	3.73	4.73
DEV	0.395	2.329	5.197	6.539	8.041

CORRECTED WEIGHT FLOW

UPSTREAM OF ROTOR	83.75
UPSTREAM OF STATOR	83.75
DOWNSTREAM OF STATOR	80.53

Table IVcc.

Blade element performance for complete stage.

PERCENT DESIGN SPEED = 109.96

CORRECTED WEIGHT FLOW = 100.38

CORRECTED ROTOR SPEED = 9201.36

PRESSURE RATIO = 1.2506

ADIABATIC EFFICIENCY = 82.2562

OPTIMUM BLEED

ROTOR 1

STATION 1 - STATION 2

	10	30	50	70	90
DIA 1	29.150	27.080	25.060	23.020	20.948
DIA 2	29.048	27.302	25.516	23.730	21.944
BETA 1	21.805	22.564	24.360	25.690	25.855
BETA 2	37.080	39.138	43.823	45.028	45.449
BETA(PR) 1	57.418	54.234	50.475	46.707	43.307
BETA(PR) 2	46.813	44.043	35.253	24.623	15.329
V 1	633.33	643.31	646.47	656.38	662.74
V 2	761.14	783.37	841.08	911.90	961.11
VZ 1	588.02	592.33	588.91	591.50	596.40
VZ 2	607.23	607.60	606.83	644.50	674.26
V-THETA 1	235.25	250.99	266.65	284.54	283.02
V-THETA 2	458.92	494.46	582.39	645.13	684.91
V(PR) 1	1091.9	1013.4	935.3	962.6	806.4
V(PR) 2	922.1	845.3	743.1	709.0	699.1
VTHETA PR1	920.1	822.3	726.6	627.8	542.3
VTHETA PR2	694.0	587.6	429.9	295.4	184.8
U 1	1155.34	1073.29	993.23	912.38	831.84
U 2	1152.98	1082.09	1011.21	940.52	869.73
M 1	0.5950	0.6050	0.6082	0.6183	0.6247
M 2	0.6836	0.7147	0.7700	0.8404	0.8911
M(PR) 1	1.0258	0.9531	0.8799	0.8125	0.7602
M(PR) 2	0.8342	0.7712	0.6803	0.6534	0.6482
TURN(PR)	8.605	10.190	15.721	22.084	26.979
LOSS COEF.	0.2043	0.1542	0.1648	0.1295	0.0873
DFAC	0.2285	0.2423	0.3031	0.2876	0.2497
EFFP	0.6929	0.7717	0.8024	0.8737	0.9270
EFF	0.6824	0.7640	0.7948	0.8680	0.9234
LOSS PARA.	0.0474	0.0365	0.0413	0.0334	0.0219
INCID	-2.18	-2.67	-2.73	-3.09	-2.59
DEV	3.713	5.243	4.453	3.923	3.629

CORRECTED WEIGHT FLOW

UPSTREAM OF ROTOR	100.38
UPSTREAM OF STATOR	100.38
DOWNSTREAM OF STATOR	97.56

STATOR 1

STATION 2 - STATION 3

	10	30	50	70	90
DIA 3	29.164	27.422	25.672	23.874	22.034
BETA 2	37.080	39.138	43.823	45.028	45.449
BETA 3	-9.363	-5.306	-5.481	-8.827	-24.320
V 2	761.14	782.37	841.08	911.90	961.11
V 3	546.65	583.68	633.85	634.90	531.89
VZ 2	607.23	607.60	606.83	644.50	674.26
VZ 3	535.37	581.18	630.95	627.38	484.69
V-THETA 2	458.92	494.46	582.39	645.13	684.91
V-THETA 3	-88.93	-53.58	-60.54	-97.42	-219.05
M 2	0.6886	0.7147	0.7700	0.8404	0.8911
M 3	0.4830	0.5193	0.5640	0.5642	0.4676
TURN	46.443	44.445	49.304	53.855	69.769
LOSS COEF.	0.1780	0.0855	0.0582	0.1638	0.3325
DFAC	0.5709	0.5187	0.5152	0.5700	0.7307
LOSS PARA.	0.0705	0.0336	0.0204	0.0529	0.0915
INCID	-15.00	-13.00	-8.88	-8.97	-10.50
DEV	9.597	12.734	12.269	8.853	-8.520

Table IVdd.

Blade element performance for complete stage.

PERCENT DESIGN SPEED = 109.95

CORRECTED WEIGHT FLOW = 99.45

CORRECTED ROTOR SPEED = 9199.41

PRESSURE RATIO = 1.4298

ADIABATIC EFFICIENCY = 82.4708

Optimum Bleed

ROTOR 1

STATION 1 - STATION 2

	10	30	50	70	90
DIA 1	29.150	27.080	25.060	23.020	20.988
DIA 2	29.088	27.302	25.516	23.730	21.944
BETA 1	21.238	23.388	24.870	26.164	26.428
BETA 2	47.102	49.075	50.416	51.726	53.625
BETA(PR) 1	58.479	55.066	51.369	47.217	43.121
BETA(PR) 2	44.627	39.271	32.653	23.910	16.372
V 1	622.23	635.93	647.18	655.62	656.93
V 2	832.17	849.61	869.55	900.87	900.26
VZ 1	579.77	583.68	587.17	588.44	588.27
VZ 2	566.45	556.55	554.08	558.02	533.92
V-THETA 1	225.91	252.44	272.18	289.09	292.39
V-THETA 2	609.62	641.93	670.15	707.23	724.85
V(PR) 1	1109.0	1019.3	940.5	866.4	806.0
V(PR) 2	795.9	718.9	658.1	609.9	556.5
VTHETA PR1	945.3	835.6	734.7	635.8	550.9
VTHETA PR2	559.1	455.1	355.1	246.2	156.9
U 1	1171.24	1088.07	1006.91	924.94	843.29
U 2	1168.75	1096.99	1025.23	953.47	881.71
M 1	0.5752	0.5887	0.5999	0.6083	0.6096
M 2	0.7297	0.7512	0.7740	0.8073	0.8092
M(PR) 1	1.0252	0.9437	0.8718	0.8038	0.7479
M(PR) 2	0.6980	0.6357	0.5857	0.5466	0.5002
TURN(PR)	13.852	15.796	18.716	23.407	26.749
LOSS COEF.	0.1194	0.0877	0.0752	0.0508	0.0916
DFAC	0.4051	0.4179	0.4241	0.4237	0.4369
EFFP	0.9815	0.9171	0.9340	0.9600	0.9318
EFF	0.9740	0.9120	0.9301	0.9577	0.9283
LOSS PARA.	0.0297	0.0224	0.0194	0.0132	0.0229
INCID	-1.12	-1.63	-2.33	-2.58	-1.88
DEV	-0.473	0.471	1.853	3.110	7.672

CORRECTED WEIGHT FLOW

UPSTREAM OF ROTOR	99.45
UPSTREAM OF STATOR	99.45
DOWNSTREAM OF STATOR	95.68

STATOR 1

STATION 2 - STATION 3

	10	30	50	70	90
DIA 3	29.164	27.422	25.672	23.874	22.034
BETA 2	47.102	49.075	50.416	51.726	53.625
BETA 3	-8.469	-4.693	-3.005	-14.041	-21.530
V 2	832.17	849.61	869.55	900.87	900.26
V 3	505.39	503.56	544.50	517.92	470.89
VZ 2	566.46	556.56	554.08	558.02	533.92
VZ 3	499.88	501.89	541.51	502.45	436.04
V-THETA 2	609.62	641.93	670.15	707.23	724.85
V-THETA 3	-74.44	-41.20	-56.97	-125.65	-172.81
M 2	0.7297	0.7512	0.7740	0.8073	0.8092
M 3	0.4295	0.4311	0.4696	0.4465	0.4048
TURN	55.371	53.768	56.421	65.767	75.155
LOSS COEF.	0.2465	0.1944	0.0985	0.1224	0.0936
DFAC	0.7228	0.7102	0.6678	0.7274	0.7782
LOSS PARA.	0.0979	0.0730	0.0344	0.0388	0.0263
INCID	-4.58	-3.07	-2.28	-2.27	-2.32
DEV	10.491	13.347	11.745	3.639	-3.730

Table IVee.

Blade element performance for complete stage.

PERCENT DESIGN SPEED = 109.90 *Optimum Blade*

CORRECTED WEIGHT FLOW = 97.61

CORRECTED ROTOR SPEED = 9195.19

PRESSURE RATIO = 1.4714

ADIABATIC EFFICIENCY = 84.1403

ROTOR 1

STATION 1 - STATION 2

	10	30	50	70	90
DIA 1	29.150	27.080	25.060	23.020	20.989
DIA 2	29.088	27.302	25.516	23.730	21.944
BETA 1	21.495	23.147	25.111	26.883	28.940
BETA 2	49.165	50.354	52.617	54.217	55.487
BETA(PR) 1	53.181	56.166	52.623	48.591	43.822
BETA(PR) 2	44.552	39.237	33.495	25.943	17.207
V 1	607.44	615.85	624.84	631.29	643.72
V 2	833.72	848.76	856.01	870.25	881.22
VZ 1	565.19	566.27	565.79	563.07	574.87
VZ 2	545.15	541.54	519.72	508.85	499.29
V-THETA 1	222.58	242.09	265.17	285.46	291.54
V-THETA 2	630.79	653.55	680.18	705.98	726.13
V(PR) 1	1103.2	1017.0	932.0	851.3	795.4
V(PR) 2	765.0	699.2	623.2	565.4	522.7
VTHETA PR1	747.4	644.4	740.6	633.5	550.7
VTHETA PR2	536.7	442.2	343.9	246.5	154.5
U 1	1169.97	1086.87	1005.81	922.93	842.38
U 2	1167.48	1095.80	1024.11	952.43	880.75
M 1	0.5610	0.5693	0.5782	0.5845	0.5949
M 2	0.7242	0.7461	0.7569	0.7753	0.7879
M(PR) 1	1.0189	0.9402	0.8624	0.7883	0.7375
M(PR) 2	0.6642	0.6163	0.5525	0.5037	0.4673
TURN(PR)	14.629	16.929	19.128	22.745	26.615
LOSS COEF.	0.0958	0.0429	0.0394	0.0494	0.1133
DFAC	0.4378	0.4432	0.4619	0.4867	0.4725
EFFP	0.9112	0.9626	0.9680	0.9635	0.9213
EFF	0.9050	0.9600	0.9660	0.9613	0.9169
LOSS PARA.	0.0241	0.0110	0.0101	0.0126	0.0241
INCID	-0.42	-0.73	-1.08	-1.21	-1.13
DEV	-0.548	0.437	2.695	5.143	6.517

CORRECTED WEIGHT FLOW

UPSTREAM OF ROTOR	97.61
UPSTREAM OF STATOR	97.61
DOWNSTREAM OF STATOR	93.55

STATOR 1

STATION 2 - STATION 3

	10	30	50	70	90
DIA 3	29.184	27.422	25.672	23.874	22.034
BETA 2	49.165	50.354	52.617	54.217	55.487
BETA 3	-12.775	-4.781	-6.648	-16.400	-24.860
V 2	833.72	848.76	856.01	870.25	881.22
V 3	516.50	511.76	525.73	461.64	430.72
VZ 2	545.15	541.54	519.72	508.85	499.29
VZ 3	503.71	509.57	523.70	442.86	390.81
V-THETA 2	630.79	653.55	680.18	705.98	726.13
V-THETA 3	-114.22	-42.65	-79.65	-130.34	-181.08
M 2	0.7292	0.7461	0.7569	0.7753	0.7879
M 3	0.4377	0.4372	0.4551	0.3956	0.3681
TURN	61.941	55.135	61.265	70.617	80.347
LOSS COEF.	0.2562	0.2096	0.1171	0.1537	0.1223
DFAC	0.7394	0.7061	0.6933	0.7838	0.8222
LOSS PARA.	0.1063	0.0785	0.0407	0.0482	0.0335
INCID	-2.91	-1.79	-0.08	0.22	-0.46
DEV	9.184	13.259	5.102	1.280	-7.060

Table IVff.

Blade element performance for complete stage.

PERCENT DESIGN SPEED = 109.36

CORRECTED WEIGHT FLOW = 95.01

CORRECTED ROTOR SPEED = 9191.42

PRESSURE RATIO = 1.4761

ADIABATIC EFFICIENCY = 82.9948

Optimum Bleed

ROTOR 1

STATION 1 - STATION 2

	10	30	50	70	90
DIA 1	29.150	27.080	25.060	23.020	20.988
DIA 2	29.088	27.302	25.516	23.730	21.964
BETA 1	21.803	22.547	25.017	28.585	36.040
BETA 2	50.895	51.580	54.691	56.927	57.921
BETA(PR) 1	60.223	57.396	54.115	50.042	46.453
BETA(PR) 2	44.185	39.274	34.128	26.122	15.392
V 1	586.71	594.79	600.34	609.91	608.33
V 2	840.49	848.38	847.93	861.48	886.49
VZ 1	544.74	549.32	544.02	545.42	546.57
VZ 2	530.13	527.20	490.09	470.11	470.80
V-THETA 1	217.91	228.07	253.88	272.95	267.05
V-THETA 2	652.22	664.69	691.95	721.90	751.14
V(PR) 1	1096.9	1019.5	928.1	849.3	793.6
V(PR) 2	739.3	681.0	592.1	523.6	488.3
VTHETA PR1	952.1	858.8	751.9	651.0	575.3
VTHETA PR2	515.3	431.1	332.2	230.5	129.6
U 1	1169.97	1086.69	1005.81	923.93	842.38
U 2	1157.48	1095.80	1024.11	952.43	880.75
M 1	0.5405	0.5484	0.5539	0.5632	0.5617
M 2	0.7316	0.7457	0.7489	0.7650	0.7904
M(PR) 1	1.0106	0.9400	0.8562	0.7843	0.7327
M(PR) 2	0.6435	0.5986	0.5229	0.4650	0.4354
TURN(PR)	16.038	18.122	19.987	23.920	31.076
LOSS COEF.	0.0935	0.0298	0.0392	0.0485	0.0691
DFAC	0.4664	0.4704	0.5008	0.5241	0.5309
EFFP	0.9182	0.9752	0.9695	0.9654	0.9551
EFF	0.9121	0.9734	0.9675	0.9632	0.9523
LOSS PARA.	0.0236	0.0076	0.0100	0.0124	0.0174
INCID	0.62	0.50	0.41	0.24	1.47
DEV	-0.915	0.474	3.328	5.422	6.692

CORRECTED WEIGHT FLOW

UPSTREAM OF ROTOR	95.01
UPSTREAM OF STATOR	95.01
DOWNSTREAM OF STATOR	90.90

STATOR 1

STATION 2 - STATION 3

	10	30	50	70	90
DIA 3	29.164	27.422	25.672	23.874	22.034
BETA 2	50.895	51.580	54.691	56.927	57.921
BETA 3	-17.480	-5.481	-9.721	-21.080	-30.080
V 2	840.49	848.38	847.93	861.48	886.49
V 3	563.72	560.66	510.39	414.60	372.04
VZ 2	530.13	527.20	490.09	470.11	470.80
VZ 3	537.69	558.10	503.06	386.85	321.94
V-THETA 2	652.22	664.69	691.95	721.90	751.14
V-THETA 3	-169.33	-53.55	-86.18	-149.12	-186.47
M 2	0.7316	0.7457	0.7489	0.7650	0.7904
M 3	0.4774	0.4791	0.4366	0.3530	0.3160
TURN	68.375	57.061	64.412	78.007	88.001
LOSS COEF.	0.2441	0.1812	0.1652	0.2226	0.2191
DFAC	0.7219	0.6561	0.7208	0.8494	0.8999
LOSS PARA.	0.0935	0.0079	0.0572	0.0679	0.0573
INCID	-1.18	-0.56	1.99	2.93	1.97
DEV	1.480	12.559	8.029	-3.400	-12.280

Table IVgg.

Blade element performance for complete stage.

PERCENT DESIGN SPEED = 109.48

CORRECTED WEIGHT FLOW = 92.95

CORRECTED ROTOR SPEED = 7193.41

PRESSURE RATIO = 1.5125

ADIABATIC EFFICIENCY = 80.3659

OPTIMUM BLEED

ROTOR 1

STATION 1 - STATION 2

	10	30	50	70	90
DIA 1	29.150	27.080	25.060	23.020	20.938
DIA 2	29.086	27.302	25.516	23.730	21.944
BETA 1	21.024	23.495	25.044	26.859	28.398
BETA 2	51.730	52.857	55.927	58.275	59.095
BETA(PR) 1	61.036	58.303	55.198	51.343	47.711
BETA(PR) 2	43.813	39.519	34.181	26.127	15.785
V 1	572.36	576.99	582.48	588.60	594.34
V 2	846.41	846.04	847.22	859.21	877.92
VZ 1	533.98	529.15	527.72	525.99	527.88
VZ 2	524.24	510.84	474.66	451.80	450.91
V-THETA 1	205.24	230.03	246.57	267.38	262.02
V-THETA 2	664.52	674.41	701.77	730.83	753.28
V(PR) 1	1102.7	1007.1	924.6	842.1	794.5
V(PR) 2	726.5	662.2	573.8	503.2	468.6
VTHETA PR1	964.7	856.9	759.2	657.6	580.4
VTHETA PR2	503.0	421.4	322.3	221.6	127.5
U 1	1169.97	1086.89	1005.61	923.95	842.38
U 2	1167.48	1095.80	1024.11	952.43	880.75
M 1	0.5264	0.5312	0.5365	0.5435	0.5432
M 2	0.7344	0.7416	0.7463	0.7610	0.7809
M(PR) 1	1.0146	0.9271	0.8517	0.7762	0.7231
M(PR) 2	0.6303	0.5805	0.5054	0.4457	0.4168
TURN(PR)	17.223	18.784	21.017	25.216	31.925
LOSS COEF.	0.1115	0.0392	0.0470	0.0541	0.0752
DFAC	0.4838	0.4852	0.5244	0.5495	0.5530
EFFP	0.9059	0.9686	0.9648	0.9632	0.9530
EFF	0.8996	0.9663	0.9624	0.9608	0.9501
LOSS PARA.	0.0284	0.0100	0.0119	0.0138	0.0188
INCID	1.44	1.40	1.50	1.54	2.71
DEV	-1.287	0.719	3.381	5.427	7.086

CORRECTED WEIGHT FLOW

UPSTREAM OF ROTOR	92.95
UPSTREAM OF STATOR	92.95
DOWNSTREAM OF STATOR	88.76

STATOR 1

STATION 2 - STATION 3

	10	30	50	70	90
DIA 3	29.164	27.422	25.672	23.874	22.034
BETA 2	51.730	52.857	55.927	58.275	59.095
BETA 3	-14.584	-6.529	-13.137	-24.680	-30.440
V 2	846.41	846.04	847.22	859.21	877.92
V 3	581.25	572.83	482.67	376.37	342.31
VZ 2	524.24	510.84	474.66	451.80	450.91
VZ 3	562.52	569.11	470.04	341.99	295.13
V-THETA 2	664.52	674.41	701.77	730.83	753.28
V-THETA 3	-146.36	-65.13	-109.70	-157.15	-173.43
M 2	0.7344	0.7416	0.7463	0.7610	0.7809
M 3	0.4907	0.4882	0.4109	0.3188	0.2898
TURN	66.314	59.386	69.064	82.555	89.535
LOSS COEF.	0.2512	0.1759	0.2166	0.2784	0.2457
DFAC	0.6980	0.6523	0.7671	0.8959	0.9290
LOSS PARA.	0.0976	0.0658	0.0742	0.0827	0.0640
INCID	-0.35	0.72	3.23	4.28	3.15
DEV	4.376	11.511	4.613	-7.000	-12.640

Table IVhh.

Blade element performance for complete stage.

PERCENT DESIGN SPEED = 109.93 *Optimum Bleed*

CORRECTED WEIGHT FLOW = 90.80

CORRECTED ROTOR SPEED = 9197.78

PRESSURE RATIO = 1.5276

ADIABATIC EFFICIENCY = 78.3808

ROTOR 1

STATION 1 - STATION 2

	10	30	50	70	90
DIA 1	29.150	27.080	25.060	23.020	20.998
DIA 2	29.088	27.302	25.516	23.730	21.944
BETA 1	21.020	23.401	25.044	26.856	28.759
BETA 2	53.921	53.510	57.043	58.889	59.562
BETA(PR) 1	62.510	59.616	56.478	52.775	48.108
BETA(PR) 2	44.231	40.427	35.870	26.766	16.236
V 1	543.51	553.85	561.60	568.21	568.45
V 2	845.08	836.13	830.47	852.82	871.86
VZ 1	507.34	508.30	508.80	506.93	507.75
VZ 2	497.67	497.23	452.05	440.64	441.69
V-THETA 1	194.95	219.97	237.74	256.65	256.03
V-THETA 2	682.99	672.21	697.25	730.16	751.71
V(PR) 1	1099.1	1004.9	921.3	838.0	775.6
V(PR) 2	594.6	553.2	557.8	533.5	550.2
VTHETA PR1	975.0	866.9	768.1	667.2	586.3
VTHETA PR2	484.5	423.6	326.9	223.3	129.1
U 1	1159.97	1086.83	1005.81	923.93	842.38
U 2	1167.48	1095.80	1024.11	953.43	880.75
M 1	0.4990	0.5090	0.5165	0.5229	0.5233
M 2	0.7304	0.7814	0.7301	0.7535	0.7740
M(PR) 1	1.0092	0.9235	0.8473	0.7712	0.7138
M(PR) 2	0.6003	0.5714	0.4902	0.4341	0.4085
TURN(PR)	18.279	19.188	20.409	25.007	32.823
LOSS COEF.	0.1301	0.0404	0.0590	0.0406	0.0720
DFAC	0.5254	0.4956	0.5414	0.5619	0.5603
EFFP	0.8950	0.9484	0.9564	0.9601	0.9570
EFF	0.8807	0.9060	0.9534	0.9575	0.9542
LOSS PARA.	0.0329	0.0101	0.0147	0.0154	0.0180
INCID	2.91	2.72	2.78	2.97	4.11
DEV	-0.869	1.527	5.070	5.068	7.536

CORRECTED WEIGHT FLOW

UPSTREAM OF ROTOR	90.80
UPSTREAM OF STATOR	90.80
DOWNSTREAM OF STATOR	88.55

STATOR 1

STATION 2 - STATION 3

	10	30	50	70	90
DIA 3	29.164	27.422	25.672	23.874	22.034
BETA 2	53.921	53.510	57.043	58.889	59.562
BETA 3	-12.235	-7.934	-16.218	-29.180	-32.960
V 2	845.08	836.13	830.97	852.82	871.86
V 3	588.07	565.44	474.77	384.93	346.99
VZ 2	497.67	497.23	452.05	440.64	441.69
VZ 3	574.71	566.03	455.88	336.08	291.14
V-THETA 2	682.99	672.21	697.25	730.16	751.71
V-THETA 3	-124.63	-78.65	-132.60	-187.67	-138.78
M 2	0.7304	0.7814	0.7301	0.7535	0.7740
M 3	0.4947	0.4804	0.4029	0.3254	0.2933
TURN	66.155	61.444	73.261	88.069	92.522
LOSS COEF.	0.2307	0.1780	0.2052	0.2713	0.2446
DFAC	0.6379	0.6618	0.7796	0.9006	0.9279
LOSS PARA.	0.0984	0.0664	0.0893	0.0775	0.0820
INCID	1.84	1.37	4.34	4.69	3.61
DEV	6.725	10.106	1.532	-11.500	-15.160